AN ANALYSIS OF THE ROLE OF T-BOX GENES IN DEVELOPMENT OF THE MAMMALIAN RETINA

James Keith Langford Holt

A thesis submitted for a degree of Doctor of Philosophy (Ph.D.)
to the University of London, 2003

Institute of Child Health
30 Guilford Street
London
WC1N 1EH

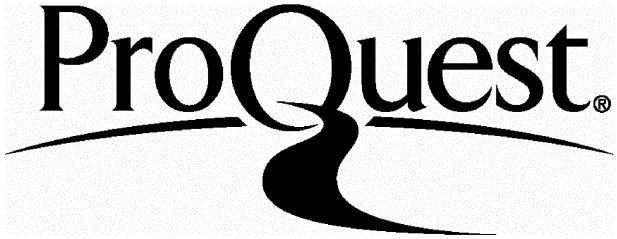

Abstract

Exploring how the eye develops is of great value in the understanding and ultimately the treating of human eye disease. Genetic eye disease is a significant cause of congenital blindness and retinal degeneration in man. Studying the molecular basis of eye development also teaches us about basic mechanisms of neural development and patterning. One flourishing area of research in eye development is that of retinal patterning. Patterns/gradients of gene expression across the retina confer positional identity to retinal cells, essential for eye morphogenesis and the guidance of retinal ganglion cell axons into the brain. I have studied patterning of the retina along its dorso-ventral axis, in particular the putative role of T-box transcription factor genes in this process. T-box (*Tbx*) genes are known to be involved in many developmental events such as heart patterning and the provision of forelimb identity, yet their roles in eye development are not clear. *omb*-related *Tbx* gene expression was restricted to the dorsal retina during early mouse and human development and showed lamina-specific patterns at later stages. Embryonic expression of *Tbx2* and *Tbx5* was disrupted in *Pax6*-null mice, as was expression of ventral homeobox gene *Vax2*. *Tbx2* and *Tbx5* expression was induced by the implantation of BMP4-soaked beads and whole mouse embryo culture. Transgenic mice were generated to investigate the effect of retinal misexpression of *Tbx5* in dorso-ventral patterning, eye morphogenesis and retinal stratification. These data provide insight into T-box gene regulation and function in the eye and more generally into the interactions of transcription factors and signalling molecules in the patterning of neural structures.

Table of Contents

List of Tables

List of Figures

Figure

Acknowledgements

This thesis is my own composition and the studies presented here are the results of my own work. This thesis has not been, is not concurrently being and will not be submitted for any degree or professional qualification other than 'PhD Child Health' to University College London.

The Child Health Research Appeal Trust (CHRAT), to whom I am extremely grateful, funded the work presented in this thesis. Thanks to ex-Dean Roland Levinsky, second supervisor Andy Copp and Unit leader Patrizia Ferretti. Thanks to everyone in NDU and DBU, particularly Adam Rutherford, Morritz Meins, Karen Willis and Esta Adams, but also Sarah Reid, Fang Zhang, Paul O'Neill, Sally Walder and Melanie Mackay. Thanks also Diane Vaughn and Alan Simpkins. Specific thanks to Katy Gardener for help with the generation of transgenic mice, to Caroline Patternotte and Simon Lee for help sequencing, to Diane Gerrelli for *Sonic hedgehog* mutant mouse embryos and to Hourinaz Behesti for continuing the embryo culture work. Thanks to David Latchman (the current ICH Dean), to the British Society of Developmental Biologists and to the Company of Biologists for Conference funding. Thanks to Hazel Smith (Cruciform Building, UCL, London) for help with the *Small eye* mice and to the numerous other individuals and institutions that provided essential materials for my work (acknowledged in **Chapter 2**, Materials).

Thank you to my family, particularly my parents, for financial support and trust over my long and continuing studies. Thanks to friends, some of who consistently expressed an interest in seeing me. Thanks to Arantza Barrios for reading my Introduction and being my friend. Thanks to ICH for being generally kind and for its refreshing abundance of youth and vitality. Biggest thanks go to my supervisor Jane, for supervising me with patience, making time for me and reading endless draughts of this thesis.

Abbreviations

AER	apical ectodermal ridge
BCIP	5-bromo-4-chloro-3-indolyl-phosphate
bHLH	basic helix-loop-helix
BMP	bone morphogenetic protein
bp	base pair(s)
BSA	bovine serum albumen
cDNA	complementary DNA
CNS	central nervous system
CSHB	cryostat section hybridisation buffer
DAB	3,3'-diaminobenzidine
DEPC	diethyl pyrocarbonate
DNA	deoxyribonucleic acid
dNTPs	phosphorylated deoxyribonucleotides
E(number)	embryonic day
EDTA	ethylenediamine tetraacetic acid
EFG	epidermal growth factor
EGTA	ethyleneglycol tetraacetic acid
FGF	fibroblast growth factor
GDF	growth/differentiation factor
hCG	human chorionic gonadotropin
HGF	hepatocyte growth factor
INL	inner nuclear layer
kb	kilobase pair(s)
LGN	lateral geniculate nucleus/nuclei
mg	milligrams
ml	millilitres
MOPS	3-(N-Morpholino)propanesulfonic acid
mRNA	messenger RNA
µg	micrograms
µl	microlitres
NBT	nitro blue tetrazolium

ONL	outer nuclear layer
PBS	phosphate-buffered saline
PBT	phosphate-buffered saline with 0.1% Tween-20
PCR	polymerase chain reaction
pg	picograms
pmol	picomoles
PMS	pregnant mare's serum
RA	retinoic acid
RD	retinal dystrophies
RGC	retinal ganglion cell
RNA	ribonucleic acid
RPE	retinal pigmented epithelium
rpm	revolutions per minute
RT-PCR	reverse transcriptase-polymerase chain reaction
SC	superior colliculus/colliculi
SDS	sodium dodecyl sulphate
TBE	Tris borate EDTA
TGFβ	transforming growth factor beta
Tm	melting temperature (of oligonucleotide primers from DNA)
WMHB	whole mount hybridisation buffer
wpc	weeks post-conception
utr	untranslated region

Gene names approved by nomenclature committees are used throughout. In some cases original gene names are also given for clarity and continuity with literature.

- Gene names are written in *italics* with the first letter only in UPPERCASE. Exceptions are writing the first letter of zebrafish genes (and some *Drosophila* genes, depending on the mode of gene inheritance) in lowercase and writing all letters of human genes in uppercase.
- The protein that the gene encodes is written without italics, in UPPERCASE. Exceptions are non-human vertebrate transcription factors, where usually only the first letter is capitalised, and zebrafish proteins, written in lower case.

CHAPTER 1

Introduction

THE BEGINNING

In the beginning, from the molecular soup in the waters of primeval Earth, a rather special molecule was born. This molecule, über-ancestor of modern nucleic acids and probably most analogous to contemporary ribonucleic acid (RNA), was special in that it encouraged its own construction. Nucleic acids soon came to be dominant among many unique but short-lived peers and those better at self-replication naturally became more dominant. They became longer and able to encode and build protein molecules. Further down the road came the evolution of the cell – the self-replicating molecules found themselves better able to do so when enclosed by a bubble of fat. From here it was but a few skips (relatively speaking) to the creation of multi-cellular organisms that could exist for longer and duplicate more efficiently than ever before. Nervous systems developed to organise and allow multi-cellular creatures to function as a single organism. Parts of these primitive nervous systems evolved into specialised sensory organs enabling perception of and interaction with the environment. Such are the roots of the eyes you use to read this page.

Our eyes allow us to receive visual information from the environment and transform it into neural impulses that are directed into the brain for interpretation. Light passes through the pupil and is focused, by the lens, onto the retina at the back of the eye (**Fig. 1.1**). The light passes through the retina and activates photoreceptors at the back before being absorbed by the retinal pigmented epithelium (RPE). Photoreceptor activity, which is strongest in the central (macula) part of the retina, is translated into retinal ganglion cell (RGC) activity via a modulating layer of interneurons. RGCs project their axons into the brain through the optic nerve. The information is processed in the visual centres of the brain and conscious image perception is generated.

The study of how eyes evolved, how they develop and how they function, as well as being interesting, is of great practical value. Understanding what happens when they develop normally and function properly enables us to understand what happens when they don't. Genetic eye disease is hugely debilitating and is an important cause of congenital blindness. 1.5 million children worldwide are blind, in the UK 1-2 children per 1000 are visually impaired. Many genes involved in eye development have been

Figure 1.1

Schematic diagram demonstrating the basic anatomy of the mammalian eye. Light is shown entering the eye to be refracted by the lens (pink) onto the retina (green). Photoreceptors (blue) at the back of the retina are activated by light. Activated photoreceptors stimulate retinal ganglion cells (orange). Retinal ganglion cell axons connect to central brain areas via the optic nerve. Retinal signals can then be processed to generate an internal representation of the outside environment.

Anatomy of the mammalian eye

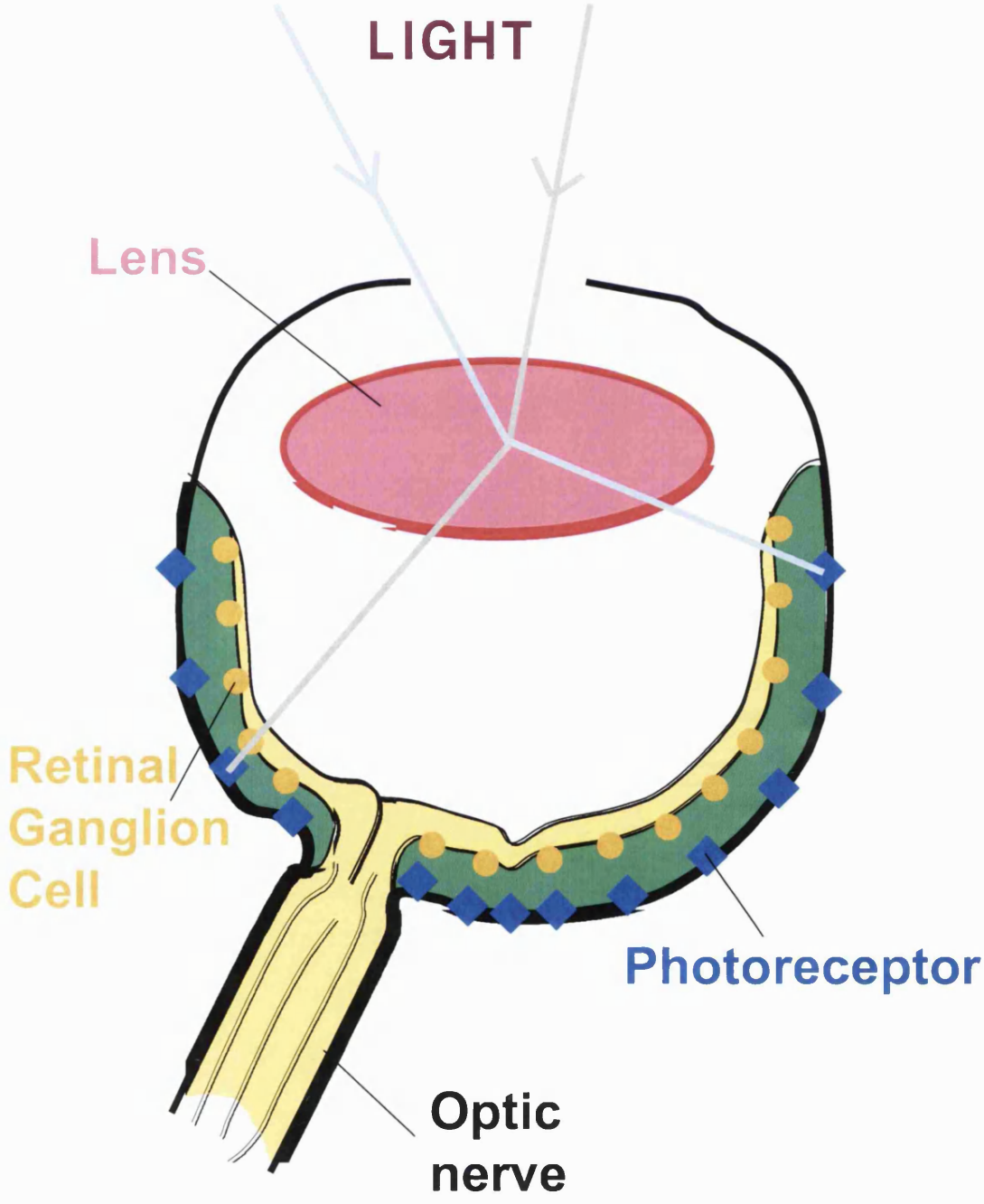

implicated in human eye disease. For example, mutations in the *PAX6* gene (which encodes a paired-box homeodomain transcription factor with pivotal roles in early eye development) are now known to cause aniridia and other anterior segment malformations, such as Peters' anomaly, in humans (Hanson and Van Heyningen, 1995). Genetic defects are also responsible for some adult-onset eye disorders, for example some retinal degenerative disorders (retinal dystophies or RD) present late in life and are caused or contributed to by genetic mutations. More than sixty genes, many encoding transcription factors, are known to cause human RD, which are thought to affect over 15 million people worldwide (Bessant *et al.*, 2001; Stone *et al.*, 2001; Chader, 2002). As well identifying key genes, developmental biology has contributed to the understanding of morphogenetic processes and tissue interactions during eye development. Moreover, study of the developing visual system teaches us much about the general mechanisms governing cellular transitions towards final differentiation (Livesey and Cepko, 2001). It teaches us about control of the cell cycle and apoptosis, which has relevance for the study of degenerative disease and tumourigenesis as well for developmental biology (Dyer and Cepko, 2001). The developing retina is a functional sub-unit of the central nervous system (CNS) that is anatomically distinct and therefore highly amenable to investigation and experimentation. This makes development of the retina a favoured model for the study of neural development and differentiation.

In this thesis the roles of T-box transcription factors in retinal development and dorso-ventral patterning of the retina are explored. I introduce this work by giving an extensive review of background relevant literature in the next section. I outline our current understanding of how the vertebrate eye forms during embryonic development. Some of the putative molecular players involved in the provision of positional identity to cells across the dorso-ventral axis of the retina are discussed. At the end of this chapter I state the aims of this thesis and how I set about achieving them.

BACKGROUND

In this chapter, early eye development is described from its beginnings in the anterior neural plate to formation of recognisable eye structures, the optic cups. Development of the neural retina is then described from the undifferentiated pool of multipotent precursors at the optic cup stage to the formation of the mature layers of the adult retina. In this first section (**1.1.**), a description of the developmental sequence of morphogenetic events precedes a more detailed discussion of the important genes involved. The next section (**1.2.**) explores the development of axonal projections from the retina to the brain and the influence of patterning molecules of the Eph and ephrin families. From then on the focus becomes dorso-ventral patterning of the retina (**1.3.**) and the T-box family of transcription factors (**1.4.**).

1.1. Retinal development and differentiation

The two eyes begin to form as outpouchings of neuroectoderm at the lateral sides of the prosencephalon (**Fig. 1.2A, B**). In mammals these first appear as a pair of dimples in the anterior neural plate called the **optic pits**. The optic primordia evaginate further to form the **optic vesicles** (**Fig. 1.2C, D**). Their bases constrict to form the **optic stalks**. The dorso-distal optic vesicles make contact with the overlying **surface ectoderm** (which thickens to form the **lens placode**) and they become tightly associated. Invagination of the optic vesicles occurs on their ventral aspects (**Fig. 1.2E, F**). This gives the developing retina the appearance of a cup deficient on its ventral aspect. Retinal tissue grows ventrally around the developing lens to form the **ventral fissure** and complete a bi-layered **optic cup**. A ventral invagination also occurs in the optic stalk, forming a ventral groove where optic nerve fibres and blood vessels subsequently pass. The ventral groove later seals to form a double-layered tube. Tissue derived from the ventral optic vesicle and stalk (blue and magenta in **Fig. 1.2D** respectively) thus gives rise to central inner optic cup/neural retina and inner optic stalk/nerve (blue and magenta in **Fig. 1.2G**). Tissue derived from the dorsal optic vesicle and stalk (green/orange and lilac in **Fig. 1.2D** respectively) gives rise to the peripheral neural retina, the outer optic cup (future RPE) and outer stalk/nerve (green, orange and lilac in **Fig. 1.2G**).

Figure 1.2

Schematic overview of optic cup development in the mouse embryo (**A-G**):

A Cartoon of an antero-lateral view of the developing head of a mouse embryo at the optic pit stage. The locations of the optic pits on the anterior neural plate, which is closing to form the prosencephalon, are indicated. Broken line indicates the plane of section for **B**.

B Schematic representation of a transverse section through the developing head shown in **A**. The developing head consists of neuroepithelium (cyan), mesoderm (yellow) and surface ectoderm (red) at this stage. The lateral head folds are coming together dorsally (arrows) to seal the developing forebrain into a tube (the prosencephalon). Dorsal (**d**) and ventral (**v**) regions are indicated. The first morphological signs of eye development occur at this stage with the bilateral evagination of neuroepithelium to form the optic pits, indicated.

C Cartoon of a lateral view of the developing head of a mouse embryo at the optic vesicle (**ov**) stage. The lateral head folds have fused to form the dorsal midline (arrows) and the optic pits have deepened to form optic vesicles. The right **ov** (cyan; indicated) is visible underneath the surface ectoderm. The dorso-ventral (**d-v**) and naso-temporal (**n-t**) axes of the developing **ov** are indicated for this figure and for **E**. Broken line indicates the plane of section for **D**.

D Schematic representation of a frontal section through the developing optic vesicle shown in **A**. The optic neuroepithelium now forms an **ov** joined proximally to the brain by an optic stalk (**s**). Dorsal, **d**, and distal, **D**, directions are indicated (also for **F** and **G**). The dorso-distal **ov** (green) makes contact with the overlying surface ectoderm (red). Through reciprocal signalling, the surface ectoderm thickens to form a lens placode (**l**) and the dorso-distal **ov** is specified as neural retina (**n**). As the developing lens and optic vesicle become further associated the ventro-distal optic vesicle (blue) will also become specified as neural retina. The dorso-proximal optic vesicle (orange) is specified as retinal pigmented epithelium (RPE) by the peri-ocular mesenchyme (yellow). Following invagination of the optic vesicle, the dorsal (lilac) and ventral (magenta) optic stalk give rise to the outer and inner optic stalk (later optic nerve).

E Cartoon of a lateral view of the developing head of a mouse embryo at the optic cup stage. The lens placode has thickened and begun to invaginate (red). The optic vesicle has invaginated and then grown ventrally (indicated by arrows) around the developing lens to form an optic cup (cyan). Broken line indicates the plane of section for **F**.

F Schematic representation of a frontal section through the developing optic cup shown in **E**. The neural retina (**n**) is thickened with respect to the RPE (**p**). The optic vesicle (and stalk) has invaginated to create a cup with a ventral deficiency (cyan). Optic tissue grows ventrally (dark green) around the developing lens (**l**) to complete a cup shape (the optic cup, **oc**). Optic stalk tissue similarly grows ventrally, transforming the optic stalk (**s**) into a double-layered tube.

G Same as **F**, but when the **oc** has fully formed and the lens vesicle (**l**) has detached from the surface ectoderm. Dorsal **oc** = cyan, ventral **oc** = dark green. The lower figure is identical to the upper, but coloured green, blue, orange, lilac and magenta as in **D** to show tissue of origin in the **ov**.

Eye development (I): development of the optic cup

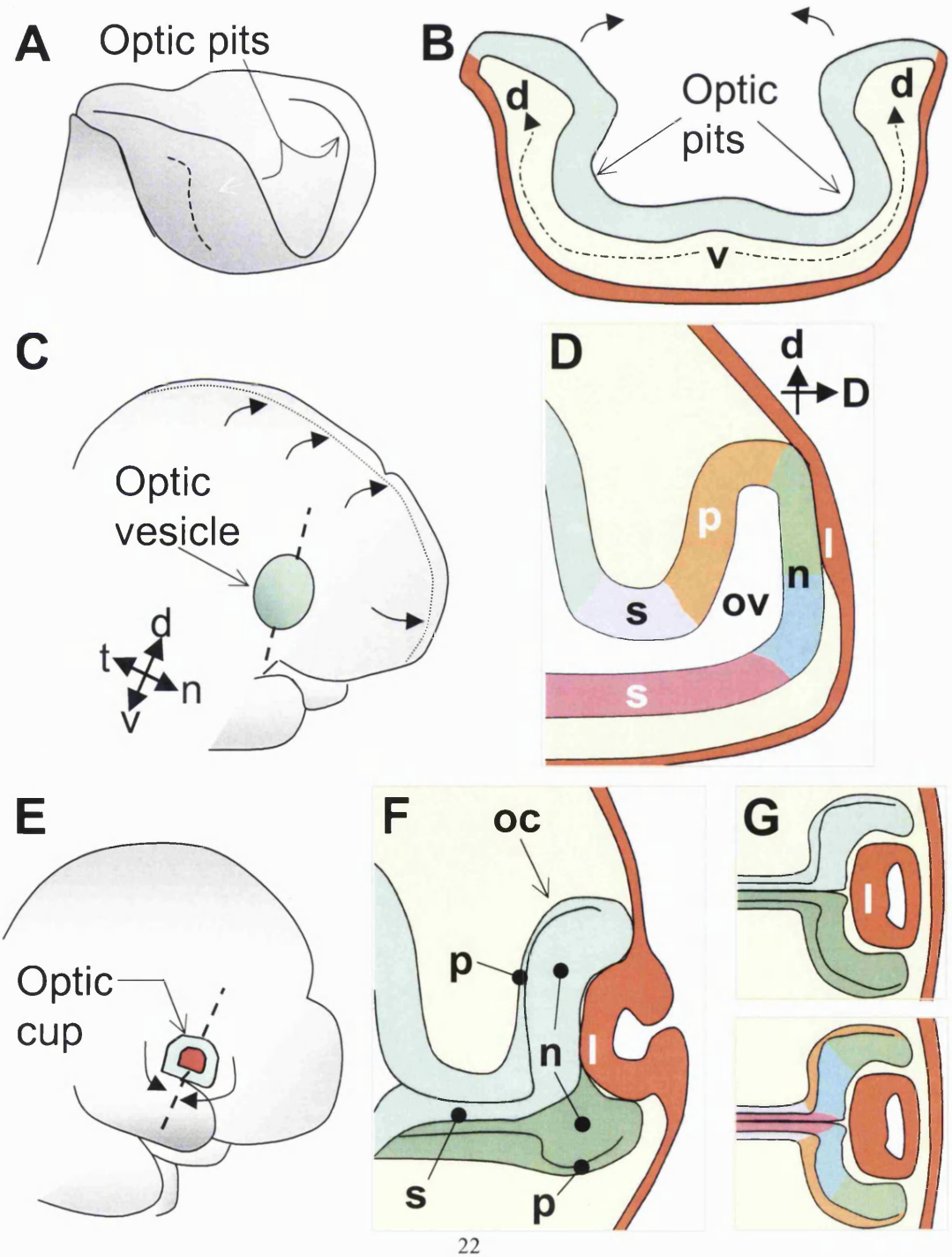

During the process of optic vesicle invagination the neuroepithelium of the presumptive retina remains closely associated with the developing lens. Thus as the optic cups are forged from the optic vesicles, the lens placode deepens and forms a **lens vesicle** that ultimately detaches from the surface ectoderm (**Fig. 1.2F, G**). The surface ectoderm now overlying the lens will give rise to the corneal epithelium. The inner layer of the optic cup (presumptive neural retina) proliferates greatly and thickens with respect to the outer layer (presumptive RPE) immediately prior to and during invagination. The developing eye now resembles the adult structure and retinal differentiation is ready to begin (Silver and Sapiro, 1981; Kaufman, 1992; Bellairs and Osmond, 1998; Chow and Lang, 2001).

Bisection of the eye field and dorso-ventral patterning of the early optic vesicles

The vertebrate nervous system begins dorsally in the ectoderm layer of the pre-gastrulation embryo. Ectodermal cells are directed to a neural rather than an epidermal fate by the inhibition of bone morphogenetic protein (BMP) signalling with antagonists such as Noggin and Chordin (Harland, 2000). BMPs are secreted morphogens from the transforming growth factor beta (TGFβ) family of secreted proteins. By defining the domain of the presumptive neural plate, BMP inhibition is one of the earliest steps in retinal determination. The anterior neural plate becomes subdivided into fields that will give rise to different CNS domains. This process is largely mediated by the differential localisation of transcription factors. Misexpression of several transcription factors known to be important for eye development in neural cells will promote a retinal fate at the expense of other CNS fates in *Xenopus* embryos (Kenyon *et al.*, 2001). These include paired homeobox gene *Pax6* and paired-like homeobox genes *Rx1* and *Otx2*.

There is evidence that two laterally placed retinal primordia originally arise from a single eye field in the anterior neural plate in developing vertebrates, though there are variations between species. In *Xenopus*, the genes *ET* (otherwise known as *Tbx3* and encoding a T-box transcription factor) and *Pax6* are expressed in a continuous band in the anterior neural plate (Li *et al.*, 1997). Down-regulation of retina primordial genes in the ventro-medial prosencephalon leads to separation of the early eye field into two lateral domains (Li *et al.*, 1997). Signals in the underlying prechordal mesoderm are seemingly essential for this medial suppression. Removal of prechordal mesoderm

leads to cyclopia and ectopic grafting of it can suppress *Pax6* in retinal primordial tissue in Xenopus and in chick embryos (Li *et al.*, 1997; Pera and Kessel, 1997 1428).

In the mouse, *Pax6* is expressed in retinal primordial cells, as are *pax6* and *tbx2* (a closely related paralogue of *tbx3*) in zebrafish. Expression of these genes is widespread throughout the anterior neural plate in these species and does not define which of the anterior neural plate cells will form eyes (Puschel *et al.*, 1992; Dheen *et al.*, 1999). Fate-mapping studies in zebrafish suggest that retinal precursors arise from a single domain in the antero-medial prosencephalon. Invading ventral diencephalic precursors are then believed to bisect the early eye field which are displaced bilaterally to give the two optic primordia (Woo and Fraser, 1995). Analysis of cyclopic mutant zebrafish suggest that the prechordal mesoderm – and the nodal (of the TGFβ family) signalling pathway – are essential for resolution of the two eye fields and development of the ventral diencephalon (Chow and Lang, 2001; Vetter and Brown, 2001).

Vertebrate orthologues of Drosophila patterning gene *hedgehog* (*hh*) are also implicated in bisection of the eye field. Mutations in *Sonic hedgehog* (*Shh/SHH*) cause cyclopia in mammals (Belloni *et al.*, 1996; Chiang *et al.*, 1996; Roessler *et al.*, 1996). In the ventral diencephalon, zebrafish *shh* seems to be regulated by the nodal-related cyclops (cyc) (Krauss *et al.*, 1993; Sampath *et al.*, 1998; Muller *et al.*, 2000). Zebrafish mutations in *shh* do not cause cyclopia (Schauerte *et al.*, 1998). This is likely to be due to compensation by related *hh* gene *tiggy-winkle hedgehog* (*twhh*) which has only been identified in zebrafish and displays similar expression and function to *shh* in the ventral diencephalon (Ekker *et al.*, 1995).

Over-expression of *shh* in the zebrafish optic vesicles suppresses dorso-distal *pax6* expression and promotes expression of proximo-ventral gene *pax2* leading to reduced retinas and enlarged optic stalk-like structures (Macdonald *et al.*, 1995). These data implicate *Shh* in more than just the suppression of eye development in the ventral midline. *Foxgl*-deficient mice exhibit a selective loss of *Shh* expression from the caudal aspect of the ventral telencephalic midline. They show an expansion of *Pax6* expression and a virtual eradication of *Pax2* expression with enlarged retinas and absent optic stalks (Huh *et al.*, 1999). SHH signalling thus appears to regulate early

dorso-ventral patterning of the optic neuroepithelium (therefore proximo-distal patterning of the developing eye), presumably through some form of diffusion gradient from the ventral (diencephalic and telencephalic) midline source.

In summary, Nodal and Hedgehog signalling pathways direct the establishment of two eye fields in a wide range of species. This may be achieved through the regulation of genes such as *Pax2* and *Pax6* to pattern the ventral diencephalon and the early eye.

Development of the optic cup from the optic vesicles

Pax6 is an important early regulator of eye development with conserved roles across a wide range of vertebrate and invertebrate species (Baker, 2001). *Pax6* is able to induce complete though imperfect ectopic eyes in *Drosophila* (Halder *et al.*, 1995) and in *Xenopus* (Chow *et al.*, 1999). *Pax6* expression in the distal optic vesicle and the surface ectoderm is essential for the close association of these structures and for development of a single neural retina and lens (Ashery-Padan *et al.*, 2000; Collinson *et al.*, 2000). In the *Pax6*-null mouse mutant, eye development is arrested at the optic vesicle stage, lens development is not initiated and the optic cup does not form (Grindley *et al.*, 1995). *Pax6* is later expressed throughout the neural retina and the lens with a complex regulation that employs different promoters and enhancer elements for transcription in different parts of the eye (Kammandel *et al.*, 1999; Xu *et al.*, 1999).

Expression of *Pax2*, a *Pax6*-related paired box transcription factor, complements that of *Pax6* at early stages, being localised to the proximal (ventral) optic vesicle and optic stalk. It is later expressed in the optic nerve and in ventral retina. Following closure of the optic fissure, for which it is essential, *Pax2* is found only in the optic disc and nerve (Nornes *et al.*, 1990; Macdonald and Wilson, 1996). *Pax2* and *Pax6* can each repress transcription of the other (Schwarz *et al.*, 2000). This is likely to contribute to the sharp expression boundaries of these genes that emerge at the optic stalk/optic cup boundary. *Vax2*, an *Emx*-related homeobox gene expressed in a similar domain to *Pax2*, has recently been identified in human, mouse and *Xenopus* (Barbieri *et al.*, 1999; Ohsaki *et al.*, 1999). Over-expression of frog or human *Vax2/VAX2* in *Xenopus* leads to optic stalk expansion, aberrant in-folding of the ventral retina towards the brain and failure of the optic fissure to close (Barbieri *et al.*, 1999). *Vax2*-

null mice also do not close their optic fissures (Barbieri *et al.*, 2002). Related *Vax1*, expressed in cells derived from the ventral anterior midline, is similarly essential for optic fissure closure in the mouse (Bertuzzi *et al.*, 1999).

Mouse LIM homeobox gene *Lhx2* is expressed in the optic vesicles where it is essential for optic cup and lens placode formation from the closely associated optic vesicle and surface ectoderm. *Lhx2* appears to act independently of *Pax6* and may allow the presumptive neural retina to respond to signals from the overlying ectoderm (Porter *et al.*, 1997). *Bone morphogenetic protein 4* (*Bmp4*), encoding a secreted morphogen from the TGFβ family, is initially expressed in the dorso-distal optic vesicle and over-lying surface ectoderm (Furuta and Hogan, 1998). *Bmp4* becomes downregulated in the lens placode and during formation of the optic cup expression is restricted to the dorsal neural retina. *Bmp4*-null mice usually suffer from severe defects in posterior mesodermal structures and do not develop far beyond gastrulation. On a mixed genetic background some embryos can progress to the 20- to 27-somite stage enabling analysis of early eye development. Studies of *Bmp4*-null and wild type mice using explant culture and BMP4-soaked beads reveal that BMP4 signalling in the dorsal optic vesicles of mice is essential, but not sufficient, for lens formation from the closely associated surface ectoderm (Furuta and Hogan, 1998). *Bmp7* is expressed in the optic vesicle and also appears to be necessary for lens induction (Wawersik *et al.*, 1999).

Unlike BMP4, BMP7 appears to lie upstream of *Pax6* in the lens placode where it may act in synergy with fibroblast growth factors (FGFs). *Pax6* expression in the lens placode is positively regulated by FGF and BMP7 signalling (Faber *et al.*, 2001) and by earlier *Pax6* expression in the pre-placodal surface ectoderm (Grindley *et al.*, 1995). FGFs are a family of secreted signalling molecules that can function synergistically with BMPs elsewhere during development (Lough *et al.*, 1996; Ericson *et al.*, 1998; Dudley *et al.*, 1999). It is not clear which FGF molecules are involved in lens induction and from where they are derived. Multiple *Fgf* genes are expressed in the developing lens and retina (see below). FGFs are also known to have a later role in lens development. FGF signalling is both necessary and sufficient for the differentiation of lens-fibre cells (McAvoy *et al.*, 1991).

Signals from the surface ectoderm to the optic vesicle are essential for development of the neural retina and may also involve FGFs. Basic-helix-loop-helix-zipper transcription factor gene *Mitf* is normally expressed in the optic vesicles, but becomes downregulated in the distal optic vesicles. It remains in the proximal optic vesicles where it specifies the RPE (Bora *et al.*, 1998). Homeobox gene *Chx10* is first expressed in the distal optic vesicles and is essential for proliferation of the neural retina, but not for optic cup invagination (Liu *et al.*, 1994; Burmeister *et al.*, 1996). Following removal of the surface ectoderm in mouse head explants, *Mitf* was not downregulated in the distal neuroepithelium, which formed a pigmented monolayer, and expression of *Chx10* was not initiated (Nguyen and Arnheiter, 2000). Development of the neural retina was rescued by the application of FGF1, FGF2 or epidermal growth factor (EGF) soaked beads in these experiments (Nguyen and Arnheiter, 2000). Removal of the surface ectoderm in the chick (which does not show initial pan-optic *Mitf* expression like the mouse) led to an unspecified but pigmented optic vesicle. Neural retina/RPE specification was restored by ectopic FGF1 (Hyer *et al.*, 1998). In the developing eye, FGF1 and FGF2 proteins localise strongly to the surface ectoderm and can also be detected in the optic vesicle (Nguyen and Arnheiter, 2000). Taken together, these data suggest that FGFs from the surface ectoderm are essential for neural retina induction. An additional possibility is that FGF or non-FGF signals from the surface ectoderm activate autocrine FGF signalling in the distal optic vesicle to initiate neural retina development. Expression of *Fgf1*, *Fgf8*, *Fgf9* and *Fgf15* have all been reported in the neural retina (de Iongh and McAvoy, 1993; McWhirter *et al.*, 1997; Vogel-Hopker *et al.*, 2000; Zhao *et al.*, 2001). In *Fgf9*-null mouse mutants, the ventral RPE boundary shifts into presumptive neural retina (Zhao *et al.*, 2001). *Fgf1*, *Fgf2* and *Fgf1/Fgf2* knockout mice show no overt eye phenotype, suggesting a certain level of redundancy in this system (Dono *et al.*, 1998; Ortega *et al.*, 1998; Miller *et al.*, 2000).

Development of the RPE appears to be dependent on signals from the extra-ocular mesenchyme. Removal of peri-ocular mesenchyme leads to a failure of *Mitf* induction and of RPE development in the chick optic vesicle. TGFβ family member Activin can substitute for the peri-ocular mesenchyme by promoting *Mitf* expression and downregulating neural retina markers such as *Chx10* and *Pax6* (Fuhrmann *et al.*, 2000). *Fgf9* misexpression in mouse presumptive RPE induces formation of a

secondary neural retina, over-riding any RPE-promoting peri-ocular signals. In these experiments optic cup formation still occurred, but a mirror-image secondary neural retina was formed in place of RPE (Zhao *et al.*, 2001). Similarly, when FGF1 or FGF2 (but not EGF) soaked beads were placed behind mouse optic vesicles in explant cultures, pigmentation of the developing RPE was disrupted (Nguyen and Arnheiter, 2000). In the chick, *Fgf1* misexpression in prospective RPE (or an ectopic FGF1 source) similarly induced ectopic neural retina (Hyer *et al.*, 1998).

In summary, the optic vesicle is patterned across the proximo-distal axis through the expression of transcription factor genes such as *Pax6*, *Pax2* and *Vax2*. *Pax6* allows the dorso-distal optic vesicle and the overlying surface ectoderm to become closely associated with each other. A series of inductive events then occur, to form the optic cup and lens. BMP signalling and perhaps also FGF signalling from the optic vesicle allows lens development to be initiated in the surface ectoderm. FGF signalling and/or other signals from the surface ectoderm similarly seem essential for induction of a single neural retina, whilst Activin and/or other signals from the peri-ocular mesenchyme specify the RPE. These signalling events, perhaps through the actions of various transcription factors such as Lhx2, allow the development of the optic cup and lens from the optic vesicles and surface ectoderm.

Retinal stratification and the formation of RGCs

Once the presumptive neural retina has formed, it proliferates and the retinal progenitor cells begin to differentiate into neurons. Initially an inner layer of differentiating cells emerges from a multipotent pool of retinal precursors. From these two layers ultimately emerge the three cellular layers of the mature retina: the outer nuclear layer, the inner nuclear layer and the ganglion cell layer, each populated by different types of neurons (**Fig 1.3**).

The six major neuronal types, their many subtypes and Müller glial cells are specified in an orderly and overlapping temporal sequence from the multipotent retinal precursors (Altshuler *et al.*, 1991). In contrast with other neuronal systems the determination of cell type occurs concomitantly with the final mitosis and is not dependent on cell lineage (Holt *et al.*, 1988; Wetts and Fraser, 1988; Turner *et al.*, 1990). Local environmental cues and continuing intercellular communication are

Figure 1.3

Once the optic cup has formed during development, the neural retina starts to differentiate and becomes stratified. Figures **A-D** show different stages of retinal lamination during human development:

A Light micrograph of a section through the 7 week post-conception human embryonic retina (20 mm crown-rump length) taken from Spira and Hollenberg, 1973. At this stage the optic cup has formed and the neural retina has separated into inner and outer cellular layers, separated in humans by the transient layer of Chevitz. Outer retina is at the top of the figure. This is also the case for **B**, **C** and **D**. **C**, transient layer of Chevitz; **il**, inner layer; **ol**, outer layer; **pe**, pigmented epithelium.

B Light micrograph of a section through the 12 week post-conception human embryonic retina (83 mm crown-rump length) taken from Spira and Hollenberg, 1973. At this stage the inner nuclear layer is emerging at the inner aspect of the proliferating zone in the outer layer of the retina. In the outermost neural retina putative cone photoreceptors are seen (arrow). Ganglion cells of the innermost ganglion cell layer are projecting axons through the nerve fibre layer towards the optic disc and nerve. **gcl**, ganglion cell layer; **inl**, inner nuclear layer; **ipl**, inner plexiform layer; **nfl**, nerve fibre layer; **pz**, proliferating zone.

C Light micrograph of a section through the 21 week post-conception human embryonic retina (200 mm crown-rump length) taken from Rhodes, 1979. The three cellular layers of the mature retina are readily distinguished at this stage. **gcl**, ganglion cell layer; **inl**, inner nuclear layer; **ipl**, inner plexiform layer; **nfl**, nerve fibre layer; **onl**, outer nuclear layer; **opl**, outer plexiform layer.

D Cartoon of a section through an adult retina taken from Nicholls *et al.*, 2001. The three cellular layers of the mature retina are depicted with the major cell types they are composed of: photoreceptors in the ONL, interneurons in the INL and projection neurons (RGCs) in the GCL.

Eye development (II): stratification of the neural retina

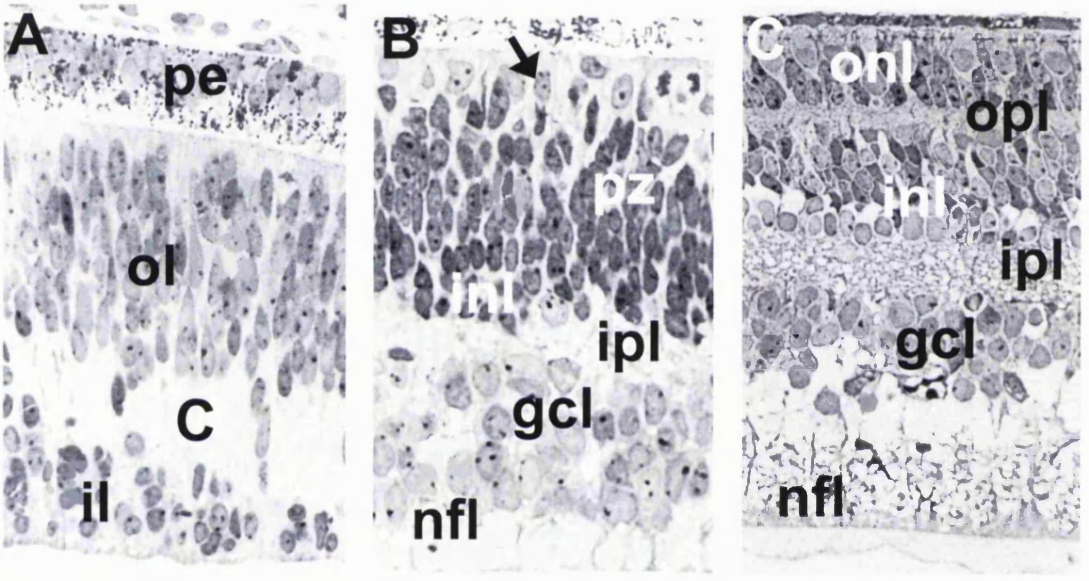

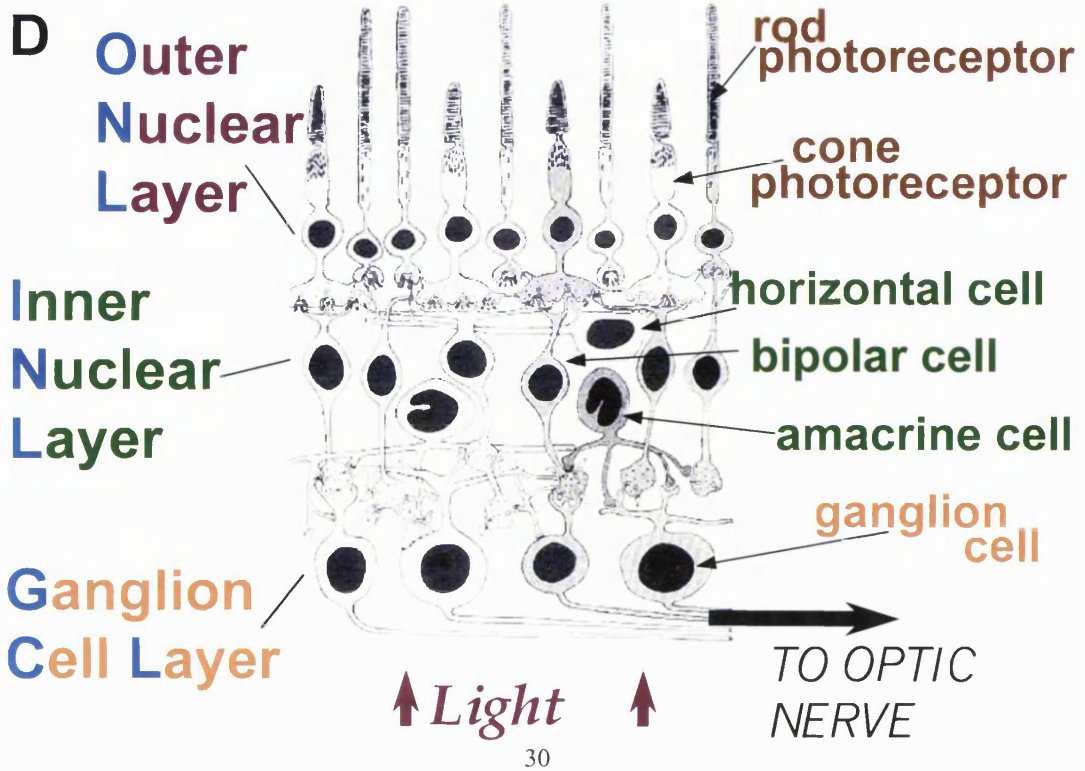

believed to gradually restrict the developmental potential of individual mitotic precursor cells and specify development of distinct cell types through the differential expression of transcription factors (Cepko *et al.*, 1996). Exactly which factors are involved in cellular determination and laminar patterning in the developing retina and how such factors operate is at present very poorly understood.

Though multiple cell types are generated throughout retinal development (Sidman, 1961; Young, 1985), the first post-mitotic retinal cells are specified as RGCs in the embryonic retina. This specification is known to involve Notch (a cell surface receptor for inhibitory signalling), SHH and FGF signalling pathways (Guillemot and Cepko, 1992; Austin *et al.*, 1995; McCabe *et al.*, 1999; Zhang and Yang, 2001). Development of RGCs, indeed of the retina as a whole, progresses in a dorsal to ventral and a central to peripheral gradient (Silver and Sapiro, 1981).

With processes attached to the inner and outer retinal surfaces, cell bodies of the earliest post-mitotic RGCs migrate inwards towards the vitreal surface (Maslim *et al.*, 1986; Watanabe *et al.*, 1991). Scleral attachments retract and vitreal endfeet transform into a growth cone that extends towards the optic nerve head while somata continue to migrate inwards to form the inner neuroblastic layer (Prada *et al.*, 1981). Thus the early neural retina is composed of two layers, an inner layer dominated by differentiating RGCs and an outer dividing region dominated by undifferentiated neuroblasts.

Extensive histological analysis by Mann led her to conclude that some cells of this inner layer migrate inwards to form the ganglion cell layer while others migrate outwards to form the amacrine and Müller cell components of the future inner nuclear cell layer (Mann, 1964). Indeed analysis of amacrine cells of the outer neuroblastic layer in the embryonic day 15 (E15) mouse retina led Hinds and Hinds to propose that they were derived only from RGCs of the inner layer that have transformed and lost their axon (Hinds and Hinds, 1978). By E17, amacrine cells appeared to develop from both inner and outer retina (Hinds and Hinds, 1983). Transcription factor expression domains that show initial restriction to the inner neuroblastic retina and subsequent localisation to the ganglion cell and inner nuclear layers have recently been described

(Thor *et al.*, 1991; Davis and Reed, 1996; Zhou *et al.*, 1996). These data support the notion that the inner neuroblastic retina contains future occupants of both layers.

With the development of amacrine interneurons the inner nuclear layer emerges. The inner nuclear layer forms at the inner border of the outer neuroblastic layer. It is separated from the developing ganglion cell (inner) layer by the inner plexiform layer. The inner plexiform layer is acellular and contains only cell processes. In humans it is derived from the transient layer of Chevitz that separates the inner and outer neuroblastic layers of the early retina. The inner nuclear layer is histologically distinguished from the outer neuroblastic layer by the small round differentiated nuclei of the former and the mitotic spindle-shaped nuclei of the latter (**Fig 1.3A**).

From the proliferating zone in the outer neuroblastic layer emerge photoreceptors to line the outer limits of the neural retina and interneurons to occupy the expanding inner nuclear layer (**Fig 1.3B**). Eventually an acellular outer plexiform layer divides the proliferating zone from the outer nuclear (photoreceptor) layer (**Fig 1.3C**). In the mature retina, when proliferation and differentiation are complete, the neural retina consists of three cellular layers (**Fig 1.3D**). The outer plexiform nuclear separates the outer nuclear layer (which contains rod and cone photoreceptors) from the inner nuclear layer (which contains Müller glia and amacrine, bipolar and horizontal interneurons). The inner plexiform layer separates the inner nuclear layer from the ganglion cell layer (which contains RGCs and some displaced amacrine cells). The innermost layer is the nerve fibre layer that contains RGC axons travelling to the centrally located optic disc. At the optic disc RGC fibres form the optic nerve head where they leave the retina and head for the brain through the optic nerve (derived from the optic stalk).

A number of transcription factors are implicated in the development of RGCs, most notably members of the POU-domain family of transcription factors. POU-domain factors Pou4f1, Pou4f2, Pou4f3 (previously called BRN3 factors) and RPF-1 are expressed in RGCs throughout development and in the mature retina (Xiang *et al.*, 1995; Gan *et al.*, 1996; Zhou *et al.*, 1996; Xiang, 1998; Gan *et al.*, 1999). In *Pou4f2*-null mice, although ~70% of RGCs are lost during development, numbers of inner retinal neurons containing tyrosine hydroxylase and glutamic acid decarboxylase

(enzymes synthesising dopamine, DA, and γ-aminobutyric acid, GABA, respectively) remain unchanged (Gan *et al.*, 1996). This shows that DA and GABA releasing amacrine cells do not require *Pou4f2* for survival and suggests that a specific requirement for *Pou4f2* may be limited to RGCs. Analysis of mutant cells within the mouse retina reveals that *Pou4f2* is not required for initial cell fate specification or migration of RGCs, but is essential for their proper differentiation, axon guidance and continued survival. RGC axons were extended at appropriate times in *Pou4f2*-null embryos, but were disorganised with dentritic features and exhibited pathfinding difficulties throughout their course to retino-recipient brain areas (Gan *et al.*, 1999; Erkman *et al.*, 2000).

Pou4f2, but not *Pou4f1* or *Pou4f3*, has recently been implicated in the regulation of *Pax6* in the embryonic neuroretina (Plaza *et al.*, 1999). *Pax6* expression, described above in the context of its prime roles in early eye development, is specifically maintained in the ganglion and amacrine cell layers of the mature retina (Davis and Reed, 1996; Macdonald and Wilson, 1996). Other transcription factors, such as homoeodomain LIM protein Islet-1 and helix-loop-helix protein O/E-1 (Olf-1) can be detected in mature RGCs (Thor *et al.*, 1991; Davis and Reed, 1996). Their precise functions are not yet known, but presumably they maintain cell type-specific features within individual cells.

Pou4f genes have recently been demonstrated to lie downstream of *Ath5* (Hutcheson and Vetter, 2001; Wang *et al.*, 2001). Targeted deletions of *Ath5* block the initial differentiation of 80% of RGCs and those that are generated do not survive (Brown *et al.*, 2001; Wang *et al.*, 2001). *Ath5* encodes a basic helix-loop-helix (bHLH) transcription factor that (along with other *Ath* genes such as *NeuroD*) is homologous to *Drosophila* proneural gene *atonal*. These bHLH factors are described as 'proneural' because they promote neuronal differentiation. Expression of other *Ath* genes in the retina coincides with the birth of other retinal neuron types and is required by them for survival (Vetter and Brown, 2001).

To summarise, proliferating retinal progenitors become post-mitotic and differentiate after formation of the optic cup. Inductive environmental events and the intrinsic actions of transcription factors gradually restrict cell fate. As cells differentiate they

migrate to distinct cellular layers. The retina first becomes segregated into two layers and then into three cellular layers separated by plexiform layers. RGCs are the first differentiated cell types to be born in the developing neural retina. Notch, SHH and FGF signalling all regulate the genesis of RGCs. *Ath5* and *Brn3b* encode transcription factors that are particularly important for their differentiation and survival.

1.2. Retinal projections and patterning

RGCs are the only projection neurons of the vertebrate retina. The development of their projections into central brain areas is well characterised, particularly those terminating in the optic tectum (the superior colliculus in mammals). Here a very precise retinotopic map becomes established, *i.e.* neighbouring RGCs make connections to neighbouring regions in the target areas. This map is inverted along the dorso-ventral and antero-posterior embryonic axes. Thus ventral retinal axons project to dorsal tectum/colliculus while dorsal axons project to ventral areas. Likewise nasal (anterior) axons project to posterior tectum/colliculus and temporal (posterior) axons project to anterior areas. This inverted retinal topography is observed in other target regions, but there are added levels of complexity involved. In the lateral geniculate nucleus of primates for example, axon terminals are separated into 12 different sub-layers according to the RGC type (Rodieck, 1998).

In the study of the development of retinal projections into the vertebrate brain, most interest has focused on the formation of retinotopic maps. The tectum/superior colliculus offers a relatively uncomplicated example of topographical map formation and accessible study of axon guidance in the developing brain. It is for these reasons that developmental biologists have often focused their research on the tectum/superior colliculus over other retino-recipient areas of the brain. For the rough anatomy of the retinofugal projections and an illustration of topographic mapping to the superior colliculus, see **Fig 1.4**.

Roger Sperry demonstrated the existence of a topographical representation of the retina in the tectum in the early 1940's. He rotated newts eyes 180° after severance of the optic nerve and studied their visuomotor behaviour following nerve regeneration (Sperry, 1943). Based on findings in newts and in similar experiments on frogs where

Figure 1.4

A drawing of the adult primate visual system viewed in a transverse slice through the head at the level of the eyes is shown. This drawing is taken from Polyak, 1941. Information from the left and right visual fields is carried along axons (marked *white* and *black* respectively) from retinal ganglion cells (RGCs) in the eye (**e**) through the optic nerve (**on**). Axons derived from nasal retina cross at the optic chiasm (**oc**) to travel along the contralateral optic tract (**ot**), whilst those derived from temporal retina project to the ipsilateral side. The net result is that fibres from both eyes that carry information about the left visual field (white/dotted fibres) project to the right side of the brain, and those carrying information about the right visual field (black fibres) project to the left side of the brain. (This is a conserved feature in vertebrates as the degree of binocular vision correlates with the significance of the ipsilateral pathway; vertebrates with monocular vision project all RGC axons to the contralateral brain.) The primary target of the retina is the lateral geniculate nuclei (**lgn**) of the thalamus. Relay neurons in the **lgn** project to the primary visual cortex (essential for vision) through the optic radiations (**or**). As well as projecting to the **lgn**, there are a number of secondary targets of the retina. Of these the best studied is the superior colliculus (**sc**), which simultaneously interprets information from visual, aural and somatosensory modalities to direct saccadic eye movements.

The retinofugal connections form topographical maps of the retina in the **lgn** and the **sc** that are inverted across their embryonic axes (antero-posterior and dorso-ventral). This is shown in a schematic representation of a retina projecting axons to the **sc**. The axes across the surface of the retina and the **sc** are marked: **A**, anterior; **P**, posterior; **D**, dorsal; **V**, ventral. Anterior (nasal) axons project to posterior **sc** and posterior (temporal) axons project to anterior **sc**. At the same time, dorsal axons project to ventral **sc** and ventral axons project to dorsal **sc**. In this diagram a projection from the dorso-nasal retina (in blue) projects to the ventro-posterior **sc** and a projection from the ventro-temporal retina (in red) projects to the dorso-anterior **sc**.

Anatomy and topography of the retinofugal projections

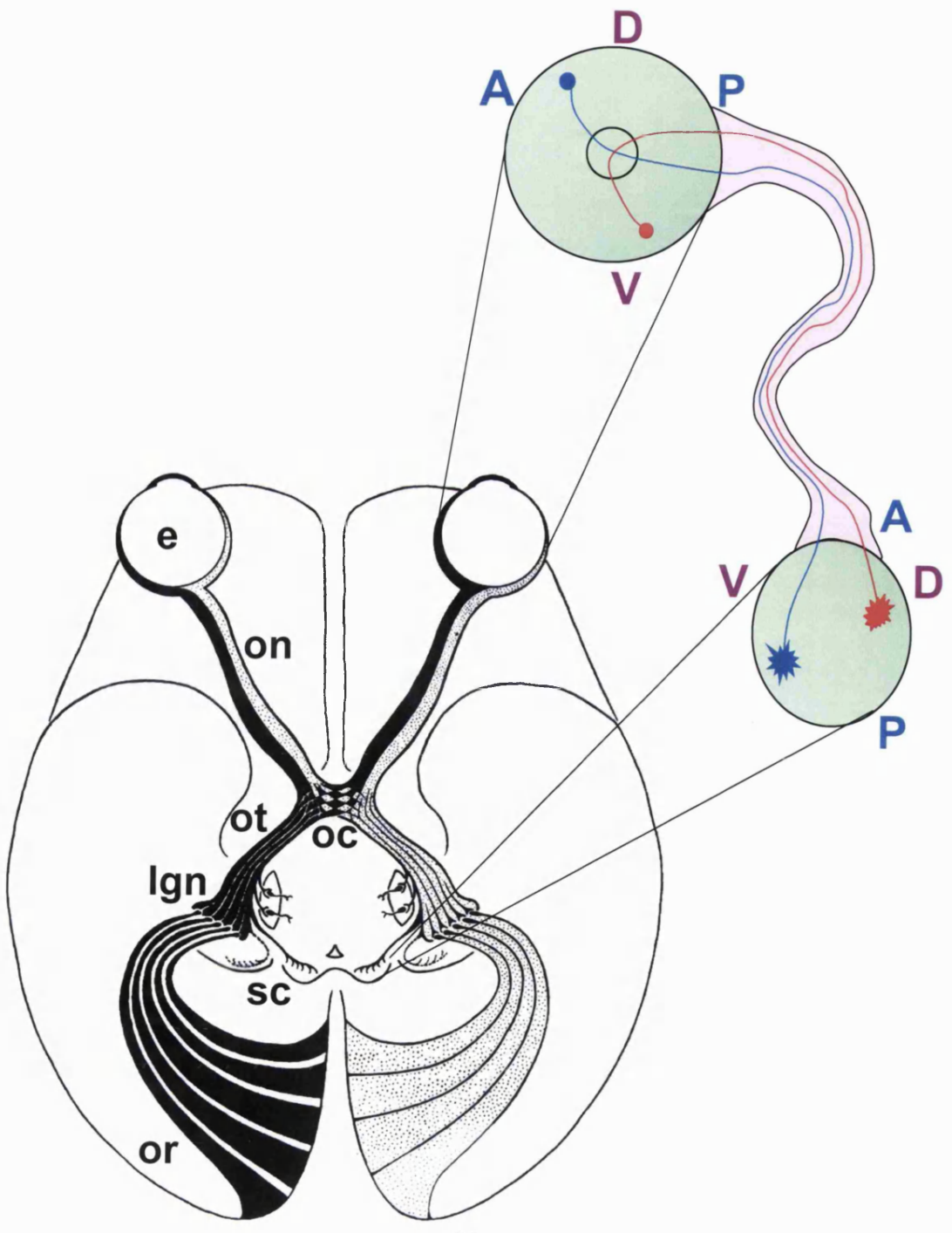

the animals behaved as though their visual world were upside-down and back-to-front, Sperry formulated the chemoaffinity hypothesis (Sperry, 1963). He suggested that topographic connections were formed by complementary gradients of matching cytochemical tags. These 'tags' were proposed to reside on invading RGC axons and their tectal targets across at least two perpendicular axes. This work spawned considerable interest in patterning of the retina (and of central target regions). The search for molecular asymmetry across the developing retina has recently uncovered numerous factors and revealed molecular distinctions across the dorso-ventral and naso-temporal (antero-posterior) axes. Within the past decade, Eph receptor tyrosine kinases and their ephrin binding partners have been identified as molecules that effect retinal polarity and aid in the establishment of retinal topography, as envisaged by Sperry (Harris and Holt, 1995). In the next section, the development of RGC projections to central brain areas are described and the roles of Eph and ephrin molecules in this process are discussed.

The formation of RGC connections to the central brain

The ventral wall of the vertebrate optic cup is formed when its nasal and temporal aspects meet and fuse. The development of the ventral retina then lags behind that of the dorsal retina (Silver and Sapiro, 1981). The opposite is true of the chick tectum (ventral areas develop first; Rager and von Oeynhausen, 1979). Differentiation is also more advanced in central regions of the vertebrate retina compared to the periphery (Silver and Sapiro, 1981). Fish are an exception to the above; development is most advanced in the ventro-nasal retina of zebrafish (Schmitt and Dowling, 1996; Schmitt and Dowling, 1999). Thus in mammals, birds and frogs the first RGCs emerge from the dorsal aspect of the newly formed retina, sending axons along the optic stalk through the ventrally located optic fissure (Silver and Sapiro, 1981).

Chick RGC axons are topographically arranged across the dorso-ventral axis of the optic nerve, while axon bundles from nasal and temporal retina are mixed (Ehrlich and Mark, 1984). In mammalian systems, naso-temporal as well as dorso-ventral topography is apparent in the optic nerve (Reese and Baker, 1993; Chan and Guillery, 1994; Chan and Chung, 1999). This early retinotopy becomes increasingly impoverished as fibres scatter throughout the nerve. Only loose spatial relationships are maintained as axons grow into the optic chiasm (Simon and O'Leary, 1991; Reese

and Baker, 1993; Chan and Guillery, 1994; Chan and Chung, 1999). Dorsal and ventral RGC axons are re-segregated in the optic chiasm, entering the caudal and rostral aspects of the optic tract respectively (Reese and Baker, 1993; Chan and Guillery, 1994; Chan and Chung, 1999). The changing expression of chondroitin-sulphate proteoglycans in the mouse optic chiasm could aid in the sorting of dorsal from ventral axons because of temporal differences in times they reach the chiasm (Chung *et al.*, 2000).

RGC axons enter the lateral geniculate nucleus and the superior colliculus at their anterior (rostral) aspects. As they enter, dorsal and ventral axons are biased to the correct location with respect to the dorso-ventral (medio-lateral) axis of the target structure (Godement *et al.*, 1984; Wagner *et al.*, 2000). This targeting is very rough and by no means absolute (Godement *et al.*, 1984; Simon and O'Leary, 1991; Simon and O'Leary, 1992). In fish, dorso-ventral order along the optic tract is not essential for retinotopy. Three zebrafish mutants with a disruption of axon sorting in the optic tract show conserved tectal mapping (Trowe *et al.*, 1996). Along the antero-posterior (rostro-caudal) axis of the superior colliculus, axons enter anteriorly and grow posteriorly. In rats, the axons preferentially branch around the correct retinotopic termination areas (Simon and O'Leary, 1991; Simon and O'Leary, 1992; Simon and O'Leary, 1992). In the chick, axons tend to stop growing in roughly the correct antero-posterior location of the tectum, thus a coarse topography can be observed. In frogs and fish initial axon targeting is far more precise (Roskies *et al.*, 1995).

In the final phase of the development of RGC axon projections, substantial remodelling occurs. This results in a focused termination zone for axons derived from a particular retinal location, with a loss of inappropriate arborisations and some axonal re-routing (Nakamura and O'Leary, 1989; Simon and O'Leary, 1992). Nitric oxide, which has repellent activity, has been implicated in this remodelling process. Reduced synthesis leads to delayed remodelling in mice (Wu *et al.*, 2000). After remodelling in the P12 rat, although the most widely mispositioned axons have disappeared, axon distributions from a single point in the retina remain widespread across the dorso-ventral extent of the superior colliculus relative to the now very tight termination zone (Simon and O'Leary, 1992). In the chick, axons from identical retinal areas will

sometimes travel through opposing tectal areas to reach a common termination zone (Ehrlich and Mark, 1984).

In summary, the establishment of the very precise retinotopic connections from the vertebrate retina to target central brain areas can be simplistically viewed as occurring in two phases. The first is characterised by the invasion of large numbers of RGC axons into the target regions with a positional bias for roughly the correct topographical locations. The second phase is dominated by the dying back of numerous inappropriate connections to leave precise termination zones from precise retinal locations.

Eph and ephrin molecules

Prior to the identification of the Eph and ephrin families and their importance in the developing visual system, many studies had searched for cytochemical asymmetry within the retina with limited success. Antibody studies yielded a number of cell surface molecules with asymmetric retinal distributions, some with complementary gradients in the tectum (Constantine-Paton *et al.*, 1986; Moskal *et al.*, 1986; Trisler and Collins, 1987; Trisler, 1990; McLoon, 1991). Despite some evidence for their involvement in growth cone motility and synaptogenesis, roles in axon topography and patterning were not established (Trisler and Collins, 1987; Mendez-Otero and Friedman, 1996; Araujo *et al.*, 1997). Interest in them waned as exciting work on Eph/ephrin interactions in the developing visual system emerged.

Eph receptor tyrosine kinases are a subfamily of transmembrane proteins now known (with their ephrin binding partners) to be involved in the establishment of topographical connections by RGCs. They are also involved in axon guidance in other contexts, axon fasciculation and the formation of anatomical boundaries (Holder and Klein, 1999). Eph and ephrin molecules are classed 'A' or 'B' depending on sequence homologies and binding affinities. Thus Eph A (EPHA) receptors bind ephrin A (EFNA) ligands, and EphB (EPHB) receptors bind ephrin B (EFNB) ligands. EPHA4 is an exception to this as it will bind ephrins from both classes (Gale *et al.*, 1996; Eph Nomenclature Committee, 1997; see also Mouse Genome Informatics). Ephrins, like their Eph partners, are membrane-bound and are capable of transducing signals to

mediate a cellular response (Holland *et al.*, 1996; Xu *et al.*, 1999; Davy and Robbins, 2000).

'A' class Eph and ephrin molecules are distributed in complementary gradients along the embryonic antero-posterior axes of the retina and target brain areas at early stages of development. Chick *Epha3* is highly expressed in the temporal (posterior) retina and anterior tectum, while *Efna5* is expressed in the nasal (anterior) retina and posterior tectum (Cheng *et al.*, 1995; Drescher *et al.*, 1995; Connor *et al.*, 1998). Their interactions are known to repel temporally derived RGC axons from posterior target areas and promote retinotopy (Cheng *et al.*, 1995; Drescher *et al.*, 1995; Winslow *et al.*, 1995; Hornberger *et al.*, 1999). *In vitro* and *in vivo* assays have demonstrated an inhibitory effect of posterior target tissue on temporal retinal axon growth and arborisation **(Walter *et al.*, 1987a;** Simon and O'Leary, 1992; Roskies and O'Leary, 1994).

'B' class Eph and ephrin molecules are asymmetrically distributed across the dorso-ventral axis of the retina and its targets. From early optic cup stages, *Efnb* and *Ephb* genes are more prominently expressed in dorsal and ventral retina respectively (Braisted *et al.*, 1997; Sefton *et al.*, 1997; Connor *et al.*, 1998; Birgbauer *et al.*, 2000). They are expressed uniformly across the chick tectum, though EFNB1 seems to be more prominently localised to the dorsal neuroepithelium (Braisted *et al.*, 1997; Connor *et al.*, 1998). EPH/EFNB interactions, like those of the 'A' class, can lead to axon repulsion in the developing visual system. *Ephb2* and *Ephb3* double null mice exhibited Eph kinase-independent defects in RGC axon guidance to the optic disc, particularly affecting dorsal axons (Birgbauer *et al.*, 2000). Follow-up work suggested that during development, EPHB promotes dorsal axon guidance by repelling EFNB-containing axons into the optic nerve (Birgbauer *et al.*, 2000; Birgbauer *et al.*, 2001). At the optic chiasm, midline EFNB repels EPH-containing axons derived from ventro-temporal retina in order to form the ipsilateral retinal projection (Nakagawa *et al.*, 2000). Repulsive EPH/EFNB interactions have been shown to guide axons during the development of other systems and they could contribute to the sorting of dorsal and ventral axons in the optic tract (Henkemeyer *et al.*, 1996; Orioli and Klein, 1997; Wang and Anderson, 1997). In retinal target areas however, neither EPH/EFNB

interactions nor any repulsive guidance mechanisms have been shown to contribute to dorso-ventral retinal topography (Walter *et al.*, 1987b).

EPH/EFNB interactions may yet be important for dorso-ventral topography in retinal targets, just as across the antero-posterior axis, EPH/EFNA interactions may guide axons to topographically correct locations via additional mechanisms to chemorepulsion. Co-localisation of ephrin ligands with Eph receptors can modulate their function, presumably by binding Eph molecules and reducing their availability. For example, EPHA-mediated repulsion of RGC axons is abolished by overexpressing *Efna* genes, while ephrin removal sensitised them (Hornberger *et al.*, 1999). The co-localisation of Eph receptors with ephrin ligands in the tectum/superior colliculus could modulate interactions with incoming axons and provide an alternate response to chemorepulsion. For example the correct Eph/ephrin 'match' with target tissue may provide survival signals to topographically appropriate connections. Recently the interaction of guidance mechanisms across both retinal axes was demonstrated by the analysis of double homozygous mice for *Efna2* and *Efna5* disruptions. Although antero-posterior order was almost lost, impairments were also seen along the dorso-ventral axis (Feldheim *et al.*, 2000). This could be due to subtle asymmetries in *Epha* expression along the dorso-ventral axis, as reported for *Epha7* (Sefton *et al.*, 1997; Sefton and Nieto, 1997). Alternatively, EPHA4 could link dorso-ventral guidance to that across the antero-posterior axis by virtue of its ability to bind both A and B class ephrins. EPHA4 tyrosine phosphorylation is asymmetric across both axes in the retina consistent with the imposition of two ligand gradients and could thus guide axons along both axes in target structures (Connor *et al.*, 1998). If this were so, the loss of one set of ligands would alter the EPHA4 phosphorylation status and disrupt guidance across both axes.

To summarise, Eph and ephrin molecules are heavily implicated in the formation of topographical connections from the retina to the brain, though the precise nature of their involvement and the degree of their importance are not fully known. Asymmetric EPH and EFN distributions are present in the retina well before the invasion of RGC axons into the central target regions. As well as roles in axon guidance Eph/ephrin interactions are likely to compartmentalise the retina and control intra-retinal organisation.

1.3. Dorso-ventral patterning of the developing eye

Early events across the dorso-ventral axis of the developing eye have been described in **1.1.** with discussion of bisection of the eye field and formation of the optic cup. Since this thesis investigates the mechanisms of dorso-ventral retinal patterning, the current section explores some of the molecular events thought to confer positional identity to cells of the developing neural retina along its dorso-ventral axis.

Positional identity across the dorso-ventral axis of the neural retina is essential for the exit of RGC axons from the retina and their guidance to appropriate targets in the brain (Schulte *et al.*, 1999; Birgbauer *et al.*, 2000; Koshiba-Takeuchi *et al.*, 2000). It is necessary for co-ordinated growth and development of the eye and for regional variations in the density and organisation of different retinal cell types. Such regional differences include a thicker nerve fibre layer with less axons in ventral compared to dorsal chick retina (Imagawa *et al.*, 1999). Analysis of the pigeon retina shows an irregular distribution of cells of the ganglion cell layer, with an area of increased density in the dorsal retina (Snow and Robson, 1994). Blue cones in mammalian species are restricted to ventral retina while green cones are primarily localised to dorsal retina (Rohlich *et al.*, 1994). *Xenopus* RGCs are generated asymmetrically along the dorsoventral axis up to metamorphosis and beyond (Straznicky and Tay, 1977) and bullfrogs synthesise rhodopsin in ventral retina, but porphyropsin in dorsal regions (Reuter *et al.*, 1971). Other processes such as pigmentation or the apoptosis of quail RGCs occur in a dorsal to ventral direction (Marin-Teva *et al.*, 1999). This may be due to the developmental lag of ventral retina behind dorsal retina (Silver and Sapiro, 1981).

In attempting to understand patterning of the neural retina it is useful to define axes and divide it into different territories (**Fig. 1.5**). These will be used throughout this thesis. These axes and territories are useful to describe asymmetries in gene expression and morphology across the longitudinal plane of the neural retina. The **naso-temporal axis** describes the developing eye with reference to adjacent nasal and temporal regions of the embryonic head. This axis through the retina runs along the longitudinal extent (the antero-posterior axis) of the embryo. In describing the embryonic eye, naso-temporal is preferable to antero-posterior because in the adult,

Figure 1.5

Retinal polarity can be described using different axes. These can be used to define different territories of the developing retina. Point locations on the retinal surface can be described with reference to the naso-temporal and dorso-ventral axes. The **naso-temporal axis** describes the developing eye with reference to adjacent nasal and temporal regions of the embryonic head and the **dorso-ventral axis** describes the retina with reference to more dorsal and ventral regions of the diencephalon (**A**):

A Cartoon of the lateral (right) aspect of the head of a 30-40 somite stage mouse embryo. The newly formed optic cup is labelled and the naso-temporal and dorso-ventral axes are indicated. The boxed region around the optic cup is enlarged in a schematic diagram to illustrate the neural retina, lens and ventral fissure. **d**, dorsal; **n**, nasal; **t**, temporal; **v**, ventral.

The schematic diagram in **A** is employed to illustrate territories described with reference to the naso-temporal and dorso-ventral axes of the developing retina (**B-D**):

B The neural retina can be divided in half into a dorsal and a ventral hemiretina with reference to the position of the ventral fissure.

C The neural retina can be divided into nasal, temporal, dorsal and ventral quadrants. **D**, dorsal; **N**, nasal; **T**, temporal; **V**, ventral.

D The neural retina can alternatively be divided into corner-quadrants: dorso-temporal, dorso-nasal, ventro-temporal and ventro-nasal. **D-N**, dorso-nasal, **D-T**, dorso-temporal; **V-N**, ventro-nasal; **V-T**, ventro-temporal.

Point locations on the retina can be described across its radial dimension as being *central* (*i.e.* close to the centre of the retina) or *peripheral* (*i.e.* away from the centre). Points can also be described as *inner* and *outer* retina with respect to the **laminar axis** of the retina. These dimensions are illustrated in **E**.

E This cartoon shows a plane of section through the newly formed optic cup across the dorso-ventral and proximo-distal axes of the developing eye. The laminar axis of the retina and central and peripheral regions of the retina are marked. **c**, central; **d**, dorsal; **D**, distal; **p**, peripheral; **P**, proximal; **v**, ventral.

Axes and territories of the developing neural retina

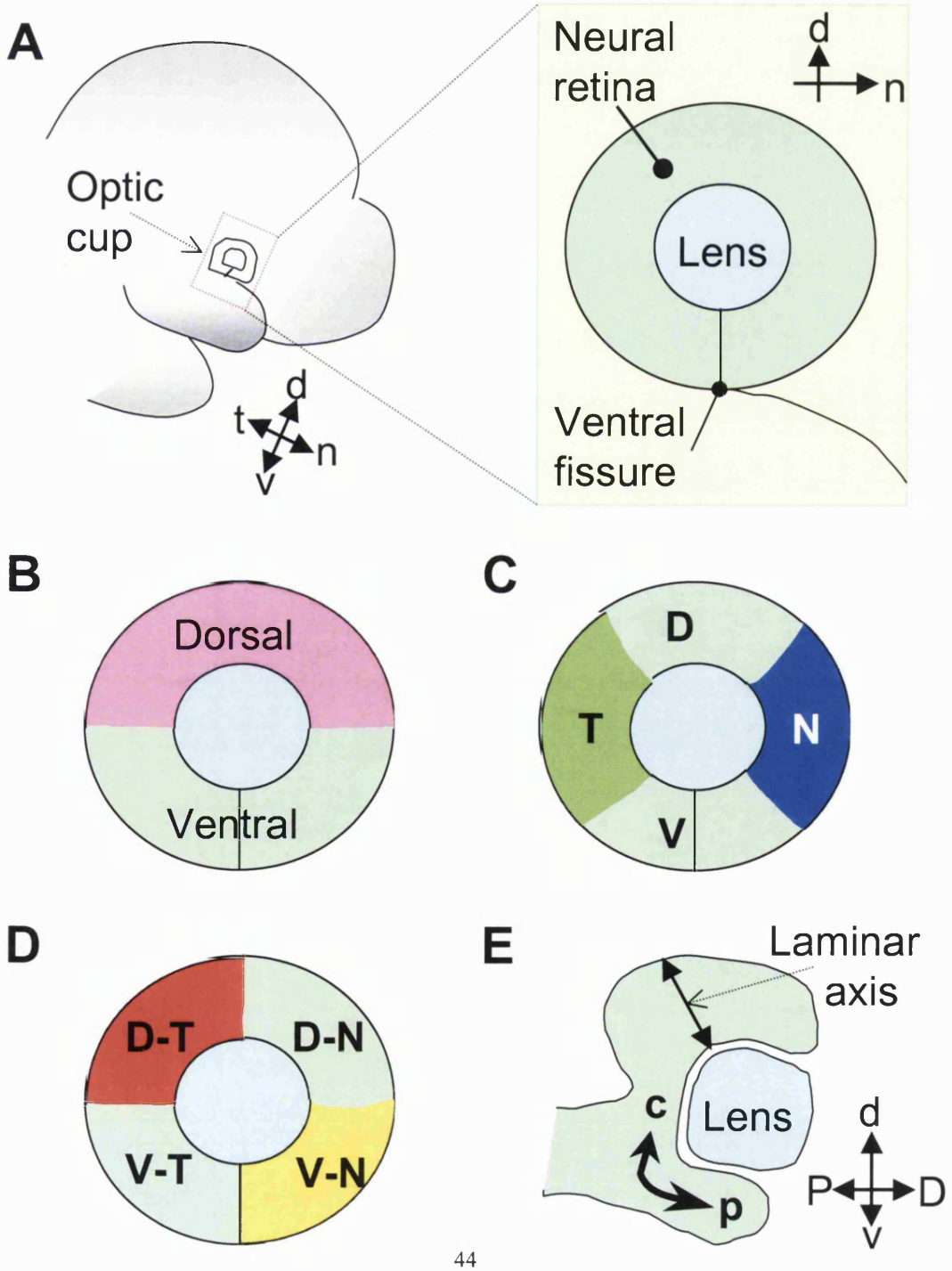

the terms anterior and posterior are used to describe distal and proximal areas of the mature eye respectively. The **dorso-ventral axis** describes the retina with reference to more dorsal and ventral regions of the diencephalon. In the adult eye, dorsal regions are described as superior, and ventral regions are described as inferior. Point locations on the retina can additionally be described with reference to the radial dimension as being *central* (close to the centre of the retina, the macular region of the mature eye) or *peripheral* (distal retina, away from the centre). To describe points across the thickness of the retina (the **laminar axis** of the retina), *inner* refers to points close to the inside of the optic cup (towards the vitreous) and outer refers to points close to the outside of the optic cup (towards the RPE).

This introduction to the molecular basis of dorso-ventral patterning of the developing eye begins with the presentation of sonic hedgehog (SHH) and bone morphogenetic protein 4 (BMP4) as signalling molecules with likely roles in dorso-ventral patterning of the neural retina. The influence of the retinoic acid (RA) system in dorso-ventral patterning is then described. Possible links of these different signalling systems to the regulation of dorsal and ventral transcription factors and cell surface molecules is discussed.

SHH and BMP4 signalling

The importance of SHH in patterning the proximo-ventral optic vesicle and optic cup has been described in **I.I.**. Recent work has implicated SHH in patterning of the ventral neural retina well after formation of the optic cup. Levels of SHH were altered in the chick eye before and after formation of the optic cup using viral misexpression and antibody producing cells to increase and reduce SHH activity respectively (Zhang and Yang, 2001). Both decreasing and increasing SHH signal levels at both timepoints reduced growth and disrupted development of the eye, affecting the ventral half more than the dorsal half of the eye. Changes in gene expression patterns occurred in a manner consistent with a role for SHH as a ventralising factor for the retina. Ventral markers *Vax* and *Pax2* appeared to be positively regulated and the dorsally expressed *Bmp4* gene was negatively regulated by SHH signalling (Zhang and Yang, 2001). Similar results have been reported in *Xenopus*, though *Bmp4* was not downregulated by SHH (Sasagawa *et al.*, 2002). Later in development, *Shh* is expressed in the inner neural retina and, as the retina becomes stratified, the ganglion cell layer (Jensen and

Wallace, 1997; Zhang and Yang, 2001). Work in chick suggests that this retinal source of SHH serves as a negative regulator of RGC production (see **1.1.**) behind the differentiation wave front (Zhang and Yang, 2001). Later in rodents it appears to act as a RGC axon-derived signal for the proliferation of astrocytes in the optic nerve (Wallace and Raff, 1999).

TGFβ family member BMP4 has been introduced previously in the context of lens development (see **1.1.**). In addition to the established role of BMP4 in lens induction, it has recently been implicated in dorso-ventral patterning of the neural retina. As well as being regulated by ventral signalling molecule SHH (Zhang and Yang, 2001), *Bmp4* appears to be involved in the regulation of dorsal identity and proliferation in the chick eye (Koshiba-Takeuchi *et al.*, 2000; Trousse *et al.*, 2001). Since the role of BMP4 in patterning of the mammalian retina is explored in this thesis, the biochemical mechanisms of BMP4 signalling are described here.

The mechanism by which BMP4 binds transmembrane cell receptors and transduces signals to target genes is similar for all TGFβ family members. The TGFβ family member ligand reaches the cell surface and brings together two types of serine/threonine protein kinase, designated type I and type II. BMPs seem to do this by co-operative binding, whilst other TGFβ family members tend to bind sequentially, associating with the type II receptor first. The complex that forms becomes phosphorylated and in turn phosphorylates SMAD proteins, which move to the nucleus and transduce the TGFβ family member signal. Immunophilin FKBP12 can bind the leucine-proline motif of type I receptors and may serve to inhibit basal or background signalling (signalling in the absence of ligand). Whether other signal transducers for the TGFβ family exist aside from the SMAD proteins is not known, though other signalling pathways can modulate the SMAD pathway. For example, the MAP kinase pathway (activated by agonists that include epidermal and hepatocyte growth factors) can inhibit the accumulation of SMADs in the nucleus (Massague, 1998).

SMADS, so named because of genetic homology to *sma* genes in *C. elegans* and *Mad* (the founding SMAD-encoding gene) in *Drosophila*, can be divided into three subtypes. These are: (1) SMADs that are direct substrates of TGFβ family

serine/threonine receptor kinase domains, (2) SMADs that assist signalling by association with type (1) SMADs and (3) SMADs that inhibit signalling by association with the other SMAD subtypes. Different SMADs act as substrates for different TGFβ family type I receptors. For example, SMAD1 (and probably close homologues SMAD5 and SMAD8) is a substrate for BMP type I receptors. When SMAD1 is over-expressed in *Xenopus*, it mimics the ability of BMP4 to ventralise the embryonic mesoderm. Activated (phosphorylated) SMADs associate with other SMADs such as SMAD4 and move into the nucleus. There they generate complexes with various nuclear cofactors (one example in *Xenopus* is FoxH3, previously known as FAST1, a forkhead transcription factor) and bind DNA to regulate target genes (Massague, 1998).

BMPs can bind the BMP type I receptors BMPR-IA and BMPR-IB (previously known as ALK3 and ALK6 - or BRK1 and BRK2 - respectively) and the BMP type II receptor (BMPR-II, previously known as BRK3) independently. When representatives from type I and type II are co-expressed, binding is greatly facilitated (Koenig *et al.*, 1994; ten Dijke *et al.*, 1994; Liu *et al.*, 1995; Nohno *et al.*, 1995; Rosenzweig *et al.*, 1995). This co-expression and the heteromeric receptor complexes that form appear to be essential for a transcriptional response and thus for signal transduction (Liu *et al.*, 1995). Other TGFβ receptor subtypes can get involved in receiving the BMP signal. For example, activin type II receptors, ACTR-II and ACTR-IIB (that bind activin and its type I receptor ACTR-I), can bind BMPs in co-operation with BMPR-IA or BMPR-IB (Yamashita *et al.*, 1995). This finding shows similarities with the receptor system of the *Drosophila* BMP2/4 orthologue, decapentaplegic (DPP), where ACTR-II/-IIB related Punt only binds DPP effectively in the presence of type I receptors TKV (Thick veins) or SAX (Saxophone) (Letsou *et al.*, 1995).

During eye development, *Bmpr-IB* is expressed throughout the optic stalk and in the neural retina from the 18-somite stage to at least E12.5, with much higher levels in the ventral retina. *Bmpr-IA* is far more widely expressed than *Bmpr-IB*; it is found throughout the optic vesicles and later the neural retina and the lens from the 18-somite stage to at least E12.5 (Dewulf *et al.*, 1995; Furuta and Hogan, 1998). Of the *Bmp* genes themselves, *Bmp7* and *Bmp4* are expressed in the mouse neural retina. *Bmp7* is more diffusely expressed in the retina than *Bmp4* (which is expressed

dorsally) in the mouse (Dudley and Robertson, 1997; Furuta and Hogan, 1998). *Bmp7* and *Bmp5* expression has been reported in the dorsal chick retina, though at weaker levels than for *Bmp4* (Belecky-Adams and Adler, 2001). *Bmp7* (and/or *Bmp5*) could co-operate with dorsally expressed *Bmp4* to regulate dorso-ventral patterning. Strong evidence suggests BMP4/7 (and also BMP2/7) heterodimers will form when the two are co-expressed. Moreover, these heterodimers will convey a far more potent activity than either molecule alone (Hazama *et al.*, 1995, Aono, 1995 #702; Suzuki *et al.*, 1997; Nishimatsu and Thomsen, 1998). *Bmp7* transcripts are also detected in the developing RPE, as are those of *Bmp2*. *Bmp3* is expressed in the mesenchyme around the optic stalk.

Other TGFβ family members, bar Activin family members in the chick, have not been detected in the eye of higher vertebrates (Belecky-Adams *et al.*, 1999). However, *Gdf6* (*Growth/differentiation factor 6*), of the GDF5 subfamily of the TGFβ family, is expressed in the dorsal retina of frogs and fish. In *Xenopus*, *Gdf6* expression is detected in the dorsal eye fields early in development and is later found in the dorsal eyes of tailbud embryos where it is co-incident with *Bmp4* expression (Hemmati-Brivanlou and Thomsen, 1995; Chang and Hemmati-Brivanlou, 1999). Zebrafish *radar*, orthologous to mammalian *Gdf6*, is similarly expressed in the dorsal aspect of the developing retina (Rissi *et al.*, 1995; Davidson *et al.*, 1999). Co-translation of GDF6 and BMP2 in the same cells leads to direct association and heterodimer formation (Chang and Hemmati-Brivanlou, 1999). The same is likely to be true with BMP4. Dominant negative GDF6 blocks the inductive actions of BMP4 when co-injected into *Xenopus* embryos (Chang and Hemmati-Brivanlou, 1999).

BMP signalling is affected by BMP antagonists, some of which are expressed in the developing retina. *Noggin* is expressed in the dorsal chick optic cup (Belecky-Adams and Adler, 2001; Trousse *et al.*, 2001). GDF6 can bind Noggin with an affinity approaching that of BMP2, which binds Noggin only marginally less effectively than BMP4; BMP7 binds Noggin with an affinity around one hundred times less than BMP4 (Zimmerman *et al.*, 1996; Chang and Hemmati-Brivanlou, 1999). Ventroptin is another BMP antagonist that binds BMP4 with high affinity and it is strongly expressed in the developing ventral and temporal retina. It does not bind other TGFβ family members BMP7, TGFβ and Activin (Sakuta *et al.*, 2001).

In summary, Shh and BMP4 are diffusible signalling molecules implicated in patterning ventral and dorsal retina respectively. BMP4 is a member of the TGFβ family of secreted molecules. It signals via cell surface receptors, perhaps in co-operation with other TGFβ family members in the retina such as BMP7, BMP5 and/or GDF6, to activate SMAD proteins leading to regulation of gene expression in the nucleus. Dorso-ventral asymmetry in the BMP system of the developing eye has been reported in the expression of *Bmp4*, *Bmp5*, *Bmp7*, *Bmpr-IB*, *Noggin* and *Ventroptin*.

Retinoic acid and other factors implicated in dorso-ventral patterning of the retina

Retinoic acid (RA), a morphogen known to play a wide role in pattern formation throughout the vertebrate embryo, is richly synthesised in the developing eye. Retinoids (including RA) are synthesised by aldehyde dehydrogenases from dietary vitamin A. In the developing world, vitamin A deficiency is an important cause of blindness (West, 2000). Virtually all vitamin A function is mediated by two metabolites: retinaldehyde, which forms the light sensitive chromophore bound to opsin; and RA, which regulates gene transcription (Dowling and Wald, 1960).

RA functions through binding with two families of nuclear receptor, the RAR (RARα, RARβ and RARγ; activated by all physiological RA variants) and the RXR (RXRα, RXRβ and RXRγ; activated by 9-cis RA) receptor families (Kastner *et al.*, 1997). These form homodimers or heterodimers with each other or additional types of nuclear receptor and bind DNA response elements to regulate transcription (Mangelsdorf and Evans, 1995; Chambon, 1996). Orphan nuclear receptors in particular have been implicated in the modulation of RA signalling. Chicken ovalbumin upstream promoter transcription factor II (COUP-TFII), from the COUP family of orphan nuclear receptors, can modulate RA actions and is localised to the dorsal retina in mice (McCaffery *et al.*, 1999). Another orphan nuclear receptor, TLX, can modulate RA actions in the mouse eye by promoting sensitivity to RA signalling (Kobayashi *et al.*, 2000).

RA seems to be particularly important for development of the ventral retina. Specific inhibition of ventral retinoic aldehyde dehydrogenase in 2- to 11-somite stage zebrafish embryos for 2 hr (using low concentrations of competitive inhibitor citral)

results in complete failure to form a ventral retina (Marsh-Armstrong *et al.*, 1994). Vitamin A deprivation in rats and genetic removal of retinoid receptors in mice (RARβ/γ and RXRα knockout animals) caused a shortening of the ventral portion of the retina (Warkany and Schraffenberger, 1946; Kastner *et al.*, 1994; Kastner *et al.*, 1997). In some RARγ/RXRα knockout mice, the ventral retina failed to form completely (Kastner *et al.*, 1997). Interestingly, immersion of zebrafish embryos in RA treated tank water during the period of the formation of the primary optic primordia affected the ventral and not the dorsal eye. Duplicate retinas formed from future RPE cells derived from the ventral region of the developing optic cups (Hyatt *et al.*, 1992). RA seems to promote ventral identity as well as growth in mice and zebrafish. Post-gastrulation treatment with RA in *Xenopus* expanded the expression domain of ventral marker *Vax2* (Sasagawa *et al.*, 2002). Treatment with RA at the end of zebrafish gastrulation expanded the ventral *pax2* domain and reduced that of dorsal *mshC*, homologous to mouse *Msx3* (Hyatt *et al.*, 1996; Ekker *et al.*, 1997). In mice, *Pax2* expression is positively regulated by TLX, an enhancer of RA signalling (Yu *et al.*, 2000). Furthermore, some RARα/γ mouse knockouts display complete retinal coloboma (failure of the optic fissure to close), a defect seen in *Pax2* knockout mice (Lohnes *et al.*, 1994; Torres *et al.*, 1996). When RA-soaked beads were inserted into the dorsal zebrafish retina, optic fissure-like structures – a ventral retinal characteristic – were induced (Hyatt *et al.*, 1996). Study of the effect of RA on *Shh* expression in *Xenopus* suggested that RA does not pattern the ventral retina by upregulating *Shh*. If anything, forebrain *Shh* expression was reduced with post-gastrulation RA treatment (Sasagawa *et al.*, 2002).

RA is synthesised in an asymmetric fashion along the dorso-ventral axis by aldehyde dehydrogenases. RA synthesis is initially greatest in the ventral retina, but in the postnatal eye more RA is synthesised dorsally (McCaffery *et al.*, 1992; McCaffery *et al.*, 1993). *Raldh2*, the gene encoding Retinaldehyde dehydrogenase 2 (RALDH2, originally designated V2), is expressed early in E8 mouse in the ventral optic pits (McCaffery *et al.*, 1993; Berggren *et al.*, 1999). This is believed to set up an early ventral-high to dorsal-low RA gradient that could lead to the polarised expression domains of various transcription factors. This initial RA polarising event has also been hypothesised to induce expression of the later RA synthesising enzymes that maintain the dorso-ventral asymmetry of its distribution. In the ventral retina, the

activity of RALDH2 is quickly superseded (E8.5-E9 in mice) by that of RALDH3 (originally designated VI and also named ALDH6) (McCaffery *et al.*, 1993; Grun *et al.*, 2000; Mic *et al.*, 2000; Suzuki *et al.*, 2000). At the same time, dorsal RA synthesis by RALDH1 (also named AHD2 and ALDH1) begins (McCaffery *et al.*, 1992; McCaffery *et al.*, 1993; Ang and Duester, 1999). Put more simply, ocular RA is first synthesised in the ventral optic pits by RALDH2. Activity of this dehydrogenase ceases and is replaced in the optic vesicles by RALDH1 (in dorsal retina) and RALDH3 (in ventral retina).

Prior to the onset of *Raldh1* expression, *Cyp26*, encoding the RA-degrading oxidase CYP26, is expressed throughout the dorsal mouse optic vesicles (McCaffery *et al.*, 1999). In the optic cup, *Cyp26* becomes expressed in a narrow horizontal stripe between the dorsal and ventral domains of RALDH1 and RALDH3 activity. This creates a trough between very high ventral and moderately high dorsal RA signalling levels (Drager *et al.*, 2001). This 'equatorial' region between the dorsal and ventral optic cup has been shown to be devoid of RA signalling. RARβ (but not other retinoid receptors) was downregulated in the *Cyp26* expressing stripe of tissue (McCaffery *et al.*, 1999). More significantly, LacZ was never detected in the equatorial region when *β-galactosidase* expression was driven by a retinoic acid response element (RARE) in transgenic mice. In these mice, RA signalling was equally prevalent, if not more so, in the early dorsal retina. RA signalling was greater ventrally from E14.5, though by P17 levels were higher dorsally (Enwright and Grainger, 2000; Stull and Wikler, 2000; Wagner *et al.*, 2000). In the chick, the distribution and activities of RALDHs and RA degradation were similar to those of the mouse, but were not apparent until the optic cup had already formed (Mey *et al.*, 2001). This suggests that RA signalling does not initially specify the dorso-ventral axis of the chick retina.

These data indicate that varying levels of RA signalling divide the mouse retina into dorsal, ventral and equatorial zones (Enwright and Grainger, 2000; Stull and Wikler, 2000; Wagner *et al.*, 2000; Drager *et al.*, 2001). Interestingly, these dorsal, ventral and equatorial zones are correlated with the functional compartments of the oculomotor system (Wagner *et al.*, 2000). While RA is crucial for formation, growth and identity of the ventral retina, it does not appear to be restricted to this function and may regulate compartmentalisation and identity in both dorsal and ventral retina. RA

signalling has been implicated in *Pax2* regulation; it may contribute to the asymmetric expression domains of other dorsal and ventral retinal transcription factors, a number of which have been identified in vertebrates.

Many patterning transcription factors are of the homeobox family, originally named so because mutations in them led to 'homeotic' transformations of one body part to another. In the mammalian ventral retina, these include homeobox genes *Vax2* (Barbieri *et al.*, 1999; Ohsaki *et al.*, 1999), *Pax2* (Nornes *et al.*, 1990) and *Six9/Six6/Optx2* (Jean *et al.*, 1999; López-Ríos *et al.*, 1999). Expressed in the dorsal mouse retina are homeobox genes *Hmx3* (Weidong *et al.*, 2000) and *Msx2* (Monaghan *et al.*, 1991; Furuta and Hogan, 1998) and T-box genes *Tbx2*, *Tbx3*, *Tbx5* (Chapman *et al.*, 1996) and *Tbx20* (Carson *et al.*, 2000; Kraus *et al.*, 2001). These transcription factors are likely to regulate the effector molecules of dorso-ventral identity. Such ideas have acquired good supporting evidence through misexpression studies by Schulte *et al.* in the chick retina. Analysis of territorial markers and axon projections suggested that asymmetrically expressed transcription factors could provide positional identity and regulate Eph and ephrin genes across both naso-temporal and dorso-ventral axes (Schulte *et al.*, 1999; Schulte and Cepko, 2000). Across the dorso-ventral axis of the chick retina, *Vax/Vax2* misexpression promoted *Ephb2* and *Ephb3* expression, inhibited *Efnb1* and *Efnb2* expression and increased RGC axon guidance to dorsal areas (Schulte *et al.*, 1999). Recent analyses of *Vax2*-null mice suggested similar roles for *Vax2* in the mouse (Barbieri *et al.*, 2002; Mui *et al.*, 2002). Chick *Tbx5* has been shown to positively regulate *Efnb1* and *Efnb2*, negatively regulate *Ephb2* and *Ephb3* and promote guidance of RGC axons to ventral target areas (Koshiba-Takeuchi *et al.*, 2000).

To summarise, RA is essential for the proper growth and development of the ventral retina and seems to be important for the establishment of dorsal and ventral compartments in the retina. This could permit and/or define the expression boundaries of genes encoding dorsal and ventral transcription factors. These in turn could regulate the cell surface molecules (such as Eph/ephrin molecules) and internal programs that affect position-dependent cellular identity. The relationship between RA and other signalling pathways (such as BMP4 and SHH) remains unclear.

1.4. Conserved regulatory networks in vertebrate and fly eye development and the T-box transcription factors

Transcription factors are nuclear proteins that positively or negatively regulate gene transcription by binding to DNA sites within promoters or other regulatory regions of target genes. When bound to regulatory DNA sequences, transcription factors modulate transcription levels by interacting with the basal transcriptional complex of a target gene (Latchman, 1998). The ability of transcription factors to control genes within a cell casts them as critical players in the efficient implementation of cellular programs. This is most crucial during the development of an organism, where transcription factors control changing cellular identities. Transcription factors often act in association with others to function in self-regulating networks. Strikingly, the genes encoding transcription factors are often highly conserved throughout evolution. This is evidenced by the homologous networks of transcription factors that operate in analogous systems between quite different species. The remarkable similarities in how the *Drosophila* compound eye and the vertebrate eye are regulated during development provide a good example of this (Wawersik and Maas, 2000). These similarities have prompted the search for the involvement of vertebrate homologues of *Drosophila* genes during visual system development. In this section I first look at some similarities and differences between the networks of transcription factors that control eye specification in *Drosophila* and vertebrates. An aim of this thesis (see **1.6.** below) is to explore the function of mammalian homologues of *Drosophila* T-box gene *optomotor blind* (*omb*) during visual system development. Thus I will introduce *omb* and the T-box gene family and describe the roles of *omb* homologues during vertebrate development.

Similar regulatory networks govern eye development in vertebrates and flies

Eye specification in Drosophila depends on an inter-regulatory network of genes that encode transcription factors. Misexpression studies suggest that these form a rough hierarchy with *twin of eyeless* (*toy*) at the top and *eyeless* (*ey*) immediately downstream. Further downstream lies *eyes absent* (*eya*), *sine oculis* (*so*) and *dachshund* (*dac*). All these genes can induce ectopic eyes when misexpressed in non-eye imaginal discs. Two other genes *teashirt* (*ts*) and *so*-related *optix* (*opt*) can also induce ectopic eyes when misexpressed, but how they are involved and their

relationship to other master control genes is not yet clear. Although some regulatory genetic hierarchy does exist, extensive inter-regulation and positive feedback loops within this network make the perception of it as a linear pathway inaccurate. It is perhaps best viewed as a self-regulatory network of transcription factors for which mutual activity is required to lock into an eye development program. Such a view is compounded by evidence that suggests some of these factors may function as part of a transcriptional complex *in vivo* (Chow and Lang, 2001).

In vertebrates, despite radically different eyes to those of *Drosophila*, there are conserved features in how the eyes are specified. Vertebrate eyes appear to be specified by a network of transcription factors, some of which are homologous to those in *Drosophila*. In place of the related genes *toy* and *ey* is a single orthologue, *Pax6* (introduced above in **1.1.**). *Six3* and *Optx2* (also known as *Six6* or *Six9*, briefly introduced in **1.3.**) are members of the SIX-homeobox family (of which *sine oculis* is the founding member) that are particularly homologous to *optix* (Toy *et al.*, 1998). Like the master control genes in *Drosophila* eye development, those in vertebrates such as *Pax6*, *Six3*, *Optx2* and *Rx1* can upregulate each other's expression and induce ectopic retinal tissue when over-expressed (Andreazzoli *et al.*, 1999; Chow *et al.*, 1999; Loosli *et al.*, 1999; Zuber *et al.*, 1999; Bernier *et al.*, 2000). There are however important differences between the fly and vertebrate networks. Vertebrate homologues of *Drosophila eya* (*Eya1-4*) appear to play non-essential roles in eye development, so far only mutations in human *EYA1* have been associated with (mild) ocular abnormalities (Azuma *et al.*, 2000). Similarly the *Drosophila* homologue of *Rx* is not expressed in the eye-antennal disc (Mathers *et al.*, 1997). *Dach1*, homologous to *Drosophila dac*, is expressed in the developing eye of chick and mouse, but seems to be regulated independently of *Pax* and *Eya* genes (Heanue *et al.*, 2002). Still, the similarities in mechanisms of transcriptional regulation between vertebrates and flies are such to encourage the search for vertebrate orthologues of Drosophila genes.

The T-box gene family

In the past decade the T-box gene family has become established as a family of transcription factor-encoding genes implicated in many critical aspects of development. Mutation of the *T* (*Brachyury*) locus in the mouse has been known to be important for embryonic viability and tail development (hence *T* - for tail) for over

seventy years. In 1990 the *T* gene was cloned (Herrmann *et al.*, 1990), and in 1992 sequence homology was discovered between the *T* gene and a newly cloned *Drosophila* gene, *optomotor blind* or *omb* (Pflugfelder *et al.*, 1992). The discovery of *T*-related genes in the mouse led to the naming of the T-box (abbreviated *Tbx*) gene family after the region of homology encoding a novel DNA binding domain (Bollag *et al.*, 1994). The *T* gene product was shown to function as a transcription factor, a function dependent on the 'T-box' DNA-binding domain or 'T domain' (Kispert *et al.*, 1995). Later X-ray crystallography of the protein showed that it bound to DNA as a dimer and interacted with both the major and minor grooves of DNA in a novel manner (Muller and Herrmann, 1997 ~~1478~~). Many more T-box genes have now been described in a wide range of species (**Fig 1.6**) and found to encode transcription factors. They are involved in numerous aspects of development and can be organised into subgroups based on sequence homology and intron structure. These are the *Tbx1*, *Tbx2*, *Tbx6* and *Tbr1* subfamilies, though some T-box genes do not readily fall into any of these categories (**Fig. 1.6**; Papaioannou, 2001).

omb is expressed in neuronal and glial cells of the developing *Drosophila* visual system, including at the dorsal and ventral margins of the eye disc and in the optic lobe primordia (Poeck *et al.*, 1993). The gene is named after the visual phenotype that is characterised by abnormal turning responses of the fly through a maze of rotating drums (Pflugfelder and Heisenberg, 1995). Anatomically the impairment of *omb* gene function leads to disruption of neuronal connectivity in the fly optic lobes. Some lethal *omb* alleles fail to develop an optic lobe completely (Pflugfelder and Heisenberg, 1995). *omb* is the only known *Drosophila* member of the *Tbx2* subfamily of T-box genes. The completion of genome sequence projects means that confident identification of orthologous genes (those derived from a common ancestral gene) between diverse species is possible, for example between human and *C. elegans*. *Tbx2*, *Tbx3*, *Tbx4* and *Tbx5* are all highly conserved vertebrate members of the *Tbx2* subfamily. Further variants of these genes seem to exist in frogs and fish (Dheen *et al.*, 1999; Takabatake *et al.*, 2000).

Phylogenetic analysis suggests that *Tbx2* and *Tbx3* form a cognate pair (as do *Tbx4* and *Tbx5*), which means they are paralogous *i.e.* they arose from the duplication of a common ancestor gene. The *Tbx2*/*Tbx3* and *Tbx4*/*Tbx5* common ancestor genes are

Figure 1.6

Phylogenetic tree of the T-box family members from Fig. 2 in Papaioannou *et al.*, 2000. Phylogenetic analysis was conducted by Papaioannou *et al.* using the ClustalW software package (http://www.ebi.ac.uk/clustalw/) accessed via the European Bioinformatics Institute (EBI; http://www.ebi.ac.uk/). The T-domain amino acid sequences of all the T-box family members listed in this table were aligned with ClustalW. Aligned sequences were subjected to Phylip analysis in the same EBI interface. Outputs were then interpreted using the tree drawing program NJplot obtained from Pôle Bio-Informaitique Lyonnaise (http://pbil.univ-lyon1.fr/). The following genes were excluded from analysis due to insufficient sequence data: *AmphiTbx4/5*, *AmphiTbx20*, *ChTbr2*, *CpTbx2*, *CpTbx3*, *CpTbx6R*, *HsTBX10*, *NvTbox1*, *NvTbox2*, *NvTbox3*, *NvTbox4*, *XTbx4* and *Zftbxa*. The following species abbreviations are used in this table: *Am* or *Amphi*, amphioxus; *Ap*, *Asterena pectinifera* (starfish); *As*, ascidian; *Ce*, *Caenorhabditis elegans*; *Ch*, chicken; *Ci*, *Ciona intestinalis* (ascidian); *Cp*, *Cynops phyrrhogaster* (Japanese newt); *Hp*, *Hemicentrotus pulcherrimus* (sea urchin); *Hs*, *Homo sapiens*; *Hy*, hydra; *Mm*, *Mus musculus*; *Nv*, *Notophthalmus viridescens* (newt); *Pf*, *Ptychodera flava* (acorn worm); *X*, *Xenopus laevis*; *Zf*, zebrafish.

Phylogenetic tree of the T-box gene family

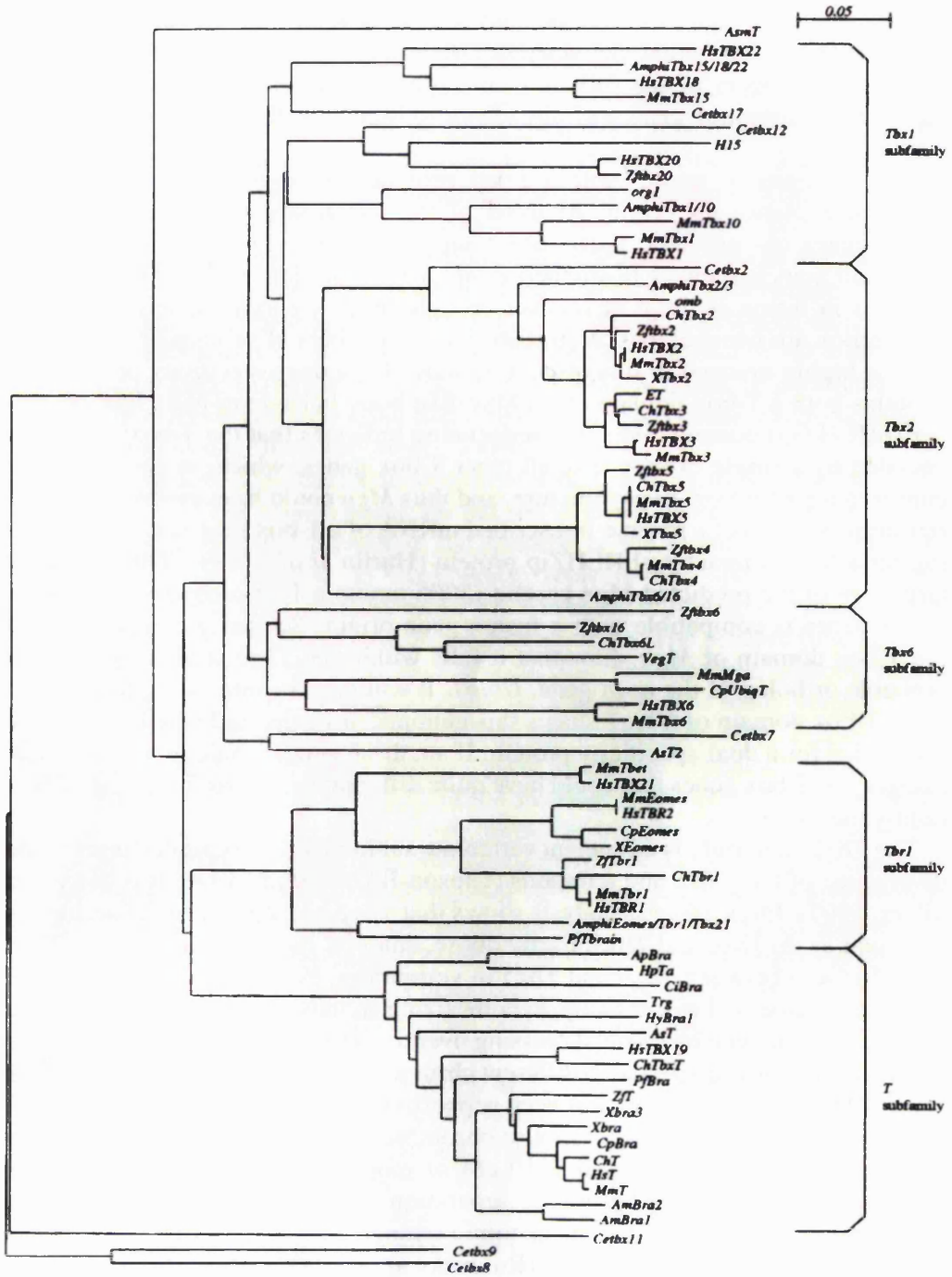

themselves hypothesised to have arisen from an initial tandem duplication by an unequal crossing-over event. This initial duplication is believed to have occurred over 450 million years ago in a common metazoan ancestor to vertebrates, flies and nematodes. *Drosophila omb* is believed to be descended from the *Tbx2/Tbx3* ancestral gene and so is orthologous to vertebrate *Tbx2* and *Tbx3*. En masse duplication of the *Tbx2/Tbx3* and *Tbx4/Tbx5* cluster in vertebrates would have separated the cognate pairs onto separate chromosomes. In the mouse genome, *Tbx2* and *Tbx4* lie together on chromosome 11 and *Tbx3* and *Tbx5* lie together on chromosome 5 (Agulnik *et al.*, 1996; Ruvinsky *et al.*, 2000).

The involvement of *omb* in *Drosophila* visual system development and the known similarities between *Drosophila* and vertebrates in the transcriptional regulation of eye development prompted the interest of my laboratory in the function of *omb*-related genes in the vertebrate eye. *Tbx2*, *Tbx3* and *Tbx5*, but not *Tbx4*, were found to be expressed in the developing mouse retina at optic vesicle and optic cup stages in the laboratory of Virginia Papaioannou (Chapman *et al.*, 1996). Furthermore, gene expression was apparently restricted to the dorsal aspect of the developing retina (see **1.3.**). This raised the possibility that the Tbx2, Tbx3 and Tbx5 transcription factors were involved in dorso-ventral patterning of the developing retina. This could mean regulation of axon guidance molecules on the growth cones and axons of dorsal RGCs. Given the role of *omb* in the guidance of axons in the optic lobes of *Drosophila*, this was an attractive idea. It became my main focus of research to study the role of *omb*-related T-box genes in the developing mammalian retina. In view of this aim, the known functions of the T-box gene family in mammals are reviewed in the next section, focusing on human T-box mutations and the *omb*-related vertebrate T-box genes.

T-box gene function in mammals

Eighteen T-box genes have now been identified in humans, more than in any other species (Papaioannou, 2001). The near completion of the human genome project means most and perhaps all of the human T-box genes have been uncovered. Mutations in T-box genes are now known to give rise to a number of developmental disorders in humans. *TBX1* mutations cause DiGeorge syndrome (Jerome and Papaioannou, 2001; Merscher *et al.*, 2001), *TBX3* mutations cause Ulnar-mammary

syndrome (Bamshad *et al.*, 1997), *TBX5* mutations cause Holt-Oram syndrome (Basson *et al.*, 1997; Li *et al.*, 1997) and *TBX22* mutations cause X-linked cleft palate and ankyloglossia (Braybrook *et al.*, 2001). The only other mammalian species in which T-box genes have been extensively studied is the mouse, where orthologues for all but 3 of the human genes have been uncovered (Papaioannou, 2001).

Numerous functional studies of T-box genes have been performed in mice that (for obvious reasons) could not be performed in humans. These studies have yielded considerable insight into the functions of T-box genes. The high level of homology between mouse and human *Tbx/TBX*, the analysis of human *TBX* expression profiles and the study of human developmental syndromes caused by mutant *TBX* genes all suggest conserved roles for T-box genes during mouse and human development (Papaioannou, 2001). This makes the mouse an invaluable model for the study of mammalian T-box gene function, though of course differences do exist and care must always be excised when extrapolating mouse data to humans (for example, see Fougerousse *et al.*, 2000).

Tbx2 (*omb*-related) subfamily genes are expressed in developing and adult mammals (Bollag *et al.*, 1994; Campbell *et al.*, 1995; Law *et al.*, 1995; Bamshad *et al.*, 1997; Li *et al.*, 1997). Amplification of *TBX2* mRNA in a subset of human breast cancers, particularly in those associated with BRCA1 and BRCA2, implicates *TBX2* in the development of this disease (Jacobs *et al.*, 2000; Sinclair *et al.*, 2002). *Tbx2* subfamily genes have been most consistently implicated in development of the vertebrate heart, limbs and eyes. *TBX3* mutations cause the limb, apocrine, genital and dental abnormalities of Ulnar-Mammary Syndrome (thought to be due to haploinsuffiency). The hypoproliferative features of this disorder may be partially attributable to upregulation of p14ARF, which is normally inhibited by TBX3 (and TBX2) and causes proliferation arrest (Brummelkamp *et al.*, 2002; Lingbeek *et al.*, 2002). Most individuals with Ulnar-Mammary Syndrome have posterior (postaxial) forelimb defects that range from minor defects in the ulnar (posterior) ray to loss of the forearm and hand (Bamshad *et al.*, 1997). Holt-Oram syndrome patients caused by *TBX5* haploinsufficiency exhibit heart and anterior (preaxial) forelimb defects that show an extremely variable expression, even within families. Upper limb deformities tend to be more severe in the left limb and range from sloping shoulders, limited supination

and clinodactyly to severe reduction deformities primarily affecting the radial (anterior) ray (Basson *et al.*, 1997; Li *et al.*, 1997). These data demonstrate critical and complementary roles of *TBX3* and *TBX5* in development of the anterior-posterior axis in the upper limb.

Heart problems in Holt-Oram syndrome include conduction disease (sinus and atrio-ventricular nodal abnormalities) and septation defects (atrio-septal defects, ventriculo-septal defects and tetralogy of Fallot). Other anomalies suggestive of aberrant cardiac chamber specification may also be present (Basson *et al.*, 1997; Li *et al.*, 1997). Interestingly, missense mutations near the amino-terminal end of the T domain cause predominantly cardiac malformations whereas those near the carboxyl-terminal primarily cause limb defects (disrupting binding to the major and minor DNA grooves respectively). Putative null mutations substantially affect both heart and limb (Basson *et al.*, 1999). The severe cardiac problems seen in some mutations may be contributed to by loss of association between TBX5 and homeobox transcription factor NKX2-5. These transcription factors are capable of synergistic action in developing cardiomyocytes (Hiroi *et al.*, 2001). This co-operation provides a basis for the similar cardiac defects observed in humans with *NKX2-5* mutations (Schott *et al.*, 1998; Benson *et al.*, 1999). A mouse model of Holt-Oram Syndrome now exists carrying a heterozygous null mutation of *Tbx5* (Bruneau *et al.*, 2001). This indicates conservation of the role of *Tbx5* in limb and cardiac morphogenesis between mice and humans. Transcription of the genes encoding atrial naturetic factor (ANF, a peptide secreted into the blood) and connexin 40 (cx40, a component of gap junctions) was reduced in these mice. In addition, Tbx5 and Nkx2-5 were found to be capable of direct and co-operative transactivation of the *cx40* and *Anf* promoters. This offers a basis for the cardiac conduction defects seen in Holt-Oram Syndrome as *cx40* is normally expressed within the conduction system. *Tbx5* deficiency in homozygous mice caused severe hypoplasia of the posterior heart (where *Tbx5* is normally expressed) and the mice died at E10.5. The developing eyes of these homozygotes were not examined (Bruneau *et al.*, 2001). Ocular anomalies such as nystagmus and Duanes anomaly have been reported in Holt-Oram patients though this is not a consistent feature (Newbury-Ecob *et al.*, 1996).

Work in chick has highlighted an additional role for *Tbx5* during limb development: the establishment of forelimb identity. An analogous role for paralogue *Tbx4* has been demonstrated in the hindlimb. The expression of *Tbx5* and *Tbx4* in developing forelimbs and hindlimbs respectively in different vertebrate species suggests that this is a conserved function of these genes (Chapman *et al.*, 1996; Gibson-Brown *et al.*, 1996; Ruvinsky *et al.*, 2000; Takabatake *et al.*, 2000). In manipulated chick embryos, the preponderance of forelimb or hindlimb features in FGF-induced ectopic limbs is highly correlated with respective expression of *Tbx5* or *Tbx4* (Gibson-Brown *et al.*, 1998; Ohuchi *et al.*, 1998). More significantly, when either gene is misexpressed in the inappropriate limb bud, limb identity is transformed (albeit incompletely) into that associated with the ectopic T-box gene (Rodriguez-Esteban *et al.*, 1999; Takeuchi *et al.*, 1999). Misexpression of *Pitx1*, a paired-like homeobox gene related to *Otx* genes, in the chick wing bud induces *Tbx4* and promotes leg identity (Logan and Tabin, 1999). In *Pitx1*-null mice, *Tbx4* was downregulated in a forelimb-like hindlimb (Szeto *et al.*, 1999). Forelimb identity may be a default state occurring in the absence of *Pitx1* and *Tbx4*. *Tbx4* is downregulated when *Tbx5* is misexpressed in the inappropriate limb bud (but not *vice versa*) and this may be sufficient for the promotion of forelimb identity. If so, this might explain why no loss of upper limb identity is observed in Holt-Oram Syndrome.

Tbx2 and *Tbx3* are expressed in similar patterns in developing forelimb and hindlimb buds. In the mouse, *Tbx2* is expressed in the anterior and posterior aspects of the developing limbs, but lacks the expression in the apical ectodermal ridge (AER) seen for *Tbx3* (Chapman *et al.*, 1996). In the chick the reverse is true: *Tbx2* is expressed in the AER whilst *Tbx3* expression is restricted to the shared anterior and posterior expression domains (Gibson-Brown *et al.*, 1996). The anterior domain is mostly fated for apoptosis, perhaps explaining why only posterior skeletal elements are affected in human ulnar-mammary syndrome (Logan *et al.*, 1998). All ~~orthologous~~ *Tbx2* subfamily members, excluding *Tbx4* (excluding *tbx3* in zebrafish), are expressed in the developing dorsal retina in a wide range of species (Chapman *et al.*, 1996; Gibson-Brown *et al.*, 1996; Ruvinsky *et al.*, 2000; Takabatake *et al.*, 2000). The exploration of the function of these genes in the developing eye is one of the aims of this thesis.

SUMMARY AND AIMS

The research discussed in the introduction to this thesis includes literature published before and during the course of my investigations. It describes the early morphogenetic events surrounding genesis of the developing eyes in the vertebrate embryo (**1.1.**). It explains retinal stratification and the genesis of RGCs, the projection neurons of the retina. The development of RGC projections to central brain targets and the putative roles of Eph/ephrin interactions in axon guidance and retinal patterning were described (**1.2.**). Together these reviews provided a background for the discussion of the molecules implicated in dorso-ventral patterning of the neural retina (**1.3.**), the central interest of this thesis. Finally, the T-box family of transcription factors were introduced (**1.4.**). This was because in this Ph.D. project I have focused on the role of the *omb*-related subclass of this family in dorso-ventral retinal patterning.

It now leaves me to list the specific aims of this thesis and describe how I have attempted to achieve them:

(1) To explore the expression patterns of T-box genes, more specifically those of the omb-related subclass, in development of the mammalian retina.

(2) To explore the regulation of *omb*-related T-box genes, in particular with reference to a putative relationship with BMP4 in the developing mammalian dorsal retina.

(3) To explore the function of *Tbx5* in the developing mammalian eye, especially with regards to a proposed role in dorso-ventral patterning of the retina.

This first aim is realised in **Chapter 3**, where the expression patterns of *omb*-related T-box genes during retinal development in humans and mice are investigated. I then go on to look at the place of *omb*-related genes *Tbx2* and *Tbx5* in the regulatory hierarchy controlling dorso-ventral patterning of the retina in mice. In **Chapter 4**, the expression pattern of *Bmp4* is compared with those of *Tbx2* and *Tbx5* (and other asymmetrically expressed retinal genes). In addition, *Tbx2*, *Tbx5* and *Vax2* expression in mutant mice is examined in this chapter to look for disruptions in dorso-ventral patterning. In **Chapter 5**, a whole mouse embryo culture system is employed to test

the effect of ectopic human recombinant BMP4 on *Tbx2* and *Tbx5* regulation. **Chapter 6** focuses on the role of *Tbx5* in the mammalian retina. The generation of a construct to misexpress *Tbx5* in the developing ventral mouse eye is described. This will allow the direct examination of *Tbx5* function in the mammalian retina. It will also enable analysis of the role of mammalian *Tbx5* in dorso-ventral patterning of the retina through the analysis of gene expression profiles and RGC projections. In **Chapter 7** the various elements of this PhD thesis are brought together and the ways in which the research described aids our current understanding of mammalian retinal development are discussed. Two main research areas are discussed, the genetic basis of dorso-ventral patterning of the developing eye and the roles of T-box genes during retinal development. Finally, the future directions of study in these fields to follow the work of this thesis are given. Related work, not included into the body of the thesis, is described in **Appendix I** and **Appendix II**. Published research papers are listed in **Appendix III**.

CHAPTER 2

Materials and Methods

MATERIALS

The reagents, solutions and equipment used for the different branches of my experimental work are documented here. Solutions were sterilised by autoclaving, or, where stated, by filter-sterilisation with a 50 ml syringe (Becton Dickenson Labware, NJ, USA) and a 0.22 μm filter (Millipore corporation, MA, USA).

2.1. Plasmids

A variety of different bacterial plasmids were used during the course of my studies. These were electroporated into electrocompetent *Escherichia-coli* of the DH5α strain (originally from Promega, WI, USA) and amplified for use in sub-cloning or to prepare RNA probes for *in situ* hybridisation. The plasmids and their origin are listed in **Table 2.1**.

2.2. Reagents for bacterial work

Agar plates

4 g **L-agar** (Lennox L-Agar 'LB Agar'; Gibco BRL, Paisley, UK) was heated in a microwave in 200 ml distilled water until completely dissolved and cooled until comfortable to touch. Ampicillin or kanamycin (both from Sigma-Aldrich Company Ltd., Poole, UK; made up in sterile distilled water to respective stock concentrations of 50 mg/ml and 10 mg/ml and stored at –20°C) were added to give respective concentrations of 50 μg/ml and 20 μg/ml. The mixture was poured into petri dishes (20-25 ml each) in a sterile environment. The agar plates were then allowed to dry at room temperature.

L-Broth

3.5 g **L-Broth** (Lennox L-Broth 'LB Broth'; Gibco BRL, UK) was added to 100 ml distilled water and autoclaved. Above concentrations of antibiotic were added just prior to use to make selective.

Table 2.1. Plasmids acquired and their providers

Insert	Vector	Provider
α-p0-ires-gfp-intron-pA	pSL1180	P. Gruss (Germany)
Foxg1	pBK-CMV	H. Smith (UK)
Bmp4	pSP72	B. Hogan (USA)
Pax2	pBS31-1	P. Gruss (Germany)
Tbx2	pBK-CMV	J. Sowden (UK)
TBX2	pGEM-3Zf(+)	J. Sowden (UK)
Tbx3	pBluescript II KS(-)	V. Papaioannou (USA)
TBX3	pBluescript II SK(-)	D. Law (UK)
Tbx5	pBK-CMV	J. Sowden (UK)
TBX5	pBluescript II SK	D. Brook (UK)
Tbx20	pGEM-T	J. Sowden (UK)
Vax2	pBluescript II KS	C. Cepko (USA)

SOC medium

SOC medium was made by the addition of 50 times filter-sterilised 125 mM potassium chloride/500 mM magnesium sulphate/1 M Glucose (reagents from Sigma, UK) in distilled water to L-Broth.

2.3. Reagents for gel electrophoresis

DNA loading buffer

6 times **DNA loading buffer** (50% sucrose, 0.024% orange G, 0.0024% sodium azide) was made by adding 5g sucrose (Sigma, UK), 2.4 mg orange G (Sigma, UK) and 0.24 mg sodium azide (BDH, Poole, UK) to a tube and making up to 10 ml with distilled water. As an alternative to adding sodium azide (which is highly toxic) the solution could be filter-sterilised.

MOPS buffer

10x **MOPS buffer** (0.2 M MOPS, 50 mM sodium acetate, 10 mM EDTA) was made up with 41.85 g 3-(N-morpholino) propanesulfonic acid (MOPS), 6.81 g sodium acetate, 3.76 g EDTA and DEPC-treated water to a volume of 1 L (reagents from Sigma, UK). Sodium hydroxide (Sigma, UK) was used to bring the solution to pH 7.0. The solution was not autoclaved and it was stored in the dark at room temperature because MOPS buffer is heat and light sensitive.

RNA denaturing loading buffer

3.72 ml **RNA denaturing loading buffer** was made up with 24 mg orange G (Sigma, UK), 300 µl glycerol (Sigma, UK), 450 µl 10x MOPS buffer, 720 µl formaldehyde (BDH, UK) and 2.25 ml formamide (BDH, UK) to be stored at –20°C.

TBE buffer

1 times **TBE buffer** (0.09 M Tris-borate, 0.001 M EDTA) was made up with 108 g Tris base, 55.5 g boric acid, and 3.65 g EDTA (tetrasodium salt) made up to 10 L with distilled water (reagents from Sigma, UK).

2.4. Reagents for *in situ* hybridisation

Plasmids with the cDNA templates used for probe synthesis with the enzymes used to linearise and transcribe them for antisense and sense probes are listed below in **Table 2.2**.

Cryostat section hybridisation buffer

50 ml **cryostat section hybridisation buffer (CSHB)** was made up and stored in 10 ml aliquots at –20°C. In preparation for this, a number of solutions were first made up. 50 mg yeast tRNA (Sigma, UK) was dissolved in 5 ml DEPC-treated distilled water to give a concentration of 10 mg/ml. 5 g dextran sulphate (Sigma, UK) was dissolved in DEPC-treated water by vigorous vortexing to give a 50% solution. 10 times Salts solution (2 M sodium chloride, 0.05 M sodium dihydrogen orthophosphate monohydrate, 0.05 M di-sodium hydrogen orthophosphate anhydrous, 0.05 mM EDTA, 0.1 M Tris pH 7.5) was made up with:

57 g sodium chloride (Sigma, UK)
3.45 g sodium dihydrogen orthophosphate monohydrate (BDH, UK)
3.55 g di-sodium hydrogen orthophosphate anhydrous (BDH, UK)
50 ml 0.5 mM EDTA (Sigma, UK)
50 ml 1 M Tris pH 7.5

This mixture was made up to 500 ml with DEPC-treated water and autoclaved.

50 ml CSHB (50% formamide, 10% dextran sulphate, 0.5% Denhardts solution, 0.1% tRNA, 1x Salts) was made up by mixing:

25 ml formamide (BDH, UK)
10 ml 50% dextran sulphate
5 ml 10 mg/ml tRNA
5 ml 10x Salts
250 µl Denhardts solution (Sigma, UK)
4.75 ml DEPC-treated water

Table 2.2. Enzymes used for linearisation and transcription of cloned cDNA

cDNA	Size of cDNA insert	Linearised with:		Transcribed with:	
		sense	antisense	sense	antisense
Foxg1	2.4 kb	*Cla*I	*Bam*HI	T3	T7
Bmp4	1 kb	*Sma*I	*Eco*RI	T7	Sp6
Pax2	500 bp	*Eco*RI	*Bam*HI	T7	T3
Tbx2	2.2 kb	*Xho*I	*Sal*I	T3	T7
TBX2	498 bp	*Hind*III	*Eco*RI	T7	Sp6
Tbx3	180 bp	*Hind*III	*Xho*I	T3	T7
TBX3	1.4 kb	*Hind*III	*Bam*HI	T3	T7
Tbx5	3 kb	*Xho*I	*Sal*I	T3	T7
TBX5	2.4 kb	*Xba*I	*Eco*RI	T7	T3
Tbx20	891	*Pst*I	*Sac*II	T7	Sp6
Vax2	700 bp	*Kpn*I	*Eco*RI	T7	T3

Embedding mixture

200 ml **embedding mixture** was made by adding 0.9 g gelatine (300 Bloom; Sigma, UK) to 20 ml PBS and heating to dissolve with continuous stirring. A further 160 ml PBS was added once the mix had dissolved. The solution was cooled to room temperature. 56 g albumin grade II (Sigma, UK) was stirred in by mixing overnight with a stirrer. 36 g sucrose was added and stirring was continued until dissolution. The embedding mixture was stored at –20°C in 5 ml aliquots.

Embryo powder

Embryo powder was prepared as follows: E12.5 mouse embryos in a minimal volume of PBS were homogenised using a sterilised electric homogeniser. 4 volumes of ice-cold acetone (BDH, UK) were mixed into the homogenised tissue, and the mix was incubated on ice for 30 minutes. The mixture was spun in a centrifuge for 2 hours and the supernatant discarded. The pellet was washed with another volume of acetone and pulse-spun. The supernatant was removed and the pellet spread out on filter paper and allowed to air dry. The spread pellet was then ground to a very fine powder using a pestle and mortar and stored in an airtight tube at –20°C.

MABT

MABT was made from a sterile 5 times MABT stock, diluted in distilled water and mixed with Tween-20 to give a 0.1% concentration. 5 times MABT (0.5 M maleic acid, 0.75 M sodium chloride) was made up with 58.1 g maleic acid (Sigma, UK) dissolved into 900 ml distilled water. Sodium hydroxide was added to raise the pH to 7.5, causing the maleic acid to first come out of solution, and then go back into solution. 43.8 g of sodium chloride (Sigma, UK) was added, the pH checked again and the solution made up to 1 litre with distilled water.

M-block

50 ml **M-block** was made up and stored at –20°C in 10 ml aliquots: Blocking Reagent (Roche Molecular Biochemicals, Lewes, UK) was added to MABT to give a 10% solution in MABT and stored at –20°C in 10 ml aliquots. 10 ml 10% Blocking Reagent was added to 10 ml heat-inactivated (by heating to 56°C for 30 minutes) sheep serum (Sigma, UK) and made up with 5 times MABT stock and Tween-20 (Sigma, UK) to give 50 ml blocking solution in 1 times MABT (M-block).

SSC

20 times SSC (3 M sodium chloride, 0.3 M sodium citrate) was made up by dissolving 175.3 g of sodium chloride (Sigma, UK) and 88.2 g of sodium citrate (Sigma, UK) into 900 ml of DEPC-treated water. The pH was adjusted to 7.0 with concentrated sodium hydroxide solution and made up to a litre with DEPC-treated water. For SSC pH 4.5, citric acid was used to adjust the pH.

TBST

250 ml **TBST** was made from 25 ml sterile 10 times TBST stock, 2.5 ml Tween-20 (to give a 1% concentration), 24 mg levamisol (Sigma, UK) and distilled water. 10 times TBST stock contained 8% NaCl, 0.2% KCl, and 0.25 M Tris HCl (pH 7.5).

Whole mount hybridisation buffer

50 ml **whole mount hybridisation buffer (WMHB)** was made up at a time and stored in 10 ml aliquots at –20°C. 25 ml formamide (BDH, UK), 12.5 ml 20 times SSC pH 4.5, 5 ml 10% sodium dodecyl sulphate (SDS), 250 µl 10 mg/ml yeast tRNA (Sigma, UK) and 250 µl 10 mg/ml heparin (Sigma, UK) were mixed and made up to 50 ml with DEPC-treated water.

2.5. Primers

Oligonucleotide primers were designed, checked with the *Amplify* program on the Apple Macintosh, and ordered from Sigma, UK, or Thermo Hybaid, Ashford, UK. Primers used for PCR are listed in **Table 2.3**. Primers used for sequencing are listed in **Table 2.4**. For site directed mutagenesis of *Tbx5* the following complementary primers were used to introduce the mutation:

MMTbx5-mut	gga gtg aga ata gct aac cgc gga cct gtg cca g
MMTbx5-mut-R	ctg gca cag gtc cgc ggt tag cta ttc tca ctc c

2.6. Culture reagents

Explant and culture saline

1 litre of the following solution was made with distilled water and autoclaved:

Table 2.3. Primers used for PCR

Gene amplified	Primer name	Sequence	Product size	T_a°C
αp0Tbx5/gfp Construct	Con-5'F	gct gcc cag tat cta gag aac c	522	60
	Con-5'R	gga tcc act agt tct aga gcg g		
	1191F	ggc ctg agt acc tct tac agg a	600	60
	JHConR-2	caa acg cac acc ggc ctt att c		
Pax6	M130	ctt tct cca gag cct caa tgt g	147	56
	SeyB	gca aca gga agg agg ggg aga		
PGM1	PGMF	gaa aaa tca aag cca ttg gtg gg	417	55-60
	PGMR	ggc acc gag ttc ttc aca gag gat		
TBX2	736F	acg aca tcc tga agc tgc ct	209	57
	923R	cct cgt aca agc gta gag ac		
TBX3	hTBX3-F	cca gaa tga taa gat aac cca g	261	55
	hTBX3-R	ggg aca taa atc ttt aag agg c		
TBX5	TBX5F	ggg ata gtt gga gag cag aac c	295	60
	TBX5R	gaa aca tcc gcc ttc cag cct t		

T_a = annealing temperature

Table 2.4. Primers used for sequencing of *Tbx5*

DNA for primer	Primer name	Sequence
pBK-CMV (5' MCS)	CMV-5'F	gac ctt gat tac gcc aag ctc g
Pax6 (p0 promoter)	JHConF-1	gcc taa gag caa gta cag tgg g
Tbx5 (coding region) 5' ↓ 3'	24x2F	cgc ctc tgg agc ctg att cc
	MM310R	gga act tca gcc aca gtt cac g
	840F	ggg cag tga tga cct gga gtt a
	1191F	ggc ctg agt acc tct tac agg a
	1868F	ccc cca gag ttt ctc tac act c
Tbx5 (3' utr)	231R	agg atg gga ctc gac act ctt t

MCS = multiple cloning site, utr = untranslated region.

0.118 M sodium chloride
4.02 mM potassium chloride
0.406 mM magnesium sulphate
0.246 mM magnesium chloride
0.641 mM sodium dihydrogen orthophosphate
1.8 mM calcium chloride

50 ml of this solution was taken and to it was added 0.75 g glucose and 0.25 g sodium bicarbonate for **explant saline**, and 0.1 g glucose and 0.1 g sodium bicarbonate for **culture saline**. The solutions were then filter-sterilised, ready for use.

Other culture reagents

Foetal calf serum (**FCS**; Sigma, UK) was heat inactivated by placing in a water bath at 56°C for 30 minutes. Dulbecco's Modified Eagle Medium (**D-MEM**; with L-Glutamine, 25 mM HEPES and 4500 mg/L D-Glucose, without sodium pyruvate) was from GibcoBRL, UK. Alpha modification of Eagle's minimal essential medium with ribosides and deoxyribonucleosides (**α-MEM**) was also from GibcoBRL, UK. Penicillin/streptomycin solution (100,000 units per ml) was from Sigma, UK.

2.7. Other reagents

DEPC treatment of distilled water

Distilled water was **DEPC-treated** by the addition of 1 ml 0.05% (v/v) DEPC (Diethyl pyrocarbonate; Sigma, UK) to 1 L of distilled water in a fume hood (DEPC is very toxic). The water was then shaken vigorously and incubated for at least 12 hours at 37°C. DEPC-treated water was autoclaved to sterilise the solution and to inactivate the DEPC.

Injection buffer

30 ml **injection buffer** (10 mM Tris pH 7.5, 0.1 mM EDTA, 25 mM sodium chloride) was made up with 300 µl 1M Tris buffer pH 7.5, 6 µl 0.5 M EDTA, 600 µl 5 M sodium chloride and 29.1 ml Embryo Water (Reagents all from Sigma, UK). The solution was then filter-sterilised.

Methyl green solution

Methyl green solution (0.5% methyl green, 0.1 M sodium acetate) was made up by first dissolving 4.1 g sodium acetate (Sigma, UK) into 460 ml distilled water. Acetic acid (BDH, UK) was used to bring the pH to 4.0 and 2.5 g methyl green (Sigma, UK) was added. The solution was mixed well to allow the methyl green to dissolve fully. The solution was filtered, made up to 500 ml with distilled water and autoclaved.

4% paraformaldehyde

4% paraformaldehyde was made up in a fume hood with 20g paraformaldehyde (Sigma, UK) in 500 ml of PBS (made with DEPC-treated water) and heated to 60°C on a hotplate with continual stirring to dissolve. 10 ml aliquots were made up and stored at –20°C.

PBS and PBT

Phosphate-buffered saline (**PBS**) was made up using one PBS tablet (Oxoid Ltd., Basingstoke, UK) dissolved in 100 ml distilled water, or 100 ml DEPC-treated distilled water for RNase-free solutions. **PBT** was made by adding 0.1% Tween-20 (Sigma, UK) to PBS.

METHODS

The various experimental techniques used during the course of my studies are described here. Many protocols required preparatory procedures and different methods were used at various stages of a particular experiment. Where this is the case they were listed in the order in which they were used or grouped together in a single section. At the beginning of each section I give a brief explanation of the methods that follow, before describing in detail how I have carried them out. Materials highlighted in bold are described under subheadings in the preceding section. All data from these methods presented in this thesis was observed in at least three independent experiments using tissue from more than a single animal, unless stated otherwise.

2.8. Amplification of cDNA using *Escherichia-coli*

Many of the most important techniques in molecular biology demand the cloning of complementary DNA (cDNA; derived from specific messenger RNAs) into a bacterial plasmid vector. To amplify cDNA, the DH5α strain of *Escherichia-coli* was used for all large-scale plasmid preparations. Electroporation was used to transform these bacteria, a procedure that uses an electric shock to force uptake of plasmid DNA by *Escherichia-coli.* For this technique to be effective, bacteria need to have first been made *electrocompetent.* This involves arresting bacteria while in their log phase of multiplication and storing them at ultra low temperatures until use.

By using plasmids that contain a resistance gene for an antibiotic present in the growth medium, successfully transformed bacteria can be selectively grown. The plasmids are harvested from bacteria cultures. To check the identity and quantity of the plasmid it is digested into linear fragments with restriction enzymes and visualised using gel electrophoresis. Restriction enzymes are biological enzymes that bind DNA at specific sites and cleave it at points within the binding site. These sites are invariably palindromic, *i.e.* the sequence of bases is the same when read from either the sense or anti-sense direction. Cleaving of DNA leaves 'blunt ends', where both DNA strands are cut in the same place, or 'sticky ends', where the two DNA strands are cleaved at different points (within the recognition site) to leave 3' or 5' overhangs.

Digested DNA is mixed with a loading buffer containing sugar (to give weight) and dye (to visualise the sample). The mixtures are loaded into wells within an agarose gel that has been immersed in buffer inside an electrophoresis tank. The gel is made up with ethidium bromide that binds DNA to allow visualisation under ultra violet light. An electric current is applied across the gel and the linearised DNA, which possesses a net negative charge, is drawn towards the positive electrode at a rate dependent on the size of the DNA fragment. Once the dye has passed sufficiently far across the gel, the gel is removed from the tank and placed under an ultraviolet light source. Ethidium bromide, bound to the different DNA fragments, is visualised and distinct bands corresponding to the location of different DNA fragments are seen.

If the digested DNA is run alongside a DNA 'ladder', a selection of DNA fragments of known size and quantity, both the size of the fragments (by comparing location across the gel) and their amount (by comparing intensity of signal) can be determined. If the number and sizes of fragments of the digested DNA corresponds to that predicted by analysis of the plasmid map and knowledge of the insert, then the plasmid has indeed been amplified, the DNA region of interest successfully cloned.

This DNA may now be used as a template for the manufacture of RNA probes for *in situ* hybridisation (**2.12.**) or can be further manipulated for the building of an artificial DNA construct (**2.15./2.16.**) for *in vivo* genetic modification of an experimental organism (see **Chapter 6/Appendix I**). This section is concerned with the cloning of DNA, from the preparation of electrocompetent cells to the identification and quantification of the amplified plasmid.

Preparation of electrocompetent cells

4 x 5 ml of sterile **L-Broth** medium in 30 ml universal tubes (Phillip Harris Scientific, Ashby de la Zouch, UK) were inoculated with DH5α strain *Escherichia-coli*. 200 µl pipette tips dipped into a stock aliquot of DH5α cells (in 50% glycerol aqueous solution, stored at –80°C) were dropped into each tube. These starter cultures were incubated overnight at 37°C shaking at 200 rpm. 4 x 100 ml of L-Broth medium were made up in 4 x 500 ml glass conical flasks that were then bunged with cotton wool, covered with aluminium foil, and autoclaved.

The 4 x 100 ml L-Broth medium were pre-heated to 37°C before one of the 4 x 5 ml overnight DH5α cultures was added to each flask. These were then incubated shaking at 37°C for approximately 1.5 hr until the OD_{550}, as measured using a spectrophotometer (Amersham Pharmacia Biotech, St. Albans, UK), was in the range 0.5 - 0.6. The cultures were transferred into 4 x 100 ml chilled centrifuge bottles and kept on ice for 30 min. Hereon, great care was taken to ensure the cells remained at 0°C.

The tubes were spun for 15 minutes in a Sorvall SLA-1500 rotor (pre-chilled to 0°C) at 4,000 g (5,130 rpm). Following the spin, the supernatant was immediately discarded. Any solutions to be discarded (during all procedures) that have come into

contact with bacteria were placed in a beaker with a small volume of chloros overnight (to kill any remaining bacteria) before pouring down the sink. The bacterial pellets in the 4 tubes were each re-suspended in chilled 25 ml sterile distilled water, more water was then added, 25 ml at a time, to each tube until each tube contained 100 ml. The tubes were again spun for 15 minutes at 4,000 g spin at 0°C, the supernatant discarded, and 100 ml chilled sterile distilled water added to each tube, 25 ml at a time, as before.

The tubes were spun again for 15 minutes at 4,000 g at 0°C and the supernatant carefully discarded. Each pellet was resuspended in 4 ml chilled 10% glycerol in sterile distilled water and the solutions were transferred with a chilled 5 ml pipette to 4 x 15 ml chilled falcon tubes (Greiner Laborotechnik, Germany). These were spun for 15 min at 4,000 rpm at 0°C. The supernatants were discarded and the pellets re-suspended with vigorous vortexing in 200 µl chilled 10% glycerol in sterile distilled water (giving a volume of 350 µl). 28 x 1.5 ml eppendorfs (Anachem, Luton, UK) were chilled on dry ice and the bacteria were transferred to the eppendorfs, 50 µl to each tube. The electrocompetent cells were stored at –80°C until use.

Electroporation of electrocompetent Escherichia-coli cells

An electroporation cuvette (Invitrogen, Paisley, UK) and an aliquot of electrocompetent cells for each plasmid to be electroporated was placed on ice, as was the plasmid. One falcon 2059 tube (Becton Dickenson, USA) per DNA sample was placed in a rack and labelled. An electroporator ('Electroporator II'; Invitrogen, UK) set to 'ARMED', 1800 volts, 150 ohms, and 'PULSE', was plugged into a power source (Consort, Belgium) set to 1500 volts, 25 milliamps and 25 watts. After ensuring correct polarity, the power source was switched on and the electroporator set to 'CHARGE'. The unit was allowed to charge fully (at least 30 seconds) and then discharged by setting to 'PULSE', recharged and discharged again, then recharged as to be ready for use

Approximately 10 pg of plasmid DNA was added to a single aliquot of thawed out cells. Each mixture in turn was added to a chilled electroporation cuvette, tapped on the bench to remove any bubbles and wiped dry with a tissue. The electroporator was set to 'DISARMED', a cuvette inserted and the machine set back to 'ARM', then the

unit discharged by setting to 'PULSE'. The machine was temporarily set to 'DISARM' whilst removing the cuvette and then recharged ready for the next cuvette. When all cuvettes were done the electroporator was disconnected and the power supply turned off. The cells flushed out of each cuvette with 1 ml **SOC medium** and transferred to a labelled falcon 2059 tube.

Once all the cells had been electroporated and transferred to falcon 2059 tubes, they were all grown for 30 minutes at 37°C shaking at 200 rpm. 10-100 µl was spread (using a moulded glass pipette) onto a selective **agar plate**. Following electroporation of ligated DNA, the culture was spun down for 5 minutes in a bench centrifuge, the supernatant discarded, the pellet re-suspended in residual supernatant, and all the cells (~100µl) were spread onto a selective plate. The plates were then incubated upside-down overnight at 37°C.

The following morning plates were checked for bacterial colonies. The number of colonies per microgram of DNA, or the *transformation efficiency* of the cells, was calculated to determine the competence of cells by electroporating a known 10 pg plasmid sample. 100 colonies with 10 µl plated following electroporation of 10 pg plasmid DNA gives a transformation efficiency of 10^9 col/µg transformants. This efficiency was routinely achieved. Plates could be stored for a few weeks at 4°C or colonies immediately picked for further multiplication and DNA harvesting.

Mini preps for DNA harvesting

To isolate the multiplied plasmid from bacteria in a purified form, a QIAprep Spin Miniprep Kit (which provides buffers and spin columns; Qiagen Ltd., Crawley, UK) was used. This would typically yield 20-25 µg of plasmid DNA from a 1-5 ml culture volume. For a greater yield a maxiprep using a 100 ml culture volume must be performed (Plasmid Maxi Kit; Qiagen, UK). A single colony was picked from a selective agar plate containing bacteria with the plasmid of interest and used to inoculate 3 ml of selective L-Broth in a 30 ml universal tube (using concentrations of 50 µg/ml for ampicillin and 20 µg/ml for kanamycin). Bacterial cultures were left at 37°C overnight shaking at 200 rpm.

The following morning overnight cultures were spun at 4,000 rpm on a bench centrifuge and the supernatants discarded. Bacterial pellets were re-suspended in 250 µl of buffer P1 (with RNase added) from the Qiagen kit and the suspension transferred to a 1.5 ml eppendorf. 250 µl of buffer P2 was added to each eppendorf and immediately mixed by inversion. After a maximum of 5 minutes 350 µl of buffer N3 were added to each tube. These were immediately mixed by inversion and spun at 13,000 rpm for 10 minutes. The supernatants from each tube were decanted into a Qiagen spin column and spun for 1 minute at 13,000 rpm. The filtrates were discarded and 750 µl of buffer PE (with ethanol added) was added to each column. These were spun at 13,000 rpm for 1 minute, the filtrates were discarded, and the columns were spun again at 13,000 rpm for 1 minute to remove residual buffer that was then discarded from each column.

The DNA was eluted from the column. 50 µl of buffer EB (10 mM Tris buffer pH 8.8, 1 mM EDTA) was placed in the centre of the column. After standing for 1 minute the columns were spun at 13,000 rpm for 1 minute. The elutant was transferred to an eppendorf labelled with the plasmid name and the date. Yield and identification of the DNA was then carried out by digestion of 1 µl with diagnostic restriction enzymes and gel electrophoresis. DNA was stored at –20°C.

Restriction digests and gel electrophoresis

A 10 µl restriction volume was used for diagnostic digests. 1 µl of the miniprepped plasmid DNA was placed into a 500 µl eppendorf and 1 µl 10 times restriction enzyme buffer was added. The optimal buffer was chosen by examination of Promega charts (contained in their catalogue) listing the varying enzyme activities in different buffers (buffers and enzymes were all supplied by Promega, USA). 0.4 µl of each restriction enzyme (enzymes at concentrations of 10-12 units/µl) was added. Enzymes were vortexed on removal from –20°C and kept on ice at all times when in use. When two enzymes were used in one reaction, the reaction volume was increased so that the volume of enzyme did not exceed 10% of the reaction volume. High enzyme concentrations may inhibit the reaction either through the rising glycerol concentration from the enzyme mixture or by encouraging star activity. The reaction mixture was then made up to 10 µl with distilled water, vortexed and pulse-spun on a centrifuge before incubating in a water bath at 37°C from 1 hour to overnight.

Following digestion, 2 µl of 6 times **DNA loading buffer** was added to the 10 µl reaction. 1 µl uncut plasmid was similarly prepared for electrophoresis by adding 2 µl 6 times DNA loading buffer and 9 µl distilled water. Two tubes with DNA ladder were prepared (to be run either side of the plasmid samples): 2.5 µl Hyperladder I (Bioline, London, UK), 2 µl 6 times DNA loading buffer, and 7.5 µl distilled water in each tube. On some occasions 0.5-1 µl of a 1 kb ladder was used (Promega, USA). The tubes were vortexed, pulse spun on a centrifuge and placed on ice until ready to be loaded into an agarose gel. The agarose gel was prepared as follows:

A 90 ml volume of **TBE buffer** was added to 0.9 g electrophoresis grade agarose (Sigma, UK) for a 1% agarose gel. If the expected band sizes were large (in excess of 3 kilobase pairs) then a lower (≥ 0.75%) percentage of agarose was used; if expected bands were small (less than 500 base pairs) a higher percentage (≤ 2 %) gel was used. This is because a low percentage of agarose within the gel gives a better separation of bands of high molecular weight and a high percentage gives better separation of low molecular weight bands. The agarose was dissolved into the TBE buffer by heating in a microwave at full power for 2 minutes, or until the mixture was boiling for at least 15 seconds. Volume was restored after heating by adding distilled water until the weight returned to that prior to heating. 1 µl 10 mg/ml ethidium bromide was added with care (ethidium bromide is highly mutagenic and a suspected carcinogen) to the liquid agarose, mixed by swirling, and the gel mixture was poured into the gel former with a gel comb inserted, and allowed to set at 4°C.

Once set, the gel was placed in an electrophoresis tank (Bio-Rad Laboratories, CA, USA) and immersed in TBE buffer. Positioning was such that the positive electrode was at the opposite end to the gel comb, which was removed to reveal a row of wells. Each DNA sample was loaded by careful pipetting into a separate well. The tank was plugged into a power source (Bio-Rad, USA) and a potential difference applied across the tank of 90-150 volts. When running a gel overnight, a voltage of 10-16 volts was applied across the tank. When the orange G from the loading buffer was seen to reach the end of the gel (orange G runs much faster than most DNA fragments), the power source was turned off and the gel transferred to a tray. The gel was then carefully

carried to the gel imaging apparatus to be viewed under ultraviolet light and photographed (Alphaimager™ imaging equipment; Flowgen, Lichfield, UK).

2.9. Preparation of human and mouse tissue for molecular analysis

Immunohistochemistry (**2.11.**), *in situ* hybridisation (**2.12.**) and reverse transciptase-polymerase chain reaction (RT-PCR; **2.13.**) were used to analyse biological tissues at the molecular level. The acquisition and dissection of developing human and mouse tissues for these procedures is described below. Human embryos and foetuses were staged using hand and foot measurements to estimate the number of weeks post conception (England, 1996). For some foetuses the age was determined by subtracting 2 weeks from the number since the last maternal period.

Acquisition of developing human tissue

Embryonic and foetal human tissue was received on ice in DEPC-treated PBS from the Developmental Biology Resource, Institute of Child Health and the Medical Research Council (MRC) tissue bank, Hammersmith Hospital. Ethical approval was obtained and informed consent was sought and granted.

Dissection of mouse embryos

Mus musculus of the CBA/Ca strain kept at the Institute of Child Health Western Laboratories were mated together overnight. The following morning females that had mated were identified by the presence of a waxy white vaginal plug. As the mice are presumed to have mated at approximately midnight the night before, this day is described as embryonic day 0.5 (E0.5).

When pregnancies were sufficiently advanced, mice were isolated and humanely killed using cervical dislocation, a Home Office designated Schedule 1 procedure. A small volume of 70% ethanol (Hayman, Witham, UK) in distilled water was spread over the abdominal area and, lifting the skin clear with forceps (Raymond A. Lamb, London, UK), a horizontal incision was made using a pair of scissors (Raymond Lamb, UK). The skin was torn apart to widen the incision and the anterior abdominal wall was lifted with forceps to be cut from side to side with scissors to open the abdominal cavity. The intestines were lifted out of the abdomen to expose the two

horns of the mouse uterus, with embryonic conceptuses clearly visible. The uterus was cut at the tips of the horns and at the cervix to be transferred into **PBS** or into 10% heat-inactivated **FCS** in **D-MEM**. The dead mouse was stored at –20°C before disposal by incineration. Embryos were then carefully dissected out from the extra-embryonic layers using No. 5 watchmaker's forceps (Raymond Lamb, UK).

2.10. Cryosectioning of human and mouse tissue for molecular analysis

The cryosectioning of developing human and mouse tissues for immunohistochemistry and *in situ* hybridisation is described below. Histological tissue staining of cryosections is also described.

TESPA-coating of slides

Silverfrost slides (BDH, UK) were TESPA-coated prior to use. Slides were placed into glass racks and washed (in a fume hood) for a minimum of 30 seconds each in a series of three baths. These contained (in order) 10% hydrochloric acid/ 70% ethanol in **DEPC-treated water**, DEPC-treated water, and 95% ethanol in DEPC-treated water. Slides were then placed overnight in an oven at 65°.

Four new baths were prepared in a fume hood for the slides. The first contained 2% TESPA (3-aminopropyltriethoxy-silane; Sigma, UK) in acetone. The next 2 baths contained acetone, and the final one contained DEPC-treated water. Ethanol was from Hayman, UK; acetone and hydrochloric acid were from BDH, UK. The slides were passed through the baths, 10 seconds only in the TESPA/acetone bath, and a minimum of 30 seconds in the others. The slides were then covered and dried in a 37°C oven, then stored at room temperature until use.

Cryosectioning of tissue

Tissues to be cryosectioned were placed into **4% paraformaldehyde** in PBS and placed at 4°C overnight. They were then washed in PBS and placed into a filter-sterilised 20% sucrose in PBS overnight at 4°C. Tissues were transferred directly from the sucrose solution into plastic moulds filled with OCT compound (Sakura, Holland). Tissues were orientated within the OCT compound under a dissecting microscope

(Zeiss, Germany) and the orientation recorded. For rapid freezing of tissue a plastic weighing boat filled with isopentane (Sigma, UK) was placed on dry ice in an ice bucket. The mould with OCT compound and orientated tissue was then placed in the isopentane with a few pieces of dry ice. When frozen, blocks of OCT were transferred on dry ice to a –80°C freezer to be stored between 1 and 14 days before cryosectioning.

A single OCT block to be sectioned was transferred on dry ice from –80°C to a cryostat. A small amount of OCT compound was used to stick a tissue specimen to a metal chuck, which was then placed in the cryostat (Bright, Huntingdon, UK). After allowing about 20 minutes to bond, the plastic mould was peeled away from the tissue specimen and the metal chuck fitted into the cryostat. 10 μm sections of the tissue specimen were cut and placed in sequence onto a set of numbered and labelled TESPA-coated slides. When a section had been placed on each slide in the set a second section was placed on the slides in sequence, followed by a third if so desired. This allowed adjacent slides to contain adjacent sections and a single slide to contain sections from different points of the tissue specimen. Slides were left to dry overnight at room temperature, covered to protect from dust. After drying, slides were wrapped concertina-style 20 at a time back-to-back in strips of aluminium foil to allow easy access to individual slides. These were placed at –80°C until use.

Haematoxylin and eosin staining of cryostat tissue sections

Cryosectioned tissue mounted on slides were stained with haematoxylin and eosin for histological analysis and for comparison with adjacent sections processed for immunohistochemistry (**2.11.**) or *in situ* hybridisation (**2.12.**). These were removed from –80°C and allowed to thaw for 20-30 minutes at room temperature. Slides were baked at 37°C for 30 minutes to aid adhesion of sections to slides.

The slides were immersed briefly in distilled water to remove the OCT compound and placed in Enrlich's haematoxylin solution (BDH, UK) for 5 minutes. They were then washed in distilled water for 1 minute and placed in a trough to be washed for 5 minutes under running tap water. Slides were immersed in 10% hydrochloric acid, 70% ethanol in distilled water for 10 seconds only and returned to the trough and the running tap for a further 5 minutes. This was followed by immersion in aqueous 1%

Eosin solution (Raymond Lamb, UK) for 5 minutes and a further 5 minutes in the water trough with running tap water. Slides were dehydrated through a series of alcohol solutions: 2 minutes in 70% ethanol (in distilled water), 2 minutes in 95% ethanol, and 2 x 5 minutes in 100% ethanol. After 2 x 5 minute washes in Histoclear (National Diagnostics, Hessle, UK), slides were immediately mounted with 20 x 40 mm (or 50 mm) coverslips (BDH, UK) using Vectamount™ (Vector Laboratories Inc., CA, USA) and allowed to dry at room temperature. Sections were examined under bright field with an Axiophot microscope (Zeiss, Germany) and photographed with Tungsten 64 colour slide film (Leeds Photovisual Ltd., London, UK) using '+1' and '+2' exposure (using an MC exposure control; Zeiss, Germany). Slides were scanned (using an Epson 32-bit scanner) into *Adobe Photoshop* in PDF format. Some images were scanned (using a digital camera) directly into *Openlab* for the Apple Macintosh in TIF format. Images were saved as JPG files to be imported into *Microsoft Powerpoint*.

2.11. Immunohistochemistry

Immunohistochemistry involves the use of specific immunoglobulins, mostly from the IgG class, to examine the distribution of a molecule (usually a protein) within sections (or larger specimens) of biological tissue. Antibodies are raised against a protein of interest by introduction of the protein into a foreign animal species, which then recognises the protein as an antigen. The immune response that follows in the host species results in the production of large quantities of polyclonal immunoglobulin antibodies specific to the foreign protein. These circulate in the animal's blood stream and can be purified from the blood serum. Purified immunoglobulins can be tagged with a fluorescent label or with an enzyme capable of catalysing a colour reaction. This enables antibodies to be visualised. Hence, when antibodies are applied to tissue specimens for specific binding, the protein of interest can be localised.

Many procedures do not involve the use of tagged antibodies against the protein of interest (the *primary* antibody), but use tagged *secondary* antibodies that specifically recognise immunoglobulins from a foreign host species. Thus, the secondary antibodies will specifically recognise bound primary antibodies when applied to the specimen. This allows an amplification of the signal when tagged secondary

antibodies are visualised, as more than one secondary antibody molecule will bind a single primary antibody. Similar amplifications may be achieved in the chemistry of the visualising colour reaction to enable a strong signal over even very small areas of protein localisation.

Untagged primary antibodies were used, followed by secondary antibodies tagged with *biotin*, for analyses of POU4F2 and TBX2 protein distribution on cryostat tissue sections. Complexes of avidin and biotin, tagged with horseradish peroxidase (HRP), were applied to fuse with the biotinylated secondary antibodies and further amplify the signal. HRP will catalyse a colour reaction between hydrogen peroxide and 3,3'-diaminobenzidine (DAB) to give a brown product (or black when developed in a nickel or cobalt chloride solution) and allow visualisation. The immunohistochemistry step in the *in situ* hybridisation protocol (see **2.12**) uses an enzyme-tagged primary antibody. The enzyme is *alkaline phosphatase*, which catalyses a reaction between nitro blue tetrazolium (NBT) and 5-bromo-4-chloro-3-indolyl-phosphate (BCIP) to form two new products, both of which are blue.

Immunohistochemistry for BRN3b and TBX2 on cryostat sections

Slides with cryosectioned tissue (see **2.10.**) were removed from storage at −80°C and allowed to thaw for 20 to 30 minutes. A grease pen (DAKO, High Wycombe, UK) was used to draw around the thawed out sections and the slides were placed in an incubation chamber humidified with PBS. Sections were washed with PBS by carefully pipetting a small volume (~0.5 ml) onto them within the margins of the grease enclosure. After 5 minutes, the solution was tipped off the slide and replaced to wash the sections again for 5 minutes. All washes and incubations were carried out in this manner at room temperature (unless stated otherwise) and solutions were replaced hastily to ensure sections did not dry out.

0.1% Hydrogen peroxide solution was made from a 30% stock solution (Sigma, UK) diluted in PBS. Slides were incubated for 15 min in a 0.1% hydrogen peroxide solution in PBS at room temperature to reduce activity of endogenous peroxidases. Sections were washed twice in PBS. Slides were incubated for 1 hour with a blocking solution: 2% normal serum (Vector Laboratories, USA) and 0.1% Tween-20 (Sigma, UK) in PBS (**PBT**). The normal serum blocks non-specific binding of the antibody.

Serum is taken from the same species of animal used to generate the secondary antibodies to minimise cross-reactivity with serum proteins. Use of a detergent (Tween-20) on the tissue allows better permeation of the antibodies. Primary antibodies goat polyclonal anti-POU4F2 (Brn-3b; Santa Cruz, USA) or rabbit polyclonal anti-TBX2 (kindly provided by C. Campbell, USA) were diluted 1:100 in blocking solution and applied to the slides. These were incubated overnight at 4°C.

The slides were returned to room temperature and washed twice in PBS. Biotinylated secondary antibody (DAKO, UK) was diluted 1:200 in PBS and applied to the sections. These were incubated for 2 hours. 'A' (avidin) solution was diluted 1:400 in PBS then mixed 50:50 with 1:400 'B' (biotin) solution ('A' and 'B' solutions supplied in an ABC kit; Vector Laboratories, USA) in PBS and allowed to stand (for complex formation) for 20 minutes. Sections were washed twice in PBS and treated with prepared avidin and biotin solution for 2 hours. Slides were washed twice with PBS and freshly prepared DAB kit mix (Vector Laboratories, USA) was applied. The DAB mix was prepared by adding a drop of Buffer, a drop of DAB solution, and two drops of hydrogen peroxide solution to 2.5 ml of distilled water. Development was carried out protected from light, and slides were checked frequently to avoid over-labelling. After about 2-20 minutes the reaction was halted by a wash in distilled water.

The slides were dehydrated by immersion in butanol (BDH, UK) for 5 minutes. They were then washed twice in histoclear for 5 minutes each, and mounted in Vectamount™. These washes were performed in glass coplin jars (Raymond Lamb, UK). Slides to be counterstained with methyl green were immersed in **methyl green solution** and washed 3 times in distilled water just prior to butanol treatment. Sections were examined, photographed, scanned and stored as described in **2.10.**.

2.12. *In situ* hybridisation

In situ hybridisation is a very powerful molecular technique that allows localisation of messenger RNA for a specific gene on sections of biological tissue, or whole specimens. The first step in this method is to clone the cDNA of the gene to be analysed into a vector containing T3, T7 or Sp6 RNA polymerase promoters.

Following amplification of the plasmid (see **2.8.**), the cDNA can be used as a template for the manufacture of labelled RNA probes.

The plasmid is linearised by cutting at the 5' end of the gene insert and cleaned by phenol extraction. The RNA polymerase binding site (T3, T7 or Sp6) contained at the 3' end is then utilised for transcription of antisense probes. For sense probes the plasmid is cut at the 3' end and the 5' RNA polymerase binding site is used for transcription. See **Table 2.2** for details of the enzymes used for linearisation and transcription of the different cDNAs that I have used. Distilled water treated with DEPC is used when working with pre-hybridised RNA, to reduce the potential threat of RNase contamination. Antisense probes are used so they can bind or *hybridise* with the endogenous *sense* messenger RNA (mRNA) transcribed from the gene of interest in biological tissues. Sense probes are made for use in control experiments. Control experiments using the sense probes were carried out to test whether labelling with new probes was specific and so a reliable indicator of mRNA localisation. In the protocol that follows, the probes were labelled by using digoxygenin-UTP (the 'U' base unique to RNA, with an added chemical tag) during transcription. Following hybridisation, immunohistochemistry for the digoxygenin label (see **2.11.**) is performed on the tissues to allow visualisation of the hybridised probes *in situ.*

Linearisation of DNA

The plasmid DNA to be transcribed was allowed to thaw then vortexed. 2 x 10 µg was placed into a pair of 500 µl eppendorfs (Anachem, UK) and labelled very clearly as *sense* and *antisense.* An appropriate restriction enzyme was chosen for the sense and the antisense tubes to cut the plasmid at the 3' and the 5' end of the insert respectively. 12 µl of relevant 10 times restriction enzyme buffer was added to each tube followed by 5 µl of the chosen enzyme. Each tube was made up to 120 µl volume with distilled water, vortexed, pulse spun and placed in a 37°C water bath for 1 hour to overnight. Following incubation, 5 µl of each digest was run on a 0.8% agarose gel alongside 0.5 µg of uncut plasmid and a DNA ladder to ensure linearisation of the plasmid.

Phenol extraction

The volume of each digest was made up to 150 µl with distilled water and 150 µl of phenol equilibrated with Tris pH 7.0 (Sigma, UK) was added to each tube in a fume hood. The tubes were vortexed for 30 seconds and spun in a centrifuge for 5 minutes. The (top) aqueous layer (120 µl) was carefully decanted into a new set of clearly labelled (II) eppendorfs. A further 60 µl distilled water was added to the original tubes, which were re-vortexed (30 seconds) and spun (5 minutes) before removing with care 80 µl of the aqueous phase and adding to the new (II) tubes. Phenol contaminated tubes and pipette tips were discarded into refuse labelled as phenol solid waste. An equal volume (200 µl) of chloroform/iso-amyl alcohol 24:1 (Sigma, UK) was added to each tube. The tubes were vortexed (30 seconds) and spun (5 min). The top aqueous phase (180 µl) was carefully removed from each tube and placed in a set of 1.5 ml eppendorfs. The (II) tubes were now discarded. To each of the 1.5 ml tubes 0·1 volume (18 µl) was added of 3 M sodium acetate solution and 2·5 volumes (495 µl) 100% ethanol. The tubes were placed at –20°C overnight to allow the DNA to precipitate.

The tubes were removed from –20°C and immediately spun at high speed (13,000 rpm) for 30 minutes at 4°C in a microfuge. As soon as the microfuge stopped, the supernatant was carefully tipped out. The pellet was washed with chilled 200 µl 70% ethanol in DEPC-treated water and spun for 8 minutes at 4°C. The supernatants were carefully discarded, and the tubes were pulse-spun. The final drop of 70% ethanol was removed with a 200 µl pipette and the tubes were allowed to stand for 5-10 minutes to air dry. The pellets were re-suspended in 21 µl DEPC-treated water, and 1 µl from each tube was run on a 0.8% agarose gel with a DNA ladder to check DNA recovery. 1 µg (as judged from the gel photograph) cleaned linear DNA was set aside for the probe synthesis and remaining DNA stored at –20°C for future syntheses.

Probe synthesis

Sense and antisense 500 µl eppendorfs were labelled and for each 2 µl of 10 times digoxygenin-labelled UTP mix, 2 µl 10 times transcription buffer (all from Roche, UK), 0.5 µl RNase inhibitor (Promega, USA) and ~1 µg linearised cDNA were added. Each tube was made up to 19 µl with DEPC-treated water. 1 µl of RNA polymerase was then added to each tube, ensuring that the appropriate polymerases (T3, T7, or

Sp6), were added to the sense and antisense tubes, binding 5' to the sense and antisense strands respectively. T3, T7, and Sp6 polymerases (Roche, UK) were thawed on ice and vortexed prior to use. They were kept on ice at all times when in use and otherwise stored at –20°C.

The tubes were vortexed, pulse spun on a centrifuge and immediately incubated at 37°C for 2 hr only, then placed on ice. 1 µl from each tube was retained at this point for electrophoresis and placed at –20°C. 1 µl RNase-free DNase I (Roche, UK) was added to each tube. These were then incubated at 37°C for 15 min only. Tubes were returned to ice and 80 µl DEPC-treated water, 10 µl 3M sodium acetate (made up using DEPC-treated water) and 300 µl 100% ethanol was added to each tube. The tubes were vortexed, pulse spun and placed at –20°C overnight to precipitate the newly synthesised RNA. DNase treatment and precipitation are carried out to deliver a pure sample of clean RNA.

The tubes were removed from –20°C and immediately spun at high speed (13,000 rpm) for 30 minutes at 4°C. As soon as the centrifuge stopped, the supernatant was carefully tipped out. The pellet was washed with chilled 200 µl 70% ethanol in DEPC-treated water and spun for 8 minutes at 4°C. Supernatants were carefully discarded and the tubes were pulse-spun. The final drop of 70% ethanol was removed with a 200 µl pipette and the tubes were allowed to stand for 5-10 minutes to air dry. The pellets were re-suspended 60 µl DEPC-treated water, and 3 µl from each tube was run on a 1% agarose RNA gel with an RNA ladder (3 µl) and the 1 µl samples retained prior to the DNase treatment and precipitation. This allows quantification of the RNA, a check of the recovery following precipitation and examination of the success of DNase treatment. A special denaturing gel was used for RNA electrophoresis. The denaturing gel was used to prevent RNA secondary structure formation and to minimise RA degradation (see below). The RNA probes were stored at –20°C until use for *in situ* hybridisation.

RNA gel electrophoresis

0.95 g electrophoresis grade agarose was dissolved into 81 ml DEPC-treated water (for a 1% agarose gel) by boiling for a minimum of 15 seconds in a microwave. Volume was restored after heating by adding DEPC-treated water and 9.5 ml of 10

times **MOPS buffer** was added. 5 ml formaldehyde was then added to the mixture in a fume hood and mixed by manual vortexing. The gel mixture was poured into the gel former with a gel comb inserted, and allowed to set at 4°C.

16 µl of **RNA denaturing loading buffer** was added to each 3 µl RNA sample (or 1 kb RNA ladder; Promega, USA) in 500 µl eppendorfs. 1 µl 1 mg/ml ethidium bromide in DEPC-treated water was added to give 20 µl for each sample. The tubes were pulse-spun in a microfuge and then incubated at 70°C for 5 minutes, using a PCR machine (MJ Research Inc., MA, USA) or a waterbath, to denature the RNA. The samples were placed on ice, ready to load. Once set, the gel was placed in an electrophoresis tank and immersed in 1 times MOPS buffer, the positive electrode at the opposite end to the gel comb. The comb was removed and the denatured RNA samples were loaded by careful pipetting into separate wells. The gel was then run and photographed as for a DNA gel (see **2.8.**).

In situ hybridisation for cryostat sections

Up to 20 slides (per experiment) with cryosectioned tissue (see **2.10.**) were removed from –80°C and laid out for 20-30 minutes at room temperature to thaw. RNA probes to be hybridised were diluted to an appropriate concentration (~1 ng/µl), usually around 1 part in 100 (this is best determined empirically), in **cryostat section hybridisation buffer**, allowing 75-100 µl for each slide. Probe mixes were placed at 70°C for 5 minutes using a PCR machine to denature the RNA. 75-100 µl mix was then added to each of the thawed out slides. Probe mix was evenly spread across the slides with no bubbles over the sections. 20 x 40 mm (or 50 mm) coverslips were washed in 100% ethanol, dried, and carefully placed on the slides so as to cover the sections entirely. Slides were placed on a slide moat (Grant Instruments Ltd., Shepreth, UK) heated to 65°C and humidified with DEPC-treated distilled water and left overnight.

Slides were removed from the slide moat, placed in a glass rack, and immersed in preheated Washing Solution (50% formamide, 1x **SSC** (pH 7.0), and 0·1% Tween-20 in distilled water) within a glass trough in a 65°C water bath for 1 hour. Slides were then carefully transferred into plastic modified coplin jars (Raymond Lamb, UK) containing preheated Washing Solution (maximum 5 slides per coplin jar). Any

coverslips that had not fallen off the slides were gently nudged off using a 200 µl pipette tip. After 30 minutes, the Washing Solution was replaced (in a fume hood) and washed a further 30 minutes at 65°C. The slides were transferred in a fume hood to fresh modified coplin jars containing **MABT** and washed twice for 30 minutes each at room temperature. Slides were then removed one by one from the modified coplins, their edges dried with a tissue and the sections encircled using a grease pen, and placed in a humidified incubation chamber. 200-300 µl **M-block** was immediately applied to each slide. The slides were incubated for a minimum of 1 hour at room temperature. Anti-digoxygenin antibody tagged with alkaline phosphatase (Roche, UK) was diluted 1:1000 in M-block and applied to the slides. The slides were then incubated overnight at 4°C.

The slides were removed from 4°C and transferred back into modified coplin jars to be washed 4 x 5 min in MABT. The slides were placed in fresh modified coplins to be washed 2 x 10 min in Staining Buffer (100mM sodium chloride, 100 mM Tris pH 9.5, 50 mM magnesium chloride and 0.1% Tween-20 in distilled water). They were then returned to the incubation chamber. 200-300 µl of Staining Buffer with 18 µl/ml NBT/BCIP stock solution (18.75 mg/ml NBT and 9.4 mg/ml BCIP; Roche, UK) were applied to each slide and incubated at room temperature protected from light for 1-24 hours until satisfactorily developed. The length of time necessary for development is related to the strength of the probe during hybridisation. Hybridisations with new probes should be checked regularly to avoid over-development. The reaction can be slowed, a good idea for overnight development, by placing at 4°C. Labelling was checked under a dissecting microscope and slides were washed in distilled water. Slides were dehydrated in 100% butanol for 5 minutes and washed 2 x 5 minutes in histoclear. Slides were immediately mounted with 20 x 40 mm (or 50 mm) coverslips using Vectamount™ and left to dry at room temperature. Sections were examined, photographed, scanned and stored as described in **2.10.**.

In situ hybridisation for whole mouse embryos

Mouse embryos to be processed whole for whole mount *in situ* hybridisation were obtained as described in **2.9.** and fixed overnight in 4% paraformaldehyde. The next day they were transferred from 4% paraformaldehyde to 30 universal tubes and washed twice in PBT. Solutions were changed using fine tipped glass pipettes (John

Poulton Ltd., Barking, UK) and embryos were kept covered by solution at all times. Washes used 2-5 ml of solution and were carried out rocking gently at room temperature for 5 minutes, except where stated otherwise. Additions of new solutions to the embryos were preceded by a brief rinse in the new solution to aid removal of residual amounts of the previous solution.

The embryo tubes were next placed on ice and embryos were washed for 15-30 minutes each in an ascending set of methanol concentrations: 25%, 50%, 75% then 2 x 100% methanol (BDH, UK) in PBT. Embryos were transferred to 5 ml round-bottomed tubes (falcon 2054; Becton Dickenson, USA) in methanol and could be stored at –20°C for preferably not longer than 4 weeks. Whole mouse embryos stored in methanol were rehydrated on ice prior to use, through a descending series of methanol diluted in PBT. The embryos were kept in 5 ml round-bottomed tubes. 15 ml falcon tubes were used when the embryos were large and numerous. Following rehydration (20 minutes each in 75%, 50%, and 25% methanol in PBT) the embryos were washed 2 x 5 min in PBT.

The embryos were bleached with 6% hydrogen peroxide in PBT for 1 hr and washed 3 times in PBT. They were then separated according to size in readiness for treatment with proteinase K (Sigma, UK) diluted in PBT. Larger embryos required stronger treatment to allow better penetration of reagents in subsequent steps. The approximate lengths and strengths of proteinase K treatment for embryos at various developmental stages are listed below:

E11.5 - 8 min at 10 µg/ml
E10.5 - 7 min at 5 µg/ml
E9.5 - 2 min at 5 µg/ml
E8.5 - 1 min at 5 µg/ml
E7.5 - 1 min at 2.5 µg/ml

The embryos were immediately washed in 2 mg/ml glycine (Sigma, UK) in PBT followed by 2 washes in PBT. Next they were re-fixed with 0.2% gluteraldehyde (made from 25% gluteraldehyde; Sigma, UK) and 4% paraformaldehyde in PBS for 20 min at 4°C, and rinsed twice in PBT. 200 µl pre-warmed (to 70°C) **whole mount hybridisation buffer (WMHB)** was added and replaced with another 1 ml. The

embryos were incubated at 70°C from 2 hr to overnight. At this point, the embryos could be stored for up to 4 weeks at –20°C if so desired. Digoxygenin labelled riboprobes to be used were diluted to the chosen concentration (~1 μgml^{-1}) in preheated (to 70°C) WMHB to make the probe mix. The embryos in pre-warmed WMHB were rinsed with 200 µl probe mix and replaced with another 1 ml. The embryos were placed at 70°C overnight to hybridise with the RNA probe.

Embryo solution was prepared by placing ≥ 7.5 mg of **embryo powder** in a 15 ml falcon tube with 1.12 ml **TBST** for every 5 ml required. The mix was incubated at 70°C for 30 minutes and then cooled on ice. 125 µl heat-inactivated sheep serum and 2.5 µl sheep anti-digoxygenin antibody (Roche, UK) was added (per 5 ml required). The solution was incubated shaking at 4°C for ≥ 3 hr (to pre-absorb the antibody) and then spun at top speed for 10 min at 4°C. The supernatant was made up to 5 ml with 10% heat-inactivated sheep serum in TBST. This may be kept at 4°C for several weeks and can be used 2 or 3 times. Probe mix was removed from the embryos and kept (may be reused 2 or 3 times). Embryos were washed 2 x 30 min in Solution 1 (50% formamide, 5x SSC pH 4.5, 1% SDS, in distilled water) at 70°C, then transferred into Solution 2 (50% formamide, 2x SSC pH 4.5, in distilled water) for 2 x 30 minute washes at 65°C. The embryos were washed 3 times in TBST then pre-blocked with 10% heat-inactivated sheep serum in TBST for 90 minutes. The embryos were incubated over 1 to 3 nights at 4°C in the embryo solution.

Following incubation in embryo solution the embryos were thoroughly washed to remove all traces of the antibody: 3 times in TBST followed by 5 x 1 hr TBST washes. The embryos were left rocking overnight in TBST and then washed 3 x 10 min in NTMT (100mM sodium chloride, 100 mM Tris pH 9.5, 50 mM magnesium chloride, 1% Tween-20 and 480 μgml^{-1} levamisol in distilled water). For the colour reaction they were transferred to watchglasses and immersed in 18 μlml^{-1} NBT/BCIP in NTMT.

Colour reaction development was carried out rocking in a light-tight box. Embryos were checked every 10-20 minutes as development could be fast, though it sometimes took hours. The reaction could be slowed by placing at 4°C, speeded up by placing at 37°C, and stopped at any time by transferral of embryos to PBT. If necessary,

embryos were developed further by returning to NBT/BCIP/NTMT. After development, the embryos were washed twice in PBT and stored in the dark at 4°C with 0.018% thimerosol (Sigma, UK) in PBT. Embryos were examined under dark field in a dish of PBT with a dissecting microscope. Sometimes a small amount of 1% agarose was poured into a petri dish and set. This allowed careful positioning of embryos for photography by cutting holes in the agarose for the embryos to sit in. ~~was used for photography~~. Images were photographed (using '0' and '+1' exposure), scanned and stored as described in **2.10.**.

Embedding and vibratome sectioning of whole mount embryos

Whole mount embryos were transferred directly from PBT/0.018% thimerosol into a drop of **embedding mixture**. Embryos were left for at least 30 minutes, or overnight for embryos with more than 30 somites. Each embryo was coated with embedding mixture and placed on the side of an embedding mould. The mould was placed under a dissecting microscope in a fume hood. 50 µl 25% gluteraldehyde was placed into the mould. 500 µl embedding mixture was added and immediately mixed thoroughly by pipetting twice. The embryo was pushed to the bottom of the mould and orientated with watchmaker's forceps. This was done with haste as setting occurs in minutes and prolonged disturbance of the solution disrupts the setting. Embryos were placed at 4°C overnight to set and were then placed in PBS to be stored at 4°C until use. Poorly set and poorly orientated embryos were cut out and re-embedded.

Embedded embryos were superglued to the mounting tray of the vibratome (Agar Scientific Ltd., Stanstead, UK) and left for 20 minutes to stick. The embryo was then submerged in PBS, and 50 µm sections were cut. Each section was removed from the PBS bath and placed on a slide. The blade was lowered by 50 µm to cut again. Up to 10 sections were placed on a slide that was then mounted with 22 x 50 mm glass coverslips and 50% glycerol in PBT. Nail varnish or Tippex was used to hold the corners of the coverslip to the slide. Slides were stored at 4°C and examined promptly under differential interference contrast (DIC) with an Axiophot microscope. Images were scanned directly and stored as described in **2.10.**.

2.13. Polymerase chain reaction (PCR)

Single stranded oligonucleotides can be used to amplify regions of DNA in what is known as a *polymerase chain reaction*. Oligonucleotides may be designed to amplify specific DNA fragments, and will do so from picomolar quantities of DNA. The polymerase chain reaction (PCR) is thus a very powerful technique with a large range of applications. I have used this technique (1) to identify construct DNA from mouse tail tips and so determine transgenic status (2) to examine levels of gene expression within human and mouse tissue using *reverse transcriptase*-PCR (RT-PCR) and (3) to screen bacterial colonies for the presence of a DNA insert using primers specific to the insert.

Two oligonucleotides (small pieces of single stranded DNA) 20-25 bases long, known as *primers*, are required for PCR. The region to be amplified is optimally around 250-500 base pairs in length, though long range PCR can amplify fragments tens of kilobases long. The two primers must each be complementary to the 3' ends of the respective sense and antisense strands of this DNA region. Sense and antisense oligonucleotides are placed in a tube with the DNA sample, thermostable DNA polymerase enzyme and an excess of phosphorylated deoxyribonucleotides (dNTPs) in a reaction buffer. The tube is then passed through a series of temperature changes in a specialised PCR machine (effectively just a plate with tube slots and highly controllable temperature settings). The tube is passed through cycles of 3 separate temperature settings:

1. The first setting is at 94°C to denature DNA, to separate the double stranded DNA and to dissociate oligonucleotides.
2. Secondly it is placed at a temperature 2 or 3 degrees below that for which binding or *annealing* of the oligonucleotide primers to complementary DNA sequences becomes unfavourable (the melting temperature or *Tm*). This ensures that the oligonucleotide primers bind their complementary sites that flank the DNA region of interest specifically. This is enabled because less specific bonds are less stable and less likely to form in a high-energy environment (*i.e.* at a high temperature). The Tm was calculated thus: $Tm = 69.3 + (0.41 \times GC\ \%) - 650/N$. 'GC %' is the percentage of guanine- and cytosine-based nucleotides in the primer and 'N' is the total number of nucleotides in the primer.

3. The third temperature is that required for *extension*. This utilises the DNA polymerase and the nucleotide bases to extend the annealed primer in a 5' to 3' direction. This creates double stranded areas of DNA that include the region to be amplified on both sense and antisense strands (with their respective primers). The DNA polymerase used is derived from bacteria that have adapted to life at extreme temperatures and possesses an optimal temperature of 72°C. This is essential for the entire process. If extension were performed below the annealing temperature, non-specific binding of primers and hence DNA polymerisation would occur at many inappropriate sites. Following a short period of extension a second cycle is begun.

The mixture is returned to 94°C and the bound primers are separated from the DNA, except they are no longer 'primers', for they have been extended to include the DNA region to be amplified. At the subsequent annealing step, more specific binding sites will be presented to as yet unused primers. Previously bound sense primers will have extended far enough in the 3' direction to include the complementary site of the antisense primer (and *vice versa*), which will anneal. When extension ensues in the opposite direction (the 5' to 3' direction of the complementary strand), it will be limited by the beginning of the original primer. This process continues in subsequent cycles with primers being extended and ever more binding sites being presented. This leads to rapid amplification of the region flanked by the primer pair, which quickly dominates the DNA population (**Fig. 2.1**). The amount of PCR product at the end of the reaction depends on both the number of cycles and the original quantity of DNA containing the primer sites. PCR products are run on an electrophoresis gel to be visualised.

For the determination of the transgenic status of mice, DNA is extracted from tail tips for PCR analysis of DNA sequences specific to the transgenic construct for these reactions. For RT-PCR, RNA is extracted from biological tissues and used to synthesis DNA with *reverse transcriptase*, an enzyme used by retroviruses to build DNA from an RNA template. Oligo dT, an oligonucleotide string of 'T' bases that will bind the poly-A tail of extracted mRNA, is used as a primer for this reaction to build a complementary DNA (cDNA) library of the biological tissue.

Figure 2.1

This figure seeks to give a simplistic understanding of the polymerase chain reaction (PCR). This procedure first demands the design and synthesis of two oligonucleotide primers complementary to sense and antisense regions of DNA separated by 100-1,500 bases. If these primers are then added to even very tiny amounts of DNA containing the complementary regions, the DNA region that they flank can be amplified using a bacterial polymerase to levels detectable by gel electrophoresis.

1.1 (cycle 1, step 1). Sense and antisense primers are mixed in excess with DNA and heated to 94°C to denature and separate DNA strands.

1.2 (cycle 1, step 2). Temperature is lowered to 2-3 degrees below the primer melting temperature (Tm), usually between 50-60°C, and primers anneal to the complementary region s of DNA for which they were designed.

1.3 (cycle 1, step 3). Temperature is raised to the optimal polymerisation temperature of 72°C. Annealed primers are extended in a 5' to 3' direction by the addition of complementary phosphorylated deoxyribonucleotide bases (dNTPs).

2.1 (cycle 2, step 1). The mixture is returned to 94°C for the beginning of a second cycle. Extended primers are separated from DNA and the whole procedure begins again. This time however there are more sites for binding of the primers (2.2), and more new DNA spanning the region is synthesised (2.3).

3.1 (cycle 3, step 1). By the beginning of the third cycle DNA fragments are emerging that exactly span the region between the two primers, being synthesised from the extended primer for the complementary strand.

6.1 (cycle 6, step 1). Primer-flanked DNA fragments rapidly dominate the reaction. With further cycles the number of these DNA fragments increases in an exponential manner.

Polymerase chain reaction (PCR)

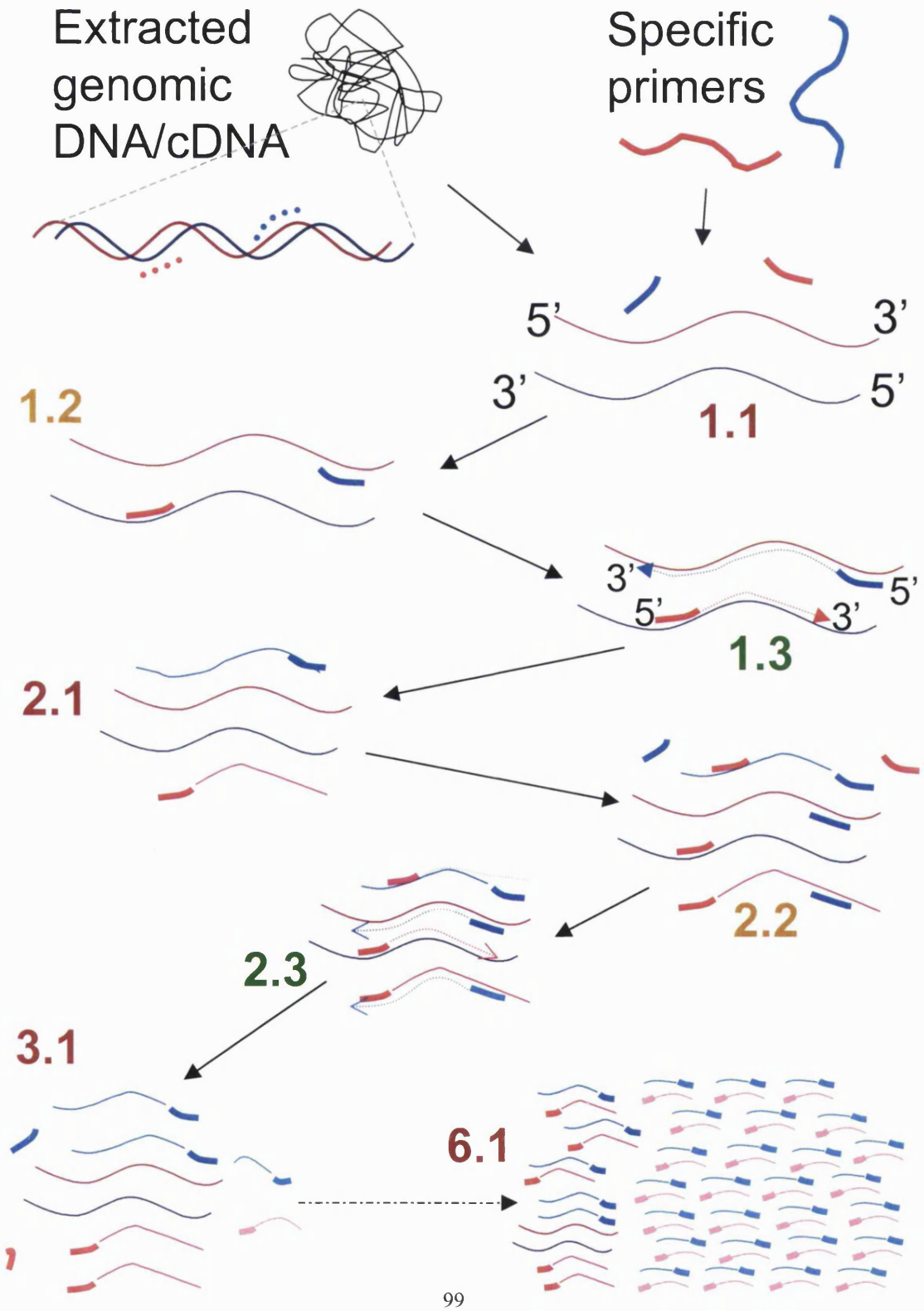

cDNA populations derived from extracted mRNA will represent only those genes that have been transcribed (or 'expressed') in the tissue of origin. The greater the levels of expression for a given gene, the greater the RNA extracted and the cDNA synthesised for that gene. The cDNA is then used in a conventional PCR reaction. The number of cycles is chosen so that the reaction is in a linear phase, usually between 20 and 35 cycles. This is the period when product yield is linearly related to the amount of starting template. After this the DNA polymerase becomes exhausted and the rate of amplification with more cycles falls sharply. If the reaction is stopped in the linear range, the expression levels of different genes (or the same gene from different tissues) can be analysed by comparing electrophoresis band intensities on a gel.

DNA extraction from tail tips

Mice were tail-tipped at post-natal day 10 (P10). The tail was anaesthetised and the tip (~5 mm) was removed with a pair of scissors. The tip was then placed in a 1.5 ml eppendorf. Where more than one mouse was tail-tipped at a time, instruments were all rinsed in 70% ethanol before removing the tail tips from the next mouse. Same-sex mice sharing a cage, were differentiated by punching a hole in the right and/or left ears.

200 µl PBS was added to each tail tip. Proteinase K (Sigma, UK) was diluted in distilled water to a concentration of 10 mg/ml and 10 µl was added to each tail tip in PBS. The eppendorfs were incubated at 52-55°C overnight. The tubes were all vortexed vigorously to break up the tissue and heated to 100°C for 5 minutes in a specialised heating block (Grant Instruments, UK) to inactivate the proteinase K. The tubes were spun in a microfuge for 2 minutes and the supernatants (containing the DNA) were transferred to a fresh 1.5 ml eppendorf. Tail-tip DNA was labelled and stored at –20°C until use for PCR. 2 µl was used for each PCR reaction.

RNA extraction for RT-PCR

An electric homogeniser was autoclaved and baked for 8 hours to destroy any RNases that may be present. Tissues to be used for RT-PCR were placed in a 5 ml bijou and PBS removed before placing –80°C. When they were to be used, they were removed from –80°C and kept on dry ice to avoid thawing. The electric homogeniser was set up in a fume hood, and 3 x 30 ml universal tubes were filled with DEPC-treated distilled

water to wash homogeniser thoroughly in each in turn after each usage. Each sample was weighed and compared with an empty bijou. Phenol- and guanidinium-based RNAzol-B (AMS Biotechnology Europe Ltd., Abingdon, UK) was added in units of 0.8 ml (0.8 per 100 mg of tissue). Use of RNAzol-B promotes the formation of RNA complexes with guanidinium and water and inhibits hydrophilic interactions of DNA and proteins. This isolates the RNA in the aqueous phase of the bi-phasic solution produced. Samples were immediately placed on ice following addition of RNAzol-B and were homogenised in turn. Homogenised samples were transferred to 1.5 ml eppendorfs and 0.1 volume of chloroform (Sigma, UK) was added to each sample. Samples were vortexed for 30 seconds and spun in a microfuge at 4°C for 30 min. The aqueous phase (which contains the RNA) was removed with extreme care to avoid DNA contamination from the interface, and an equal volume of isopropanol was added. Samples were immediately placed at –20°C overnight to precipitate RNA.

Samples were removed from –20°C and spun for 30 min at 4°C. The supernatant was carefully removed and the pellet rinsed with 200 µl RNase-free 70% EtOH and re-spun for 10 min at 4°C. The supernatant was discarded, the samples pulse-spun and the final drop removed with a pipette. Samples were air-dried for 5-10 minutes and the pellets resuspended in 20 µl DEPC-treated distilled water. 1 µl of each sample was then loaded with 3 µl of RNA ladder onto an RNA gel (see **2.12.**) to determine the concentration of extracted RNA. RNA was stored at –80°C.

cDNA synthesis

8 µl cDNA synthesis mix was made up for each RNA sample to be used for cDNA synthesis (reagents from Promega, USA):

5 µl 5x M-MLV reverse transcriptase (RT) buffer
1.25 µl dNTPs mix (each dNTP: 10 mM)
0.625 µl (50u) RNasin
1 µl (400u) M-MLV RT
0.125 µl DEPC-treated distilled water.

5 µg of each RNA sample was mixed with 1 µg (1-2 µl) of Oligo dT primer (Promega, USA). Each sample was made up to 17 µl with DEPC-treated water before

denaturation by 5 min at 70°C. 8 µl cDNA synthesis mix was added to each of the denatured RNA/Oligo dT samples to give a 25 µl reaction. Samples were immediately heated to 42°C for 90 min for the reaction to occur and then stored at –20°C.

Polymerase chain reaction (PCR) on genomic and complementary DNA

Separate reaction mixtures were made up for each set of primers to be used for DNA and control samples. Separate pipettes and filter tips were used and PCR reaction mixtures were made up in a designated PCR set-up to reduce the risk of DNA contamination. The following reagents were added for each reaction (reagents from Promega, USA):

1.25 µl 20 µM sense (or 'forward') primer
1.25 µl 20 µM antisense (or 'reverse') primer
0.8 µl 10 mM dNTPs
5 µl 10 times ammonium reaction buffer
1.5 µl 50 mM magnesium chloride
0.2 µl Taq Polymerase
38 µl distilled water

The reaction mixtures were divided into 48 µl aliquots and 2 µl DNA was added to each in a separate laboratory space again. The samples were loaded into a PCR machine that was programmed as follows:

Step 1 - 5 min @ 94°C
Step 2 - 30 sec @ 94°C
Step 3 - 30 sec @ 60°C
Step 4 - 1 min @ 72°C
Step 5 - GOTO Step 2 29 times (for 30 cycles)
Step 6 - 10 min @ 72°C

30 cycles were performed for RT-PCR and 35 cycles were performed for mouse tail-tip PCRs. 3 µl of orange G was added to 15 µl of each PCR product and run on an electrophoresis gel with a DNA ladder (see **2.8.**). The gel was examined for the presence and intensity of amplified fragments of the appropriate size.

Colony PCR

The following quantities were used per sample in the reaction mix for a colony PCR:

0.5 µl 20 µM sense (or 'forward') primer
0.5 µl 20 µM antisense (or 'reverse') primer
0.16 µl 10 mM dNTPs
1 µl 10 times ammonium reaction buffer
0.3 µl 50 mM magnesium chloride
0.04 µl Taq Polymerase
7.5 µl distilled water

The reaction mixtures were divided into 10 µl aliquots and a pipette tip was dipped into a bacterial clone, dipped into the PCR tube with reaction mixture, and finally placed into 3 ml **L-Broth** for an overnight culture at 37°C. The samples were loaded into a PCR machine that was programmed as follows:

Step 1 - 90 sec @ 94°C
Step 2 - 30 sec @ 60°C

Step 3 - 3 min @ 72°C
Step 4 - 20 sec @ 94°C
Step 5 - 20 sec @ 60°C
Step 6 - 2 min @ 72°C
Step 7 - GOTO Step 4 (8 times)
Step 8 - 20 sec @ 94°C
Step 9 - 20 sec @ 60°C
Step 10 - 3 min @ 72°C
Step 11 - GOTO Step 8 (19 times)

When the program was completed, 2 µl of orange G was added to each product and run on an electrophoresis gel with a DNA ladder. Overnight cultures from clones that did not give the desired amplified PCR product were discarded.

2.14. Manipulation of whole mouse embryos in culture

Mouse embryos removed from the uterus from E7.5 to E11.5 in the manner described in **2.9.** can be cultured whole for up to 48 hours (**Chapter 5**). Development may proceed relatively normally in good cultures. Manipulation of vertebrate embryos during development is usually restricted to chicks and zebrafish due to their accessibility. Mouse embryo culture allows interference in mammalian development without resorting to lengthy and costly transgenesis. I have implanted beads soaked with recombinant human bone morphogenetic protein-4 (BMP4) into the developing eye region of 10- to 25-somite mouse embryos (E9.5-E10.5) before culturing them for 24 hours in rat serum. Freshly extracted rat serum is essential for good cultures and this was performed in pairs by members of our department engaged in the practice of whole mouse embryo culture. Methods are based on Copp *et al.*, 1997.

Extraction of rat serum

This procedure is performed in pairs, with one individual handling the rats, spinning down the blood and preparing the serum, and the other individual operating on the rats and extracting the blood. Typically blood was extracted and serum prepared from 15 adult Wistar rats in a single morning.

A single rat was placed within a fume hood in a glass chamber containing tissue soaked in ether (BDH, UK) until unconscious. The use of ether for this procedure is essential because other anaesthetics impair the quality of the rat serum. The rat was then removed from the chamber and an ether-soaked nose cone fitted to maintain unconsciousness. Unconsciousness was checked by ensuring a lack of reflexes to a sharp pinch between the digits. A small volume of 70% ethanol in distilled water was spread over the abdominal area and, lifting the skin clear with forceps, a longitudinal incision was made using a pair of dissection scissors (Raymond Lamb, UK). The intestines were removed from the abdominal cavity to expose the posterior wall. An incision was made in the posterior tissue overlying the descending aorta using scissors. A 21 gauge needle was inserted into the descending aorta and blood extracted with a 20 ml syringe. The diaphragm was opened with a pair of scissors to ensure the rat was dead. The blood was immediately placed in a 15 ml falcon 2059 tube (Becton Dickenson, USA) spun down for 5 minutes in a centrifuge at 13,000 rpm. Forceps were used to squeeze serum out of the aggregated plasma and the blood

was spun again for 5 minutes. The clear serum was then transferred into a fresh falcon 2059 tube and spun for a further 5 minutes. The supernatant was transferred to a new tube. When the serum was extracted from all the rats to be used, it was divided into 5 ml aliquots and stored at –20°C. The approximate yield was 5 ml per rat.

Dissection of E9.5 and E11.5 mouse embryos for culture

The uteri from timed pregnant mice were removed as described in **2.9.** and placed in D-MEM/10% FCS. E9.5 and E11.5 embryos were immediately dissected out in a small petri dish in D-MEM/10% FCS under a dissecting microscope (Zeiss, Germany) with strong under and overhead lighting. All fat and blood vessels (mesometrial tissue) were cut away from the uterus using iridectomy scissors (Zeiss, Germany) and removed from the dish. No. 5 watchmaker's forceps (Raymond Lamb, UK) were used to tear the uterus along the mesometrial surface. Forceps were placed at one end of the uterus and a series of small tears were made. The forcep tips were carefully repositioned after every tear. On exposure of each conceptus, the forceps were used to carefully tease it free, and a pasteur pipette was used to transfer it to a fresh dish of D-MEM/10%FCS (transfer to a fresh dish of medium was performed after removal of each successive extra-embryonic layer). Very sharp No. 5 watchmaker's forceps (Interfocus, Haverhill, UK) were used to remove further layers.

The decidual layer of each conceptus was then removed. This was carefully torn away at the thicker placental side of the conceptus revealing the ectoplacental cone at early stages (~E10.5 and earlier). The remaining decidua was then carefully peeled away from underlying layers in its entirety. The trophoblast layer and underlying Reicharts membrane were removed right up to the cone (of which they form a part). This was done with great care as if peeling an orange, indicating the successful removal of both layers at the same time. Embryos were then cultured in their intact yolk sacs. At E11.5, when the ectoplacental cone had developed into a well vascularised placenta, the placental region was left intact if embryos were to be cultured prior to analysis. In these instances, the decidua was removed up to the placenta and trimmed with iridectomy scissors. The trophoblast layer and Reicharts membrane were similarly peeled away up to the placenta. A small incision was made in the yolk sac adjacent to the placenta, avoiding large blood vessels, and the yolk sac was lifted to expose the embryo head, leaving the embryo ready for culture.

Culture of E9.5 and E11.5 mouse embryos

Round-bottomed 20 ml universal tubes were used for culture and laboratory grease (Borer Chemie, Switzerland) was applied around the mouth of the tube to provide an airtight seal when closed. E9.5 mouse embryos dissected down to the yolk sac were rinsed in **explant saline** and placed into 1 ml rat serum per embryo in a culture tube (2-3 embryos per tube). E11.5 mouse embryos were rinsed in explant saline and transferred into individual tubes with 3-5 ml 25% rat serum in **culture saline**. A glass pipette was inserted into a tube attached to a 20% oxygen, 5% carbon dioxide source for E9.5 mouse embryos, and 95% oxygen for E11.5 mouse embryos (gas supplied by CryoService Ltd., Worcester, UK). The gas was switched on to a level detectable on the forearm before attachment of the pipette. The pipette was placed into the tube for one minute, the lid otherwise covering the mouth of the tube and the gas gently rippling the surface of the liquid. The tubes were placed on a roller incubator (B.T.C. Engineering, Cambridge, UK) at 37°C for up to 24 hours and gassed again every four hours (embryos were not gassed overnight). At the end of the culture period the yolk sac and amnion were removed in a petri dish. Embryos were placed into 4% paraformaldehyde to be prepared for whole mount *in situ* hybridisation (**2.12.**).

Preparation and implantation of BMP4-soaked beads

10 µl of agarose beads (Bio-Rad Laboratories, CA, USA) in sodium azide solution were placed in a 1.5 ml eppendorf and washed with 3 changes of 1ml embryo water (Sigma, UK). The beads were spun down in a microfuge between solution changes. After washing, 4.3 µl of 113 $\mu g ml^{-1}$ BMP4 (kindly provided by the Genetics Institute, Cambridge, MA, USA) was added to the beads. For controls 0.1% bovine serum albumen (BSA; Promega, USA) in PBS was added to the beads. The beads were incubated for 30 minutes to an hour at 37°C prior to implantation.

After 1-2 hours of culture, embryos were removed from culture (one tube at a time) to be operated on. E9.5 mouse embryos were transferred to a dish of D-MEM/10% FCS. A small tear was made using very sharp No. 5 watchmaker's forceps (Raymond Lamb, UK) in the yolk sac adjacent to the ectoplacental cone. With care to avoid vascular regions, an arc around approximately one third of the cone (on the side of the embryonic head) was cut using iridectomy scissors. The very sharp No. 5

watchmaker's forceps were passed through the opening in the yolk sac and a tear was made in the amniotic sac to expose the eye region. A small hole was made posterior to the exposed embryonic optic vesicle using a tungsten needle. 1 µl soaked beads were pipetted into the dish beside the embryo and a mouth-operated holding pipette was used to lift a bead and place it into the hole made posterior to the optic vesicle. Holding pipettes were made by flaming the centre of a 10 centimetre (cm) piece of capillary tubing and pulling hard to draw out a thin 5-10 cm region. The capillary tubing was then broken to give a tip of the desired diameter. Fresh beads were pipetted into the dish for each new operation, and one embryo from a single culture tube was usually not operated on as a control. Following the operation(s), embryos were returned to their tube of rat serum, gassed again for 1 minute with 20% oxygen and placed back at 37°C on the roller.

E11.5 mouse embryos removed from culture were transferred to a dish of explant saline. A small hole was made with a tungsten needle in the lens vesicle or just ventral to one of the eyes. 1 µl soaked beads were pipetted into the dish beside the embryo. A mouth pipette was used to lift a bead and place it into the hole made by the tungsten needle. Fresh beads and fresh explant saline was used for each new operation. After the operation, each embryo was returned to its tube of rat serum in culture saline, gassed again for 1 minute with 95% oxygen and placed back at 37°C on the roller.

Culture of E9.5 mouse eye explants

Eye explant cultures of E9.5 were carried out with BSA-soaked and BMP4-soaked beads. Embryos were obtained and dissected out of their extra-embryonic membranes as described above. The heads were removed and halved along the midline using iridectomy scissors. Beads were placed into the optic vesicles, approaching from the inside, using a mouth pipette. In one optic vesicle a BMP4-soaked bead was placed. On the other a BSA-soaked bead was placed. A falcon 35-3037 centre-well organ culture dish (Becton Dickinson, USA) was humidified with DEPC water and filter paper (baked for 8 hours at 180 C to destroy any RNases). D-MEM with 20% FCS was placed in the centre well of the organ culture dish. Isolated tissue pieces were cultured on a 0.8 µm filter (Millipore, USA), placed on a piece of gauze (Raymond Lamb, UK; also baked for 8 hours) over the centre well and floating in the medium.

These were placed at 37 C in a 5% CO_2 incubator (Heraeus Equipment Ltd., Brentwood, UK) for 24 hours.

2.15. Building of the *α-p0-Tbx5-ires-gfp-intron-pA* construct and microinjection into mouse embryos

For the building of the *α-p0-Tbx5-ires-gfp-intron-pA* construct (**Chapter 6**), a number of molecular techniques were employed. Gel extraction of DNA fragments cut by restriction digestion and run on an electrophoresis gel was used to isolate genetic elements. Ligation of gel-extracted fragments with linearised plasmids was performed to allow genetic elements to be introduced into a plasmid. Following addition of a genetic element to a plasmid a sub-cloning step was required to amplify the new recombinant DNA. Site-directed mutagenesis was used to introduce a restriction site (*Sac*II). Successfully mutated plasmids were amplified and sequenced to ensure there were no errors. Finally the construct was excised using restriction digestion (with *Nhe*I and *Xho*I) and gel extraction to be microinjected into mouse embryos. Injected embryos were implanted into pseudopregnant female mice. Cloning, restriction digestion, and gel electrophoresis are described in **2.8.**. Site-directed mutagenesis, cycle sequencing, gel extraction and DNA ligation are described in this section. Embryo injection and transplantation into pseudopregnant females was performed by Katie Gardener and is described here.

Site-directed mutagenesis of Tbx5

Site-directed mutagenesis is loosely based on the polymerase chain reaction (PCR; see **2.13.**). Complementary primers 30-35 bases long containing the mutation(s) are used to bind to the circular DNA in an annealing step (following denaturation). A particularly long extension step is used to allow synthesis of a strand of the entire vector from the primer. Cycling allows amplification of the vector with the mutations present in the primers. By the final extension the reaction will be dominated by mutated vectors. *Dpn*I restriction enzyme is used to destroy original vectors: these were cloned in *Escherichia coli* and are methylated while mutated vectors were made in a PCR machine and are not. *Dpn*I cuts only methylated DNA. The mutated vectors are amplified in *Escherichia coli* (these will repair gaps in the DNA from incomplete

extension as well as allowing plasmid amplification). Mutated plasmids must be sequenced (see below) because errors during polymerisation in PCR are common.

DNA sequencing

Cycle sequencing, now the most common type of sequencing, was used. Cycle sequencing is related to PCR, it uses standard PCR primers in a reduced concentration and larger amounts of DNA. One primer is used for one sequencing reaction. A polymerisation reaction is carried out with phosphorylated deoxyribonucleotides (dNTPs) intermixed with those that are labelled with fluorescent tags coloured according to the base type. These tagged dNTPs have their 3' hydroxyl group missing to prevent further extension. This leads to the production of DNA fragments of differing lengths all beginning with the primer and ending with a fluorescent-labelled dNTP. The reaction product is run on a polyacrylamide gel, and the different fragments are all separated according to size and will fluoresce, the colour signifying the terminal base of each fragment. Usually sufficient DNA is present at the end of the reaction so that each base 100-500 bases downstream of the primers is represented by fluorescing DNA fragments in sequential locations across the gel. Colour coding of the fluorescent tags allows the DNA sequence to be read from the gel.

125-250 ng of DNA to be sequenced was placed in a 500 µl eppendorf with 1.6 pmol of primer and 4 µl terminator ready reaction mix (Applied Biosystems, Warrington, UK). Tubes were made up to 10 µl with distilled water and placed in a PCR machine with the following program:

Step 1 - 5 min @ 94°C
Step 2 - 30 sec @ 94°C
Step 3 - 30 sec @ 60°C
Step 4 - 1 min @ 72°C
Step 5 - GOTO Step 2 29 times (for 30 cycles)
Step 6 - 10 min @ 72°C

1 µl 3M sodium acetate (pH 4.65) and 25 µl 95% ethanol was added to each tube and the tubes were incubated on ice for 10 minutes. Tubes were spun for 30 minutes at 4°C and the supernatant discarded. The DNA was washed with 200 µl 70% ethanol and the tubes were spun for 10 minutes at 4°C. The supernatant was discarded, the

tubes pulse-spun, and the final drop was removed with a pipette. The DNA was dried in a vacuum centrifuge for 5 minutes and stored at –20°C. The DNA was resuspended and run on a polyacrylamide gel. The gel was computer-analysed and the readout of the sequence was examined using *Editview 1.0.1.* software on an Apple Macintosh.

Gel extraction of DNA

Gel extraction is the extraction of a DNA fragment from an agarose gel. DNA was digested with restriction enzymes to cut out the fragment of interest (see **2.8.**). If the desired fragment was a vector destined to receive a DNA insert, the ends were in some cases de-phosphorylated with alkaline phosphatase. 1 µl calf intestinal alkaline phosphatase (Roche, UK) was added to the digested DNA and incubated at room temperature for 10 minutes. De-phosphorylation of the vector ends will inhibit re-circularisation of the vector in any subsequent ligation reactions, and thus favour uptake of a phosphorylated insert. This is because phosphorylation of at least one of the DNA ends is required for a successful ligation reaction. After incubation, alkaline phosphatase was inactivated by the addition of 0.1 volume of 200 mM EGTA and a 10 minute incubation at 65°C.

Following digestion (and treatment with alkaline phosphatase if necessary), the DNA was run on an agarose gel until good separation of the DNA fragments was achieved (see **2.8.**). Placing tape over the gel comb for setting the gel created large wells for large amounts of DNA. Samples were run at a very low voltage (10-15 volts) overnight to encourage good separation. Bands of an appropriate size were excised using a sharp scalpel and weighed in 1.5 ml eppendorfs. A Qiagen gel extraction kit (Qiagen, UK) was used for extraction of DNA from gel slices. 3 volumes of buffer QG were added to each tube (100 µg ~ 100 µl) and the tubes were incubated at 50°C for 10 minutes, vortexing the tubes every few minutes to help the gel slice to dissolve. 1 volume of isopropanol was added to the tubes and the mixtures were vortexed and decanted into Qiagen columns in 2 ml microtubes. Columns were spun for 1 minute in a centrifuge and the supernatant was discarded. 0.5 ml buffer QG was added to each column to remove traces of agarose remaining. The columns were spun for 1 minute and the supernatants discarded. 0.75 ml buffer PE was added to each column to wash the DNA. The columns were spun for 1 minute, the supernatants were discarded and the columns were spun again to clear residual buffer, which was discarded. 50 µl

buffer EB was placed in the centre of each column, the columns were transferred to a fresh microtube and spun for 1 minute to elute the DNA. Elutant was transferred into a labelled eppendorf and stored at –20°C. 0.5, 1 and 2 µl were run on a gel with a ladder (see **2.8.**) to determine the concentration and purity of the extracted DNA.

For gel extraction of the digested complete construct – to be used for microinjection into fertilised eggs, **injection buffer** was used instead of the buffer EB supplied by the Qiagen gel extraction kit. Gloves were removed because fine powder from the gloves may potentially block the injecting needle. After careful quantification by agarose gel electrophoresis the elutant was diluted to 5-10 ng/µl and spun on a SpinX column (Corning Inc., NY, USA) to ensure purity. Aliquots were kept frozen before being thawed and microinjected into mouse embryos (see below).

DNA ligation

DNA ligation is the joining of compatible ends of DNA. Where DNA has been cut using a restriction enzyme (see **2.8.**), it may be re-joined using a bacterial enzyme, T4 DNA ligase. DNA fragments may be incorporated into a vector by ligating the ends of the fragment to the ends of a linearised vector. Ligation is most effectively performed on compatible 'sticky' ends (see page 76), usually cut with the same restriction enzyme, though can be performed on 'blunt' ends.

50-100 ng of linearised vector was added to a tube with 1 µl of T4 ligase buffer and 0.5 µl T4 DNA ligase (Promega, USA) and made up to 10µl with distilled water. Where a DNA fragment was to be inserted, an equimolar amount of the fragment was added to the mixture. Thus for a DNA fragment 20% the length of the linearised vector, 10 ng would be added to 50 ng of vector. A reaction without the DNA 'insert' was always set up to act as a control. A reaction was also set up with a 3:1 molar ratio, *i.e.* 30 ng of a DNA fragment 20% the size of the linearised vector would be added to 50 ng of the vector. This was because different molar ratios may favour different ligation reactions. Ligation reactions, all made up to 10 µl with distilled water, were incubated for 3 hours at room temperature, overnight at 4°C, or for over 18 hours at 16°C. The range of reaction conditions is created by different optimal temperatures of enzyme activity (room temperature) and DNA ligation (4°C).

Ligated DNA was electroporated into *Escherichia coli* (see **2.8.**) and different clones were miniprepped and screened for the insert with restriction digestion. Alternatively, when large numbers of colonies required screening, a colony PCR was performed (see **2.13.**). Only positive colonies were subsequently miniprepped. Equal numbers of colonies on control plates (vector only) and vector-plus-insert plates was a sign that incorporation of the insert to the vector was unsuccessful. In these cases clones were usually found to contain re-circularised vector only.

Injection of DNA into mouse embryos

Female CBA/B6 mice were superovulated through the administration of gonadotropins. Pregnant mare's serum (PMS) was used to mimic follicle-stimulating hormone (FSH) and human chorionic gonadotropin (hCG) was used to mimic luteinising hormone (LH). Powdered PMS (Sigma, UK) was resuspended at 50 IU/ml in sterile 0.9% sodium chloride and 0.1 ml (5 IU) was injected intraperitoneally into female CBA/B6 mice at 3-5 weeks of age. Powdered hCG (Intervat, UK) was resuspended at 500 IU/ml in sterile water and stored at –20°C. 100 µl of this hCG stock was added to 1 ml of 0.9% sodium chloride to give a working concentration of 50 IU/ml. 0.1 ml (5 IU) was injected intraperitoneally 42-48 hours after the PMS injection. Injections were timed with the light/dark cycle of the mouse (controlled in their holding room) so that the hCG was administered prior to endogenous LH release in response to the injected PMS. Following injection of the hCG, the female is placed in a cage with a stud male and checked for a copulation plug the next morning.

Pre-implantation mouse embryos were collected the day following mating by sacrificing the mouse and exposing the uterus as described in **2.9.**. At the distal ends of the uterine horns lie the oviducts and then the ovaries. The oviducts with attached ends of uterus were cut away from the ovaries, the attached mesometrium and the distal uterus and placed into a petri dish with M2 medium (Sigma, UK) at room temperature. Oviducts were placed in ~300 mg/ml hyaluronidase solution (Sigma, UK) in M2 medium in a fresh petri dish and viewed at 20x or 40x magnification under a stereomicroscope. One pair of watchmaker's forceps (Raymond Lamb, UK) were used to hold down the infundibulum (the distal opening of the oviduct), whilst another pair was used to tear the oviduct to release the clutch of eggs from the ampulla. Eggs were incubated in the hyaluronidase solution for one minute to remove the sticky

cumulus cells that surround them and then washed by transferring into a fresh dish of M2 medium using sterile transfer pipettes. Transfer pipettes were made as described in **2.14.** except that care was taken to smooth the pipette tip to a diameter of 150-200 μm using a microforge. Eggs were transferred into IVF-20 (Vitrolife, Sweden) to be cultured for 3-5 hours until the pronuclei are readily visible (but before the nuclear membrane disappears prior to first cleavage) and are ready for microinjection.

A micropipette was used to dispense 20-40 μl drops of IVF-20 in an array on the bottom of a 35-mm petri dish. These were then covered with light paraffin oil using a 5 ml pipette and embryos were transferred into the microdrops to be kept at 37°C. The two halves of the dish were marked as injected (to be microinjected with DNA) or control (no injection to control for procedural toxicity). Microinjection was performed using an inverted microscope with a fixed stage and image-erected optics (Nikon, Japan). Bright-field microscopy was used with a 40x objective and 10x eye pieces to give a 400x magnification. Micromanipulators (Zeiss-Jena, Germany) were mounted on either side of the microscope stage. One held the holding pipette (made as described in **2.14.** except that care was taken to smooth and bend the pipette tip to a diameter of ~15 μm using a bunsen burner), which was first filled with mineral oil (Sigma, UK) using a 26-gauge fine needle. The other held the injecting pipette, which was made with thin-walled capillary tubing (Clark Electromedical Instruments, Edenbridge, UK) using a micropipette puller (Sutter Instrument Co., CA, USA) and filled with 1 μl of DNA. The holding and injecting pipettes were attached, through lengths of Tygon plastic tubing, to a Transjector 5246 (Eppendorf, Germany).

A flat ~5 mm diameter drop of M2 medium was placed on a siliconised depression slide (BDH, UK) and was covered with mineral oil. This 'injection chamber' was placed on the microscope stage with the microinjection set-up described above. Embryos from a single droplet (from the 'injected' side) on the microdrop array were transferred into the M2 medium in the injection chamber. Each single cell embryo was sucked onto the end of the holding pipette and the pronuclei were visualised. The male pronucleus, being larger and (usually) nearer the egg surface, was targeted for microinjection. The injection pipette tip was pushed through the zona pellucida and into the egg towards the pronucleus avoiding the nucleoli (they are sticky and may adhere to the pipette). DNA solution was injected when the tip was inside the

pronucleus. If successful then the pronucleus swelled visibly and the pipette was quickly removed from the egg. 15 minutes maximum was allowed for microinjection of embryos from a single droplet (embryos may become damaged if left too long at room temperature) before they were transferred back to the microdrop culture.

Implantation of injected embryos into pseudopregnant female mice

Healthy looking injected embryos (with a distinct outline and perivitelline space between the egg and the zona pellucida) were transferred into pseudopregnant female mice the same day as microinjection. Pseudopregnant mice were prepared by mating a CD1 female mouse with a vasectomised male the night before implantation of injected embryos. A waxy copulation plug still forms after mating (it is made from the coagulation of semen proteins) and the uterus becomes receptive to embryo implantation, but the females own eggs are not fertilised and they degenerate, in pseudopregnant mice. Injected embryos are transferred into the pseudopregnant mouse oviduct the day the copulation plug has been detected (E0.5). If pseudopregnant mice were not immediately available following embryo injection then the embryos could be cultured *in vitro* a further one or two days (to the two-cell or morula stage respectively) and still be implanted into the oviduct at E0.5. Alternatively the injected embryos could be cultured a further day to the blastocyst stage and transferred into the uterine horns of E2.5 (or E3.5) pseudopregnant mice.

The pseudopregnant mouse to be operated on was anaesthetised with an intraperitoneal injection of 0.015 to 0.017 ml of 2.5% avertin (Winthrop Laboratories, NY, USA) per gram of body weight and laid face down on the lid of a 9-cm plastic petri dish. Healthy looking embryos from the microdrop cultures were transferred into M2 medium and loaded into a mouth pipette-operated transfer pipette. To load the transfer pipette, it was first filled with light paraffin oil, then a small air bubble was taken up, then a short column of M2 medium and a second air bubble. 15-30 embryos were then drawn up, followed by a third air bubble and a second short column of M2 medium. Leakage of pipette contents was prevented prior to use by pressing it into a piece of Plasticine secured to the base of the stereomicroscope.

The back of the recipient mouse was wiped with 70% ethanol and a small (less than 1 cm) transverse incision was make in the skin, about 1 cm to the left of the spinal cord,

at the level of the last rib, using fine dissection scissors. The body wall was lifted with watchmaker's forceps and a small incision was made just over the ovary (orange). Blunt fine forceps were used to pick up the fat pad (white) and pull out the attached left ovary, oviduct and uterus. A Serrefine clamp (Electron Microscopy Sciences, PA, USA) was clipped onto the fat pad to secure the oviduct and ovary outside the body wall. The embryo was placed under a stereomicroscope and the infundibulum (the oviduct opening) was located. The swollen ampulla was located under the bursa (a thin, transparent membrane containing blood vessels surrounding the oviduct and ovary). A hole was made in the bursa over the infundibulum using two pairs of sharp, fine-tipped watchmaker's forceps, avoiding large blood vessels. The edge of the infundibulum was lifted with blunt forceps and the transfer pipette was inserted into the opening of the ampulla. The mouth pipette was used to push the injected embryos into the ampulla. The Serrefine clamp was removed and the fat pad (with attached ovary, oviduct and uterus) was replaced inside the body with blunt fine forceps. The body wall was sewn up with one or two stitches and the skin was closed with wound clips. The mouse was returned to its cage to be left undisturbed in a warm quiet place.

2.16. Building of the M/C-*mTbx5*/pUAST constructs

For the building of the M/C-*mTbx5*/pUAST constructs (**Appendix I**) as well as techniques such as sequencing, gel extraction and ligation (described in the previous section) additional techniques were used. Complementary pairs (sense and antisense) of oligonucleotides were designed and synthesised by Thermo Hybaid, UK. These were annealed and used as DNA linkers for insertion into plasmids. On receipt of the linkers, they were diluted in TE buffer (10 mM Tris buffer pH 8.0, 1 mM EDTA) and each complementary pair mixed to give 40 μM concentrations of sense and antisense linker in 50 μl volumes. To anneal the linkers, sense/antisense solutions were incubated at 90°C for 5 hours in a PCR machine. The temperature was reduced to 20°C gradually over a period of a further 5 hours using the PCR machine. The linkers were kept at 4°C or below thereafter to inhibit dissociation and diluted to a concentration of 2 μM in TE buffer. For the ligation of annealed linkers to cut vector, large molar ratios of linker to vector were required because of the tiny size of the linkers in proportion to the vector (which was 50-100 times larger). 6.5 μl of annealed linker at concentrations of 2 μM or 200 μM were ligated with 50 μg of *Bss*HII-cut gel-extracted vector in a 10 μl overnight reaction at 4°C.

CHAPTER 3

T-box gene expression in the developing mammalian retina

INTRODUCTION

The first step towards the elucidation of *omb*-related T-box gene function in the developing eye was to determine their exact patterns of expression in the early retina. This allows identification of cell types and retinal regions in which they are active. I aimed to provide a detailed and comparative analysis of T-box gene expression in the developing mouse and human eye; reports to date have considered early stages of mouse development only and have not examined expression in humans (Chapman *et al.*, 1996).

In *Drosophila*, the *optomotor blind* (*omb*) mutant exhibits an inability to respond appropriately to rotary stimuli in a specially designed 'optomotor' maze. Anatomical analysis revealed disrupted neuronal connectivity within the fly optic lobes (Pflugfelder and Heisenberg, 1995). This phenotype is due to non-lethal mutations in a single gene, found to encode a member of the T-box family of transcription factors. Genetic cascades that underlie *Drosophila* development are frequently conserved in vertebrate species, so much that *Drosophila* genetics is increasing being used in the study of human disease (Bernards and Hariharan, 2001). This is true of the developing eye, despite the radically different structure of fly and vertebrate visual systems (Wawersik and Maas, 2000). The importance of *omb* in the developing fly visual system meant that homologues to *omb* might be important during development of the vertebrate eye. In the mouse, members of the *omb*-related mammalian subclass of T-box genes (the *Tbx2* subclass), *Tbx2*, *Tbx3* and *Tbx5*, were expressed in the developing retina (Chapman *et al.*, 1996).

In this study I explored in detail the expression of *omb*-related mammalian T-box genes within the developing eye. Expression was examined in mouse and human tissue throughout the period of eye morphogenesis and retinal stratification. I examined human tissue to prove the relevance of T-box genes to human eye development. Since very young specimens of human tissue were not available, T-box gene expression during early stages of eye development was only examined in mice.

T-box expression in mice was also analysed to provide a basis for the functional T-box gene studies undertaken in this species in chapters 5 and 6. It was necessary to

compare mouse and human expression to validate the mouse as a meaningful model for human T-box gene function. The use of mice as an experimental model is favoured for the study of mammalian development. Small rodents have long been popular for experimentation because their anatomy and physiology is similar to larger mammals and their small size makes for easy handling and husbandry. Though rats have traditionally been the rodents of choice, the relative ease of mouse transgenesis has led to the increasing use of mice. This is particularly true in developmental biology, where transgenic technology has been most effectively applied.

RESULTS

The expression of *omb*-related T-box genes *Tbx2/TBX2*, *Tbx3/TBX3* and *Tbx5/TBX5* was examined throughout mammalian eye development. The presence and distribution of the specific T-box mRNAs in mouse and human tissue were determined using reverse transcriptase-polymerase chain reaction (RT-PCR) and RNA *in situ* hybridisation. Expression of the *omb*-related T-box genes was compared with expression of *Tbx20*, a new gene identified in my laboratory. T-box gene expression was also compared with protein distribution of human POU4F2 (BRN3B), a marker for developing retinal ganglion cells (RGCs). An analysis of POU4F2 during human retinal development was carried out.

3.1. *Tbx2*, *Tbx3* and *Tbx5* are expressed in the dorsal retina during eye morphogenesis

Expression of *Tbx2*, *Tbx3*, and *Tbx5* was examined during eye morphogenesis in the developing mouse embryo. Analysis at the earliest stages of eye development was not possible in human tissue, as the youngest available specimens were at 6 weeks post-conception (wpc). At this stage the human optic vesicle had already invaginated to form the optic cup and the lens vesicle had formed: eye morphogenesis was essentially complete.

Mouse embryos of the CBA strain were analysed at embryonic day (E) 9.5 to E12.5 by performing whole mount *in situ* hybridisation to visualise the mRNA distribution

of T-box genes. Some *in situ* hybridisations were performed on cryosections of mouse tissue. Embryos examined at these timepoints were found to be between the 9- and 53-somite stage of development. During this period the newly formed optic vesicles expand from the prosencephalon (embryonic forebrain) to contact the surface ectoderm. Reciprocal signalling between the optic vesicle and the surface ectoderm is necessary for the formation of an optic cup from the former and a lens from the latter (Chow and Lang, 2001). The maturing optic cup surrounds the lens and comprises an inner multicellular neural retina and an outer monolayered retinal pigmented epithelium (RPE). See **1.1.** for a description of eye morphogenesis.

The variability of the somite stage between embryos examined at a specific timepoint, even within a single litter, makes length of gestation a poor measure of developmental stage. At early post-gastrulation stages of development I have used the number of paired somites adjacent to the neural tube as a consistent indicator of developmental stage.

T-box gene expression in the optic vesicles

Expression of *Tbx5* was first detected in the developing mouse eye using *in situ* hybridisation at the 9-somite stage of development. At this stage the post-gastrulation mouse embryo has already turned within the yolk sac so that the embryonic head faces its tail. The neural tube has closed rostrally and the optic pits (the first morphological sign of eye development) are deepening to become optic vesicles. *Tbx5* expression was faint and diffuse in the optic vesicles at this time (**Fig. 3.1A**).

By the 15-somite stage, *Tbx5* expression was clearly detected in the dorsal optic vesicles (**Fig. 3.1B**). This expression was predominantly in the region of the dorsal optic vesicle in direct opposition to the surface epithelium, but extended a short distance into more proximal dorsal neuroepithelium (**Fig. 3.1C**). It is the neuroepithelium in direct apposition to the surface epithelium that invaginates and develops as neural retina. I hereon describe this region as presumptive (or prospective) neural retina, and the more proximal optic vesicle as presumptive (or prospective) RPE. *Tbx2* was similarly expressed to *Tbx5* in the dorsal optic vesicles at 15 somites (**Fig. 3.1D, E**). *Tbx3* mRNA was not detected in the optic vesicles by 22 somites (**Fig. 3.1F**).

Figure 3.1

Tbx5 was expressed in the dorso-distal optic vesicles (**A-C**):

A Faint and diffuse *Tbx5* expression was first detected in the expanding optic pits of the 9-somite mouse embryo (arrow). Expression was also seen in the posterior (ventricular) region of the developing heart (**h**). Dorsal (**d**) orientation of the developing eye is indicated for all figures. Scale bar = 0.5 mm.

B *Tbx5* was expressed in the dorsal optic vesicle of the 15-somite mouse embryo. Expression was seen also in the posterior developing heart (**h**) and the emerging forelimbs (**f**). Dotted line indicates section shown in **C**. Scale bar = 0.5 mm.

C Vibratome section of embryo in **B** through the coronal plane and the dorso-ventral axis of the optic vesicle. *Tbx5* expression was seen in the presumptive neural retina (demarcated by point of contact with surface ectoderm, **se**, with dotted lines) and in the dorsal-most region of presumptive pigmented epithelium (proximal optic vesicle). Scale bar = 50 μm.

Tbx2, but not *Tbx3*, was expressed in the dorso-distal optic vesicles (**D-F**):

D *Tbx2* was expressed in the 15-somite mouse optic vesicles (arrow, dotted line=section in **E**), facial primordia (**p**), otic placodes (**o**), heart (**h**), forelimb bud (**f**) and allantois (**a**). Scale bar = 0.5 mm.

E Vibratome section of embryo in **D** through the coronal plane and the dorso-ventral axis of the optic vesicle. *Tbx2* expression was seen throughout the presumptive neural retina (distal optic vesicle adjacent to surface ectoderm, **se**), in the dorsal-most presumptive retinal pigmented epithelium (RPE; outside dotted line) and in the maxillary mesenchyme (**m**). Scale bar = 50 μm.

F *Tbx3* mRNA was detected in the developing maxillary region (**m**) the otic placodes (**o**) and the allantois (**a**), but not the optic vesicles, of the 22-somite mouse embryo. Scale bar = 0.5 mm.

Tbx2 and *Tbx5* persist in the late stage optic vesicles (**G-K**):

G At 24 somites *Tbx5* remains expressed in the dorsal optic vesicles (arrow), the posterior heart (**h**) and in the forelimbs (**f**). Dotted line indicates plane of section in **H**. Scale bar = 0.5 mm.

H Vibratome section of embryo in **G** through the optic vesicle. *Tbx5* expression was seen in the dorsal region of presumptive neural retina (adjacent to surface epithelium, **se**; demarcated by dotted lines) and over the dorsal boundary with presumptive RPE. Scale bar = 50 μm.

J *Tbx2* was expressed in the 27-somite mouse retina (arrow, dotted line=section in **K**), the facial primordia (**p**), otic placode (**o**), heart (**h**) and limb buds (**l**). Scale bar = 0.5 mm.

K Vibratome section of embryo in **J** through the optic vesicle. *Tbx2* was expressed across the presumptive neural retina (demarcated by dotted lines and adjacent to the lens placode, **l**) with higher levels dorsally, in the dorsal-most presumptive RPE and maxillary mesenchyme (**m**). Presumptive neural retina is. Scale bar = 50 μm.

mTbx2 and *mTbx5* are expressed in the dorsal optic vesicles

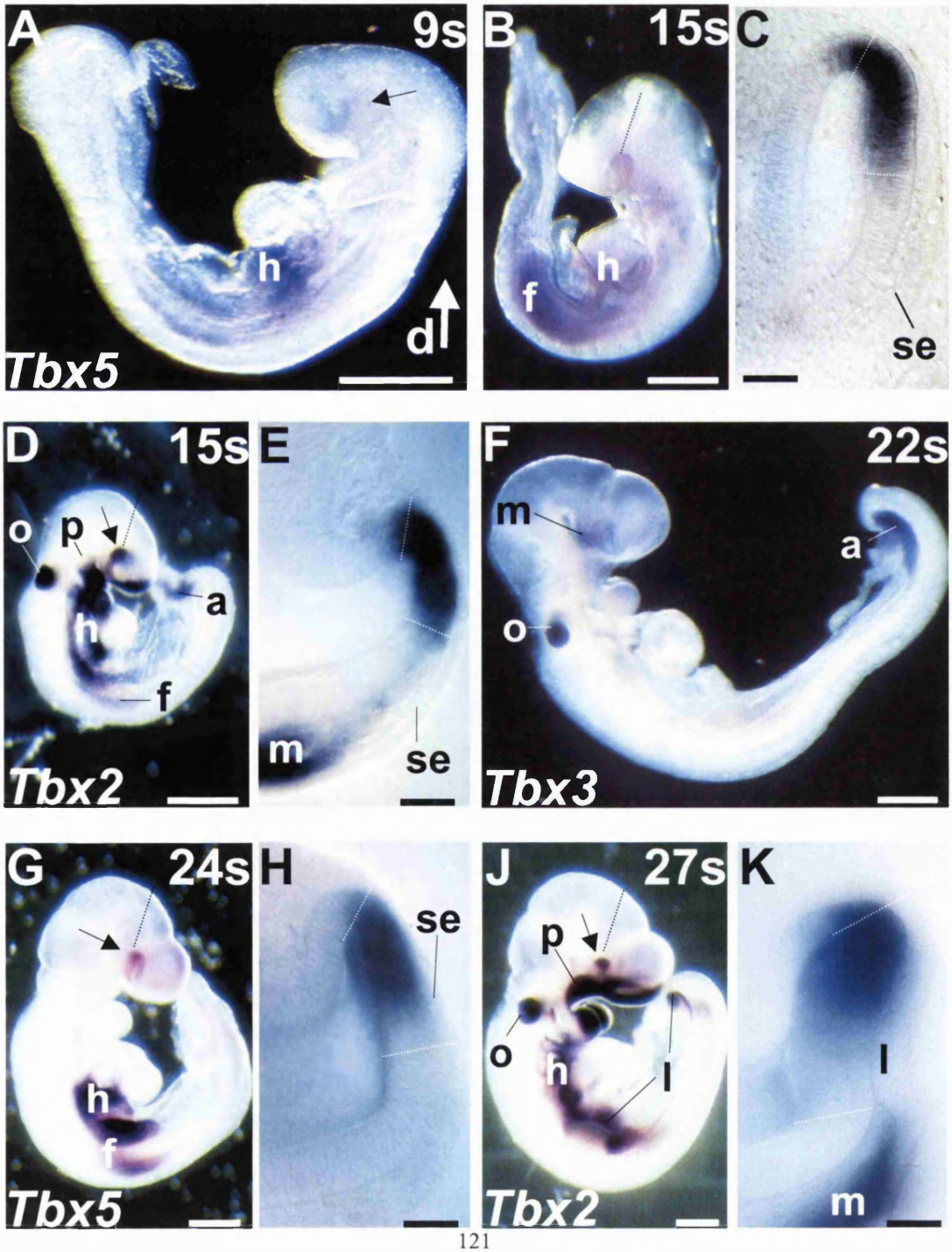

The optic vesicles flatten, presumptive neural retina thickens and invagination occurs between 25 and 30 somites. *Tbx2* and *Tbx5* expression persisted in similar patterns in late stage optic vesicles. *Tbx5* mRNA was detected in the dorsal half of presumptive neural retina and over the dorsal boundary with prospective RPE at 24 somites (**Fig. 3.1G, H**). *Tbx2* mRNA was detected across the presumptive neural retina with greatly reduced levels ventrally at 27 somites (**Fig. 3.1J, K**). *Tbx2* expression extended to the dorsal limits of presumptive RPE (**Fig. 3.1K**).

T-box gene expression in the optic cup

In the 32-somite mouse embryo *Tbx5* is restricted to the dorsal quadrant of the newly formed optic cup (**Fig. 3.2A, B**). The dorsal retina is defined relative to the ventral fissure, which is taken to be the ventral-most point in the optic cup. *Tbx2* expression is very similar to that of *Tbx5* in the optic cup. By 37 somites the *Tbx2* expression domain is of stronger intensity and expands further ventrally than that of *Tbx5* (**Fig. 3.2C, D**). *Tbx3* expression was not detected in the mouse retina at 38 somites (**Fig. 3.2E, F**).

The embryos shown in **Fig. 3.2** were sectioned using a vibratome to show slices through the dorsal and ventral optic cup (**Fig. 3.3A, B**). The thick, proliferating neural retina and the relatively thin RPE can be seen to contact the developing lens at this stage. *Tbx5* expression is restricted to the dorsal third of the neural retina and the dorsal ciliary margin (**Fig. 3.3A**). *Tbx2* shows a dorsal restriction of expression in the retina very similar to that of *Tbx5* (**Fig. 3.3B**).

In situ hybridisation reagents do not readily penetrate whole mount embryos larger than ~40 somites. Frontal cryosections of 40- and 35-somite mouse embryos were examined to more reliably look at expression of *Tbx5* and *Tbx2* (**Fig. 3.3C, D**). At 40 somites the neural retina is much thicker relative to the RPE and the lens was more fully enveloped. *Tbx5* expression was clearly seen throughout the dorsal tip of the retina, including the dorsal RPE (**Fig. 3.3C**). Graded *Tbx2* expression was seen in the 35-somite embryo across the dorsal half of the neural retina (**Fig. 3.3D**). *Tbx2* was also expressed in the dorsal RPE and in the ventral extra-ocular mesenchyme (**Fig.**

Figure 3.2

Expression of *Tbx5* and *Tbx2*, but not *Tbx3*, was detected in the dorsal quadrant of the optic cup (**A**-**F**):

A *Tbx5* expression was detected in the dorsal quadrant of the optic cup in the 32-somite mouse embryo (arrow). Expression was more strongly noted in the heart (concealed behind hindlimbs and tail) and the forelimbs (**f**). Dorsal (**d**) orientation of the developing eye is indicated for all figures.

B Close-up of the developing optic cup in **A**. Boundaries of the dorsal *Tbx5* expression domain is indicated by arrows. Dotted line indicates the plane of section for **Fig. 3.3A**. **nr**, neural retina; **vf**, ventral fissure; **le**, lens.

C In the 37-somite mouse embryo, *Tbx2* was expressed in a larger dorsal domain than that seen for *Tbx5*, within the dorsal half of the retina (arrow). Expression was also detected in the nasal, maxillary, and mandibular primordia (**p**), the otic vesicle (**o**), the heart (**h**), in anterior and posterior domains of the limb buds (**l**), and in the developing genital region.

D Close-up of the developing optic cup in **C**. Boundaries of the dorsal *Tbx2* expression domain (indicated by arrows) extend further ventrally than those of *Tbx5* in **B**. The nasal (**n**), maxillary Dotted line indicates the plane of section for **Fig. 3.3B**. **nr**, neural retina; **vf**, ventral fissure; **le**, lens.

E In the 38-somite mouse embryo, *Tbx3* expression could not be detected in the optic cup. Expression was detected in the developing maxillary and mandibular primordia (**m**), the otic vesicle (**o**), the heart (**h**), and in posterior domains of the limb buds (**l**). Scale bar = 0.5 mm for **A**, **C**, and **E**.

F Close-up of the developing optic cup in **E**. **nr**, neural retina; **vf**, ventral fissure; **le**, lens. Scale bar = 0.2 mm for **B**, **D**, and **F**.

mTbx2 and m*Tbx5* are expressed in overlapping domains in the dorsal E10.5 optic cup (l)

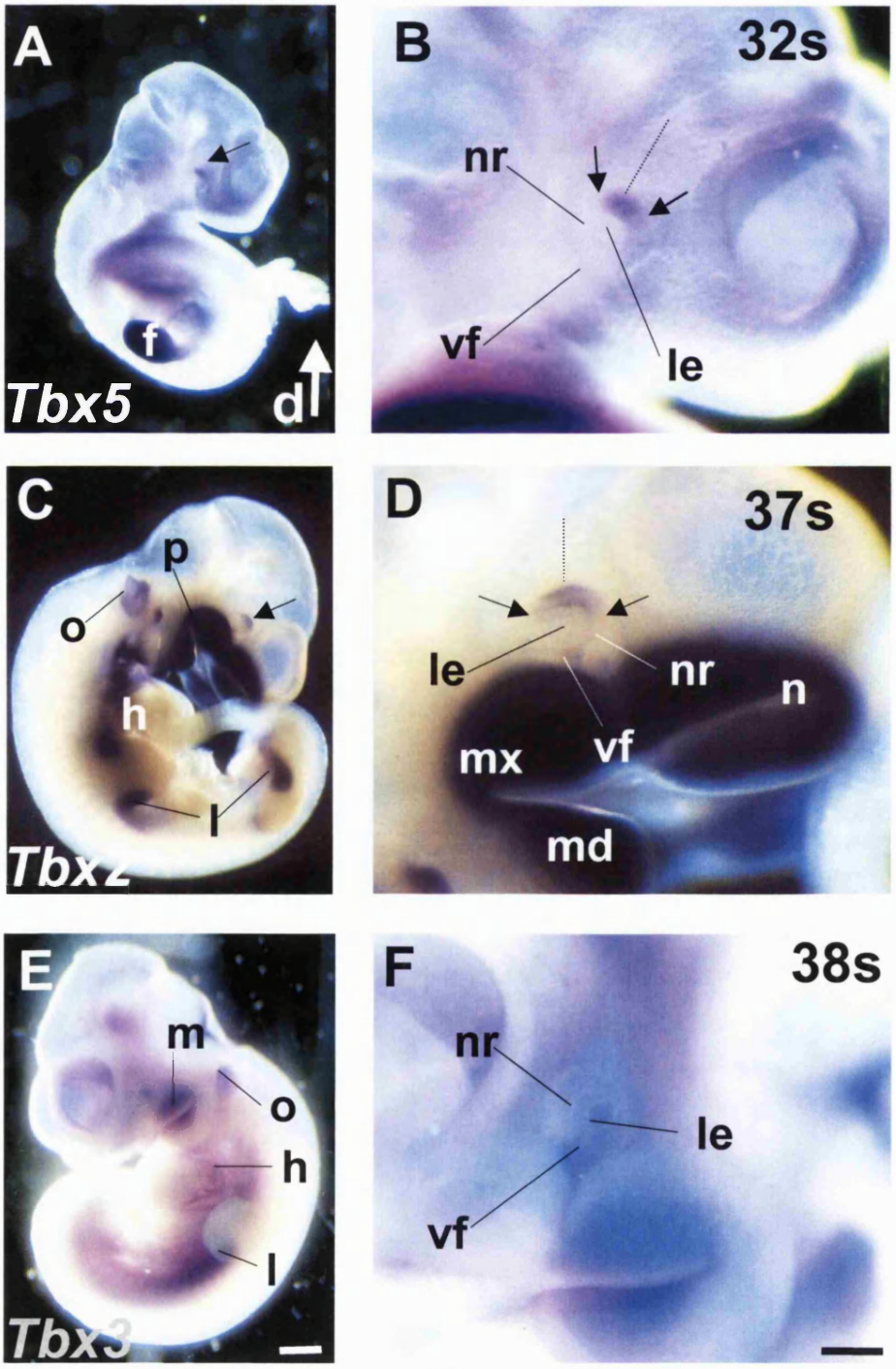

Figure 3.3

Vibratome sections of E10.5 embryos hybridised with *Tbx5*- and *Tbx2*-specific probes show gene expression in overlapping dorsal domains (**A, B**):

A Vibratome section of the embryo in **Fig. 3.2A, B**, the plane of section is indicated by the dotted line in **Fig. 3.2B**. *Tbx5* expression was detected in the dorsal pigmented epithelium and the dorsal third of neural retina at 32 somites in the mouse embryo. Dorsal (**d**) orientation of the developing eye is indicated for all figures. **nr**, neural retina; **pe**, pigmented epithelium; **le**, lens.

B Vibratome section of the embryo in **Fig. 3.2C, D**, the plane of section is indicated by the dotted line in **Fig. 3.2D**. Graded *Tbx2* expression was seen across the dorsal hemiretina and in the dorsal pigmented epithelium of a 37-somite mouse embryo. Strong expression in the maxillary mesenchyme was also seen. **nr**, neural retina; **pe**, pigmented epithelium; **le**, lens; **m**, maxillary mesenchyme.

In situ hybridisation on frontal cryosections confirm that *Tbx5* is expressed in a smaller more restricted dorsal domain across the optic cup than *Tbx2* (**C, D**):

C *Tbx5* expression was seen in the dorsal quarter of the neural and pigmented retina on frontal cryosections of a 40-somite mouse embryo. Note the pigment in the inner aspect of dorsal pigmented epithelial cells. **nr**, neural retina; **pe**, pigmented epithelium; **le**, lens.

D *Tbx2* expression was detected in the dorsal pigmented epithelium and neural retina on coronal cryosections of a 35-somite mouse embryo. Graded expression (diminishing ventrally) was seen across the dorsal hemiretina, expression was uniform across the width of the retina. *Tbx2* expression was detected in the ventral peri-ocular mesenchyme as well as in the maxillary mesenchyme. Note the pigment in the inner aspect of dorsal pigmented epithelial cells. **nr**, neural retina; **pe**, pigmented epithelium; **le**, lens; **m**, maxillary mesenchyme. Scale bar = 0.1 mm for all figures.

mTbx2 and *mTbx5* are expressed in overlapping domains in the dorsal E10.5 optic cup (II)

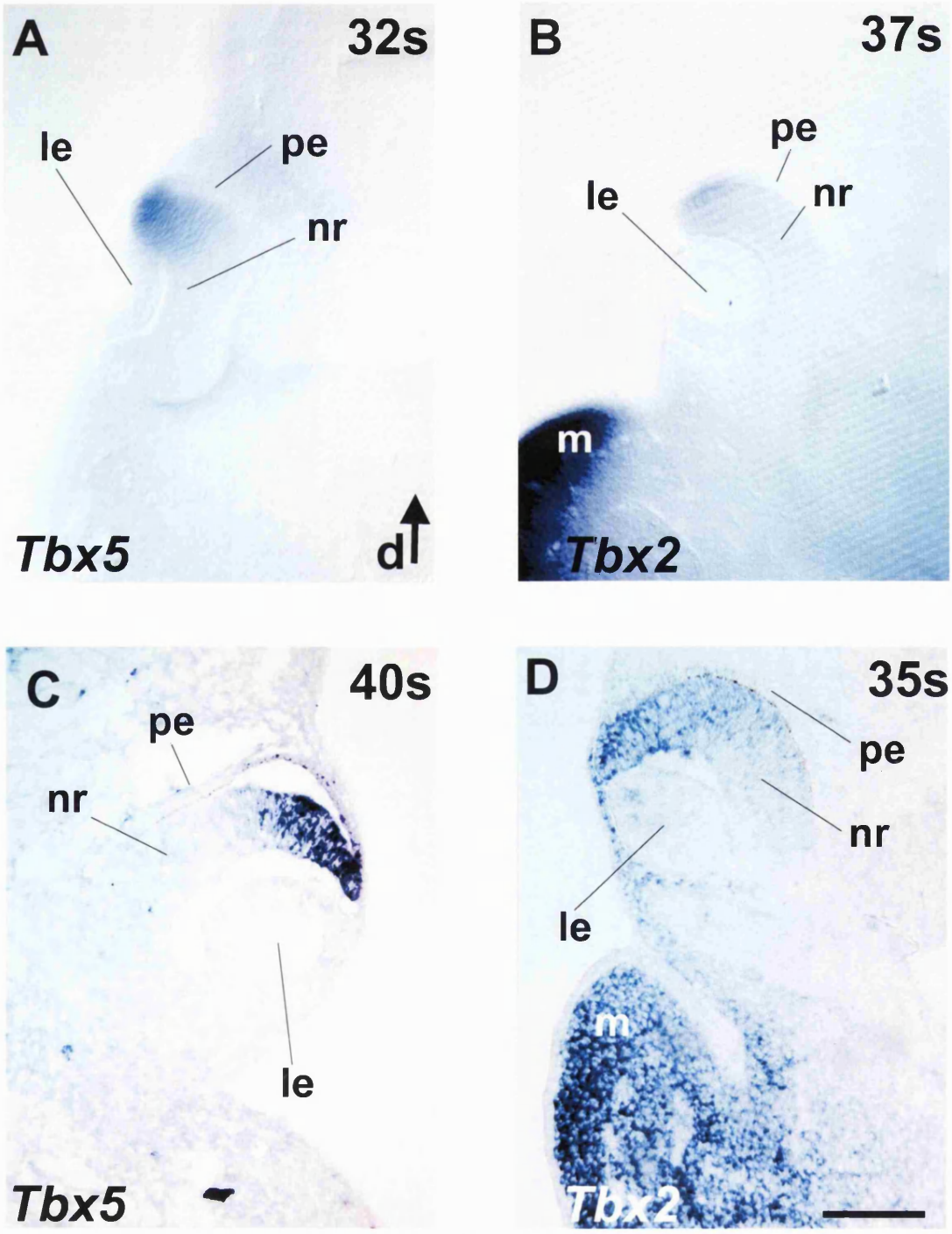

3.3D). The first signs of pigmentation in the dorsal regions of the RPE are visible in these cryosections.

At 53 somites, *Tbx5* expression is seen to occupy the dorsal quadrant of the neural retina (**Fig. 3.4A, B**), while *Tbx2* expression extends across the entire dorsal hemiretina (**Fig. 3.4C, D**). *Tbx3* expression was not detected in the retina at 53 somites (**Fig. 3.4E, F**).

3.2. *TBX2/Tbx2*, *TBX3/Tbx3* and *TBX5/Tbx5* are expressed in discrete lamina during retinal stratification

Expression of *TBX2/Tbx2*, *TBX3/Tbx3* and *TBX5/Tbx5* was examined during retinal stratification in the developing human and mouse eye. Coronal and sagittal cryosections of human and mouse retina were cut to reveal sections through dorsal and ventral neural retina from the first signs of retinal lamination to the formation of the three cellular layers of the mature retina. T-box gene expression has been analysed using *in situ* hybridisation on these sections and RT-PCR on cDNA synthesised from human eye tissue.

During the periods of development examined retinal progenitors are becoming post-mitotic, differentiating into RGCs, and migrating inwards. This process leads to a divided retina with an inner layer broadly composed of differentiating RGCs and an outer layer largely containing undifferentiated retinoblasts (human: **Fig. 3.5-3.7**; mouse: **3.8A, C, E**). As differentiation proceeds and more cell types develop, these primitive retinal layers separate further (mouse: **Fig. 3.8B, D, F**; human: **3.9**). This ultimately leads to the formation of the innermost ganglion cell layer, the interneuron-dominated inner nuclear layer, and the (photoreceptor) outer nuclear layer; layers separated by acellular inner and outer plexiform layers (human: **Fig. 3.10**). See **1.1.** for a description of retinal lamination.

Mouse embryos at these developmental timepoints were staged by recording their length of gestation. The pace of eye development slows in late mouse gestation (compared with the fast pace of the early morphogenetic events) so that variations in developmental stage within a single embryonic day are negligible. Human embryos

Figure 3.4

Tbx5 and *Tbx2* were expressed in overlapping domains of the dorsal mouse E11.5 optic cup (**A-F**):

A *Tbx5* expression was detected in the dorsal quadrant of the optic cup in the 53-somite mouse embryo (arrow). Expression was strongly detected in the forelimbs (**f**). Expression has also been noted in the heart and the genital region, but this is not evident in this figure.

B Close-up of the optic cup from **A**. Boundaries of the *Tbx5* expression domain is indicated by dotted lines. Dorsal (**d**) orientation of the developing eye is indicated for all figures. **le**, lens; **nr**, neural retina; **vf**, ventral fissure.

C ***Tbx2*** expression was detected in the dorsal half of the optic cup in the 53-somite mouse embryo (arrow). Expression was also detected in the nasal, maxillary, and mandibular primordia (**p**), the otic vesicle (**o**), the somite and dermo-myotome boundaries (**b**) and in the anterior and posterior aspects of the limb buds (**l**).

D Close-up of the optic cup from **C**. Boundaries of the *Tbx2* expression domain is indicated by dotted lines. **le**, lens; **nr**, neural retina; **vf**, ventral fissure.

E In the 53-somite mouse embryo, *Tbx3* expression could not be detected in the optic cup. *Tbx3* expression was detected in the developing maxillary and mandibular regions, the otic vesicle, the heart, the somite and dermo-myotome boundaries, and in the anterior and posterior aspects of the limb buds. Scale bar = 0.5 mm for **A**, **C**, and **E**.

F Close-up of the developing optic cup in **E**. **le**, lens; **nr**, neural retina; **vf**, ventral fissure. Scale bar = 0.2 mm for **B**, **D**, and **F**.

mTbx2 and *mTbx5* are expressed in overlapping domains in the dorsal E11.5 optic cup

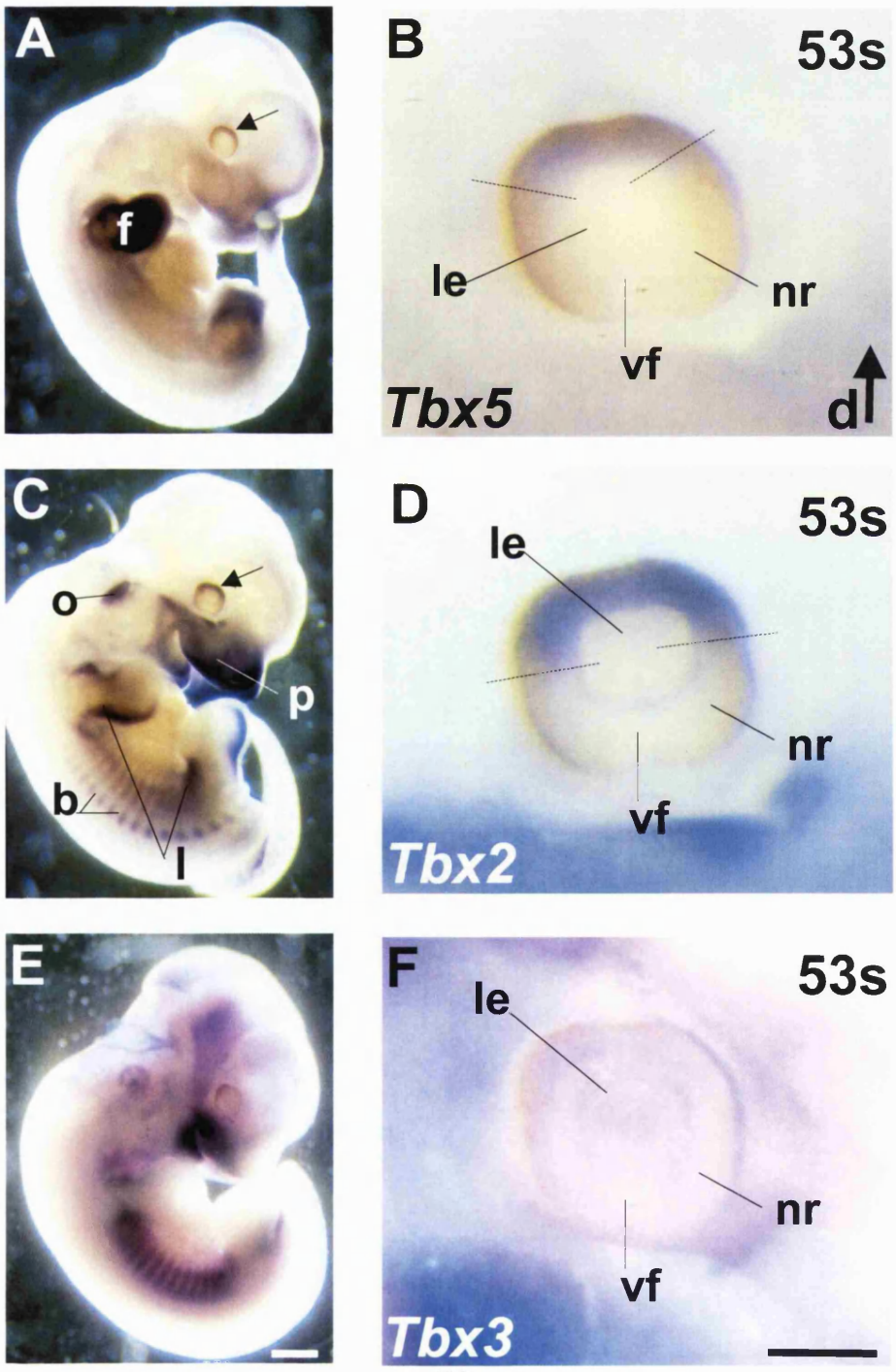

and foetuses were staged using hand and foot measurements to estimate the number of weeks post conception (wpc). For some foetuses the age was determined by subtracting 2 weeks from the number since the last maternal period.

T-box gene expression during formation of the inner and outer retinal layers

In the 6 wpc human retina (**Fig. 3.5; 3.6**), a distinct inner layer has already emerged, separated from the undifferentiated outer layer by the transient layer of Chevitz. Examination of *TBX5* expression in coronal sections showed that expression was limited to the dorsal quadrant of the neural retina (**Fig. 3.5A, B**). In sagittal sections this expression was seen to be graded and diminishing ventrally (**Fig. 3.5C, D**). *TBX5* expression extended through the undifferentiated outer retina and the emerging inner layer (**Fig. 3.5F, G**). The inner layer is the site of developing RGCs. This was demonstrated by immunohistochemical labelling of POU-domain transcription factor POU4F2 (BRN-3b/BRN-3.2) (**Fig. 3.5H**), a nuclear protein essential for the proper development and survival of RGCs (Erkman *et al.*, 1996; Gan *et al.*, 1996; Gan *et al.*, 1999).

TBX2 and *TBX3* were expressed in graded dorsal retinal domains that overlapped with *TBX5* at this stage (**Fig. 3.6**). When expression of these three genes was compared on adjacent sagittal sections through the retina, *TBX2* was expressed in a broader dorsal domain than *TBX3* and occupied the entire dorsal hemiretina (**Fig. 3.6B, C**). *TBX3* in turn was expressed in a broader domain than *TBX5* and occupied approximately half of the dorsal retina (**Fig. 3.6B, D**).

At 9 wpc, the inner and outer layers are firmly established and a nerve fibre layer composed of projecting RGC axons is evident (**Fig. 3.7A**). *TBX5* retained its graded expression in the dorsal tip of the neural retina (**Fig. 3.7B**). A dorsal restriction of expression was no longer detected for *TBX2* however (**Fig. 3.7C**), expression was limited to the inner layer of both dorsal and ventral neural retina where it co-localised with POU4F2 (**Fig. 3.7C-F**).

At 6-9 wpc, the human eye contains two distinct layers and the inner layer contains smaller, rounder cells than the outer retina, where cells are more spindle shaped (**Fig. 3.7D**). This stage is equivalent to the embryonic mouse eye at E14.5 (**Fig. 3.8A**). In

Figure 3.5

TBX5 was expressed in the dorsal quadrant of the embryonic human retina (**A-E**):

A Haematoxylin and eosin (H+E) staining of a frontal cryosection through the eye of a 6.0 weeks post-conception (wpc) human embryo. Retinal lamination had not reached the peripheral regions of retina viewed here. Dorsal (**d**) orientation of the developing eye is indicated for all figures. **nr**, neural retina; **pe**, pigmented epithelium.

B Parallel section to that shown in **A**. *TBX5* expression was seen to be restricted to the dorsal quadrant of the retina, expression domain boundaries are indicated by dotted lines. Some expression was seen in the ventral retina (arrows). Scale bar = 0.2 mm (for **A** and **B**).

C Haematoxylin and eosin (H+E) staining of a sagittal cryosection through the eye of a 6.6 wpc human embryo. In the central retina, an inner layer of differentiating nuclei was distinguished. It was separated from the neuroblastic outer layer by the transient layer of Chevitz. **C**, layer of Chevitz; **il**, inner layer; **ol**, outer layer.

D Parallel section from the same eye to that shown in **C**. ***TBX5*** expression was restricted to the dorsal retina in a graded fashion and diminishing ventrally. Expression was in inner and outer dorsal retina, but was also present in isolated innermost nuclei located ventrally (arrows). Scale bar = 0.2 mm; **C** and **D**.

E Schematic diagram of a sagittal cut through the dorsal (**d**, indicated) and ventral eye, as seen in **C** and **D**. Dotted red line indicates plane of section for **A** and **B**.

Within its dorsal domain *TBX5* was expressed in outer neuroblastic retina and in the emerging inner layer, the site of BRN3b-labelled presumptive ganglion cells (**F-H**).

F Close up of the boxed region in **C**. The dorsal limit of the emerging inner layer can be seen. **il**, inner layer; **ol**, outer layer; **C**, layer of Chevitz.

G Close up of the boxed region in **D**. *TBX5* expression is seen in the outer and inner layers of the dorsal retina.

H Parallel section to those in **F** and **G**. POU4F2, a marker of developing ganglion cells, localises to nuclei of the inner layer where *TBX5* is strongly expressed in dorsal retina (**G**). Scale bar = 50 μm for **F**, **G**, and **H**.

TBX5 expression is restricted to the dorsal quadrant of the embryonic human retina

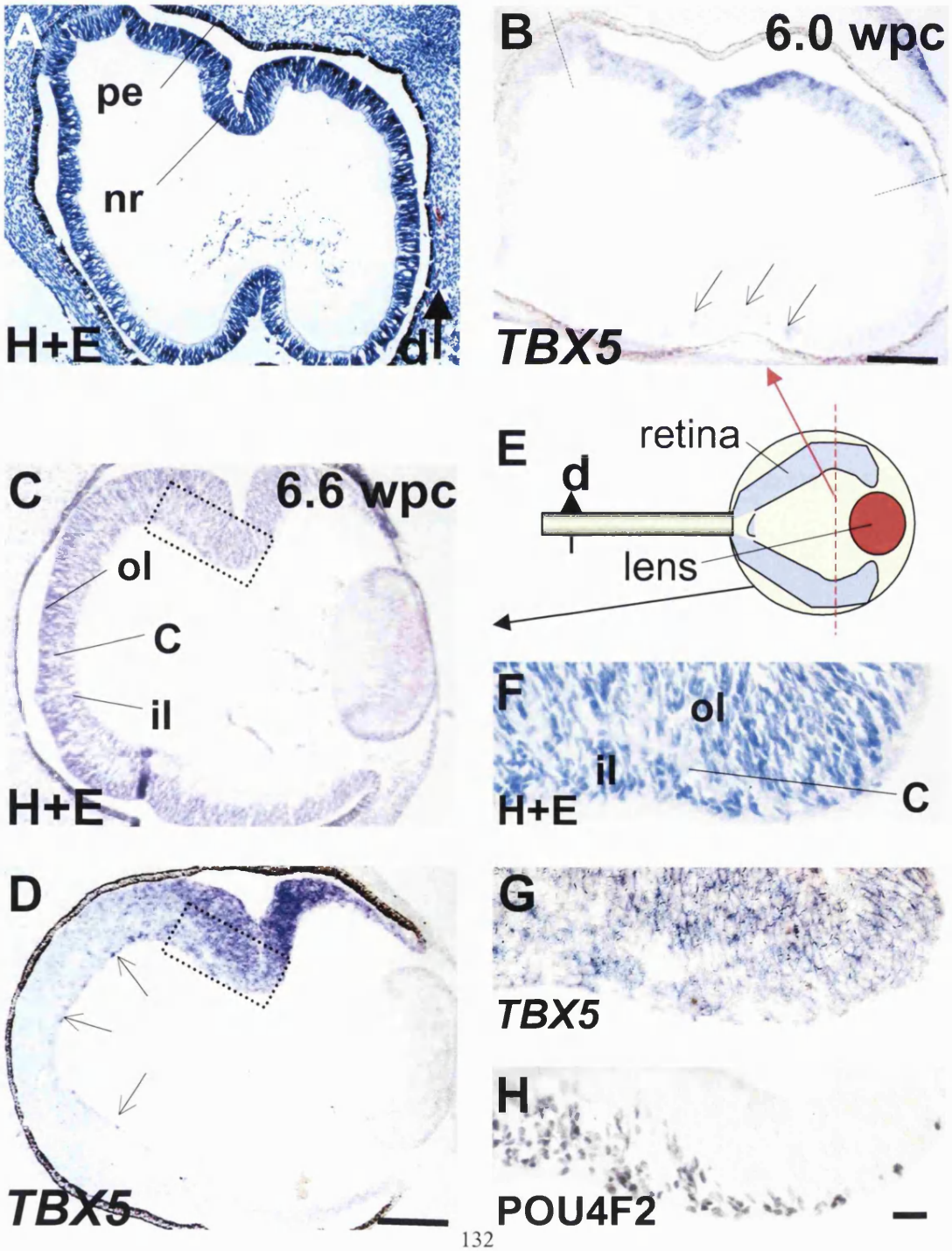

Figure 3.6

TBX2, *TBX3* and *TBX5* were expressed in overlapping dorsal domains in the embryonic human retina (**A-D**):

A Haematoxylin and eosin (H+E) staining of a sagittal cryosection through the eye of a 6.3 weeks post-conception (wpc) human embryo. An inner layer (**il**) is seen in central retina separated from the outer retina (**ol**) by the transient layer of Chevitz (**C**). Dorsal (**d**) orientation of the developing eye is indicated for all figures. **le**, lens; **pe**, pigmented epithelium.

B Parallel section from the same eye to that shown in **A**. *TBX2* expression is seen to be restricted to the dorsal two-thirds of the retina, ventral domain boundary is indicated by arrow.

C Adjacent section to that shown in **B**. *TBX3* expression is seen to be restricted to the dorsal half of the retina, ventral domain boundary is indicated by arrow.

D Adjacent section to that shown in **B**. *TBX5* expression is seen to be restricted to the dorsal third of the retina, ventral domain boundary is indicated by arrow. Scale bar = 0.2 mm for all figures.

TBX2, *TBX3* and *TBX5* are expressed in overlapping dorsal to ventral gradients in the embryonic human retina

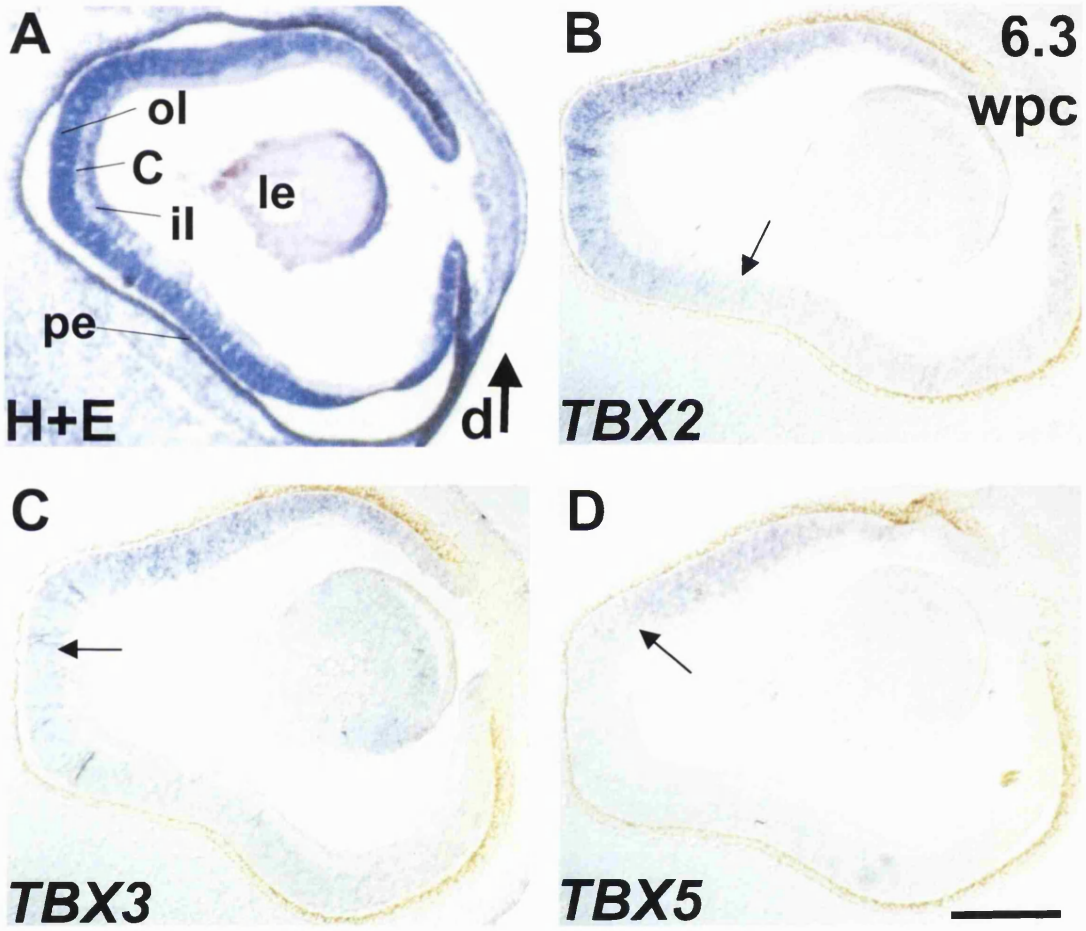

Figure 3.7

TBX2, but not *TBX5*, loses dorso-ventral asymmetry of expression in the foetal human retina, becoming restricted to the inner layer (**A-C**):

A Haematoxylin and eosin (H+E) staining of a sagittal cryosection through the eye of a 9.0 weeks post-conception (wpc) human foetus. The inner and outer layers of the retina were readily distinguished. Ganglion cell axons leaving the inner layer (**il**) form a nerve fibre layer (**nfl**) over it, in the central retina this is grossly thickened because this is the region of the optic disc. Dorsal (**d**) orientation of the developing eye is indicated and applies from **A** to **C**. **le**, lens; **ol**, outer layer; **pe**, pigmented epithelium.

B Parallel section from the same eye to that shown in **A**. Graded *TBX5* expression was retained in the dorsal retina with no laminar asymmetry. Scale bar = 0.2 mm for **A-C**; 20 μm for **D-F**.

C Parallel section to that shown in **A** and **B**. The optic nerve was seen to leave the retina in this section. *TBX2* expression was restricted to the inner layer of the retina, dorso-ventral asymmetry was no longer apparent.

TBX2 expression was restricted to the inner retina, the site of BRN3b-labelled presumptive ganglion cells (**D-F**).

D Close-up of haematoxylin and eosin (H+E) stained 9.0 wpc retina. While the outer layer (**ol**) was dominated by mitotic spindle-shaped nuclei, the inner layer (**il**) contained small round nuclei.

E Close-up of boxed region in **B** and parallel section to that in **D**. *TBX2* was expressed within the inner layer of the retina, though some nuclei appeared to be labelled in the outer layer (arrow).

F Parallel section to that in **D** and **E**. Nuclei of the inner layer are labelled with POU4F2 antibodies. Some labelling was apparent in outer nuclei (arrow), particularly those occupying the innermost aspects of the outer layer.

TBX2 becomes expressed throughout the inner nuclear layer of the foetal human retina

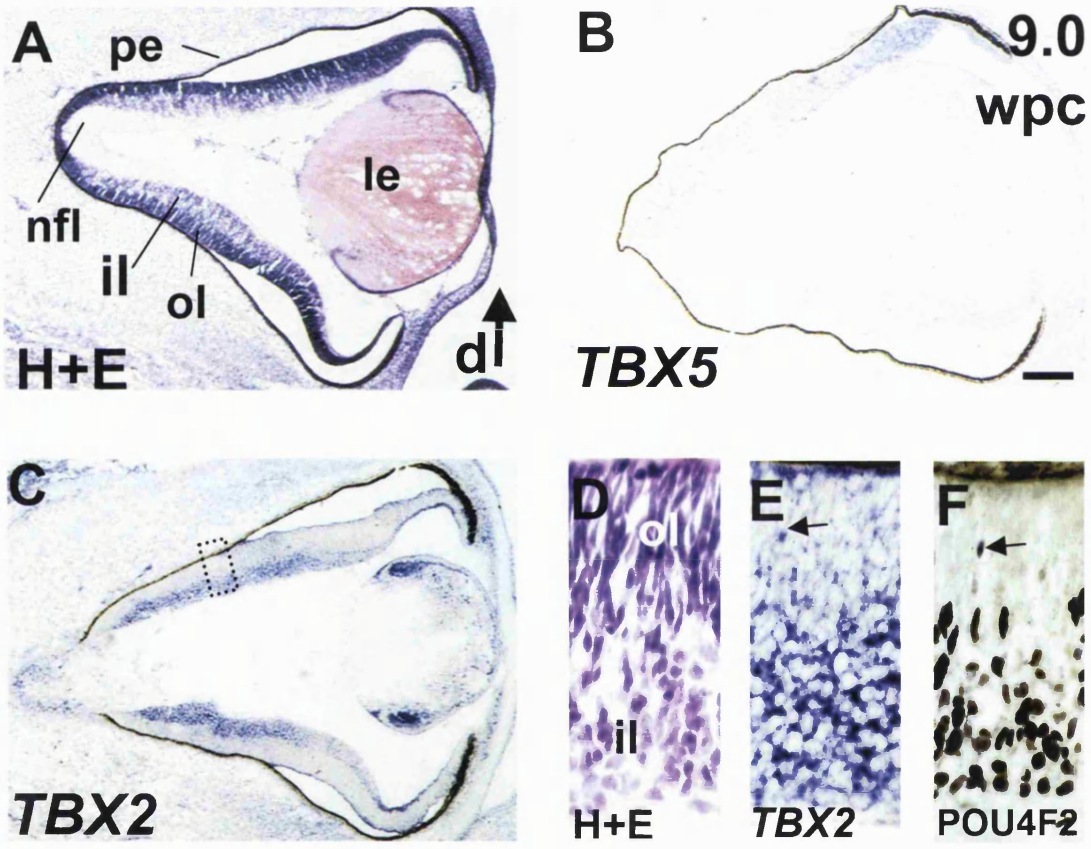

Figure 3.8

Tbx2 and *Tbx5* were expressed in overlapping dorso-ventral gradients and transiently showed localised expression to cells of the inner layer (**A-F**):

A Haematoxylin and eosin (H+E) staining of a frontal cryosection through the eye of an E14.5 mouse embryo. The retina contained two layers at this stage, an inner layer (**il**) of differentiating ganglion cells and an outer mitotic layer (**ol**). **pe**, pigmented epithelium.

B Haematoxylin and eosin (H+E) staining of a frontal cryosection through the eye of an E18.5 mouse embryo. The inner layer was further laminated at this stage, separated into presumptive ganglion cell (**gcl**) and inner nuclear (**inl**) layers by a primitive inner plexiform layer (**ipl**). **nfl**, nerve fibre layer; **ol**, outer layer.

C Parallel section to that shown in **A**. *Tbx2* was expressed throughout the E14.5 dorsal hemiretina and to a lesser degree in nuclei of the inner layer of ventral retina (arrows).

D Parallel section to that shown in **B**. Dorsal (d) orientation of the developing eye is indicated and applies from **C** to **F**. *Tbx2* was expressed in a dorsal to ventral gradient through all layers of the E18.5 retina. Stronger outer layer expression is likely to be due to the higher cell density. Expression in ventral retina was detected in two lines of outermost (presumed photoreceptors) and innermost (presumed interneurons) nuclei of the outer layer.

E Adjacent section to that shown in **C**. Graded *Tbx5* expression was present diminishing ventrally across the dorsal third of the retina. High intensity expression was also seen in a subset of inner nuclei of dorsal and ventral retina. In the dorsal inner retina, this high intensity expression in isolated nuclei was superimposed upon the dorsal to ventral gradient of *Tbx5* expression.

F Adjacent section to that shown in **D**. *Tbx5* was expressed in a dorsal to ventral gradient through all layers of the retina. No laminar asymmetry of expression was detected. Prominent outer layer expression was probably due to the increased cell density within this region. Scale bar = 15 μm for **A**, 50 μm for **B**, 120 μm for **C** and **E**, 200 μm for **D** and **F**.

mTbx2 and *mTbx5* are expressed in overlapping dorsal to ventral gradients in the E14.5 and E18.5 retina

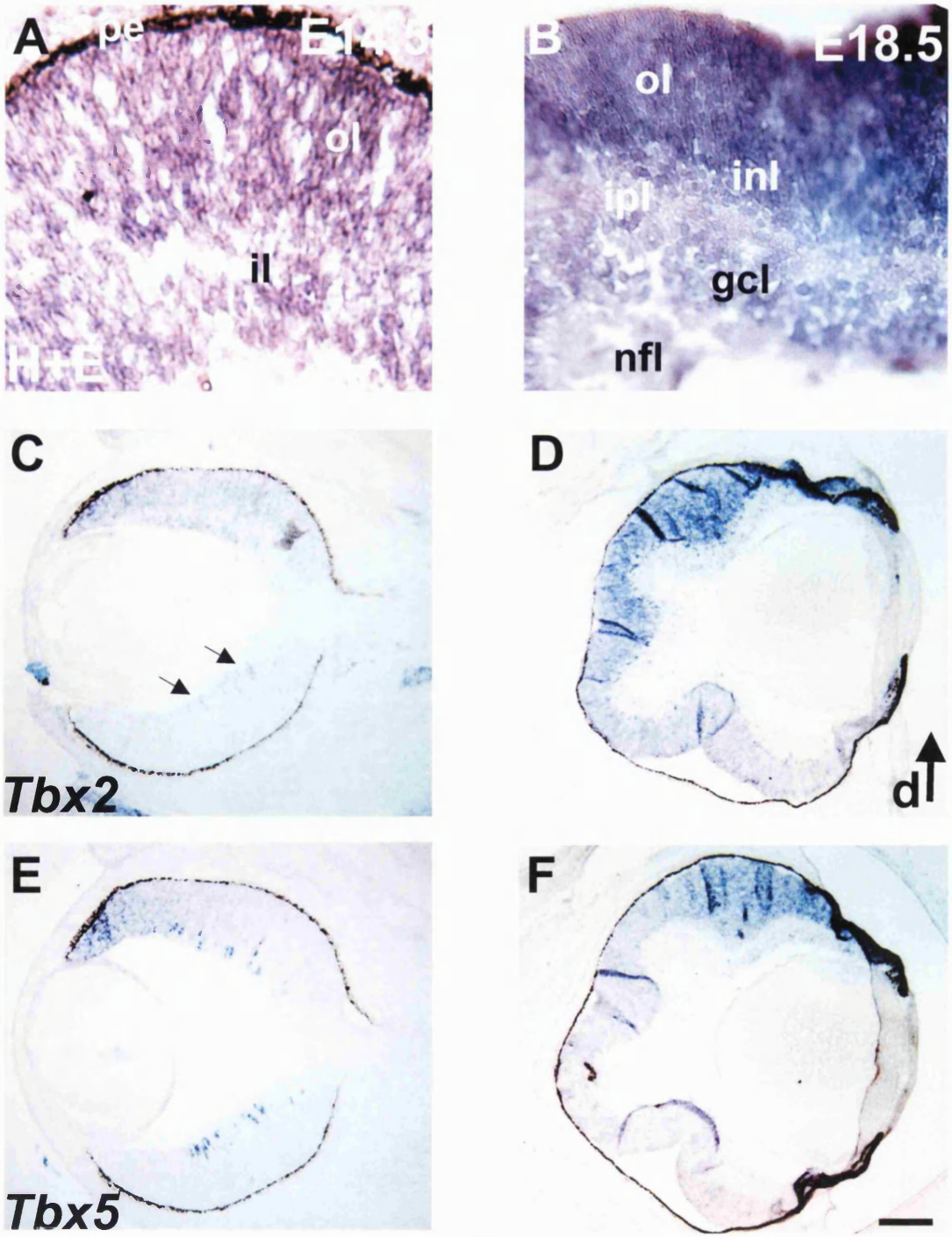

the E14.5 mouse eye the expression of *Tbx2* was seemingly identical to that of its human counterpart at 6 wpc, covering the entire dorsal hemiretina in a graded manner (**Fig. 3.8C**). Expression of *Tbx2* in the inner layer extended into the ventral retina, though at reduced levels (**Fig. 3.8C**). Expression in the ventral inner layer was not seen for *TBX2* in the 6 wpc human eye. It was certainly present at 9 wpc, when the human – unlike the mouse – had lost dorsal *TBX2* expression in the outer layer.

In the E14.5 mouse eye *Tbx5* maintained the precise expression domain across the dorsal tip of neural retina that was detected in the 6 wpc human and the early mouse optic cup, but showed an added feature. Although the dorsal *Tbx5* expression domain covered the inner and outer retina, a subset of nuclei from the dorsal and ventral inner retinal layer strongly expressed *Tbx5* (**Fig. 3.8E**). In the dorsal inner layer, the strongly expressing presumptive RGCs rested on a background of a more moderate and graded dorsal domain of *Tbx5* expression. No *Tbx3* expression was detected on mouse cryosections at this stage.

T-box gene expression during formation of the mature retinal layers

At E18.5 the mouse retina shows signs of further lamination (**Fig. 3.8B**). The inner layer can now be divided into presumptive inner nuclear and ganglion cell layers, separated by an inner plexiform layer.

Tbx2 was expressed in a dorsal-high to ventral-low gradient through all cellular layers in the E18.5 neural retina (**Fig. 3.8D**). As in the E14.5 retina, some lamina-specific expression was seen in the ventral retina: cells of the presumptive inner nuclear layer and – not seen in humans – a population of outermost retinal nuclei were expressing *Tbx2*.

Tbx5 (**Fig. 3.8F**) shared the dorsal-high to ventral-low gradient through all cellular layers in the E18.5 neural retina. The smaller dorsal domain in comparison to *Tbx2* remained. The high level expression seen in presumptive RGCs at E14.5 was no longer apparent and a restriction to the ganglion cell layer in more peripheral sections of retina, as for human *TBX5*, was not noted.

With the beginnings of an inner plexiform layer separating the inner layer into presumptive ganglion cell and inner nuclear layers, the 12 wpc human eye is at a similar stage of retinal development to the developing mouse at E18.5 (**Fig. 3.9A, B**).

Both *TBX3* and *TBX5* retained dorsal restriction of expression at 12 wpc. They also showed restrictions to distinct layers of the retina. *TBX3* was expressed in a subset of the outermost nuclei of inner differentiating cells, the region of the presumptive inner nuclear layer, within the dorsal retina only (**Fig. 3.9C, D**). In adjacent sections *TBX5* was expressed in the prospective ganglion cell layer of dorsal retina (**Fig. 3.9E**). In more central sections *TBX5* was expressed throughout the dorsal retina (**Fig. 3.9F**) while *TBX3* expression could not be detected (not shown).

By 15 wpc all three cellular layers of the mature human retina have become distinct (**Fig. 3.10A**). The outer layer has become split by the emergence of the outer plexiform layer to separate the developing photoreceptor-containing outer nuclear layer and proliferating zone of undifferentiated cells. The inner plexiform layer has thickened and the ganglion cell layer has thinned to resemble the adult retina.

TBX3 expression was no longer restricted to dorsal retina, it was expressed in dorsal and ventral regions of the inner nuclear layer (**Fig. 3.10B**). *TBX2* expression localised to the ganglion cell layer, the inner nuclear layer and to the undifferentiated proliferating zone (**Fig. 3.10C**). When a rabbit polyclonal antibody raised to the TBX2 protein (kindly provided by C. Campbell, unpublished) was used for immunohistochemistry, nuclei of the ganglion cell layer and a smaller subset of those from the post-mitotic inner nuclear layer were labelled (**Fig. 3.10D**).

TBX5 was not detected on sections of 15 wpc retina using *in situ* hybridisation (not shown), but RT-PCR analysis demonstrated that all three human T-box genes continued to be expressed in the eye into adulthood (**Fig. 3.11**). 35 cycles of PCR were performed on equal amounts of RNA. 35 cycles was found to be within the linear range of amplification (so allowing the reaction to be semi-quantitive). Expression of the housekeeping gene *PGM1* was examined to test the integrity and equality of the RNA. Expression of the three T-box genes was much greater at 10 wpc

Figure 3.9

TBX5 and *TBX3* retain dorsal restriction and attain laminar localisation of expression in the foetal human retina (**A-F**):

A Haematoxylin and eosin (H+E) staining of a sagittal cryosection through the eye of a 11.7 weeks post-conception (wpc) human foetus. The inner layer was further laminated at this stage, having been separated into presumptive ganglion cell (**gcl**) and inner nuclear (**inl**) layers by a primitive inner plexiform layer (**ipl**). Dorsal (**d**) orientation of the developing eye is indicated for all figures. **l,** lens; **nfl**, nerve fibre layer; **ol**, outer layer; **pe**, pigmented epithelium.

B Close-up of the dorsal-most tip of neural retina in a parallel section to that shown in **A**. POU4F2-labelling highlighted nuclei of the inner layer (and isolated nuclei in the outer retina) and methyl green (MeGr) counter staining illuminated unlabelled nuclei.

C Parallel section to that shown in **A**. *TBX3* expression was detected in a line of nuclei within the dorsal retina, in the region of the presumptive inner nuclear layer.

D Close-up of the boxed region in **C**. *TBX3* is expressed in a subset of nuclei lining the outer limits of the inner layer of the retina. This is the region of the presumptive (dorsal) inner nuclear layer. Although the presumptive inner nuclear layer was only morphologically distinct in more central regions of the retina, it appeared to be marked out by *TBX3* expression in the peripheral dorsal retina.

E Adjacent section to that shown in **C**. *TBX5* was expressed within the innermost cells of the dorsal retina, in the region of the developing ganglion cell layer.

F Parallel section in the region of the optic disc. *TBX5* was expressed through all layers of the dorsal retina. Scale bar = 0.2 mm for **A**, **C**, **E** and **F**; 25 μm for **B** and **D**.

TBX3 and *TBX5* are expressed in distinct layers of the dorsal 12 wpc human retina

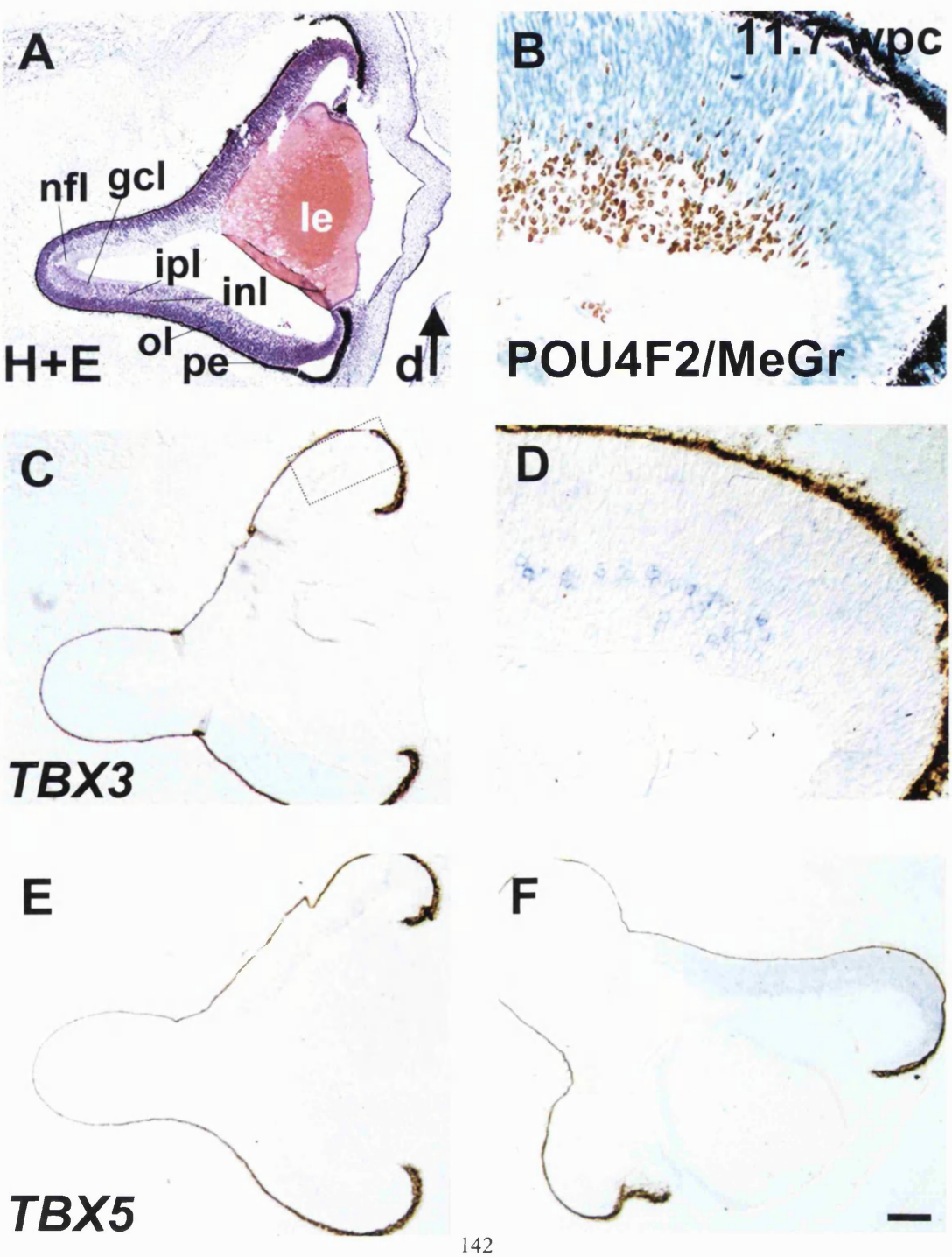

Figure 3.10

TBX2 and *TBX3* were expressed in distinct layers of the mature retina, TBX2 protein was detected only in the inner regions of its expression domain (**A-D**):

A Peripheral retina viewed on a sagittal cryosection through a 15.4 weeks post-conception (wpc) human eye stained with haematoxylin and eosin (H+E). All the mature layers of the retina were represented at this stage. An outer plexiform layer (**opl**) divided the outer layer to define a primitive outer nuclear layer (**onl**) from a proliferating zone (**pz**). The ganglion cell layer (**gcl**) was more clearly separated from the inner nuclear layer (**inl**) by the thickened inner plexiform layer (**ipl**). Photoreceptors were seen lining the outer limits of the neural retina (arrow). **pe**, pigmented epithelium.

B Parallel section to that shown in **A**. *TBX3* mRNA was found to reside throughout (in dorsal and ventral retina) the post-mitotic portion of the inner nuclear layer.

C Parallel section to that shown in **A**. *TBX2* expression was present in both the dividing and post-mitotic portions of the inner nuclear layer, and in the ganglion cell layer, throughout the neural retina.

D Parallel section to that shown in **A**. TBX2 protein was detected in only a small portion of its expression domain. TBX2 was strongly labelled in isolated nuclei of the ganglion cell layer and sporadically in nuclei of the post-mitotic region of the inner nuclear layer. Scale bar = 25 μm for **A** to **D**.

TBX2 and *TBX3* are expressed in distinct layers of the 15 wpc human retina

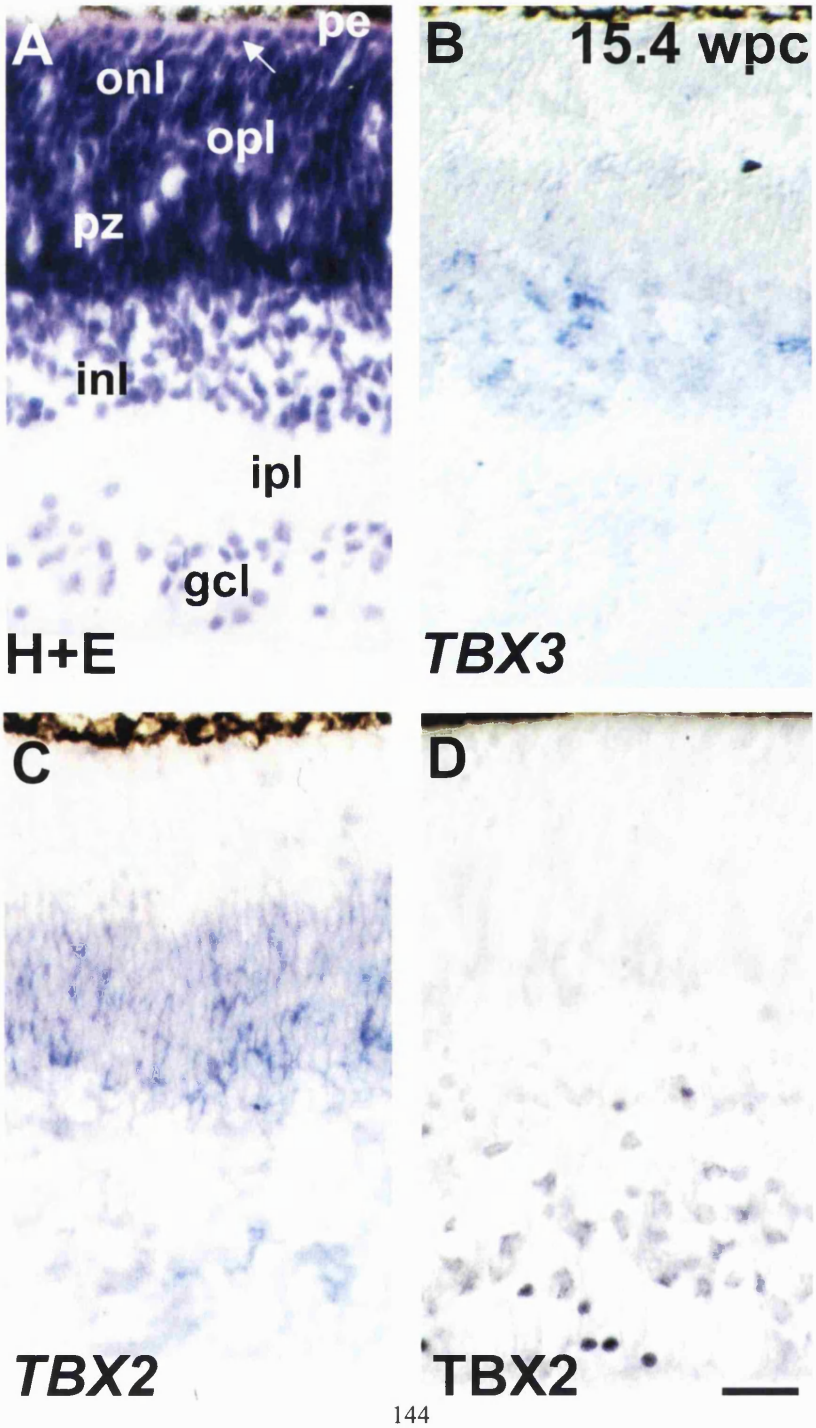

Figure 3.11

Reverse transcriptase-polymerase chain reaction (RT-PCR) results on developing human eye tissue RNA using primers specific for *PGM1*, *TBX2*, *TBX3* and *TBX5*. RNA was synthesised with RT using DNA extracted from 10, 12 and 15 weeks post-conception (wpc) human foetal eyes and an adult eye sample. *PGM1*, as a ubiquitously expressed housekeeping gene, was examined to demonstrate the uniformity of the RNA samples. Uniform bands of the expected size were obtained with *PGM1* primers from all the RNA samples. Primers specific for *TBX2*, *TBX3* and *TBX5* all amplified bands of the expected sizes. Gene expression was high for all these genes at 10 wpc and was greatly reduced – though always present - in the later samples. No DNA was amplified in control PCRs performed without RNA.

Human *TBX2, TBX3* and *TBX5* expression persists into retinal maturity

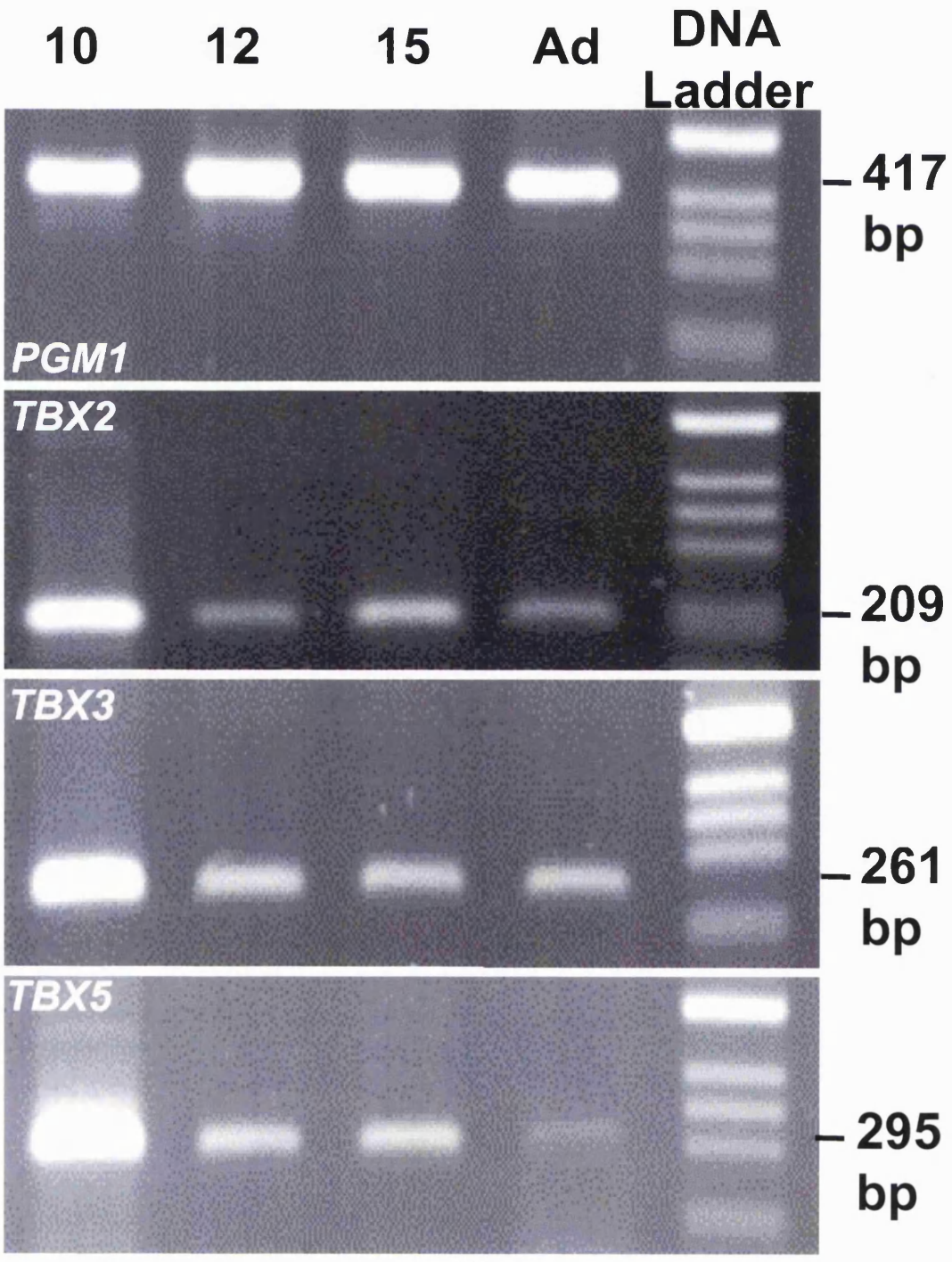

than at later timepoints, when it remained approximately constant, but for a notable reduction in the expression of *TBX5* in the adult eye.

3.3. POU4F2 is a marker for nuclei of the inner layer of the early retina and a subset of those in the mature ganglion cell layer

In this section I examine the protein distribution of the POU-domain transcription factor POU4F2 in the developing human retina. Analysis of *Pou4f2*-null mice revealed that ~70% of RGCs are dependent on *Pou4f2* for survival during development (Erkman *et al.*, 1996; Gan *et al.*, 1996). Further investigation indicated that *Pou4f2* was essential for the proper differentiation and continued survival of RGCs, but was not required for initial cell fate specification or migration (Gan *et al.*, 1999). POU4F2/Pou4f2 has previously been identified in subsets of RGCs in the adult retina of several mammalian species: human, macaque, rabbit, rat and mouse retina (Xiang *et al.*, 1993; Xiang *et al.*, 1995). In the developing retina work on Pou4f2 developmental localisation has exclusively been undertaken in mice (Gan *et al.*, 1996; Xiang, 1998). In the developing mouse eye, Pou4f2 can be detected from E11 throughout the emerging inner neuroblastic layer as well as in scattered nuclei within the outer retina (Gan *et al.*, 1996). The scattered Pou4f2-labelled outer retinal nuclei are post-mitotic and apparently migrating towards the inner layer of the retina (Xiang, 1998). In mice, Pou4f2 has been assumed to exclusively mark developing RGCs, though the labelling of other cell types with Pou4f2 antibodies has not been ruled out.

I have used POU4F2 as a marker for developing RGCs in human tissue and have compared its localisation with T-box gene expression. By examining POU4F2 protein distribution in developing human eyes I have been able to relate Pou4f2 localisation in developing mice and other vertebrates to human development and allow further insight into the comparative stages of RGC development in humans and mice.

POU4F2 localisation in the developing human retina

POU4F2 localises to most, but not all nuclei of the inner layer of the human neural retina at 6 wpc (**Fig. 3.12A**). Counter-staining with methyl green shows that a subset of nuclei in the inner layer do not contain POU4F2. Labelling extends in a central to peripheral gradient with formation of the inner layer (**Fig. 3.12A-C**). POU4F2

Figure 3.12

POU4F2 protein was localised to the emergent inner layer of the embryonic human retina (**A-C**):

A Sagittal cryosection through a 6.3 weeks post-conception (wpc) human eye that was POU4F2 immunolabelled and counterstained with methyl green. The inner layer (**il**), marked by POU4F2 (nuclei are labelled black because nickel was used during development), is clearly distinguished from the outer retina (**ol**), separated by the transient layer of Chevitz (**C**) in the central retina. The great majority, but not all, nuclei of the inner layer of the retina were POU4F2 labelled. Some POU4F2 labelling was seen in the inner regions of the outer retina. **pe**, pigmented epithelium. Scale bar = 100 μm.

B The dorsal peripheral margin of the emergent inner layer of the retina stained with haematoxylin and eosin (H+E) on a sagittal cryosection through a 6.6 wpc human eye. The inner layer (**il**) develops in a central to peripheral direction. Nuclei of the inner layer were smaller and rounder. **C**, layer of Chevitz; **ol**, outer layer.

C Parallel section to that shown in **B**. Presumptive ganglion cells become post-mitotic, migrate inwards, and produce POU4F2. Scale bar = 25 μm for **B** and **C**.

POU4F2 protein was distributed throughout the inner layer of the early foetal human retina (**D-G**):

D Central retina viewed on a sagittal cryosection through the 9 wpc human eye stained with H+E. The inner layer (**il**) was more substantial at this stage and the layer of Chevitz was no longer apparent. **ol**, outer layer.

E Parallel section to that shown in **D**. The inner layer was heavily POU4F2-labelled, some labelled nuclei were seen in the outer layer. Scale bar = 50 μm for **D** and **E**.

F Peripheral retina viewed on a sagittal cryosection through the 9 wpc human eye stained with H+E. **il**, inner layer; **ol**, outer layer.

G Parallel section to that shown in **F**. The inner layer was heavily POU4F2-labelled as in more central regions, but more outer layer nuclei were POU4F2-labelled. These outer-labelled nuclei were more prominent in the inner aspect of the outer layer, and labelling was consistently found to be of a higher intensity. Scale bar = 25 μm for **F** and **G**.

POU4F2 localises to the inner layer of the embryonic human retina

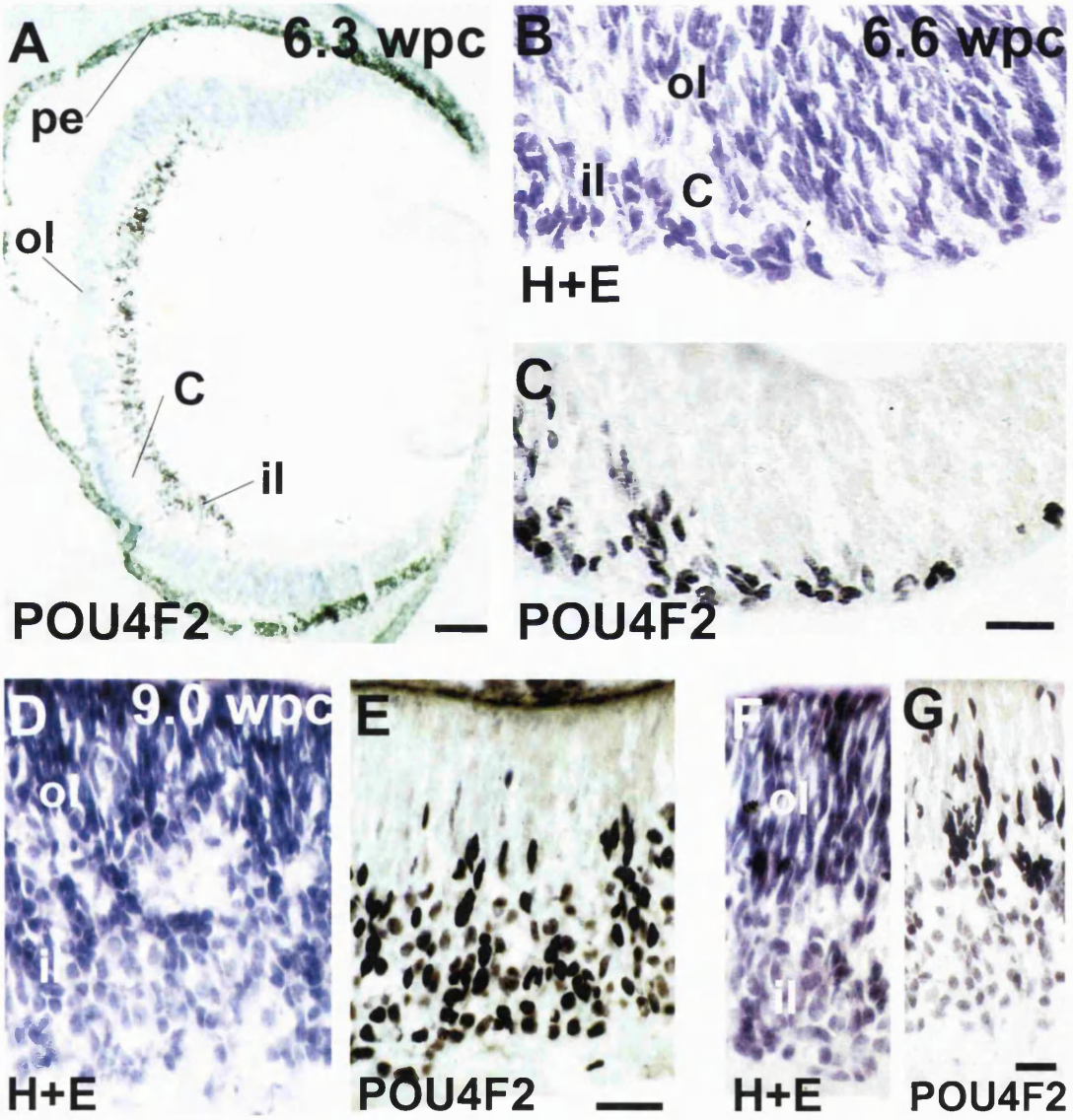

labelling is still present throughout the inner retina at 9 wpc as well as in apparently inwardly migrating nuclei of the outer layer (**Fig. 3.12D, E**). POU4F2 was typically more strongly detected in these outer nuclei; this was more readily apparent in peripheral regions of the retina (**Fig. 3.12F, G**).

At 12 wpc counter-staining with methyl green demonstrated that virtually all nuclei of the inner layer contain POU4F2, including both those of prospective inner nuclear and ganglion cell layers (**Fig. 3.13**). Only isolated nuclei of the inner retina can be identified that do not contain POU4F2 (**Fig. 3.14A**, arrows). As in the 9 wpc retina, POU4F2 was more strongly detected in the outermost labelled nuclei of peripheral regions of 12 wpc retina (**Fig. 3.14B**). In the 15 wpc retina, POU4F2 was solely restricted to the ganglion cell layer (**Fig. 3.14C, D**) where a subset of nuclei were labelled with varying intensity (**Fig. 3.14E**). 4 x 350 μm^2 areas randomly chosen from 2 sections of POU4F2-labelled and methyl green counter-stained 15 wpc central retina were analysed for numbers of unlabelled nuclei in the ganglion cell layer. The mean proportion of POU4F2 negative cells in the central ganglion cell layer was estimated to be ~30% (0.29, with a standard deviation of 0.03).

3.4. *Tbx20* is expressed in nuclei of the ventral hindbrain and in a complementary manner to *Tbx5* in the developing heart

Meins *et al.* first identified human *TBX20* and mouse *Tbx20* in my laboratory and demonstrated that both are expressed in the developing eye (Meins *et al.*, 2000). *TBX20/Tbx20* is orthologous to the *Drosophila* T-box gene, *H15*, of the *Tbx1* subfamily. *H15* is known to provide ventral identity to the developing *Drosophila* leg imaginal disc opposite *omb*, which provides dorsal identity (Brook and Cohen, 1996). It was proposed that a similar complementary relationship might exist between *Tbx20* and *omb*-related T-box genes in the mouse eye. I have examined *Tbx20* expression in the mouse to allow comparison with the *omb*-related T-box genes.

Tbx20 expression in ventral nuclei of the 27/8-somite mouse hindbrain

Mouse embryos at the 27- and 28-somite stage were sectioned frontally to give tissue slices through dorsal and ventral aspects of retina. No expression was detected in the developing eye (not shown), but strong expression was detected in a groups of nuclei

Figure 3.13

POU4F2 protein was distributed throughout the emergent ganglion cell and inner nuclear layers of the foetal human retina (**A-C**):

A Central retina viewed on a sagittal cryosection through a 12.4 weeks post-conception (wpc) human eye stained with haematoxylin and eosin (H+E). An inner plexiform layer (**ipl**) was now apparent dividing the inner layer into presumptive ganglion cell (**gcl**) and inner nuclear (**inl**) layers. **nfl**, nerve fibre layer; **ol**, outer layer; **pe**, pigmented epithelium.

B Parallel section to that shown in **A**. BRN3b labelling extends throughout the ganglion cell and inner nuclear layers. Scale bar = 25 μm.

C Sagittal cryosection through a 11.7 weeks post-conception (wpc) human eye that was POU4F2 immunolabelled (POU4F2-labelled nuclei are brown as nickel was not used during development of the colour reaction) and counter-stained with methyl green. The heavily POU4F2-labelled ganglion cell layer (**gcl**) formed the bulk of the central retina. In the periphery, some high intensity labelling was apparent. POU4F2 labelling was evident in a small number of nuclei of the outer layer (**ol**) of the retina. At this stage outer-most cells of the outer retina showed morphological evidence of photoreceptor genesis (round, darkly stained nuclei, arrows). Dorsal (**d**) is indicated. **pe**, pigmented epithelium; **inl**, inner nuclear layer; **ipl**, inner plexiform layer; **nfl**, nerve fibre layer. Scale bar = 50 μm.

POU4F2 localises to the developing inner nuclear and ganglion cell layers of the 12 wpc human retina

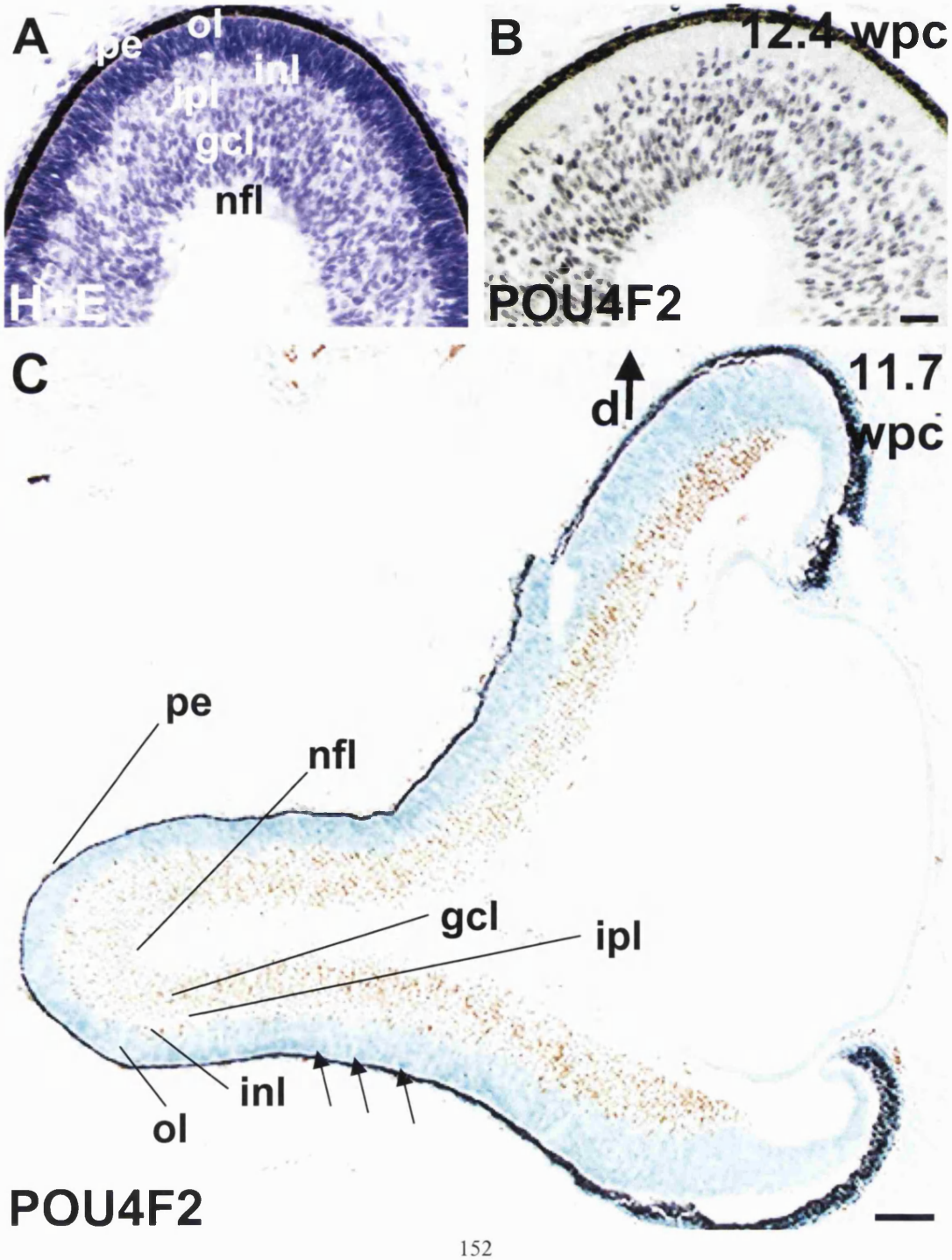

Figure 3.14

POU4F2 protein was distributed throughout the emergent ganglion cell and inner nuclear layers of the foetal human retina (**A, B**):

A Central retina viewed on a sagittal cryosection through an 11.7 weeks post-conception (wpc) human eye that was POU4F2 labelled (POU4F2-labelled nuclei were brown because nickel was not used during development of the colour reaction) and counter-stained with methyl green. A line of nuclei in the prospective nuclear layer were POU4F2 labelled, and in the ganglion cell layer (inwards of the inner plexiform layer, **ipl**) every nuclei – bar two, highlighted with arrows – was labelled.

B Peripheral retina viewed on a sagittal cryosection through an 11.7 wpc human eye that was POU4F2 labelled and counter-stained with methyl green. POU4F2 labelling intensity is stronger in the prospective inner nuclear layer and in labelled nuclei of the outer layer.

POU4F2 protein was localised to a subset of ganglion cell layer nuclei in the mature foetal human retina (**C-E**):

C Central retina viewed on a sagittal cryosection through a 15.4 weeks post-conception (wpc) human eye stained with haematoxylin and eosin (H+E). An outer plexiform layer (**opl**) separated the outer nuclear layer (**onl**) from the proliferating zone (**pz**). The inner plexiform layer (**ipl**) thickened to more clearly divide the inner nuclear (**inl**) and ganglion cell (**gcl**) layers. **pe**, pigmented epithelium; **nfl**, nerve fibre layer.

D Parallel section to that shown in **C**. POU4F2 labelling occurs only in nuclei of the ganglion cell layer.

E Close up of a parallel section to that shown in **C**. POU4F2 labelling (brown cells, nickel was not used during development of the colour reaction) occurs in a subset of ganglion cell layer nuclei with varying intensity. Scale bar = 15 μm for **A**; 50 μm for **B**; 25 μm for **C** and **D**; 10 μm for **E**.

POU4F2 localisation becomes restricted to a subset of cells in the ganglion cell layer of the foetal human retina

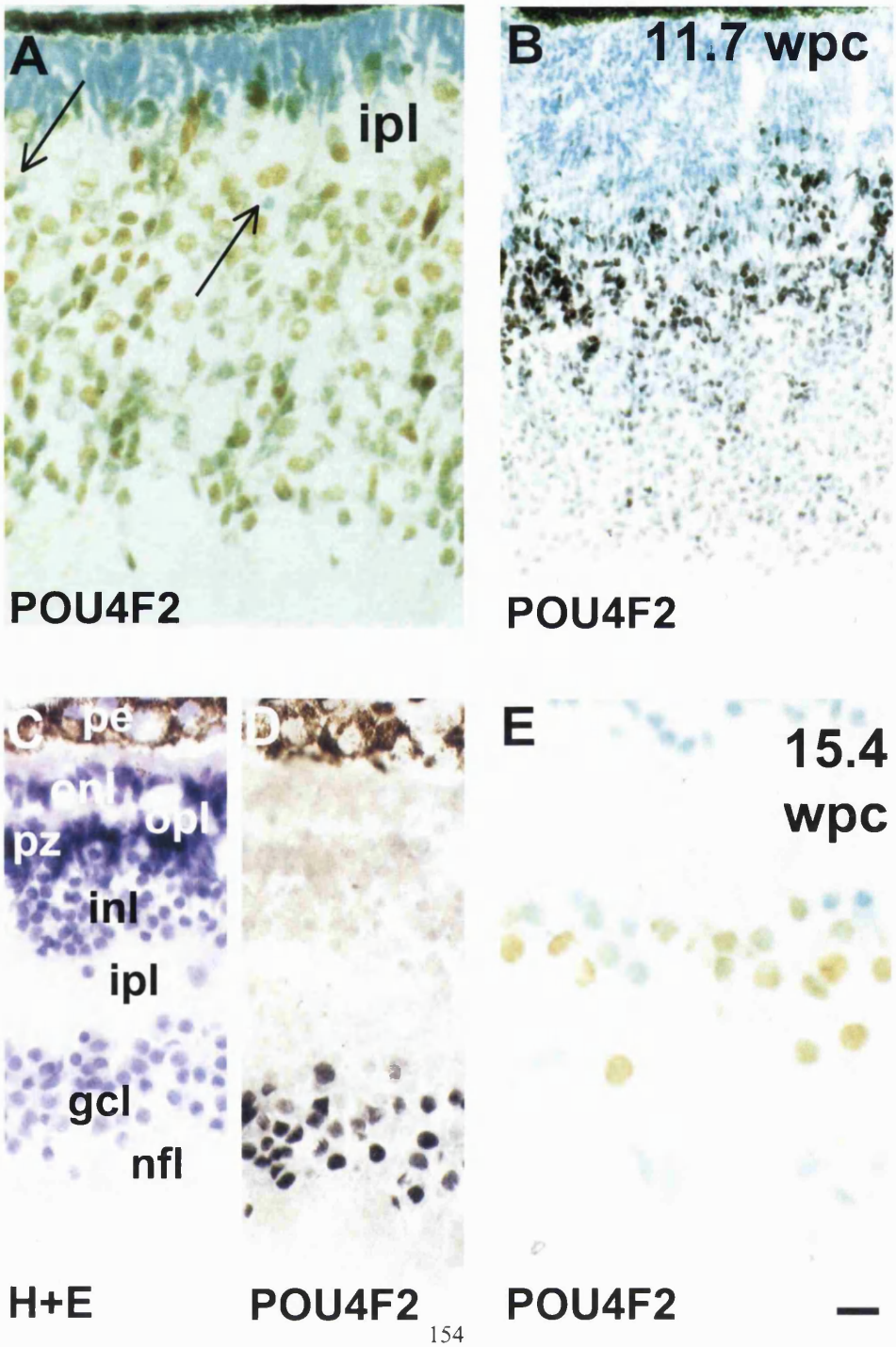

either side of the ventral rhombencephalic midline (**Fig. 3.15**). This bilateral set of labelled nuclei were first detected rostrally as bilateral lines of expressing cells in the ventral hindbrain (**Fig. 3.15D**). These became more localised to a bilateral pair of nuclear groups immediately adjacent to the ventral midline as more caudal sections through the ventral hindbrain were examined (**Fig. 3.15E, F**).

Tbx20 and Tbx5 expression in the 27/8-somite mouse heart

Tbx20 expression was seen in the heart of frontally sectioned 27/8-somite stage mouse embryos and compared with the cardiac expression of *Tbx5* (**Fig. 3.16**). Both genes were expressed throughout the developing myocardium (**Fig. 3.16**). In the developing endocardium, *Tbx5* and *Tbx20* were expressed in complementary patterns. *Tbx5* was expressed in the left ventricular endocardium while *Tbx20* was prominently expressed in endocardial cushions of the outflow tract and the atrio-ventricular canal (**Fig. 3.16**).

DISCUSSION

This chapter concludes my work on human tissue, but introduces that on mice, which I will continue to use as an experimental model in further chapters. In this section I discuss the implications of my analysis of T-box gene expression and POU4F2 distribution in retinal development, and indicate where I will go from here.

3.5. Dual roles for T-box genes during retinal development

The work described in this chapter suggests a dual role for *omb*-related T-box genes during human development: in early dorso-ventral patterning of the retina and in later lamination. All three genes are implicated in providing dorsal identity to the retina, *TBX5*/*Tbx5* and (mouse) *Tbx2* are also implicated as an upstream regulator of axon guidance molecules by virtue of their asymmetric expression in RGCs during the period when central connections are forming.

Dorsal expression of omb-related T-box genes in the developing optic cup

Tbx2 and *Tbx5* are both expressed in the dorsal optic vesicles. This expression is maintained during formation of the optic cup. *Tbx2* and *Tbx5* were also present in the

Figure 3.15

Tbx20 was expressed bilaterally in small group of nuclei either side of the ventral rhombencephalic midline (**A-F**):

A Cartoon of a mouse embryo at the 27/8 somite stage of development. Dotted lines numbered 1-4 indicate the plane of frontal sections shown in **C-F** respectively.

B Cartoon of the exposed brain of an embryo at the 27/8 somite stage of development. The brain can be divided into the telencephalon (forebrain, **f**), the mesencephalon (midbrain, **m**) and the rhombencephelon (hindbrain, **h**) at this stage. The planes of section numbered 1-4 in **A** are shown here to pass through the dorsal midbrain (1-3) and hindbrain (4), and the ventral hindbrain (1-4). The red line indicates the region where *Tbx20* was expressed.

C Section through the midbrain, and the rostral limit of the ventral hindbrain, on a frontal section through a 27/8 somite mouse embryo. The section through the head is illustrated, the '1' denotes the plane described in **A** and **B**. No *Tbx20* expression was detected at this level.

D Section through the ventral hindbrain, on a frontal section through a 27/8 somite mouse embryo. The section through the head is illustrated, the '2' denotes the plane described in **A** and **B**. Bilateral trails of nuclei either side of the ventral midline expressed *Tbx20*.

E Section through the ventral hindbrain, on a frontal section through a 27/8 somite mouse embryo. The section through the head is illustrated, the '3' denotes the plane described in **A** and **B**. Bilateral groups of *Tbx20*-expressing cells were detected immediately adjacent to the ventral midline, a thin trail of *Tbx20*-expressing nuclei extended a short distance dorsally on one side.

F Section through the ventral hindbrain, on a frontal section through a 27/8 somite mouse embryo. The section through the head is illustrated, the '4' denotes the plane described in **A** and **B**. At this level *Tbx20* expression is sharply restricted to a bilateral pair of nuclear groups either side of the cerebral aqueduct in the ventral hindbrain.

mTbx20 is expressed in ventral nuclei of the 27/8-somite stage hindbrain

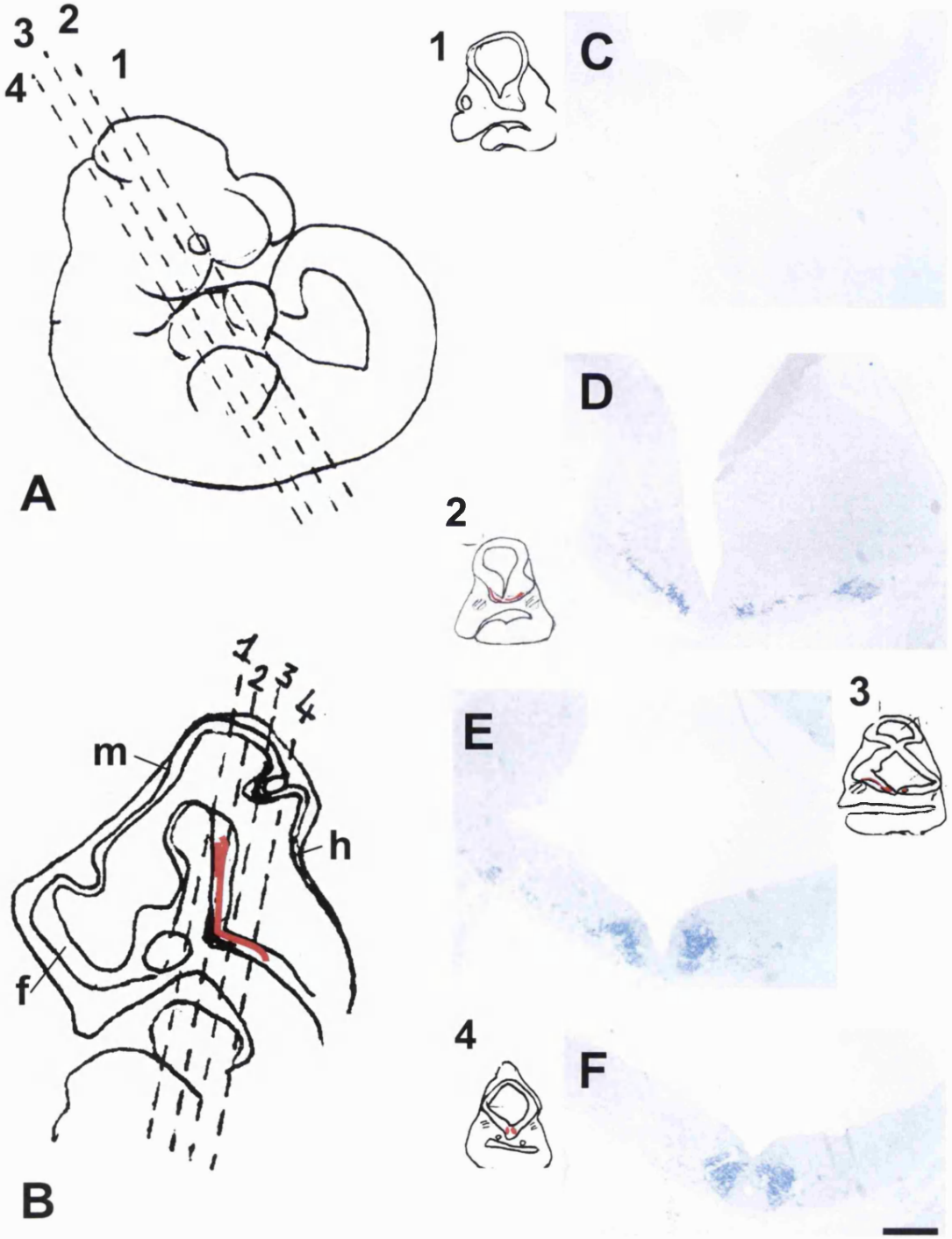

Figure 3.16

Tbx5 and *Tbx20* were expressed in complementary and overlapping patterns in the 27/8 somite stage mouse embryonic heart (**A-H**):

A Frontal section through the developing outflow tract and ventricles in the developing heart of a 27/8 somite stage mouse embryo. Cartoon (1) illustrates the whole section through the mouse embryo. See **Fig. 3.15A, B** for the relative planes of section of (1) to (4). *Tbx5* was expressed throughout the developing left ventricle (**lv**) and the right ventricular myocardium. *Tbx5* was also expressed in the pericardium (**p**). **ot**, outflow tract; **rv**, right ventricle.

B Adjacent section to that seen in **A**. *Tbx20* was expressed in the myocardium and the endocardial cushions of the outflow tract and the atrio-ventricular canal.

C Frontal section through the developing outflow tract and ventricles in the developing heart of a 27/8 somite stage mouse embryo. Cartoon (2) illustrates the whole section through the mouse embryo. *Tbx5* was expressed in the developing left ventricle (**lv**) and the right ventricular myocardium. Part of the right ventricle (**rv**) is missing on this section. **ot**, outflow tract.

D Adjacent section to that seen in **C**. *Tbx20* was expressed in the myocardium and the endocardial cushions of the outflow tract and the atrio-ventricular canal.

E Frontal section through the developing outflow tract (**ot**) and atria in the developing heart of a 27/8 somite stage mouse embryo. Cartoon (3) illustrates the whole section through the mouse embryo. *Tbx5* was expressed in the developing atria, more strongly on the left. **la**, left atrium; **ra**, right atrium.

F Adjacent section to that seen in **E**. *Tbx20* was expressed in the atrial myocardium and the endocardial cushions of the outflow tract.

G Frontal section through the developing outflow tract and atria of the developing heart of a 27/8 somite stage mouse embryo. Cartoon (4) illustrates the whole section through the mouse embryo. *Tbx5* was expressed in the atrial walls. *Tbx5* was also expressed in the tracheal mesenchyme. **ot**, outflow tract; **tr**, trachea.

H Adjacent section to that seen in **G**. *Tbx20* was expressed throughout the outflow tract and in the developing atrial myocardium. Scale bar = 0.1 mm.

mTbx20 and *mTbx5* are expressed in a complementary manner in the 27/8-somite stage heart

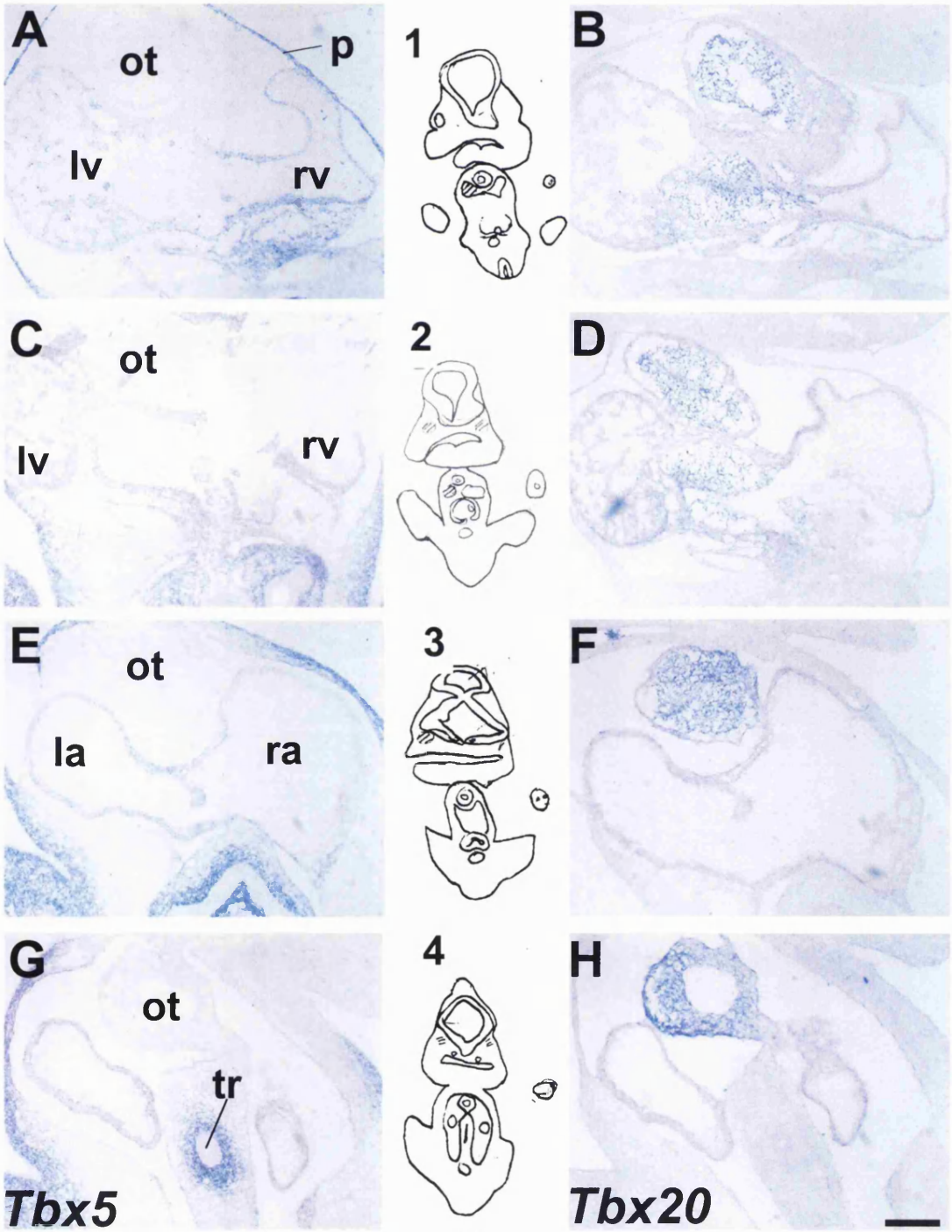

developing dorsal RPE implicating *Tbx2* and *Tbx5* in the provision of dorsal identity to RPE as well as neural retina. In the developing optic cup, *Tbx2*, *Tbx3* and *Tbx5* are all expressed in the dorsal retina (**Table 3.1**). Expression of *Tbx2* was restricted to the dorsal half and *Tbx5* was restricted to the dorsal quadrant of the retina. Although I was unable to detect *Tbx3* expression in the mouse, work out of my laboratory using S^{35} *in situ* hybridisation showed that *Tbx3* is weakly expressed in the dorsal mouse optic cup (Sowden *et al.*, 2001).

During the course of this work various studies in other species have shown that these early patterns of T-box gene expression are highly conserved. *Tbx5* is expressed in the optic vesicle at stage 11 and dorsally in the retina at least through to stage 21. Chick *Tbx2* and *Tbx3* are first detected in the dorsal optic cup from stage 14 (when the optic cup has just formed). (Gibson-Brown *et al.*, 1998; Gibson-Brown *et al.*, 1998; Ohuchi *et al.*, 1998; Koshiba-Takeuchi *et al.*, 2000). In the present study, *Tbx2* expression was detected in the newly formed mouse optic vesicle, earlier than that described in the chick. Zebrafish *tbx2* and *Xenopus Tbx3* (*ET*) expression begins much earlier than I have found in mammals. Both are strongly expressed in the anterior neural plate prior to the formation of recognisable eye structures (Li *et al.*, 1997; Dheen *et al.*, 1999; Ruvinsky *et al.*, 2000). *Xenopus Tbx3* eventually becomes restricted to the dorsal retina (Li *et al.*, 1997). *Tbx2* has a much broader dorsal expression domain than *Tbx3* in *Xenopus* whilst *Tbx5* expression is restricted to the dorsal ciliary margin (Horb and Thomsen, 1999; Takabatake *et al.*, 2000). Zebrafish genes *tbx5* and uniquely, *tbx4*, are expressed in dorsal retina. *tbx2* is expressed in a broader dorsal domain of the retina to *tbx4* and *tbx5* (Dheen *et al.*, 1999; Tamura *et al.*, 1999; Begemann and Ingham, 2000; Ruvinsky *et al.*, 2000).

I have found the dorsal restriction of T-box gene expression to be conserved in humans: *TBX2*, *TBX3* and *TBX5* are expressed dorsally in the 6 wpc retina (**Table 3.1**). These graded and overlapping domains suggest these genes work in tandem to provide positional identity along the dorso-ventral axis of the vertebrate retina. There may be some redundancy in the functions of these closely related T-box genes, though perhaps not with *TBX5*. *TBX5* appears to be primarily an activator of transcription (Bruneau *et al.*, 2001; Hatcher *et al.*, 2001; Hiroi *et al.*, 2001) while *TBX2* and *TBX3* function as transcriptional repressors (Carreira *et al.*, 1998; He *et al.*, 1999).

Table 3.1. T-box gene expression in the developing human and mouse Retina

	Weeks after Conception			
Human gene	**6**	**9**	**12**	**15**
TBX2	D	IL	GCL, INL	GCL, INL
TBX3	D	D	D, INL	INL
TBX5	D	D	D, GCL	-
	Embryonic Day			
Mouse gene	**11.5**	**14.5**	**18.5**	**Adult**
Tbx2	D	D, IL	D	GCL, INL
Tbx3	D	D	-	INL
Tbx5	D	D, IL	D	-
Level of Retinal Stratification	IL begins to emerge from uniform retina	IL and OL; NFL with RGC axons	GCL and INL; Photoreceptor cells in OL	Mature retina with GCL, INL and ONL

This table is based on data recorded in this chapter and on other work out of my laboratory (in the case of data on *Tbx3* and on adult mouse eyes). It indicates equivalent mouse and human stages in eye development as judged by the level of retinal stratification. Note that *TBX2* expression loses dorso-ventral asymmetry once the inner and outer layers are firmly established whilst *Tbx2* remains dorsally expressed in the retina when axons are forming central connections. D, expression within dorsal neural retina. Where expression becomes restricted to specific retinal layers, this is indicated as follows: IL, inner layer; GCL, ganglion cell layer; INL, inner nuclear layer. A '-' indicates a lack of data for that gene/stage. Other abbreviations used in the description of the level retinal stratification: NFL, nerve fibre layer; OL, outer layer; ONL, outer nuclear layer; RGC, retinal ganglion cell.

Positional identity is essential for what could be described as developmental fine-tuning of the retina, the establishment of the precise shape of the eyeball, the formation of appropriate connections between neurons. During early phases of eye development in particular, T-box genes may be involved in the control of morphogenetic tools such as cell cycle regulators. In the *Tbx5* null mouse, an absence of *Tbx5* expression leads to severe hypoplasia in posterior domains of the mouse heart (Bruneau *et al.*, 2001). Likewise overexpression of human *TBX5 in vitro* and *in vivo* in chick hearts has been shown to cause an arrest of cellular proliferation (Hatcher *et al.*, 2001). This effect may be indirect as proliferation was reduced in an at least partly non-cell autonomous manner (Hatcher *et al.*, 2001).

As neuronal development proceeds T-box genes may regulate axon guidance molecules so that intra-retinal axons make appropriate targets. In the case of RGCs, positional identity will be essential to equip their axons and growth cones with the guidance molecules now known to be essential for the formation of a retinotopic map in central brain targets (Harris and Holt, 1995). Human *TBX3* and *TBX5* showed polarised dorsal expression until 12 wpc, *TBX5* expression faded ventrally and became restricted to presumptive RGCs at the edges of its expression domain. In the mouse, *Tbx2* and *Tbx5* showed graded dorsal-to-ventral retinal expression until E18.5, an equivalent stage morphologically to the 12 wpc human retina (**Table 3.1**). At this stage RGC axons are reaching their targets in the brain (Godement *et al.*, 1984). Thus *TBX5* in the human and *Tbx2* and *Tbx5* in the mouse are expressed in the right patterns at the right time to be regulating axon guidance molecules whilst retinotopic maps are being formed in retino-recipient areas of the brain.

TBX3 is expressed in a small subset of cells in the region of the prospective inner nuclear layer. Although the cells of this region do contain POU4F2, in view of their location and the subsequent restriction of *TBX3* to the inner nuclear layer it is suggested that these cells are more likely to be developing amacrine cells (see **3.6.** for discussion on whether POU4F2 marks only developing RGCs). If the small subset of dorsal cells expressing *TBX3* at 12 wpc were indeed amacrine interneurons, the possibility of an indirect influence of this gene on dorsal RGCs via modulation by amacrine cells remains.

In light of this discussion, *omb*-related genes *hTBX5*, *mTbx2* and *mTbx5* are all presented as strong candidate regulators of axon guidance for dorsal RGCs. This premise is strengthened by the knowledge that *omb* itself is responsible for the proper axon guidance of optic neurons in *Drosophila* (Pflugfelder and Heisenberg, 1995). Recently, such a role has been reported for *Tbx5* in the chick. When misexpressed in the chick retina, *Tbx5* downregulated expression of ventral markers, induced dorsal ephrinB guidance molecules in ventral retina, and disrupted dorsal projections to the optic tectum (Koshiba-Takeuchi *et al.*, 2000). When *Tbx3* was overexpressed in the *Xenopus* retina, ventral markers were downregulated, but dorsal markers were not upregulated (Wong *et al.*, 2002). This is consistent with its role as a transcriptional repressor (He *et al.*, 1999). *Tbx5*, primarily a transcriptional activator (Bruneau *et al.*, 2001; Hatcher *et al.*, 2001; Hiroi *et al.*, 2001), might effect the repression of ventral markers by inducing *Tbx3* and/or *Tbx2* when it is misexpressed.

Laminar expression of T-box genes in the developing mammalian retina

As soon as the retina can be divided into an inner and an outer layer, T-box genes begin to show differential expression across the width of the retina (**Table 3.1**). For *TBX2* this was first evident at 9 wpc in humans, when dorso-ventral asymmetry was lost and expression became restricted to the inner layer. Later *TBX2* was expressed in the ganglion cell and inner nuclear layers of the 15 wpc human retina. Although expression of *Tbx2* persists throughout the dorsal mouse eye, *Tbx2* expression was restricted to the inner layer ventrally at E14.5. Differential expression of mouse *Tbx2* in different retinal layers was maintained at E18.5. *Tbx2* mRNA was detected in the innermost and outermost cells of the ventral outer layer (presumed to be amacrine interneurons and photoreceptors respectively). Thus *TBX2*/*Tbx2* appear to have roles in the development of specific cellular layers/cell types as well as in dorso-ventral patterning in the retina, though these seem likely to be different between mouse and human.

At 12 wpc the dorsal *TBX3* domain became restricted to a line of cells in the region of the prospective inner nuclear layer. At 15 wpc it was expressed throughout the post-mitotic region of the interneuron-containing inner nuclear layer with no dorso-ventral

asymmetry. This suggests *TBX3* is involved in the development of the inner nuclear layer and/or retinal interneurons.

For *Tbx5*, very strong expression was seen in isolated cells of the inner layer throughout dorsal and ventral retina in the E14.5 mouse. This strong expression was apparently superimposed upon a dorsal gradient through both layers that faded ventrally and was no longer apparent at E18.5. The different expression levels may imply a gene dosage effect. High threshold levels of transcription factor may activate different genes in a neuronal subset of the inner layer to those activated by the graded dorsal levels of expression. Human *TBX5* expression showed restriction to the developing ganglion cell layer in the margins of its dorsal domain at 12 wpc, but was not detected using *in situ* hybridisation at later stages.

RT-PCR showed that expression of all three human genes persisted into adulthood, suggesting a role in the maintenance of laminar identity (for *TBX2* and *TBX3* at least) within the mature eye. The relatively high levels of T-box gene expression detected from 10 wpc human samples for RT-PCR may represent higher expression levels at these younger stages. They may alternatively be due to the whole eye samples from which the RNA was extracted containing relatively more neural retina in the younger samples.

omb-related T-box genes join a whole host of other genes encoding transcription factors that occupy distinct cellular bands during retinal stratification. These include *Pou4f* genes (Xiang *et al.*, 1995; Xiang, 1998) and *RPF-1* (Zhou *et al.*, 1996) of the POU domain gene family, LIM homeobox genes *Islet-1* (Thor *et al.*, 1991) and *Lhx2* (Porter *et al.*, 1997), homeobox gene *Chx10* (Ferda Percin *et al.*, 2000), paired-box gene *Pax6* (Davis and Reed, 1996; Belecky-Adams *et al.*, 1997) and Olf-1/EBF-like helix-loop-helix genes O/E-1 (Olf-1) and O/E-2 (Davis and Reed, 1996; Wang *et al.*, 1997) within the developing ganglion and inner nuclear cell layers alone. The overlapping and inter-regulating networks of transcription factors that control laminar and individual cell specification within the retina are highly complex. The tangled nature of their various interactions are only beginning to be unravelled (Plaza *et al.*, 1999; Wang *et al.*, 2001). Further investigations of the interactions of different

transcription factors with each other and with their downstream targets will hopefully allow a coherent picture to emerge.

3.6. POU4F2 is most prominent in early retinal development

This is the first study to look at POU-domain transcription factor POU4F2 distribution in the developing human retina and the most comprehensive in any species to date. It demonstrates that POU4F2 is localised to most nuclei of the inner layer of the developing human retina and becomes restricted to subsets of the newly formed ganglion cell layer, as seen in other mammalian species. The antibody used was specific to POU4F2 and does not cross-react with closely related proteins POU4F1 and POU4F3 (Santa Cruz Biotechnology, UK).

POU4F2 was distributed in the vast majority cells throughout the inner layer of the early human retina (6-9 wpc) and virtually all at 12 wpc, a time when ganglion cell and inner nuclear layers are emerging. Histological studies suggest the early inner layer of the retina gives rise to amacrine cells of the ganglion cell and inner nuclear layers as well as to RGCs. Some cells migrate back towards the RPE from the prospective ganglion cell layer across the developing inner plexiform layer and form amacrine cells (Mann, 1964; Hinds and Hinds, 1978). It may be that these early POU4F2-labelled cells are not all fated to be RGCs. Some might be predicted to stop producing POU4F2 and differentiate into other cells types. The presence of *TBX3* mRNA, which became restricted to the interneuron-dominated inner nuclear layer at 15 wpc, in the region of the POU4F2-immunoreactive developing inner nuclear layer at 12 wpc, supports this idea.

The intensity of POU4F2 labelling in the inner layer of the retina varied considerably between different nuclei and strongly labelled cells frequently lay in the outer regions of the inner layer, particularly in the peripheral retina. This presents the possibility that a dosing effect of POU4F2 may be important for different functions, and could potentially directly pattern cells along the laminar axis of the retina at these early stages. Strongly POU4F2-labelled cells in the dorsal peripheral retina occupy the same regions that express *TBX3* and have been proposed to be part of the emerging inner nuclear layer in dorsal retina (see **3.5.** above). It is thus interesting to note that

displaced RGCs of the inner nuclear layer are more frequently found in the peripheral retina (Drager and Olsen, 1981).

POU4F2 was restricted to a subset of (presumably RGC) nuclei in varying amounts within the developing ganglion cell layer (~70% of ganglion layer cells in central retina) at 15 wpc. There is considerable variation between species of the different subsets of adult RGCs containing Pou4f2. In the mouse and rat a large unidentified subset are labelled and in the cat all RGCs are labelled (Xiang *et al.*, 1995). In the adult rabbit, double labelling of cells with Pou4f2 and antibodies raised specifically against adult RGCs showed Pou4f2 is exclusive to RGCs in the adult (Xiang *et al.*, 1993). In the macaque, strong immunoreactivity is detected in retrogradely labelled P-type RGCs, and weak immunoreactivity in M-type RGCs (Xiang *et al.*, 1995). In the human 15 wpc retina, the subsets of cells strongly and weakly POU4F2 labelled are likely to represent the development of distinct RGC types.

POU4F2 was distributed in virtually all cells of the presumptive ganglion cell and inner nuclear layers at 12 wpc. By 15 wpc POU4F2 remained in only a subset of RGC nuclei and was not present in the inner nuclear layer. If POU4F2 marks only future RGCs, then high numbers of POU4F2-positive presumptive RGCs must die and/or become greatly spread out during retinal growth between 12 and 15 wpc. Newly born presumptive amacrine and RGCs must then migrate inwards to repopulate the inner nuclear and ganglion cell layers. Alternatively, if some of the early POU4F2-containing cells of the inner layer do not give rise to RGCs, as I suggested above, some of the apparent loss of POU4F2 positive cells could be due to *POU4F2* downregulation in cells not fated to become RGCs.

Studies of *Pou4f2*-null mice have implicated *Pou4f2* in RGC development only (Erkman *et al.*, 1996; Gan *et al.*, 1996; Gan *et al.*, 1999). The seemingly identical localisation of POU4F2 in developing human retina to that in mice suggests a similar role. Nevertheless, it is hard to believe that the entire cellular population of the inner retina at 12 wpc are reduced to a subset of cells in the ganglion cell layer by 15 wpc.

If POU4F2 is active in cells of the inner retina not fated to be RGCs, its purpose is unclear. The inward migration of post-mitotic cells and formation of the inner layer is

not affected in the *Pou4f2* null mouse (Gan *et al.*, 1999). This could be due to redundancy, as various other transcription factors, related and otherwise, are similarly expressed in the inner layer of the early mouse retina (Davis and Reed, 1996; Zhou *et al.*, 1996; Xiang, 1998). It is possible that *POU4F2/Pou4f2* is important for the expression and/or function of genes involved in retinal patterning. Recently mouse *Pou4f2* has been implicated in RGC axon guidance and topographical mapping in the superior colliculus (Erkman *et al.*, 2000). This could be explained by interactions between *POU4F2* and the genetic pathways that control retinal patterning. Such pathways could potentially involve *TBX2*, *TBX3* and *TBX5*, shown by the present study to be expressed in POU4F2 positive cells.

3.7. *Tbx20* is implicated in the development of the cranial motor nuclei and the endocardial cushions of the heart

During the course of this work, other groups have identified *Drosophila H15*-related T-box genes in mice and in zebrafish. In zebrafish, expression of *tbx20* (also known as *hrT*) was identified in developing cranial motorneurons, the developing heart, and in the developing eye (Ahn *et al.*, 2000; Griffin *et al.*, 2000). In the zebrafish optic cup, *tbx20* was expressed in the developing eye near the choroid fissure, later in innermost ventrally located retinal cells adjacent to the lens (Ahn *et al.*, 2000; Griffin *et al.*, 2000). In the developing mouse, *Tbx20* (also known as *Tbx12*) expression was detected in the heart, lateral mesoderm, allantois, ventral hindbrain/rostral neural tube and the dorsal optic vesicle (Carson *et al.*, 2000; Kraus *et al.*, 2001). At the optic cup stage, *Tbx20* was expressed throughout the neural retina in the mouse (Kraus *et al.*, 2001).

I was unable to detect *Tbx20* expression in the mouse eye. This could be explained if the probe I used recognises a different transcript of *Tbx20* to those used by others (Carson *et al.*, 2000; Kraus *et al.*, 2001) that is not present in the eye. Alternatively it may be due to an insufficient sensitivity of my RNA probe with the protocol used for *in situ* hybridisation. The *Tbx20* expression reported in the dorsal mouse optic vesicle by others (Carson *et al.*, 2000; Kraus *et al.*, 2001) raises the possibility that it functions alongside rather than opposite the *omb*-related T-box genes. The ventrally located *tbx20* expression in zebrafish (Ahn *et al.*, 2000; Griffin *et al.*, 2000) shows

that this putative role in dorsal patterning is not conserved, unlike with the zebrafish *omb*-related T-box genes (Ruvinsky *et al.*, 2000).

The *Tbx20* expression observed in the ventral hindbrain is consistent with the description by others of *Tbx20* expression in the cranial motor neurons of developing mice and zebrafish (Ahn *et al.*, 2000; Kraus *et al.*, 2001). Based on the observations of Kraus *et al.* it is likely that the *Tbx20* expression I observed in the hindbrain are migrating cranial motor nuclei from rhombomere 2. These patterns of expression implicate *Tbx20* in the development of cranial motor nerve nuclei.

Tbx20 was prominently expressed in the developing endocardial cushions of the heart as previously described by Meins *et al.* (Meins *et al.*, 2000), suggesting an important role in the development of these structures. Endocardial expression of *Tbx5* was limited to the left ventricle. *Tbx5* was expressed in the myocardium of both ventricles. The lower *Tbx5* expression previously reported in the right ventricle at this stage (Bruneau *et al.*, 1999) may thus be due to the absence of endocardial *Tbx5* expression. If an inhibitory relationship exists between *Tbx20* and *Tbx5* in the endocardium it does not in the myocardium as both genes were expressed there in the 27/8-somite mouse embryo.

3.8. Conclusion

I have shown that *omb*-related T-box genes are expressed in the dorsal mouse and human retina during early eye development where they are likely to control dorsal retinal identity. I have also shown that their expression become restricted to different layers during retinal stratification. Thus they are likely to have separate roles in retinal lamination. Human *TBX5* and mouse *Tbx2* and *Tbx5* all show gradients of expression in RGCs across the dorso-ventral axis of the retina at a time when their projections are reaching central brain targets. These three genes are proposed as good candidates for regulating axon guidance molecules in the dorsal retina.

CHAPTER 4

Developmental expression of T-box genes and their putative regulators in normal and mutant mice

INTRODUCTION

Several avenues of enquiry in the exploration of *omb*-related mammalian T-box gene function follow from the previous chapter. These are summarised with the following questions: What is the role of T-box transcription factors in dorso-ventral patterning of the retina? How do the overlapping lamina-specific expression domains of T-box genes shape retinal stratification? How is the expression of T-box genes regulated during development? What are the target genes regulated by T-box transcription factors during retinal development?

In this chapter I address the question of what position *omb*-related T-box genes occupy in the genetic hierarchy that controls dorso-ventral patterning of the mammalian retina. I compared the expression of *bone morphogenetic protein 4* (*Bmp4*) to mouse T-box genes and other transcription factors in the mouse retina to determine whether BMP4, a known morphogen, is likely to be an upstream regulator of mammalian T-box gene expression. Expression of *Bmp4*, encoding a secreted growth factor from the transforming growth factor beta (TGFβ) superfamily, has been previously reported in the dorsal eye during chick, mouse and *Xenopus* development (Francis-West *et al.*, 1994; Hemmati-Brivanlou and Thomsen, 1995; Papalopulu and Kintner, 1996; Furuta and Hogan, 1998). Decapentaplegic (DPP), the *Drosophila* orthologue of vertebrate BMP2/4, regulates *omb* in the *Drosophila* wing, leg and genital imaginal discs (Brook and Cohen, 1996; Grimm and Pflugfelder, 1996; Gorfinkiel *et al.*, 1999). In the chick, BMP2 regulates *omb*-related T-box genes in the heart and limb (Rodriguez-Esteban *et al.*, 1999; Yamada *et al.*, 2000). Other transcription factor genes examined were *Vax2*, a ventral homeobox gene and novel forkhead gene *Foxn4*. Homeobox gene *Vax2* has been identified in the ventral retina of the developing mouse (Barbieri *et al.*, 1999; Ohsaki *et al.*, 1999), and is known to confer ventral retinal identity and regulate other asymmetrically expressed genes (Barbieri *et al.*, 1999; Schulte *et al.*, 1999). *Foxn4* encodes a forkhead (winged helix) transcription factor newly identified from a mouse eye cDNA library with low stringency hybridisation to the forkhead domain of *Foxg1* (Gouge *et al.*, 2001). *Foxg1* and related *Foxd2* (formerly known as *BF-1* and *BF-2*) are expressed in ~~developing~~ anterior and posterior domains of the developing retina respectively (Hatini *et al.*,

1994). I wanted to know if *Foxn4* was also asymmetrically expressed in the developing retina.

Gene expression was examined in mice homozygous for null mutations in genes with a potential or expected influence on dorso-ventral patterning. Expression of *Tbx5* and *Vax2* were examined as dorsal and ventral retinal markers, to detect disruptions in dorso-ventral patterning of the retina. *Small eye* (*Sey*) mice carry a null mutation in *Pax6*, a paired-box transcription factor gene generally viewed as a master control gene of eye morphogenesis (Baker, 2001). Heterozygous mutants for *Pax6* survive, but have small eyes, hence the name. Homozygous mice have no eyes and die shortly after birth – they cannot breathe whilst suckling (Hill *et al.*, 1991). Analysis of homozygous mouse embryos has shown that an optic vesicle is actually formed, but a lens placode is never induced and rather than invaginate, the optic vesicle degenerates completely (Grindley *et al.*, 1995). *Pax6* is involved in the dorsal patterning of neural structures the diencephalon (Grindley *et al.*, 1997; Pratt *et al.*, 2000), the telencephalon (Stoykova *et al.*, 2000; Toresson *et al.*, 2000) and the pituitary (Kioussi *et al.*, 1999). *Pax6* is implicated in dorsal patterning of the retina for the following reasons: (1) *Pax6* expression shows a transient restriction to the dorso-distal optic vesicle in chick and mouse (Li *et al.*, 1994; Grindley *et al.*, 1995). (2) *Pax6* interacts negatively with ventral gene *Pax2* (Schwarz *et al.*, 2000). (3) *Pax6* seems to be negatively regulated by ventral determinant Sonic hedgehog (SHH) in chick (Huh *et al.*, 1999; Zhang and Yang, 2001) and in *Xenopus* (Sasagawa *et al.*, 2002). (4) In *Xenopus*, *Pax6* has been shown to be positively regulated by dorsal retinal determinant BMP4 (Sasagawa *et al.*, 2002).

Expression of *Tbx5* and *Vax2* was examined in a second mouse model with small eyes (microphthalmia) called *ocular retardation* or *or*. In contrast to the *Sey* mutant, in the *or* mice the optic vesicle invaginates to form an optic cup, but the progenitor cells of the neural retina show reduced levels of proliferation. Naturally occurring homozygous *ocular retardation* (*or*) mutant mice are blind, their eyes are small, their retinas are disorganised and they fail to develop an optic nerve (Burmeister *et al.*, 1996). *or* mice carry a null mutation in homeobox transcription factor *Chx10*, a gene expressed throughout the undifferentiated retina in mice and in humans (Ferda Percin

et al., 2000). I have examined dorso-ventral patterning in the *or* mutant optic cup for the following reasons:

(1) The major defect in the *or* retina appears to be one of proliferation of retinal progenitor cells, particularly in the dorsal retina (Burmeister *et al.*, 1996). Recent work implicates BMP4 in promoting retinal cell proliferation in the dorsal retina (Trousse *et al.*, 2001). This suggests a possible link. If *Bmp4* expression was regulated by *Chx10* one might expect defects in dorso-ventral patterning in the *or* mutant retina.

(2) Retinoid-related orphan nuclear receptor-β is downregulated in *or* mutants raising the possibility that retinoic acid (RA) signalling could similarly be affected (Chow *et al.*, 1998). If this is the case, given the apparent importance of retinoic acid in dorso-ventral polarisation of the retina (see **1.3.**), dorso-ventral patterning could be disrupted in the *or* eye.

(3) *Foxn4* is asymmetrically expressed across both planar axes of the developing retina (see **4.3.**). Expression in retinal progenitor cells is severely diminished in the *or* mutant eye suggesting that *Foxn4* lies downstream of *Chx10* in these cells (Gouge *et al.*, 2001). If asymmetrically expressed *Foxn4* is involved in retinal patterning, then defects in dorso-ventral patterning might be observed in the *or* retina.

Mice carrying a null mutation in *sonic hedgehog* (*Shh*) were the final group of mutant mice to be examined. Mice homozygous for the *Shh* mutation exhibit severe axial and patterning defects including cyclopia and holoprosencephaly. They lack ventral midline structures. In the embryo the single eye does not develop ventral features, such as an optic stalk and expresses *Otx2*, a marker for retinal pigmented epithelium (RPE), which is derived from dorsal neuroepithelium (Chiang *et al.*, 1996). *Shh* is known to be involved in early dorso-ventral patterning of the eye and promotes ventral identity in the optic cup (Huh *et al.*, 1999; Zhang and Yang, 2001). In Chapter 3 *Tbx2* and *Tbx5* expression was demonstrated in the dorsal-most region of the developing RPE. I wanted to find out whether T-box genes were expressed in the cyclopic eye of the *Shh* homozygous mutant.

It is the aim of this chapter to: (1) Give a regulatory context for *omb*-related T-box genes in dorso-ventral retinal compartmentalisation. (2) Examine the potential of

BMP4 as a subject for further study. (3) Provide new insight into the origin of dorsal and ventral identity in the retina.

RESULTS

The expression patterns of *Tbx2*, *Tbx5*, *Bmp4*, ventrally expressed homeobox gene *Vax2* and newly identified forkhead gene *Foxn4* were compared in the developing retina of wild-type mice. *Tbx5* and *Vax2* expression were examined in homozygous mutants for *Pax6* and *Chx10* to determine whether dorso-ventral patterning was disrupted. *Tbx2* expression was analysed in *Shh* mutants to question whether it patterns the cyclopic eye.

4.1. *Bmp4* is co-expressed with *Tbx2* and *Tbx5* in the developing dorsal retina of mice

Bmp4 expression was first detected during eye development in the dorsal optic pits in the 7-somite mouse embryo. *Bmp4* was also strongly expressed in the surface epithelium (**Fig. 4.1A**). Diffuse expression of *Tbx5* and *Vax2* was detected in the optic pits in mouse embryos at the 9-somite stage (**Fig. 4.1B, C**). In the 18-somite stage mouse embryo, *Bmp4* mRNA was localised to the dorsal optic vesicle. Expression was also present in the overlying surface ectoderm, where it was more apparent in surface ectoderm that did not overlie *Bmp4*-expressing prospective retina (**Fig. 4.1D, E**). *Bmp4* expression in the dorsal optic vesicle was identical to that of *Tbx2* and *Tbx5* at this stage (**Fig. 4.1F, G**). Expression extended proximally into a small region of dorsal neuroepithelium not in direct apposition to the surface epithelium (prospective RPE). *Vax2* was expressed in the optic stalk and the ventral-most optic vesicle in the 16-somite stage mouse embryo (**Fig. 4.1H**). By the 20-somite stage *Vax2* was clearly expressed in the optic stalk and the ventral half of the optic vesicles (**Fig. 4.1J**). This 'ventral half' included presumptive RPE dorsal to the ventrally located optic stalk, and complemented the dorsal domains of *Bmp4*, *Tbx2* and *Tbx5*.

At the late optic vesicle stage (24 somites), *Tbx5* was expressed in the presumptive dorsal neural retina and over the dorsal boundary between presumptive neural retina

Figure 4.1

Dorsal *Bmp4* expression and diffuse *Tbx5* and *Vax2* expression was detected in the mouse optic pits (**A-C**):

A *Bmp4* mRNA was first detected in presumptive mouse retina in the dorso-distal aspect of the optic pits at the 7-somite stage of development (arrow). *Bmp4* was also strongly expressed in the overlying surface ectoderm. Dorsal (**d**) is indicated as up for all figures. Scale bar = 50 μm.

B *Tbx5* transcripts was first detected, faintly and diffusely, in the expanding optic pits of the 9-somite mouse embryo (arrow). Expression was also seen in the ventricular region of the developing heart. Scale bar = 0.2 mm.

C *Vax2* mRNA was first detected diffusely in the expanding optic pits of the 9-somite mouse embryo (arrow). Scale bar = 0.2 mm.

Bmp4 is co-expressed with *Tbx2* and *Tbx5* in the dorsal mouse optic vesicles (**D-G**):

D *Bmp4* was strongly expressed in the dorsal optic vesicles at the 18-somite stage of development (arrow). *Bmp4* expression was also present in the overlying surface ectoderm, this was more apparent ventrally where the ectoderm did not overlie *Bmp4*-expressing retina (arrowheads). Scale bar = 50 μm.

E In the whole embryo of that sectioned in **D** (dotted line marks plane of section), *Bmp4* expression was seen in the dorsal optic vesicle (arrow), the ventral diencephalon, the developing heart, the region of the developing gut and the developing forelimbs. Scale bar = 0.2 mm.

F In sections of a 15-somite stage mouse embryo, *Tbx2* is expressed in the dorso-distal optic vesicles in the same region as that seen for *Bmp4* in **D**. *Tbx2* mRNA was also detected in the mesenchyme ventral to the optic vesicles. Scale bar = 50 μm.

G *Tbx5* was similarly expressed to *Bmp4* and *Tbx2* in the dorso-distal optic vesicles at the 15-somite stage of development. Scale bar = 50 μm.

Vax2 is expressed in the proximo-ventral optic vesicles (**H, J**):

H Polarised *Vax2* expression was observed in the proximo-ventral optic vesicles at the 16-somite stage of development. Scale bar = 0.2 mm.

J In the 20-somite stage mouse embryo, *Vax2* mRNA was strongly detected in the ventral optic vesicles, in the ventral retina and in the optic stalk. Scale bar = 0.2 mm.

Tbx2, *Tbx5* and *Bmp4* expression co-localises in the early optic vesicles

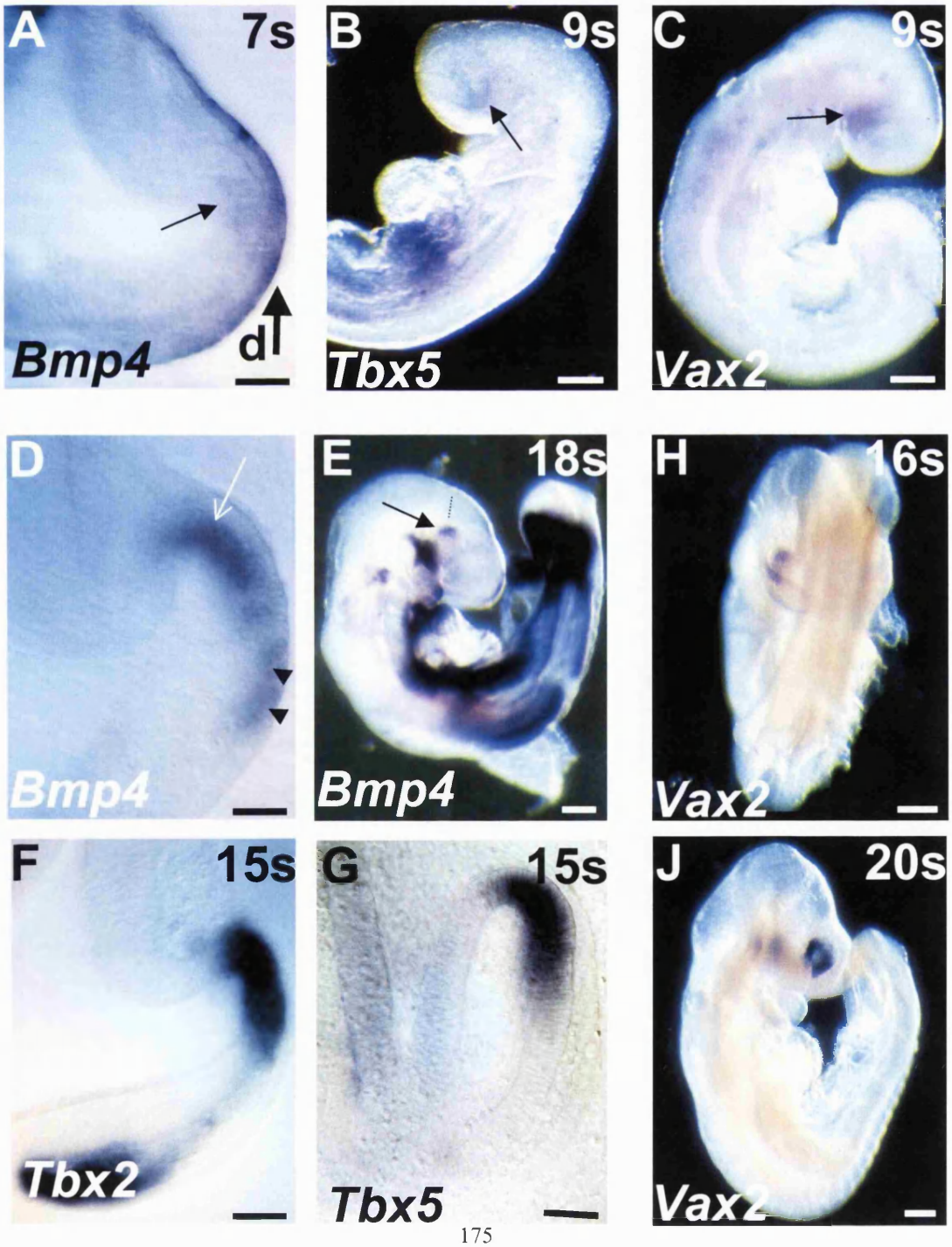

and RPE (**Fig. 4.2A, B**). In a 27-somite stage mouse embryo the optic vesicle was seen to be invaginating. *Tbx2* was expressed more broadly than *Tbx5* in the dorsal retina and the presumptive dorsal RPE (**Fig. 4.2C, D**). Unlike *Tbx5*, low level *Tbx2* expression was present in ventral neural retina. *Bmp4* in the forming optic cup at the 29-somite stage showed graded expression in the dorsal neural retina (**Fig. 4.2E, F**). The *Bmp4* expression domain lay within that of *Tbx2* and closely matched that of *Tbx5*. No *Bmp4* expression was observed in the presumptive dorsal RPE. *Bmp4*, *Tbx2* and *Tbx5* mRNA remained closely associated in the dorsal retinal quadrant of the early optic cup (**Fig. 4.3A-C**). Complementary expression of *Vax2* was similarly maintained, in the ventral quadrant of the neural retina (**Fig. 4.3D**). Expression of forkhead gene *Foxn4* was also examined at this stage (**Fig. 4.4**) and is described below.

Expression of *Bmp4* remained restricted to the dorsal quadrant of the retina at 40 somites, though on sectioning was localised to the dorsal-most tip (**Fig. 4.5A, B**). *Tbx5* mRNA also remained localised to the dorsal quadrant of the retina at the 53-somite stage (**Fig. 4.5C**), but the *Tbx2* expression domain had outgrown that of *Bmp4* to cover the entire dorsal hemiretina (**Fig. 4.5D**). In the 46-somite stage mouse embryo, *Vax2* expression covered the ventral third of the optic cup (**Fig. 4.5E**). *Foxn4* was expressed in the dorso-temporal, dorso-nasal and ventro-nasal quadrants of the retina at the 46-somite stage (**Fig. 4.5F**). See **4.2.** below for details.

4.2. *Foxn4* is expressed in an expanding dorso-nasal domain in the developing optic cup

I examined *Foxn4* expression in mouse embryos at E9 and E10. Retinal expression was first detected at the optic cup stage in the 36-somite mouse embryo (**Fig 4.4A, B**). Expression was observed in a thin band within the dorso-nasal quadrant of the optic cup (**Fig 4.4A**). Vibratome sectioning revealed strong *Foxn4* expression in the inner aspect of centro-dorsal neural retina (**Fig 4.4B**). Strong expression was also observed in the dorsal aspect of the rostral midbrain (**Fig 4.4C**) and in bilateral ventro-lateral portions of the neural tube that extended as far as the isthmic region at the midbrain/hindbrain boundary (**Fig 4.4A, D-F**). These patterns persisted in the 48-somite mouse embryo (not shown), but in the neural retina expression of *Foxn4*

Figure 4.2

Bmp4 expression was co-expressed with *Tbx2* and *Tbx5* in the dorsal retina at the stage of optic vesicle invagination (**A-F**):

A *In situ* hybridisation for *Tbx5* on a 24-somite mouse embryonic head. *Tbx5* was expressed in the dorsal aspect of the optic vesicle. Dotted line indicates section in **B**. Dorsal (**d**) is indicated as up for all figures.

B Section through the optic vesicle of the embryo in **A**. *Tbx5* expression was sharply restricted to the dorsal half of the presumptive neural retina (demarcated by dotted lines).

C *In situ* hybridisation for *Tbx2* on a 27-somite mouse embryonic head. *Tbx2* was expressed in the dorsal aspect of the optic vesicle, more broadly than *Tbx5*. Dotted line indicates section in **D**.

D Section through the invaginating optic vesicle of the embryo in **C**. The overlying surface ectoderm thickened at this stage to form a lens placode and optic vesicle was in the process of invagination. *Tbx2* was expressed in graded fashion across the presumptive neural retina (demarcated by dotted lines and thickened with respect to presumptive retinal pigmented epithelium) with high levels dorsally and lower levels ventrally. Expression extended dorsally into presumptive retinal pigmented epithelium (RPE).

E *In situ* hybridisation for *Bmp4* on a 29-somite mouse embryonic head. *Bmp4* was expressed in the dorsal quadrant of the invaginating optic vesicle in a smaller domain than *Tbx2*. Dotted line indicates section in **F**. Scale bar = 0.2 mm for **A**, **C** and **E**.

F Section through the invaginating optic vesicle of the embryo in **E**. *Bmp4* expression was restricted to the dorsal aspect of presumptive neural retina (demarcated by dotted lines), now grossly thickened with respect to the presumptive RPE. Expression was graded across the dorsal retina, with highest levels at the dorsal-most aspect of the presumptive neural retina. Expression did not extend further dorsally into presumptive RPE. The optic vesicle was further invaginated compared to the 27-somite stage and the optic cup was nearly formed. Scale bar = 50 μm for **B**, **D** and **F**.

Tbx2, *Tbx5* and *Bmp4* expression co-localises in the dorsal presumptive neural retina

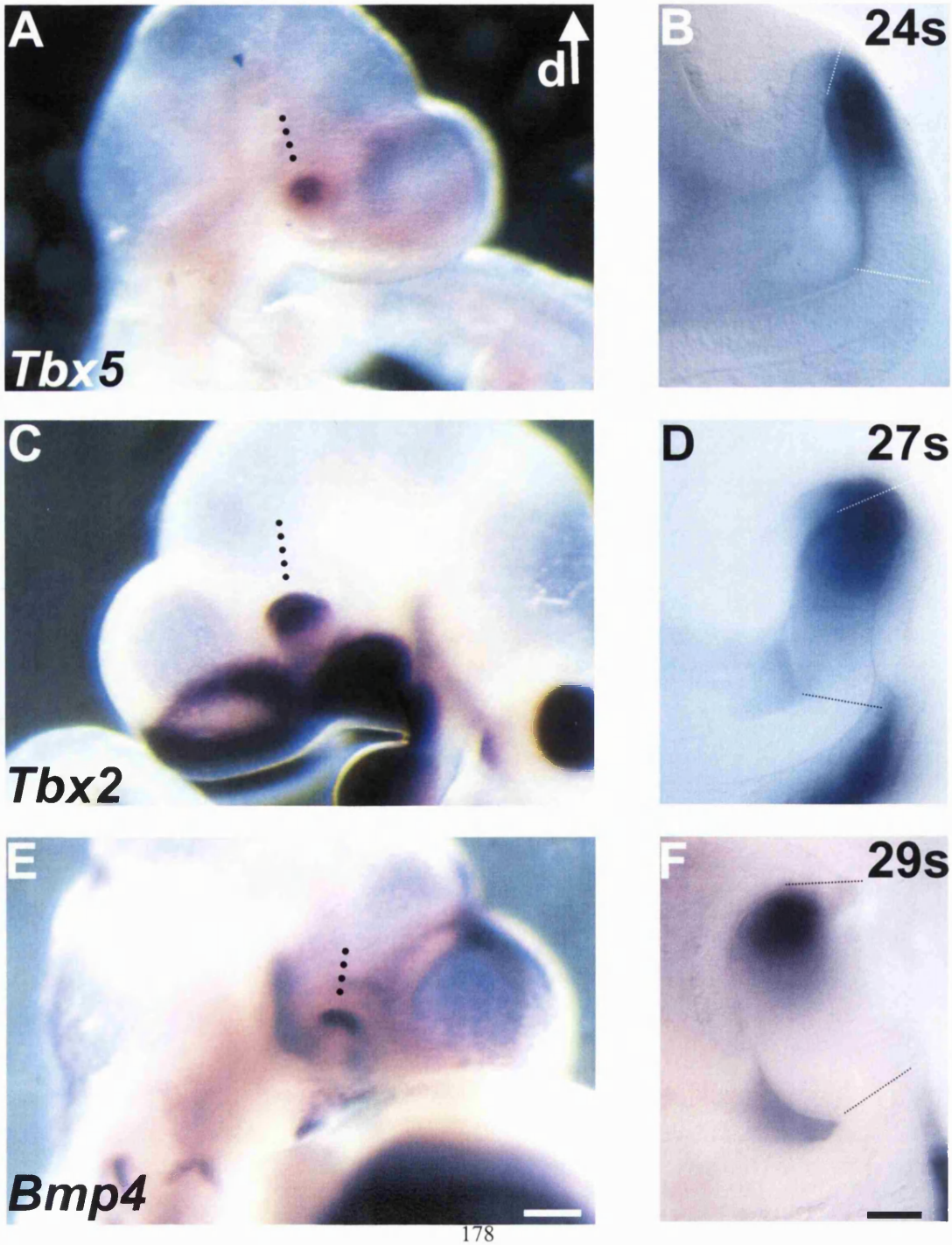

Figure 4.3

Bmp4 expression was expressed in the same dorsal domain as *Tbx2* and *Tbx5* in the newly formed optic cup, while *Vax2* was expressed in ventral retina (**A-D**):

A *In situ* hybridisation for *Tbx2* on a 32-somite mouse embryonic optic cup. *Tbx2* was expressed in the dorsal quadrant of the early optic cup (open arrow), as for *Tbx5* and *Bmp4*. **n**, nasal; **t**, temporal.

B *In situ* hybridisation for *Bmp4* on a 35-somite mouse embryonic optic cup. *Bmp4* expression was detected in the dorsal quadrant of the retina (open arrow), as for *Tbx2* and *Tbx5*. Dorsal (**d**) is indicated as up for all figures. **n**, nasal; **t**, temporal.

C *In situ* hybridisation for *Tbx5* on a 32-somite mouse embryonic optic cup. *Tbx5* was sharply expressed in the dorsal quadrant of the retina (open arrow), as for *Tbx2* and *Bmp4*, though more sharply dorsally restricted than these genes. **t**, temporal; **n**, nasal; **le**, lens; **nr**, neural retina.

D *In situ* hybridisation for *Vax2* on a 30-somite mouse embryonic optic cup. *Vax2* was expressed in the ventral quadrant of the retina (open arrow), expression was more pronounced on the temporal aspect of the ventral expression domain. **n**, nasal; **t**, temporal; **vf**, ventral fissure. Scale bar = 0.2 mm for all figures.

Tbx2, *Tbx5* and *Bmp4* expression co-localises in the early optic cup

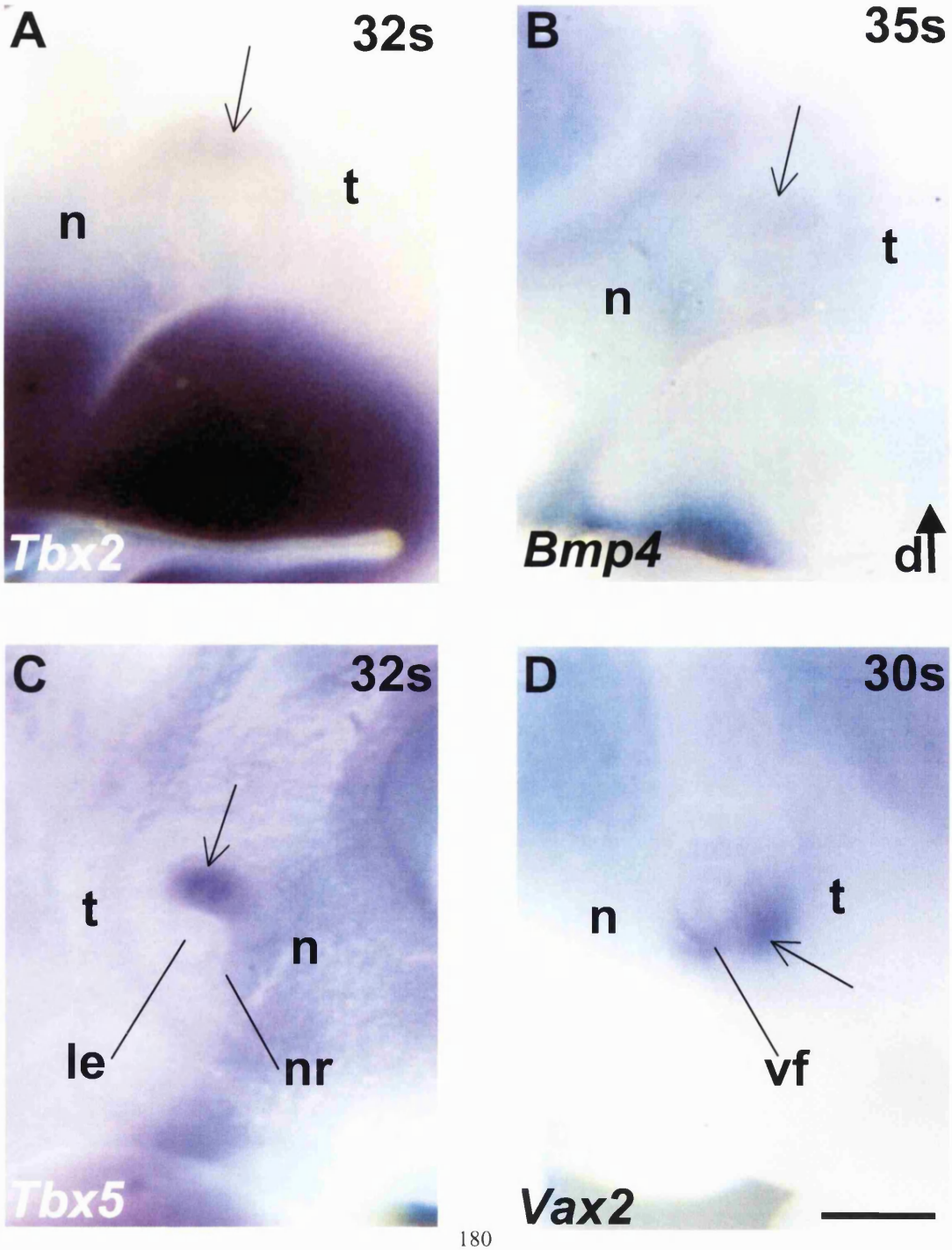

Figure 4.4

Foxn4 was expressed in the dorso-nasal retina, the rostro-dorsal midbrain and the ventral hindbrain and neural tube at E10.5 (**A-F**):

A *In situ* hybridisation for *Foxn4* on a 36-somite stage mouse embryo. *Foxn4* was expressed in the dorso-nasal retina (arrow), the rostro-dorsal midbrain and the ventral hindbrain and neural tube. Dotted lines indicate the planes of section in **B-E**. Dorsal (**d**) is indicated as up (for the head region). Dorsal is up in all figures.

B Section through the optic cup of the embryo in **A**. *Foxn4* expression was observed in the inner aspect of centro-dorsal neural retina. **nr**, neural retina; **le**, lens. Scale bar = 0.4 mm for **A**, 25 μm for **B**.

C Section through the rostral midbrain of the embryo in **A**. *Foxn4* was expressed throughout the dorsal midbrain at this level. Scale bar = 0.1 mm.

D Section through the caudal midbrain and the ventral hindbrain of the embryo in **A**. *Foxn4* expression was observed in a bilateral stream of cells of the ventral hindbrain. Expression was also observed in the dorsal midbrain. The midbrain is open on this section because the dorsal midline has ruptured during handling of the embryos. Scale bar = 0.1 mm.

E Section through the midbrain of the embryo in **A**. *Foxn4* expression was restricted to a bilateral group of cells in the ventral neural tube. **nt**, neural tube. Scale bar = 0.1 mm.

F *Foxn4* mRNA was detected in the dorsal midbrain and the ventral hindbrain and neural tube, but not in the retina, at the 32-somite stage. Scale bar = 0.4 mm.

Foxn4 expression in the developing E10.5 mouse embryo

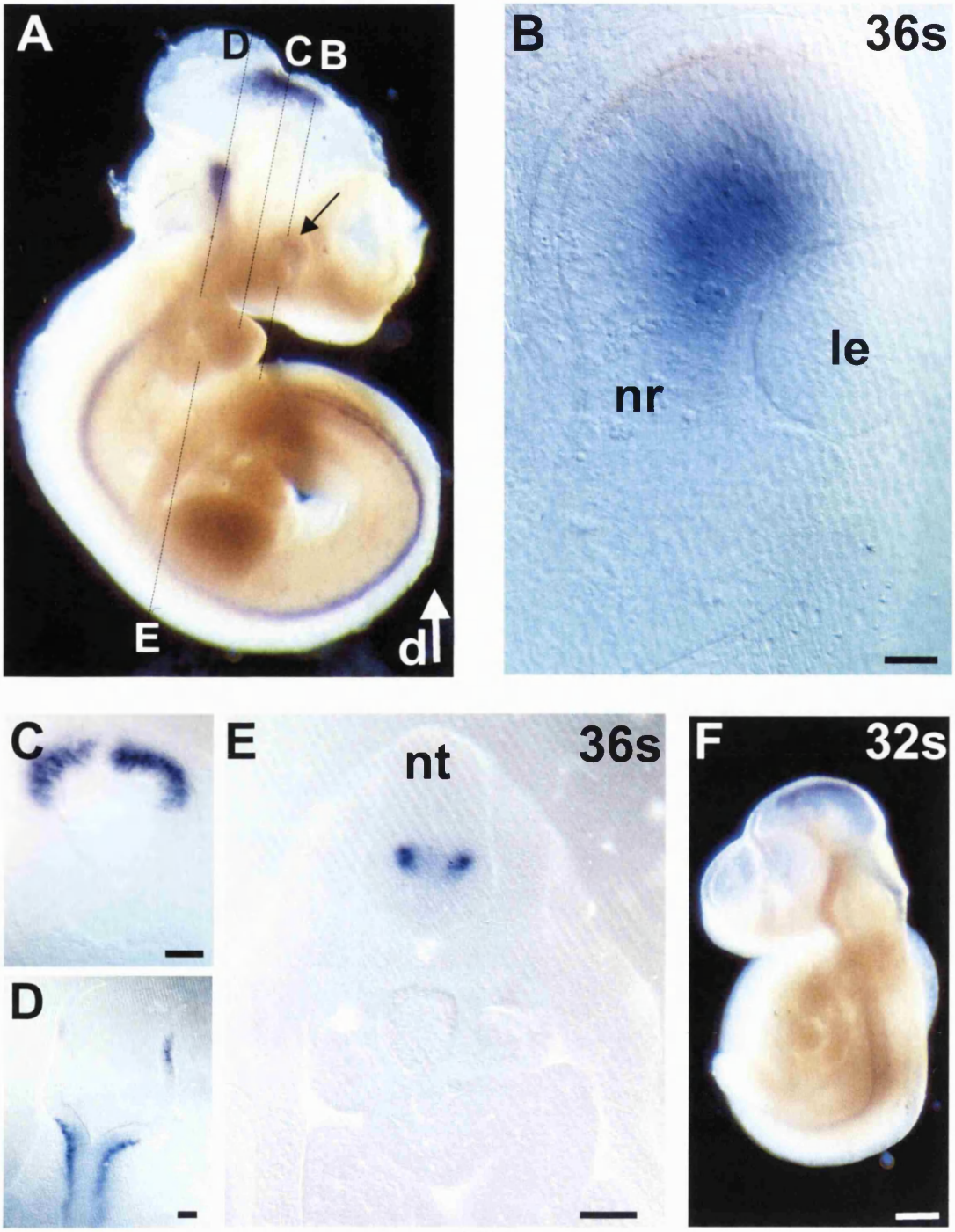

Figure 4.5

Bmp4, *Tbx5*, *Tbx2*, *Vax2* and *Foxn4* are all asymmetrically expressed across the 46- to 53-somite stage optic cup (**A-F**):

A Optic cup of a 48-somite stage mouse embryo following whole mount *in situ* hybridisation for *Bmp4*. *Bmp4* was expressed in the dorsal quadrant of the retina. Dotted line indicates section in **B**. Dorsal (**d**) is indicated as up for all figures. **t**, temporal; **n**, nasal.

B Section through the optic cup of shown in **A**. *Bmp4* expression was restricted to the dorsal-most tip of the neural retina.

C Optic cup of a 53-somite stage mouse embryo following whole mount *in situ* hybridisation for *Tbx5*. *Tbx5* was expressed in the dorsal quadrant of the retina, in the same region as *Bmp4* (**A**).

D Optic cup of a 53-somite stage mouse embryo following whole mount *in situ* hybridisation for *Tbx2*. *Tbx2* was expressed throughout the dorsal hemiretina, a larger domain than both *Bmp4* (**A**) and *Tbx5* (**C**).

E Optic cup of a 46-somite stage mouse embryo following whole mount *in situ* hybridisation for *Vax2*. *Vax2* was expressed in the ventral third of the retina.

F Optic cup of a 48-somite stage mouse embryo following whole mount *in situ* hybridisation for *Foxn4*. *Foxn4* was expressed in the dorso-temporal, dorso-nasal, and ventro-nasal quadrants of the retina. Scale bar = 0.2 mm for **A**, **C** to **F** and 0.1 mm for **B**. **dt**, dorso-temporal; **dn**, dorso-nasal; **vn**, ventro-nasal; **vt**, ventro-temporal.

Asymmetric gene expression in the developing E11.5 mouse retina

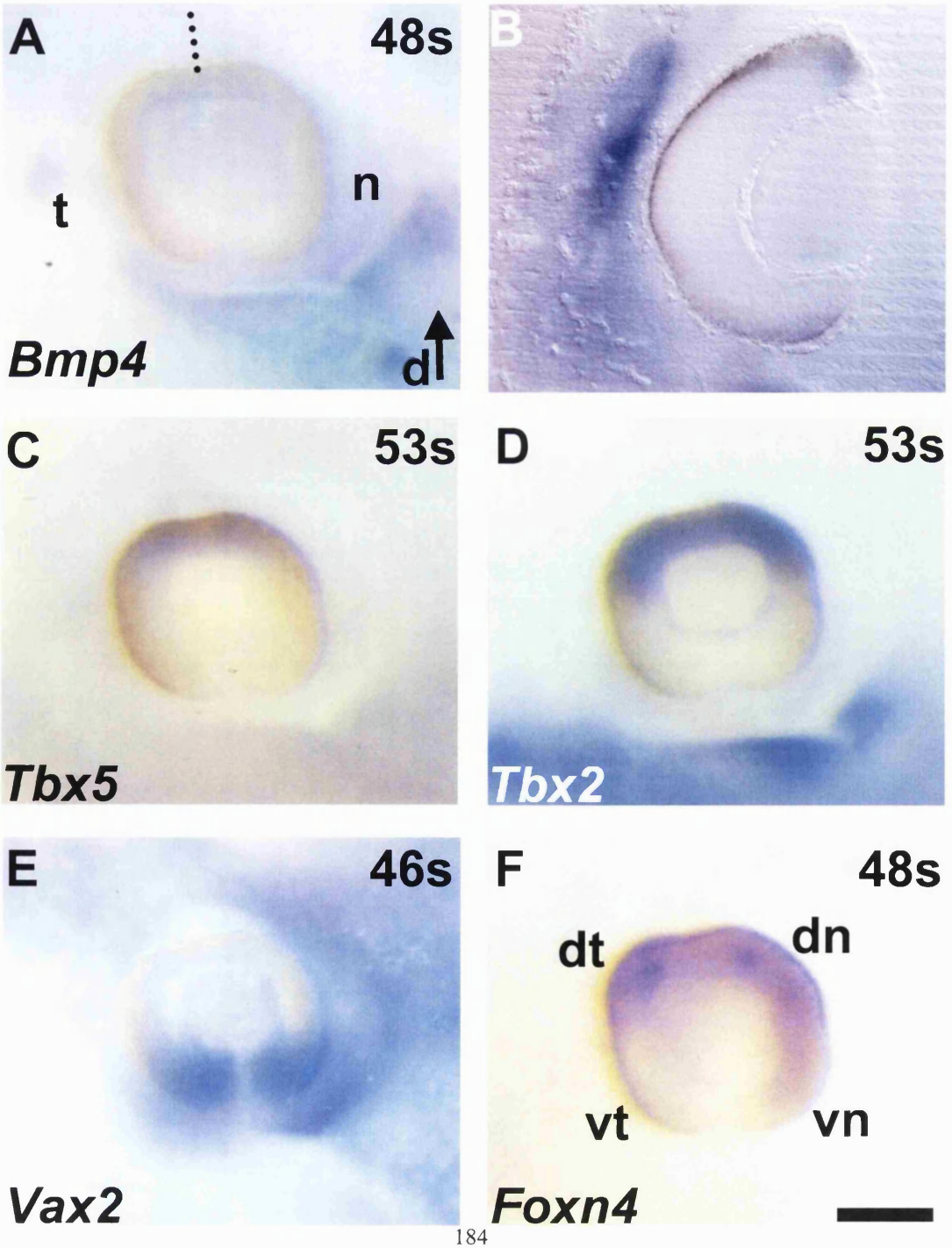

expanded into dorso-temporal and ventro-nasal domains (**Fig 4.5F**). The ventro-temporal quadrant of the neural retina was the only region to be free of *Foxn4* transcripts at this stage.

4.3. Ventral retinal identity is suppressed in the homozygous *Small eye* mouse retina

To determine whether the *Pax6*-null optic vesicle becomes polarised along its dorso-ventral axis I examined expression of dorsal and ventral markers *Tbx5* and *Vax2* in *Sey* mouse embryos using whole mount *in situ* hybridisation. Litters were removed from pregnant *Sey*/+ mice (from *Sey*/+ x *Sey*/+ matings) at E10.5 and embryos between 24 and 30 somites were examined. Homozygous mutants were readily identifiable by the absence of lens placode formation, of proximal constriction of the optic vesicles and of thickening of prospective neural retina. Heterozygous mice are indistinguishable from wild-type littermates at this stage, but by the optic cup stage heterozygotes may be distinguished by a misshapen lens (Hill *et al.*, 1991; Grindley *et al.*, 1995; Enwright and Grainger, 2000). Presumptive neural retina has been identified morphologically in all embryos as the distal portion of the developing retina that opposes the surface epithelium. This region is marked as presumptive neural retina at the molecular level in the developing optic vesicle by expression of *Chx10* (Liu *et al.*, 1994). To definitively type the embryos, PCR was used on DNA extracted from their yolk sacs to amplify a 147 base pair (bp) region of the *Pax6* gene. The *Sey* mutation is a point mutation that creates a new *Dde*I restriction site, so *Dde*I digestion was performed on the PCR products to genotype the embryos. Electrophoresis of the *Dde*I-cut PCR fragments allowed determination of whether the sample was homozygous or heterozygous for the *Sey* mutation, or wild type (**Fig. 4.6A**).

Tbx2 and Tbx5 expression in the retina of Small eye mouse embryos

Tbx2 was expressed in the dorsal half of the developing retina of wild type mouse embryos (**Fig. 4.6B, C**). In homozygous *Sey* mouse embryos (n=2), *Tbx2* was not asymmetrically expressed (**Fig. 4.6D, E**). Instead, expression was observed throughout the region identified as presumptive neural retina (demarcated by arrows, **Fig. 4.6E**). *Tbx5* was strongly expressed in the dorsal tip of the developing retina of heterozygous *Sey* mouse embryos (**Fig. 4.7A, B**). The homozygous retina showed no

Figure 4.6

Small eye mice were genotyped using PCR and *Dde*I digestion (**A**):

A Genotyping results from yolk sac samples (1-4) are shown. PCR was performed on embryonic yolk sacs using primers flanking a 147 base pair DNA region containing the mutation. PCR product was digested with *Dde*I (**d**) and run across an electrophoresis gel with uncut product (**u**) and a DNA ladder (**L**). *Dde*I cuts the wild type fragment once to give 82 and 65 base pair fragments (4). The *Small eye* mutation introduces a second *Dde*I site, so that *Dde*I digestion gives 82, 45 and 20 base pair fragments (1). Digestion of heterozygous DNA gives all sizes: a strong 82 base pair fragment (common to both alleles) and weaker 65, 45 and 20 (visible only for 1) base pair fragments (2 + 3).

Dorsal restriction of *Tbx2* expression is lost in the *Small eye* mouse retina (**B-E**):

B Whole mount *in situ* hybridisation for *Tbx2* on a wild type mouse embryo at the 32-somite stage. *Tbx2* expression can be seen in the dorsal retina (open arrow) and in the facial primordia. Dotted line indicates the plane of section in **C**. Dorsal (**d**) is indicated as up. This applies from **B** to **E**.

C Section along the dorso-ventral axis through the optic cup of the embryo shown in **B**. *Tbx2* mRNA was detected in the dorsal half of the developing neural retina and in the dorsal tip of the developing RPE. Arrows indicate boundaries of the neural retina.

D Whole mount *in situ* hybridisation for *Tbx2* on a mouse embryo at the 32-somite stage homozygous for the *Small eye* mutation (-/-). No dorsal restriction of expression was observed in the mutant eye, *Tbx2* was apparently expressed throughout the retina (open arrow). Dotted line indicates the plane of section in **E**. Scale bar = 0.2 mm for **B** and **D**.

E Section along the dorso-ventral axis through the optic cup of the embryo shown in **D**. *Tbx2* was expressed throughout the distal retina (the site where the neural retina would normally develop), which had not invaginated to form an optic cup. Expression appeared to be stronger on the inner aspect of the distal neuroepithelium. Arrows indicate boundaries of the presumptive neural retina. Scale bar = 0.1 mm for **C** and **E**.

Typing of mutant mice and *Tbx2* expression in E10.5 *Small eye* mouse embryos

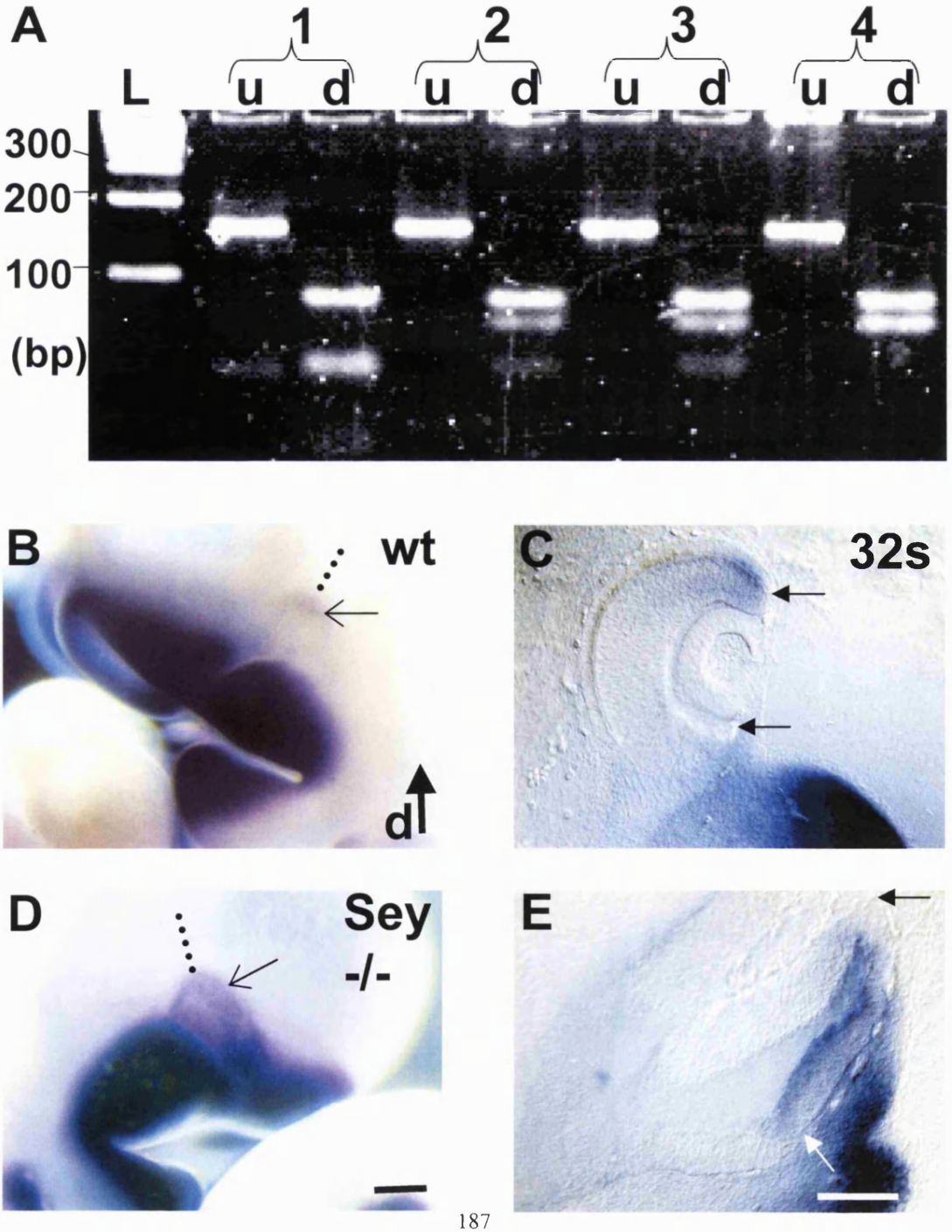

Figure 4.7

Dorsal restriction of *Tbx5* expression is lost in the *Small eye* mouse retina (**A-D**):

A Whole mount *in situ* hybridisation for *Tbx5* on a mouse embryo at the 27-somite stage. This embryo is a heterozygous (for the *Small eye* mutation, +/-) or wild type littermate of the homozygous embryo in **C** and **D**. *Tbx5* was expressed in the dorsal retina (black arrow), the heart and the upper limbs. Dotted line indicates the plane of section in **B**. Dorsal (**d**) is indicated as up for all figures.

B Section along the dorso-ventral axis through the optic cup of the embryo shown in **A**. *Tbx5* mRNA was strongly detected in the dorsal tip of the presumptive neural retina. Arrows indicate boundaries of the presumptive neural retina, dotted line indicates the outer limits of the neuroepithelium.

C Whole mount *in situ* hybridisation for *Tbx5* on a mouse embryo at the 30-somite stage homozygous for the *Small eye* mutation (-/-). *Tbx5* was expressed in the heart and the upper limbs as in the heterozygous/wild type mice, but was expressed throughout the retina. Dotted line indicates the plane of section in **D**. Scale bar = 0.5 mm for **A** and **C**.

D Section along the dorso-ventral axis through the optic cup of the embryo shown in **C**. *Tbx5* was uniformly expressed across the dorso-ventral axis of the presumptive neural retina. The hybridisation signal was faint and diffuse. Arrows indicate boundaries of the presumptive neural retina. Scale bar = 0.1 mm for **B** and **D**.

Tbx5 expression in E10.5 *Small eye* mouse embryos

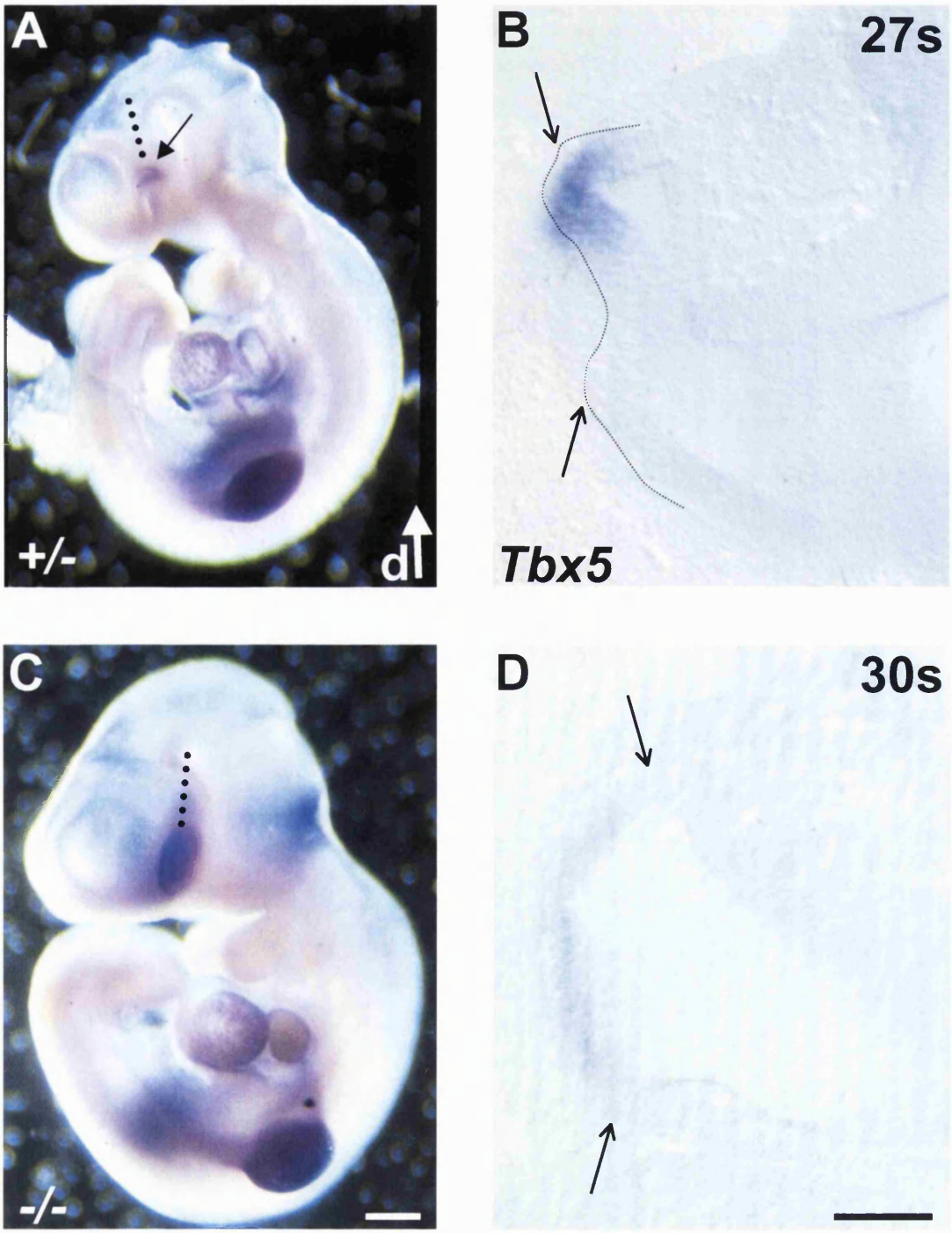

thickening of the presumptive neural retina (defined by apposition to the surface epithelium), no invagination, no lens placode formation and no constriction of the optic stalk at 30 somites (**Fig. 4.7C, D**). In the homozygous retina (n=2) asymmetric expression of *Tbx5* was never seen (**Fig. 4.7C, D**). Instead, low level *Tbx5* expression was detected throughout the region identified as presumptive neural retina (demarcated by arrows, **Fig. 4.7D**). In both cases homozygous *Sey* embryos were found to have an expanded domain of *Tbx5* expression throughout prospective neural retina that was of diminished intensity in comparison to heterozygous/wild-type littermates.

Vax2 expression in the retina of Small eye mouse embryos

At 24 somites, *Vax2* expression is clearly seen in the ventral half of the retina (**Fig. 4.8A**). Sections show *Vax2* to be strongly expressed in the ventral third of presumptive neural retina (demarcated by arrows), the ventral half of presumptive pigment epithelium and in the optic stalk (**Fig. 4.8B**). In a 24-somite homozygous *Sey* littermate, failure of the optic stalks to constrict is clear (**Fig. 4.8C**). There was no lens placode formation or retinal thickening seen on a frontal section of this embryo (**Fig. 4.8D**). The apparent infolding of the presumptive retinal neuroepithelium (and the surface ectoderm) in this homozygous embryo is an embedding and sectioning artefact. *Vax2* expression was excluded from the homozygous *Sey* presumptive neural retina altogether. Expression was seen in the optic stalk and in the presumptive pigment epithelium only (**Fig. 4.8C, D**).

4.4. Dorso-ventral retinal patterning is unaffected in the *ocular retardation* mouse optic cup

E10.5 *or* mouse embryos were examined for *Tbx5* and *Vax2* expression to look for disruptions in dorso-ventral patterning. No obvious differences in expression were observed between *or* and wild-type mice for either gene (**Fig. 4.9**). This suggests *Chx10* does not influence dorso-ventral patterning and shows that its expression is not necessary for the acquisition of retinal identity.

Figure 4.8

Dorsal restriction of *Vax2* expression is lost in the *Small eye* mouse retina (**A-D**):

A Developing retina of a 24-somite stage mouse embryo following whole mount *in situ* hybridisation for *Vax2*. This embryo is a heterozygous (for the *Small eye* mutation, +/-) or wild type littermate of the homozygous embryo in **C** and **D**. *Vax2* was expressed in the optic stalk and the ventral aspect of the developing retina. Dotted line indicates the plane of section in **B**. Dorsal (**d**) is indicated as up for all figures.

B Section along the dorso-ventral axis through the optic cup of the embryo shown in **A**. *Vax2* mRNA was strongly detected in the ventral third of presumptive neural retina and in the region of presumptive retinal pigmented epithelium just dorsal to the optic stalk. Lower level expression was detected in the optic stalk. Arrows indicate boundaries of the presumptive neural retina.

C Developing retina of a 24-somite stage mouse embryo following whole mount *in situ* hybridisation for *Vax2*. This embryo is homozygous for the *Small eye* mutation. No asymmetry of *Vax2* expression was seen in the eye. ~~se embryo at the 30-somite stage homozygous for the small eye mutation (-/-). *Tbx5* was expressed in the heart and the upper limbs as in the heterozygous/wild type mice, but was expressed throughout the retina~~. Dotted line indicates the plane of section in **D**. Scale bar = 0.5 mm for **A** and **C**.

D Section along the dorso-ventral axis through the optic cup of the embryo shown in **C**. *Vax2* was expressed in the optic stalk but not in the presumptive neural retina. Arrows indicate boundaries of the presumptive neural retina. Dotted lines demarcate the outer limits of the neuroepithelium and the surface ectoderm. Scale bar = 0.1 mm for **B** and **D**.

Vax2 expression in E10.5 *Small eye* mouse embryos

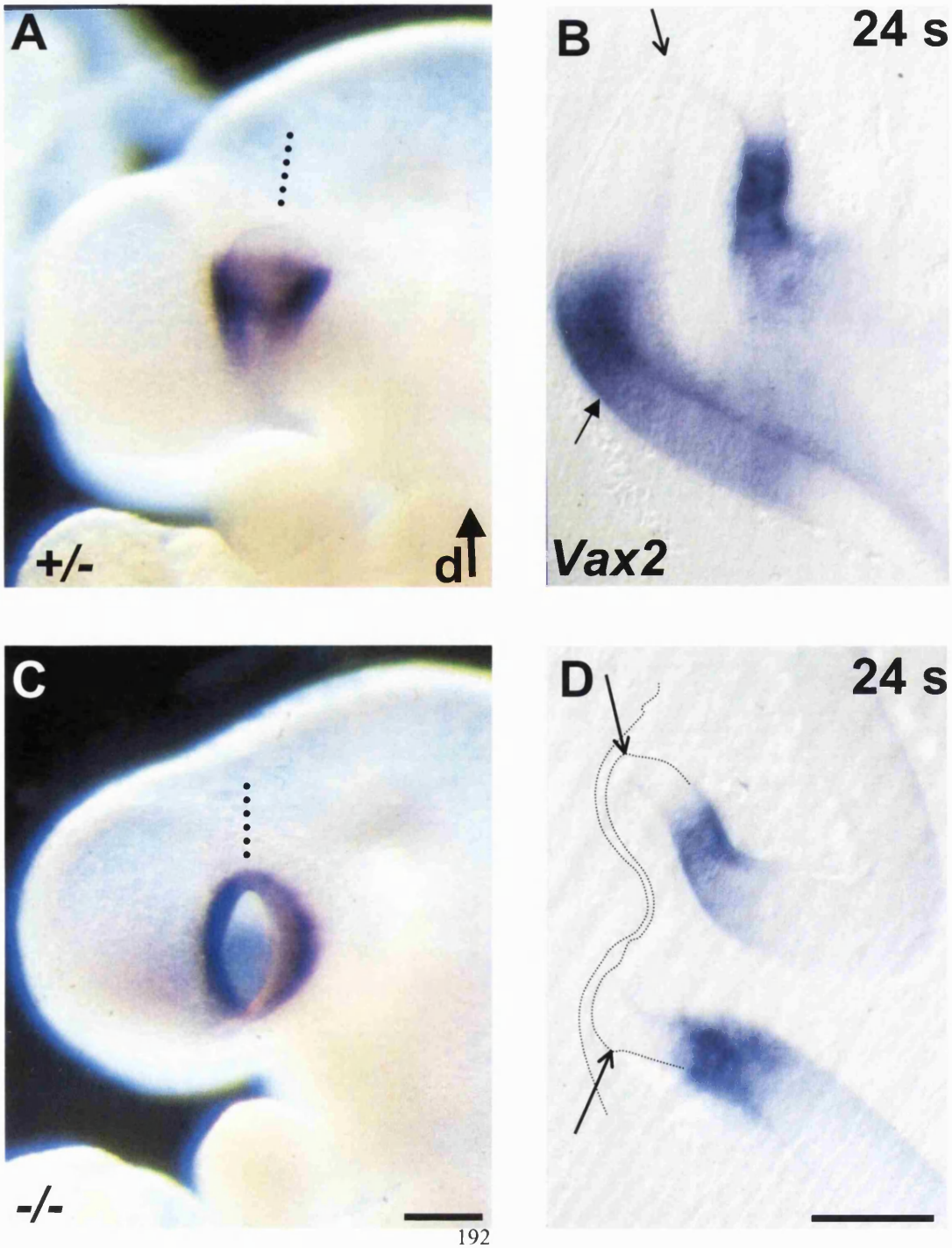

Figure 4.9

Dorsal restriction of *Tbx5* and *Vax2* expression is retained in the *ocular retardation* (*or*) mouse retina (**A-D**):

A Optic cup of a 34-somite stage *or* mouse embryo following whole mount *in situ* hybridisation for *Tbx5*. *Tbx5* was expressed in the dorsal quadrant of the developing retina, as seen in wild type embryos (**B**). Dorsal (**d**) is indicated as up for all figures.

B Optic cup of a 32-somite stage wild type mouse embryo following whole mount *in situ* hybridisation for *Tbx5*. *Tbx5* was expressed in the dorsal quadrant of the developing retina.

C Optic cup of a 32-somite stage *or* mouse embryo following whole mount *in situ* hybridisation for *Vax2*. *Vax2* was expressed in the ventral quadrant of the developing retina, as seen in wild type embryos (**D**).

D Optic cup in a 30-somite stage wild type mouse embryo following whole mount *in situ* hybridisation for *Vax2*. *Vax2* was expressed in the ventral quadrant of the developing retina. Scale bar = 0.2 mm.

Tbx5 and *Vax2* expression in E10.5 *ocular retardation* mouse embryos

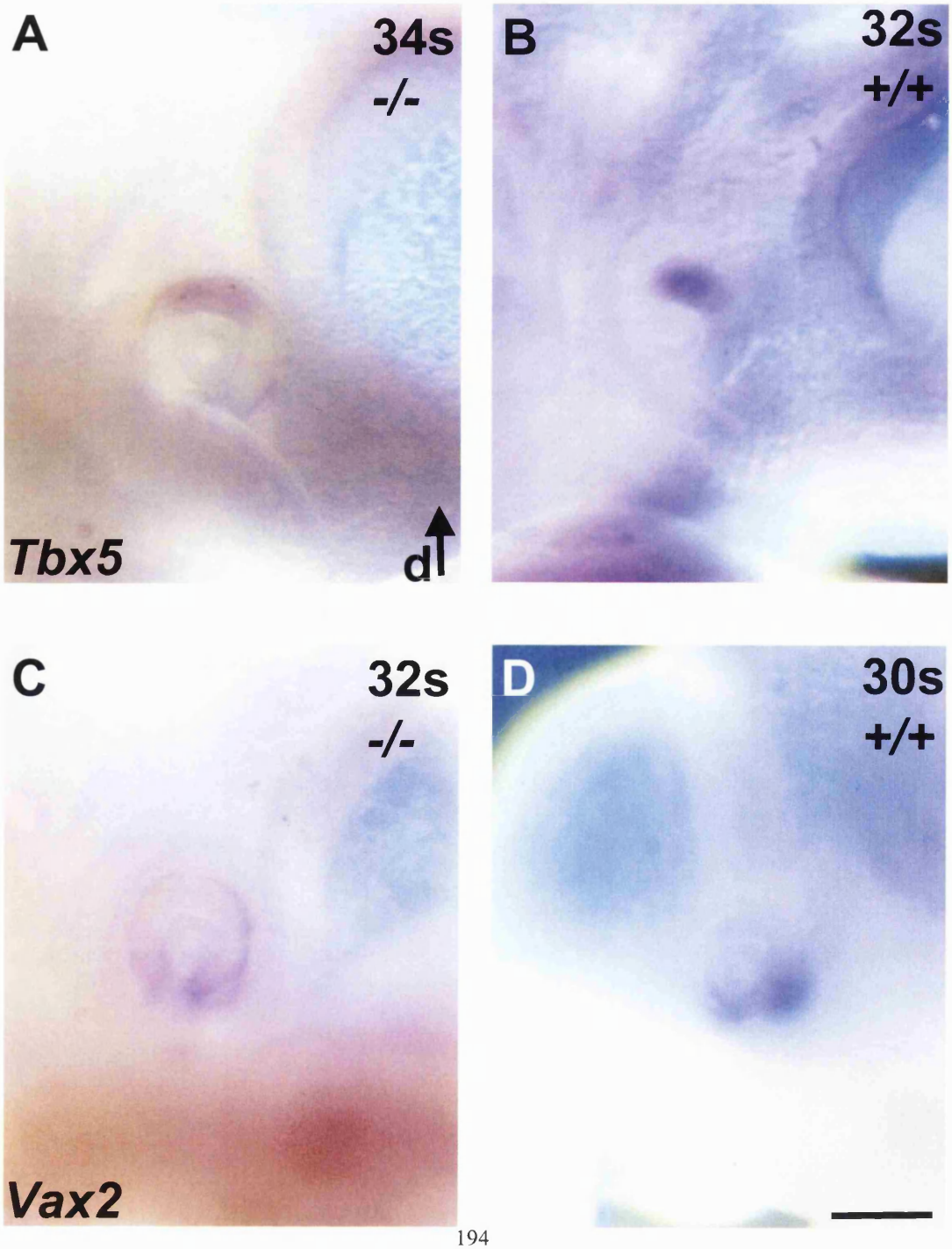

4.5. *Tbx2* expression is diminished in the hindlimbs of *Shh* null mice

Tbx2 expression was examined in *Shh* knockout mice at E9.5 and E10.5 stages of development. The differences in expression between knockout and wild type mice were examined. Mice were obtained by crossing heterozygotes for the *Shh* deletion (Chiang *et al.*, 1996). Genotyping of the yolk sacs of the offspring was performed using PCR. *Tbx2* expression was examined in a 34-somite *Shh* -/- mutant mouse embryo (**Fig. 4.10A**). *Tbx2* expression was not detected in the single cyclopic eye (**Fig. 4.10B**). *Tbx2* otherwise appeared to show quite normal patterns of expression in the mutant. A striking exception to this was a substantial reduction of *Tbx2* expression in the posterior aspect of the homozygote hindlimbs (**Fig. 4.10C**) in comparison to an equal somite stage heterozygote (**Fig. 4.10D, E**). *Tbx5* expression was examined in 2 knockout mice. Expression was not detected in the eye, but the *in situ* hybridisations had high background labelling and are not shown here. Further experiments were not carried out, but these observations on *Tbx2* are confirmed by recent unpublished work by Cheryl Tickle and colleagues. They found that *Tbx2* and *Tbx3* expression are reduced in the posterior aspects, but enhanced in the anterior aspects, of both hindlimbs and forelimbs in *Shh* null mouse embryos (Eblaghie *et al.*, 2002). *Tbx2* and *Tbx3* expression were not reported in the mutant cyclopic eye.

DISCUSSION

Here the results are discussed with an aim to inform on the regulatory context that surrounds the asymmetric expression of *omb*-related T-box genes. The scene is set for the functional studies undertaken in further chapters.

4.6. BMP4 is a candidate regulator of T-box genes in the mouse retina

The expression of *Bmp4* prior to and at the onset of *Tbx2* and *Tbx5* expression in the dorsal retina of the developing mouse makes it a strong candidate for mammalian T-box gene induction. *Bmp4* continues to be co-expressed with *Tbx2* and *Tbx5* during early development of the optic cup, but in a smaller dorsal domain than *Tbx2* in particular. Given that BMP4 is a diffusible molecule capable of operating outside its

Figure 4.10

Tbx2 expression is absent in the eye and reduced in the anterior hindlimbs of a 34-somite embryo in the absence of *Shh* (**A-D**):

A Frontal view of a 34-somite stage *Shh* knockout mouse embryo following whole mount *in situ* hybridisation for *Tbx2*. Expression of *Tbx2* was detected in the single nasal prominence (**n**), the heart (**h**) and in the flanking aspects of the developing limbs. **fl**, forelimb; **hl**, hindlimb. Scale bar = 0.5 mm.

B Lateral view of the head of the 34-somite stage *Shh* knockout mouse embryo in **A**. *Tbx2* was expressed in the nasal prominence (**n**) but absent from the cyclopic eye (**e**). **m**, midbrain; **t**, telencephalon (single vesicle).

C Posterior view of the hindlimbs (**hl**) of the 34-somite stage *Shh* knockout mouse embryo in **A**. *Tbx2* was expressed in small domains (arrows) in the posterior aspect of the hindlimbs and in the genital region (**g**). Scale bar = 0.2 mm for this figure and for **B**.

D Lateral view of a 34-somite stage heterozygous *Shh* knockout mouse embryo following whole mount *in situ* hybridisation for *Tbx2*. Expression of *Tbx2* was detected in the dorsal retina, the nasal primordia (**n**), the maxillary and mandibular primordia (**m**), the heart and in the anterior and posterior aspects of the hindlimbs. **fl**, forelimb; **hl**, hindlimb. Scale bar = 0.5 mm.

E Posterior view of the hindlimbs (**hl**) of the 34-somite stage heterozygous *Shh* mutant embryo in **D**. *Tbx2* was expressed bilaterally in large (compare to **C**) posterior hindlimb domains (arrows) and in the genital ridge (**g**). Scale bar = 0.2 mm.

Tbx2 expression in 34-somite *Shh* mutant mouse embryos

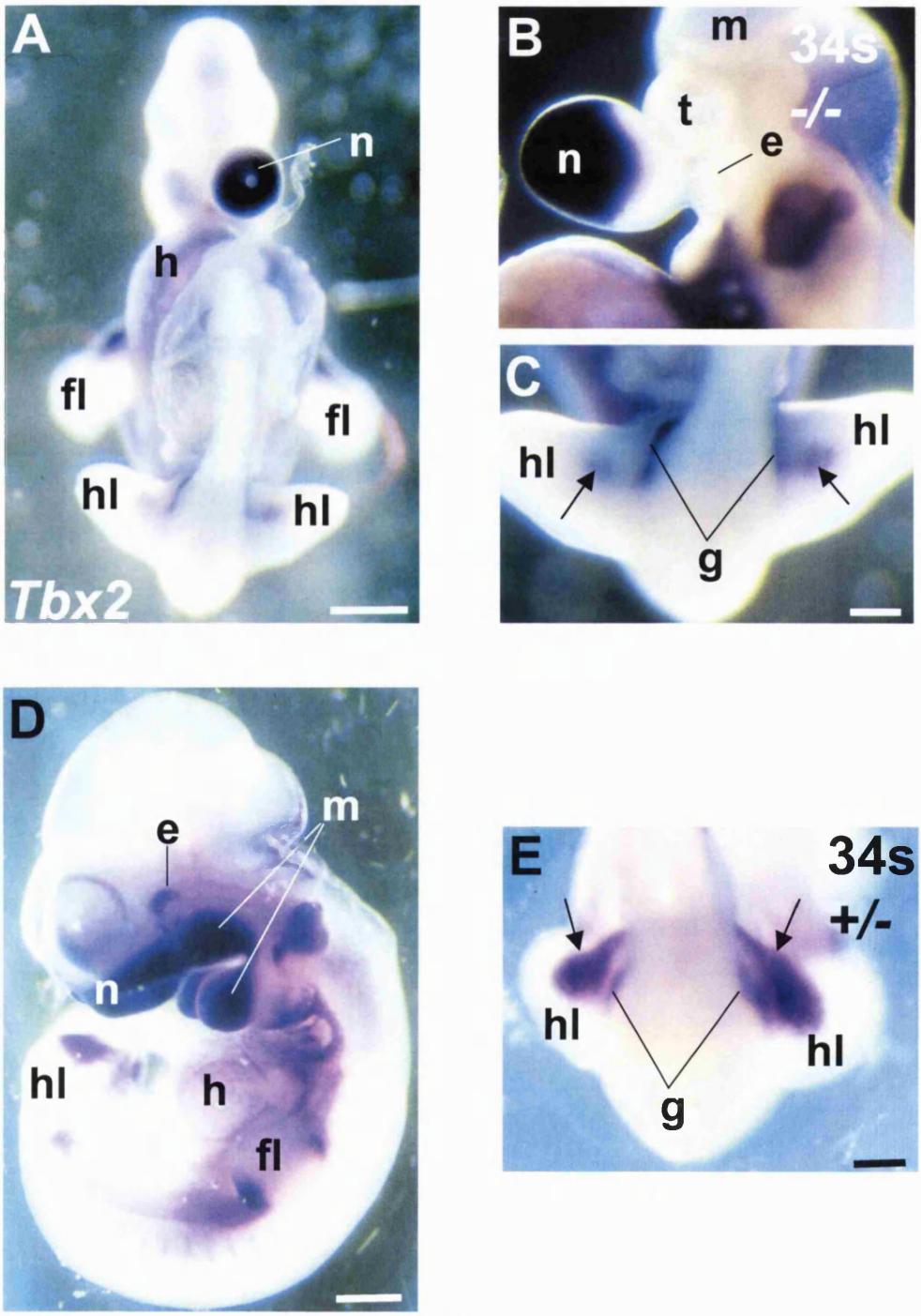

expression domain, it stands as a good candidate for the maintenance as well as the induction of restricted T-box gene expression in the mouse. *Bmp4* misexpression in the chick eye has recently been shown to induce *Tbx5* in the ventral retina (Koshiba-Takeuchi *et al.*, 2000).

Foxn4 was expressed asymmetrically across the retina, but not in a manner that suggested a role in dorso-ventral patterning or regulation by *Bmp4*. I have shown that *Foxn4* expression initially occupies central aspects of neural retina within the dorso-nasal quadrant of the optic cup. The expression domain expands into the dorso-temporal and ventro-nasal quadrants by the 48-somite stage. These 'corner' quadrants bulge outwards to give the optic cup its characteristically square shape at this stage. From E12.5, *Foxn4* is expressed throughout the retina, where it is apparently regulated by *Chx10*, an important regulator of retinal proliferation (Burmeister *et al.*, 1996; Gouge *et al.*, 2001). The *Foxn4* optic cup expression domain thus places *Foxn4* as a strong candidate for the regulation of 'corner quadrant proliferation'. If this is the case, it is possible that *Foxn4* mediates the proliferative effects of *Chx10* during later stages of retinal development.

Foxn4 was expressed in the dorsal aspect of the rostral midbrain and may be involved in the patterning of this structure. *Foxn4* transcripts were also identified bilaterally in the ventral hindbrain and neural tube. Expression of other transcription factors in these regions has been identified in the mouse where they define different groups of ventral interneurons (Matise and Joyner, 1997). *Chx10* is included in this group (Liu *et al.*, 1994) and could be regulating *Foxn4* in ventral interneurons of the neural tube as in the eye (Gouge *et al.*, 2001).

4.7. Dorso-ventral retinal polarity is dependent on *Pax6*

The loss of dorso-ventral asymmetry of *Tbx5* and *Vax2* expression in the homozygous *Small eye* mouse retina suggests that *Pax6* is essential for dorso-ventral retinal polarisation. It is unlikely that this is caused by a general developmental retardation of the eye because *Tbx5* and *Vax2* normally exhibit polarised expression as soon as a recognisable optic vesicle has been forged from the optic pits (see **4.1.** above). In addition, the sharp retention of *Vax2* in the homozygous mouse optic stalk demonstrates that (1) eye development is sufficiently advanced to define an optic stalk

at the molecular level and (2) a restricted – but diminished – *Vax2* expression domain has emerged on cue in the developing eye. The loss of dorso-ventral marker expression despite preservation of proximo-distal polarity of the mutant optic vesicle argues against general developmental retardation as the cause.

Previous data has suggested that *Pax6* have a role in establishing dorso-ventral polarity in the retina (see above, page 171). The analysis of dorso-ventral markers presented here suggests that this is indeed the case, but the nature of the disruption is more difficult to explain. The points raised on page 171 suggest that *Pax6* could be involved in the provision of dorsal identity in the early retina. This might lead one to predict a promotion of ventral identity in the *Pax6*-null retina. I have found ventral marker *Vax2* expression to be *reduced*, apparently abolished, in the presumptive neural retina of *Pax6*-null mice. The *Pax2* expression domain expands in the *Pax6* null retina (Schwarz *et al.*, 2000). *Pax2*, upregulated by *Vax2* misexpression in chick and in *Xenopus* (Barbieri *et al.*, 1999; Schulte *et al.*, 1999), clearly does not positively regulate *Vax2* – in the absence of *Pax6* at least.

A weak and diffuse domain throughout the presumptive neural retina of the mutant replaced the strong expression of Tbx5 observed in the dorsal retina of wild type mice. Is the entire distal optic vesicle of the homozygous *Sey* mouse embryo specified as dorsal retina, hence the reduced *Vax2* and expanded *Tbx5* expression domains? The presence of expression of *Pax2* (Schwarz *et al.*, 2000) and another ventral transcription factor gene, *Optx2* (*Six9/6*) (Jean *et al.*, 1999) in the *Sey/Sey* optic vesicle argues against this possibility. *Pax6* may yet prove to positively regulate *Tbx5*. If this is the case a loss of *Pax6* might directly contribute to the reduced intensity of *Tbx5* expression whilst indirectly leading to the expanded domain. Alternatively, the low-level *Tbx5* expression, rather than indicating dorsal retinal identity, may simply arise in a disorganised and unspecified retina from the loss of *Vax2* expression. This suggestion seems improbable in the light of recent findings that *Tbx5* is not upregulated in the *Vax2*-null mouse (Barbieri *et al.*, 2002; Mui *et al.*, 2002).

One mechanism to explain the apparent loss of ventral identity draws on the finding that retinoid signalling within the optic vesicle is severely reduced in the absence of *Pax6* (Enwright and Grainger, 2000). Genes encoding aldehyde dehydrogenases,

enzymes that synthesise retinoids, are expressed asymmetrically across the dorso-ventral axis of the developing eye from the optic pit stage of development. These create a ventral-high to dorsal-low gradient of retinoic acid that is perpetuated later in development by specific dorsal and ventral enzymes. These lead to opposing gradients of activated retinoids that define distinct dorsal and ventral compartments and are separated by a retinoid-poor horizontal band or meridian (McCaffery *et al.*, 1999; Enwright and Grainger, 2000; Wagner *et al.*, 2000). Work in zebrafish and in mice has implicated high levels of retinoic acid in the provision of identity to and survival of the ventral retina (Marsh-Armstrong *et al.*, 1994; Hyatt *et al.*, 1996; Kastner *et al.*, 1997). Thus the substantial reduction of retinoid signalling in the homozygous *Sey* mouse optic vesicle could lead to a failure to express ventral genes such as *Vax2*. Low levels of retinoic acid have been hypothesised to specify dorsal retina (McCaffery *et al.*, 1999). A reduction in retinoid signalling could therefore serve to promote dorsal identity (and perhaps *Tbx5* expression), or to abolish dorso-ventral identity altogether, depending on the severity of the reduction.

Although later in mouse development *Pax6* is expressed throughout the neural retina (Grindley *et al.*, 1995), finally to become restricted to the ganglion cell and inner nuclear layers (Davis and Reed, 1996; Belecky-Adams *et al.*, 1997), it may continue to influence retinal polarity. Distinct regulatory elements for *Pax6* operate in different retinal regions of the optic cup (Kammandel *et al.*, 1999; Xu *et al.*, 1999). This leads to the production of different transcripts through alternate promoters in neighbouring retinal quadrants. The potential remains for direct roles in retinal patterning for *Pax6* at all stages of retinal development.

4.8. Conclusion

This study presents BMP4 as an excellent candidate regulator for *Tbx2* and *Tbx5* in the developing mouse retina and forms a good basis for further investigation of this proposed relationship. I have also shown that null mutations in *Pax6* (known to be regulated by BMP4 in *Xenopus*; Sasagawa *et al.*, 2002), causes dorso-ventral patterning to be disrupted in mice. The question of whether *Pax6* and *Bmp4* pathways interact has arisen previously in the context of lens development (Furuta and Hogan, 1998) and arises again here in the context of dorso-ventral patterning. *Bmp4* expression was maintained in the optic vesicles of *Pax6* mutants and *Pax6* was

expressed in the optic vesicles of *Bmp4* mutants (Furuta and Hogan, 1998). However, Furuta and Hogan did not report whether or not the polarity of *Bmp4* expression was altered in the *Pax6* mutant. In chick and in *Xenopus*, BMP4 appears to act, as a dorsal regulator, opposite a midline source of SHH, which regulates ventral retinal development (Zhang and Yang, 2001; Sasagawa *et al.*, 2002). In these experiments, early expression of *Pax6* in the retina seems to be regulated by these patterning systems. My current study does not support a *direct* role for *Pax6* in dorso-ventral patterning. Regulation of *Pax6* by BMP4 and SHH may reflect the close relationship between proximo-distal and dorso-ventral patterning during early eye development. Rather than through direct regulation of polarising genes, *Pax6* seems likely to promote dorso-ventral patterning in the early retina indirectly. Defective retinoid signalling in the *Pax6* homozygous mutant optic vesicle (Enwright and Grainger, 2000) could cause a loss of ventral identity and perhaps a weak promotion of dorsal identity, leading to the observed disruptions in *Vax2* and *Tbx5* expression. How BMP4 and SHH signalling pathways might be related to the polarised activity of retinoids in the control of dorso-ventral patterning in the developing retina remains unclear.

CHAPTER 5

BMP4 induces *Tbx2* and *Tbx5* expression in the developing mouse retina

INTRODUCTION

Transforming growth factor beta (TGFβ) superfamily member *bone morphogenetic protein 4* (*Bmp4*) is expressed in the dorsal retina of several vertebrate species (Francis-West *et al.*, 1994; Hemmati-Brivanlou and Thomsen, 1995; Papalopulu and Kintner, 1996; Furuta and Hogan, 1998). *Bmp4* misexpression (using retroviral vectors) can induce *Tbx5* in the chick retina (Koshiba-Takeuchi *et al.*, 2000) and in the previous chapter (**Chapter 4**) I demonstrated that in the mouse, *Bmp4* is co-expressed with *Tbx2* and *Tbx5*. This co-expression exists from the earliest stages of expression in the dorsal optic vesicle and throughout optic cup formation.

In this study I used a post-implantation whole mouse embryo culture system to test the hypothesis that *Bmp4* is an upstream regulator of *Tbx2* and *Tbx5* expression in the developing mouse retina. Embryos were examined at two developmental stages, at the onset of polarised T-box gene expression (when the optic vesicle has developed) and later when formation of the optic cup has occurred. Beads soaked in human recombinant BMP4 protein are functionally active in numerous biological systems of the mouse and can substitute for endogenous BMP4 in the knockout mouse retina (Furuta and Hogan, 1998; Kim *et al.*, 1998; Bei *et al.*, 2000; Zhang *et al.*, 2000). In the experiments conducted in this chapter, human recombinant (hr) BMP4-soaked beads were implanted into the developing mouse eye before overnight whole embryo culture to induce *Tbx2* and *Tbx5* in ectopic locations.

An alternative system to allow the experimental manipulation of mouse eye development is to culture eye explants, *i.e.* to remove eyes and immediately surrounding tissue from mouse embryos and transplant them to a culture dish with medium. This system was used effectively for the manipulation *Bmp4* null mouse eyes by Furuta and Hogan, 1998. *Bmp4* mouse embryos die shortly after gastrulation though some survive longer to the optic vesicle stage of eye development. Explant cultures of these eyes developed a lens only in the presence of hrBMP4-soaked beads (Furuta and Hogan, 1998). Though these explants were not representative of *in vivo* development (explants were cultured for days with minimal development occurring), retinal pigmentation and lens development did eventually occur in cultured wild type eyes. Furthermore, ectopic gene expression could be induced in these explants using

hrBMP4-soaked beads (Furuta and Hogan, 1998). I tried culturing similar stage eye explants to determine the effectiveness of this method for the current study. This approach was not pursued because of the loss of retinal structure and organisation in cultured explants.

The culture system used in this chapter was one based on that described previously by Copp *et al.*, 1997. One of the aims of the present study was to assess the value of this system for the experimental analysis of mouse eye development. Embryos that grew and developed in culture were indistinguishable from those that did so *in vivo* (see below) suggesting that this system is highly representative of *in vivo* development. Whole embryo culture therefore greatly reduces the problems of many *in vitro* culture systems where results may not be directly applicable to *in vivo* development and have questionable validity. The accurate reproduction of *in vivo* development of the mouse eye allows the assessment of subtle experimentally induced changes (such as in eye morphology) as well as the more obvious alterations (such as ectopic gene induction or the presence/absence of a lens).

RESULTS

Whole mouse embryos were cultured at two different stages of development. The first was late E9.5, where the embryos had formed between 9 and 21 somites. The second was early E11.5, where the embryos had formed between 35 and 42 somites. Embryos were cultured for 15 to 24 hours after microsurgery was performed to implant beads soaked in hrBMP4 or, as a control, with bovine serum albumen (BSA). Embryos were analysed using whole mount RNA *in situ* hybridisation for *Tbx2* and *Tbx5* expression.

5.1. *Bmp4* expression at pre- and post-culture stages of development

The expression of *Bmp4* in the eye region at pre- and post-culture stages was examined to ensure that protein-soaked agarose beads could be implanted in locations where they might provide an ectopic source of BMP4 throughout the culture period. In the E9.5 embryo at the 18-somite stage, *Bmp4* was expressed in the dorsal aspect of

the optic vesicle (**Fig. 5.1A**). Expression in the ventral surface epithelium was seen on sections (see **Chapter 4**). The apparent ventro-temporal expression on the left of the optic vesicle in **Fig. 5.1A** is in fact in the ventral diencephalic midline and not in the more superficial tissues adjacent to the optic vesicle. In an E10.5 retina at the 26-somite stage (an equivalent stage to E9.5 embryos that had been cultured overnight, see **Table 5.1**), *Bmp4* was expressed in the dorsal half of the retina and in surface epithelium ventral to the developing eye (**Fig. 5.1B**). Beads placed in the peri-ocular mesenchyme temporal to the developing retina (the only location found to be technically feasible at this stage, see below) should therefore provide a truly ectopic source of BMP4 throughout the overnight culture of E9.5 mouse embryos.

Bmp4 expression was examined in the optic cup of an E11.5 and an E12.5 mouse embryo at the 40- and 48-somite stages respectively (the latter was equivalent to an E11.5 mouse embryo cultured overnight, see **Table 5.1**). *Bmp4* mRNA was detected in the dorsal quadrant of the neural retina and no longer in the surface epithelium immediately ventral to the eye at both these stages (**Fig. 5.1C, D**). Beads placed in the mesoderm ventral to the eye and in the lens (the only technically feasible location within the optic cup) in the E11.5 mouse embryo would therefore provide an ectopic source of BMP4 throughout the culture period. For further information on *Bmp4* expression in the developing mouse eye, see **Chapter 4**.

5.2. Development proceeds in whole embryo culture of E9.5 and E11.5 mouse embryos

Mouse embryos cultured for 15 to 24 hours were assessed to determine whether growth and development during culture occurred at a rate comparable to that *in vivo*. This was essential to establish that the whole mount embryo culture system utilised in this study was an accurate model of *in vivo* mouse development. Assessment was based on examining each embryo both before and after the culture period.

Two measures were taken for growth and development respectively: (1) the distance from the midbrain/hindbrain boundary to the frontal limit of the nasal prominence (termed the isthmo-nasal distance) and (2) the number of paired somites formed adjacent to the neural tube. A third assessment was made at the end of the culture

Figure 5.1

Bmp4 expression is shown in the eyes of developing mice at somite stages equivalent to pre- and post-culture E9.5 and E11.5 mouse embryos (**A-D**):

A Head region of an 18 somite stage mouse embryo following whole mount *in situ* hybridisation for *Bmp4*. This embryo is at the same stage as those placed into culture at E9.5. In the developing head, *Bmp4* was expressed in the distal tip of the mandibular primordia (**p**), the dorsal midline of the forebrain (**f**), the ventral diencephalon (**d**) and the dorsal retina (arrow).

B Eye region of a 26 somite stage mouse embryo following whole mount *in situ* hybridisation for *Bmp4*. This embryo is at the same stage as those at E9.5 after overnight culture. In the region of the developing eye, *Bmp4* mRNA was detected in the dorsal half of the retina (arrow) and in the facial primordia (**p**) ventral to the retina.

C 40 somite stage mouse eye following whole mount *in situ* hybridisation for *Bmp4*. This embryo is at the same stage as those placed into culture at E11.5. *Bmp4* transcripts were detected in the dorsal retina (arrow) and ventrally in the facial primordia (**p**).

D 48 somite stage mouse embryonic eye following whole mount *in situ* hybridisation for *Bmp4*. This embryo is at the same stage as those at E11.5 after overnight culture. *Bmp4* mRNA was detected in the dorsal retina (arrow). Expression was also observed in the facial primordia (**p**) ventral to the eye. Scale bar = 0.2 mm for **A** to **D**.

Tbx5 expression is shown in the eyes of an atypical E9.5 cultured mouse embryo where a profound left-right asymmetry of growth and development occurred (**E-G**):

E Right side of the head of a cultured E9.5 mouse embryo. 8 somites were counted on this side of the embryo. The right optic vesicle could not be seen on this embryo, an arrow marks where it should have been. An asterisk marks the location of a BMP4-soaked bead that was placed in the developing second branchial arch. Dotted line indicates the plane of section for **F**.

F Transverse section through the head of the embryo in **E** at the level of the developing eyes. The naso-temporal axis for this figure is indicated. The right side of the head is on the bottom of this figure and the neuroepithelium can be seen to be completely absent where the optic vesicle should be (marked by an arrow). The left side of the head is at the top of this figure and the optic vesicle can be seen to be invaginating. Prospective neural retina (**p-nr**), where *Tbx5* was strongly expressed, was visibly thickened with respect to the prospective retinal pigmented epithelium (**p-rpe**). In addition a lens placode formed and was invaginating to form a lens vesicle (**le**).

G Left side of the head of the cultured E9.5 mouse embryo seen in **E** and **F**. 13 somites were counted on this side of the embryo. The left optic vesicle and lens placode were invaginating to form an optic cup and lens, where *Tbx5* was expressed dorsally. The neural retina (**nr**) and developing lens (**le**) are marked. Dotted line indicates the plane of section for **F**. Dorsal (**d**) indicated for all figures bar **F**. Scale bar = 0.2 mm for **E** and **G**; 50 μm for **F**.

Bmp4 expression at pre- and post-culture stage mouse eyes and *Tbx5* expression in an atypical embryo culture

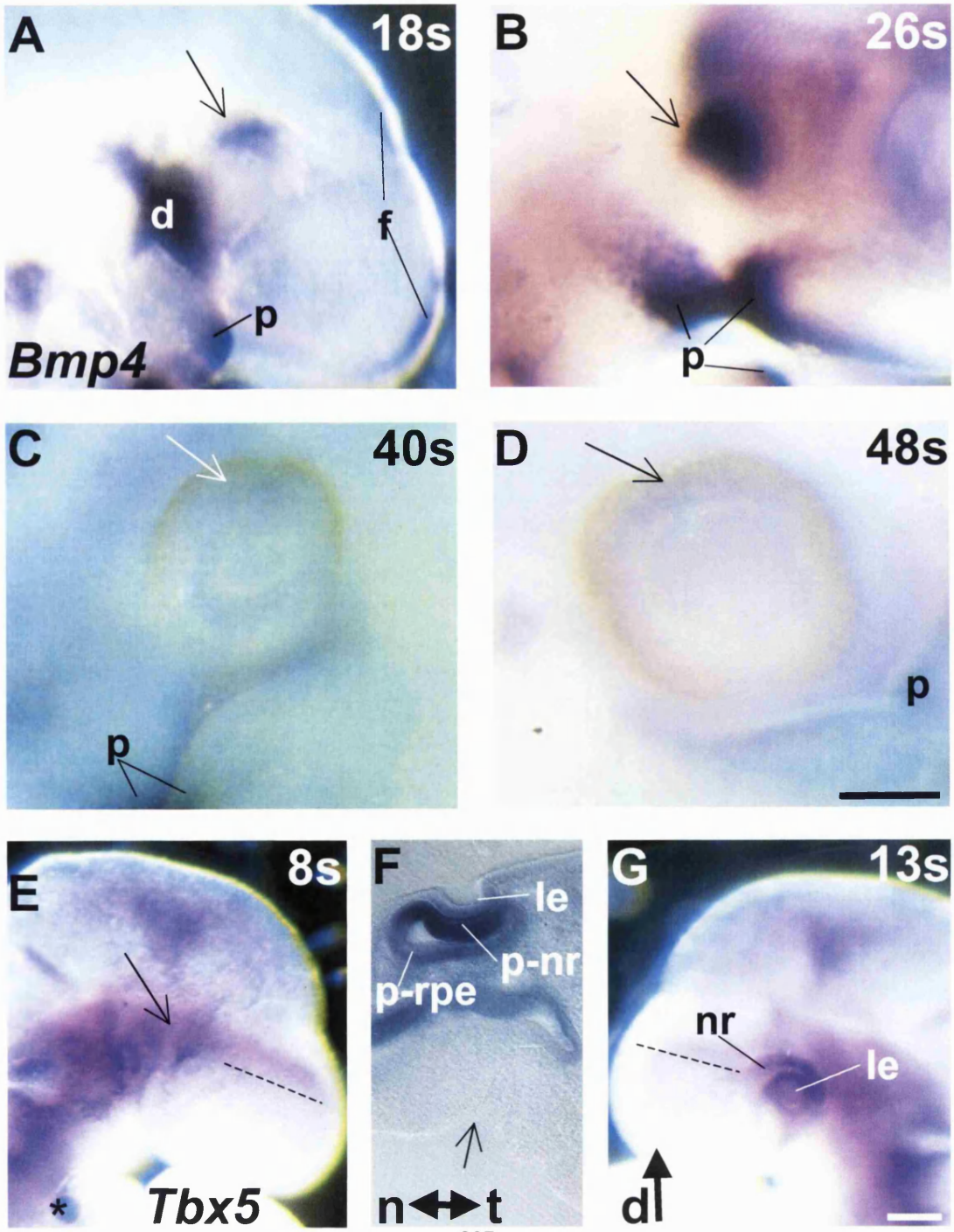

Table 5.1. Growth and development of E9.5 and E11.5 mice in culture

Length of culture	Non/pre-culture stage somite no.	head length	Post-culture quality and stage somite no.	head length	circulation	bead location	*In situ* hybridisation
16'	21	1.4 mm	22	1.3 mm	-	No op.	Normal *Tbx2*
	19	1.3 mm	21	1.6 mm	-	No op.	Normal *Tbx2*
18'	18	1.1 mm	22	1.2 mm	++	No op.	Normal *Tbx2*
	15	1.0 mm	21	1.4 mm	++	D.T. ret.	Induce *Tbx2*
	15	1.0 mm	21	1.3 mm	-	No op.	Normal *Tbx2*
			17	1.0 mm	-	D.T. ret.	Induce *Tbx2*
18'	18	1.0 mm	24	1.5 mm	++	D.T. ret.	Normal *Tbx5*
			21	1.5 mm	+	V.T. ret.	Normal *Tbx5*
			22	1.5 mm	+++	No op.	Normal *Tbx5*
			22	1.3 mm	++	No op.	Normal *Tbx5*
			21	1.2 mm	+	No op.	Normal *Tbx5*
18'	16	0.9 mm	25	1.3 mm	++	T. ret.	Induce *Tbx5*
			25	1.6 mm	+	No op.	Normal *Tbx5*
			22	1.2 mm	+++	No op.	Normal *Tbx5*
18'	20	1.2 mm	20	1.3 mm	++	No op.	_
	18	1.0 mm	19	1.2 mm	+	No op.	Normal *Tbx5*
15'	15	1.0 mm	22s	1.2 mm	+++	No op.	Normal *Tbx5*
	13	0.9 mm					
	11	0.8 mm					
24'	16	0.9 mm	23	1.5 mm	?	V.T. ret.	_
	15	1.0 mm	15	1.5 mm	?	D.T. ret.	Induce *Tbx5*
	12	0.8 mm	28	1.8 mm	?	No op.	Normal *Tbx5*
	11	0.8 mm	26	1.9 mm	?	No op.	_
	11	0.8 mm	25	1.8 mm	?	No op.	_
	9	0.8 mm	24	1.5 mm	?	No op.	Normal *Tbx5*
24'	15	1.1 mm	17	1.1 mm	?	T. ret.	Induce *Tbx5*
20'	40	3.3 mm	42	3.7 mm	-	R. + L. lens	*Tbx2* in lens
	38	3.1 mm	43	4.3 mm	+	L. + R. lens	*Tbx2* in lens
18'	40	3.4 mm	44	3.6 mm	-	lens	Normal *Tbx2*
	39	3.3 mm	46	3.7 mm	++	lens	Normal *Tbx2*
	39	3.3 mm	45	3.8 mm	++	V. ret.	Normal *Tbx2*
	36	2.9 mm	43	3.7 mm	-	V. ret.	Normal *Tbx2*
19'	42	3.3 mm	49	3.8 mm	-	lens	*Tbx2* in lens
	40	3.4 mm	48	3.8 mm	-	V. ret.	Normal *Tbx2*
	39	3.4 mm	51	3.8 mm	++	lens	*Tbx2* in lens
	38	2.6 mm	38+	3.3 mm	+	lens	Normal *Tbx2*
	35	2.5 mm	35	2.2 mm	-	V. ret.	_
20'	36	2.7 mm	43	3.1 mm	+++	V. ret.	*Tbx2* V. ret.
21'	42	3.5 mm	51	4.3 mm	+++	lens	*Tbx2* in lens
	41	3.3 mm	50	3.8 mm	+++	V. ret.	Normal *Tbx5*
19'	39	3.0 mm	48	4.3 mm	-	V. ret.	Normal *Tbx5*
	38	3.1 mm	48	3.8 mm	+++	lens	Normal *Tbx5*
	37	3.0 mm	48	4.0 mm	+	V.T. ret.	Normal *Tbx5*

Orange = non-cultured littermates Blue = control operations: BSA used

Brown = cultured unoperated embryos Red = +ve results detailed in **Table 5.2**

Yellow boxed regions = beads implanted into the lens vesicle

Green boxed regions = beads implanted into the ventral peri-ocular mesenchyme

- = no circulation detected + = circulation poor, only just detectable

++ = circulation good, but not apparent in minor blood vessels

+++ = circulation excellent, apparent even in minor blood vessels

D., dorsal; L., left; op., operation; ret., retina; R., right; T., temporal; V., ventral

period to give further indication of the embryo's health during culture, that of the embryonic circulation. This was scored with one to three plus signs on the basis of how strong and widespread the blood flow was in the embryo and/or in the yolk sac (**Table 5.1**). Where no circulation was observed the embryo was scored with a minus sign.

E11.5 mouse embryos were cultured outside their yolk sacs, which were partially cut, pulled over the head and tucked under the tail to expose the embryo whilst leaving the major blood vessels and placental attachments intact. For E9.5 mouse embryos, which have not yet developed a placenta, the culture method necessitated that they were cultured within their yolk sacs. This meant that calculation of somite numbers and the isthmo-nasal distance could not readily be carried out in E9.5 mouse embryos prior to culture. Instead, non-cultured littermates of cultured E9.5 mouse embryos were assessed to give an approximation of the pre-culture measurements. This was not ideal given the variable stages of development even within a single litter, but was sufficient to determine whether growth and development had occurred in culture.

Growth and development of E9.5 and E11.5 mouse embryos in culture

The approximate rate of somite addition in the E9.5 and E11.5 mouse embryo *in vivo* is one pair of somites every two hours (Copp *et al.*, 1997). This was mirrored in cultured embryos at both stages of development and was always accompanied by a corresponding increase in the isthmo-nasal distance (**Table 5.1**). Successful cultures tended to have a good circulation at the end of the culture period, although not in all cases as some embryos presumably came into difficulty close to the end of the culture period. Embryos that showed an appropriate level of somite addition and head growth were morphologically indistinguishable from non-cultured embryos with equivalent somite numbers.

In preliminary experiments to establish culture techniques and in a proportion of subsequent cultures, good growth and development of embryos was not observed. These embryos did not show a marked increase in somite number, tended to show a limited or absent increase in the isthmo-nasal distance and invariably had a poor circulation at the end of the culture period (**Table 5.1**). In many cases, embryos from these unsuccessful cultures looked very abnormal. In E9.5 cultures, an asymmetric

degeneration of the head was sometimes seen with a small otic vesicle and a small or absent eye on one side of the embryo. Asymmetric size and shape of the two eyes and of other structures was a feature of unsuccessfully cultured E9.5 embryos, as was a generalised loss of definition in the embryo. An example of the appearance of an embryo with poor growth and absent circulation is shown on **Fig. 1E**. In this atypical embryo, cultured for 24 hours, 8 somites were counted and the optic vesicle was absent on one side (arrows, **Fig. 1E, F**) whilst on the other side 13 somites were counted and an optic cup was forming (**Fig. 1F, G**). This shows that as well as degeneration or failure to grow, advanced growth and development of the eyes can occur in poorly cultured embryos (the optic cup normally forms between the 25- and 30-somite stages). A failed operation on the degenerate side where a bead was placed in the first branchial arch instead of the optic vesicle is likely to have contributed to the degeneration observed in this embryo. In some cases however, degeneration was observed on the unoperated side of cultured embryos. Such extreme asymmetric development observed in embryos cultured under suboptimal conditions could potentially provide a model of the human condition of unilateral microphthalmia. Further work would be required to assess whether the phenomenon could be caused by specific conditions/sham operations in a reproducible manner. E11.5 embryos that had not faired well during culture (showing limited growth and development) also showed physical abnormalities. Oedema of the heart was often seen in these embryos and less frequently abdominal oedema too. In some cases a disproportionate elongation of the trunk was observed in poorly cultured E11.5 embryos. Embryos with no circulation after culture that looked particularly abnormal were discarded and were not included on **Table 5.1**.

It was not always clear what caused a failure to survive or abnormal growth in culture, although outcomes did improve with increased expertise in dissection and surgery. The principal factors that were observed to increase the chances of growth, development and survival in culture were successful avoidance of damage to the embryo and its blood supply and a short, careful dissection. E9.5 mouse embryos that were operated on frequently faired less well than unoperated littermates, though many faired equally well showing growth and development equivalent to that one might expect *in vivo*. This was in spite of the invasive nature of the operations, which required making a small tear in the yolk sac and tearing open the amnion. A hole was

then created in the temporal mesenchyme with a tungsten needle and a bead was inserted with a mouth pipette. Good operations were those that were swift and where blood loss was minimised. The hole made in the yolk sac was neat, small and adjacent to the placental cone in good operations.

In successfully cultured E9.5 embryos, optic vesicles developed to the stage prior to invagination. At this stage the presumptive neural retina became thickened relative to the presumptive pigmented epithelium. Differences between E9.5 embryos before and after culture are shown in **Fig 5.2A** (the two embryos on the bottom left of the figure were cultured for 24 hours, the others are uncultured littermates). In cultured E11.5 embryos the corner quadrants of the retina (dorso-nasal, dorso-temporal, ventro-nasal and ventro-temporal) acquired their characteristic bulges to give the optic cup the square appearance normally seen in E12.5 mouse embryos. An E11.5 embryo is shown alongside one following 21 hours of culture in **Fig 5.2B** and **C** respectively.

5.3 BMP4-soaked beads induce *Tbx2* and *Tbx5* in the optic vesicles of mouse embryos cultured at E9.5

Operations were performed on E9.5 mouse embryos prior to culture. A small cut was made in the yolk sac and the amnion was torn. Agarose beads soaked in bovine serum albumen (BSA) or BMP4 were implanted into the temporal mesenchyme immediately adjacent to the retina. Pilot experiments were performed testing implantation at other locations ventral and nasal to the optic vesicle, but in these cases the bead could not be securely implanted without damage to the retina. Beads were placed in as ventral a location in the temporal mesenchyme as possible, so as to be distant from the endogenous dorsal expression of *Bmp4*.

Tbx5 expression is normal after overnight culture with BSA-soaked beads

In cultures of unoperated E9.5 embryos where embryos displayed good growth and development in culture (see above), *Tbx5* was normally expressed in the dorsal region of presumptive neural retina (**Fig. 5.3A, B**), but not in the ventral retina (**Fig. 5.3C**). Presumptive neural retina was thickened relative to presumptive pigmented epithelium in 25-somite stage post-culture embryos (**Fig. 5.3B**). This was in

Figure 5.2

Tbx5 expression is shown in E9.5 and E11.5 mouse embryos before and after overnight culture (**A-C**):

A Whole mount *in situ* hybridisation for *Tbx5* on 2 cultured (at the 24 and 28 somite stages, post-24 hour culture, on the bottom left) and 5 uncultured (at the 9 to the 16 somite stages) E9.5 mouse embryos. The embryo size and appearance was indistinguishable from similarly staged embryos at E10.5 that were not cultured. Growth of the embryos during culture was readily apparent when compared with uncultured E9.5 mouse embryos. *Tbx5* expression was normally expressed in the heart (**h**), the forelimbs (**f**) and the dorsal retina (arrow; see 9-somite embryo where background labelling is low). The generalised signal seen in other parts of the embryos is non-specific background labelling. Scale bar = 0.5 mm.

B Whole mount *in situ* hybridisation for *Tbx5* on a non-cultured E11.5 mouse embryo at the 37 somite stage. *Tbx5* transcripts were clearly detected in the heart (**h**), the forelimbs (**f**) and the dorsal retina (arrow). Dorsal (**d**) orientation of the developing eye is indicated and applies to **B** and **C**.

C Whole mount *in situ* hybridisation for *Tbx5* on an E11.5 mouse embryo that was cultured for 21 hours and was at the 50 somite stage (post-culture). Pre-culture number of paired somites was 41 (in brackets). The embryo size and appearance was indistinguishable from similarly staged embryos at E12.5 that were not cultured. Growth of the embryo during culture was readily apparent when compared with uncultured E11.5 mouse embryos at a similar somite stage to the embryo pre-culture (**B**). *Tbx5* expression was normally expressed in the heart (**h**), the forelimbs (**f**), the genital region (**g**) and the dorsal retina (arrow). Scale bar = 0.5 mm for **B** and **C**.

Mouse embryos at E9.5 and E11.5 grow in culture

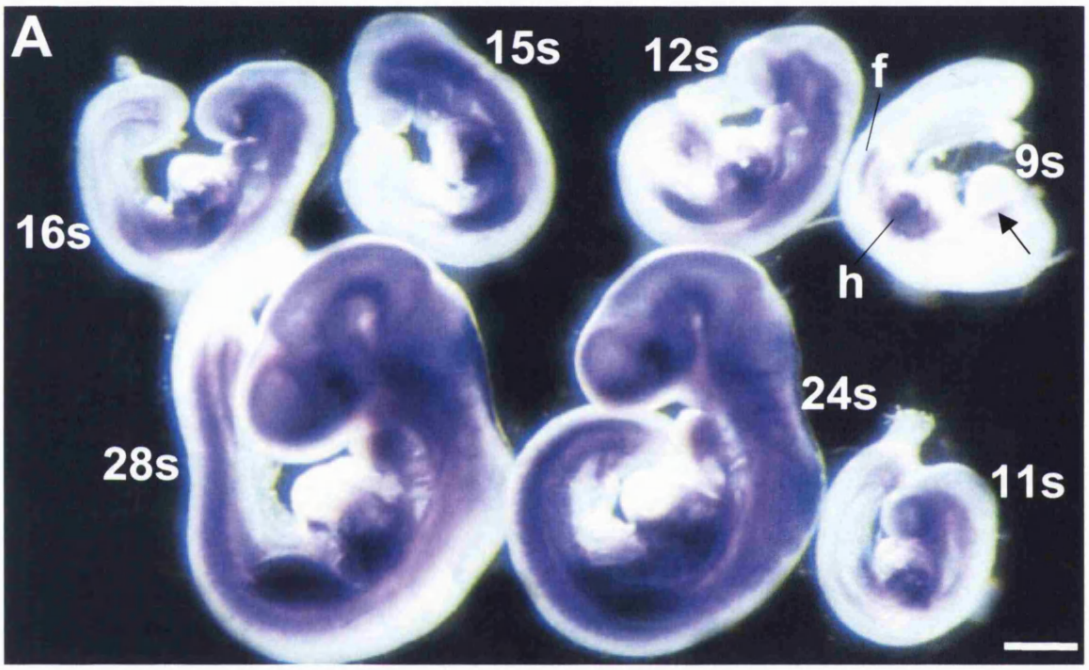

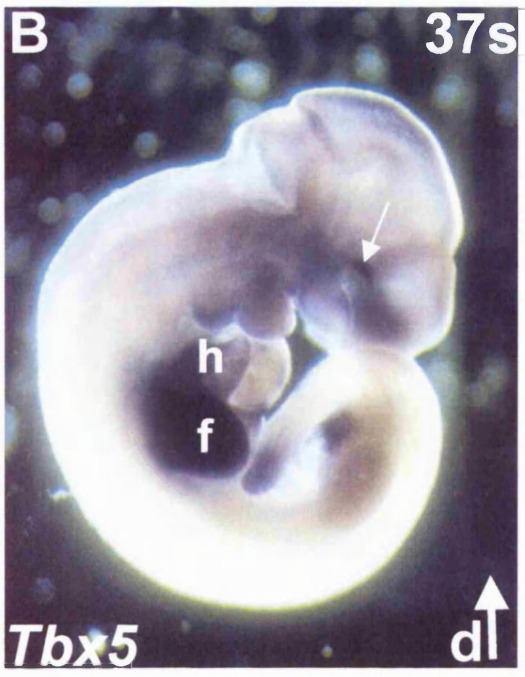

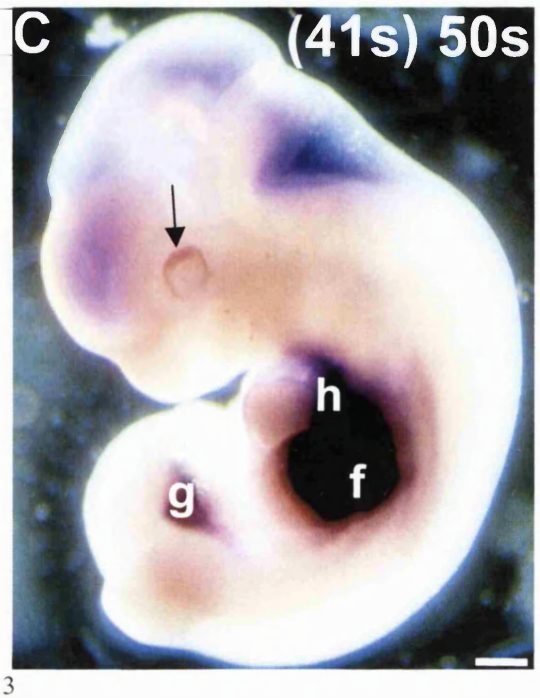

Figure 5.3

Tbx5 expression is normal in E9.5 mouse embryos after 18 hours in culture (**A-C**):

A Whole mount *in situ* hybridisation for *Tbx5* on an E9.5 mouse embryo at the 25 somite stage following culture for 18 hours. The mean somite stage of uncultured littermates was 16 paired somites. The embryo size and appearance were indistinguishable from similarly staged embryos at E10.5 that were not cultured. *Tbx5* was normally expressed in the posterior heart (**h**), the forelimbs (**f**) and the dorsal optic vesicles (arrow). The generalised signal in the brain vesicles is non-specific trapping. Dotted lines through the dorsal and ventral optic vesicle indicate the plane of sections in **B** and **C** respectively. Dorsal (**d**) orientation of the developing eye is indicated, this also applies to **D** and **F**. Scale bar = 0.2 mm.

B Section through the dorsal optic vesicle shown in **A**. Invagination of the optic vesicles had not yet begun, but the *Tbx5* expressing presumptive neural retina (**p-nr:** distal neuroepithelium, marked by dotted lines, directly opposed to the surface ectoderm, **se**) was thickened with respect to the presumptive retinal pigmented epithelium, **p-rpe** (nr: rpe thickness ratio 7:4).The naso-temporal axis for this figure and for **C**, **E** and **G** is indicated on the bottom left. The somite number (and mean of uncultured littermates, bracketed) is indicated on the right.

C Section through the optic vesicle in **A** ventral to the point of contact with surface ectoderm (**se**). No *Tbx5* expression was observed. Signal within the optic vesicle (**ov**) is non-specific trapping.

Tbx5 expression is normal in E9.5 mouse embryos after 18 hours in culture with a BSA-soaked bead placed in the ventro-temporal mesenchyme (**D-G**):

D Head of an E9.5 mouse embryo at the 21 somite stage following culture for 18 hours with a BSA-soaked bead (arrow) and whole mount *in situ* hybridisation for *Tbx5*. The mean somite stage of uncultured littermates was 18 paired somites. Although somite advancement was apparently limited in this embryo, its appearance was indistinguishable from similarly staged non-cultured embryos. *Tbx5* was normally expressed in the dorsal optic vesicles. Dotted lines through the dorsal and ventral optic vesicle indicate the plane of section in **E** and **G** respectively.

E Section through the dorsal optic vesicle shown in **D**. At 21 somites invagination of the optic vesicles (**ov**) had not yet begun, nor had the thickening of presumptive neural retina (distal **ov** opposed, dotted line, to surface ectoderm, **se**,). *Tbx5* mRNA was restricted to the presumptive neural retina. Somite number is indicated (mean of uncultured littermates is bracketed).

F Unoperated side of the head of the embryo shown in **D**. The mean somite stage of uncultured littermates was 18 paired somites. *Tbx5* was normally expressed in the dorsal optic vesicles (arrow), as for the operated side. Scale bar = 0.2 mm for **D** and **F**.

G Section through the ventral optic vesicle (and the BSA-soaked bead, marked by an asterisk) shown in **D**. *Tbx5* expression was not induced by the bead. Dotted line marks the point of contact between surface epithelium (**se**) and the optic vesicle (**ov**). Scale bar = 50 μm for **B**, **C**, **E** and **G**.

E9.5 embryos develop in culture after BSA-soaked bead insertion

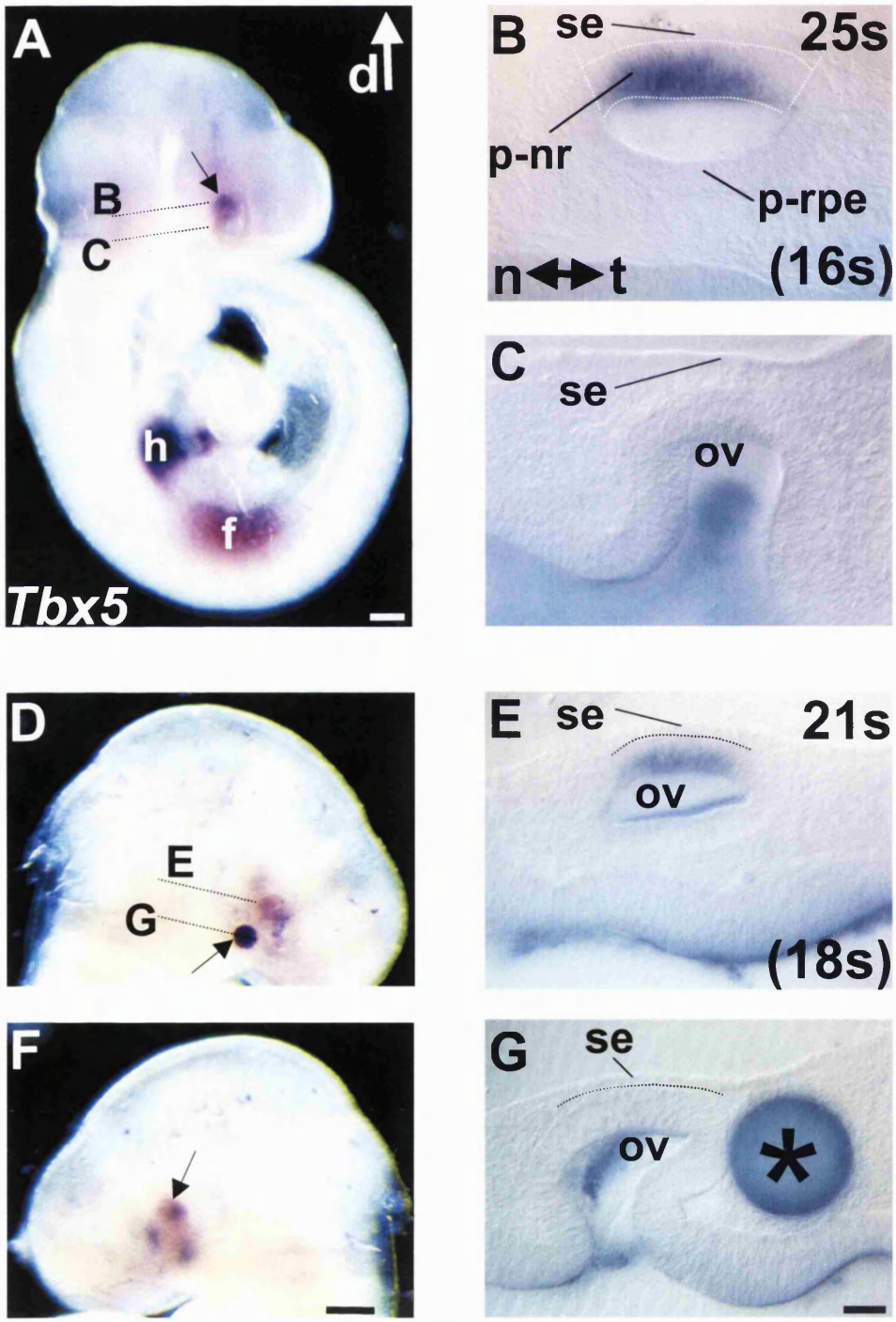

concordance with the expected appearance of a normal late stage optic vesicle at the 25-somite stage.

Beads soaked in BSA, a serum protein used as a biologically inactive control, was implanted into the ventro-temporal peri-ocular mesenchyme of E9.5 mouse embryos prior to culture. Expression of *Tbx5* was maintained in the dorsal optic vesicles of these cultured embryos and no obvious changes in morphology were observed in the presence of the bead (**Fig. 5.3D-G**; the bead is marked with an arrow in **D**, and an asterisk in **G**). Thus the implantation of a bead into the peri-ocular temporal mesenchyme does not appear to alter gene expression or disrupt eye morphology.

Tbx2 and Tbx5 are induced in the optic vesicle in response to BMP4

Beads soaked in 113 μgml^{-1} BMP4, the maximum concentration of my stock (from the Genetics Institute, MA, USA), were implanted into the temporal peri-ocular mesenchyme prior to culture of E9.5 mouse embryos. In 5 out of 5 cultured embryos, *Tbx2* and *Tbx5* expression were extended into the temporal optic vesicle in the region of the bead (**Fig. 5.4-5.6**). Both genes are normally restricted to the presumptive neural retina (that region of the optic vesicle adjacent to the surface epithelium) in the dorsal optic vesicles, with a very limited extension into the dorsal presumptive pigmented epithelium (see **Chapter 3**).

Tbx2 was clearly upregulated in the optic vesicle in response to ectopic BMP4 (**Fig. 5.4**). The extended *Tbx2* expression domain in the operated eye compared with the normal unoperated eye is clearly visible in a dorsal view of the embryos (**Fig. 5.4A**; the bead is marked with arrow). *Tbx2* was ectopically expressed in the temporal optic vesicle adjacent to the bead (marked by arrow, **Fig. 5.4B**) and was not present on the operated side (**Fig. 5.4C**). Transverse sections showed that *Tbx2* was upregulated in a temporal region of the presumptive RPE (bead marked by an asterisk, **Fig. 5.4D**) that normally does not express *Tbx2* and did not do so on the unoperated side (**Fig. 5.4E**). *Tbx2* expression was even upregulated in a region of temporal optic vesicle not in contact with the bead but ventral to it (arrow, **Fig. 5.4F**, compare with **Fig. 5.4G**). *Tbx5* expression was similarly upregulated after growth and development with a BMP4-soaked bead in culture (bead marked by arrow, **Fig. 5.5A**). *Tbx5* expression in the optic vesicle extended temporally to meet the bead on the operated side (**Fig.**

Figure 5.4

Tbx2 is upregulated in the temporal optic vesicle by a BMP4-soaked bead placed in the temporal peri-ocular mesenchyme of E9.5 mouse embryos after 18 hours in culture (**A-E**):

A Dorsal view of an E9.5 mouse embryo at the 21 somite stage following culture for 18 hours with a BMP4-soaked bead (arrow) and whole mount *in situ* hybridisation for *Tbx2*. The mean somite stage of uncultured littermates was 15 paired somites (bracketed). *Tbx2* was upregulated in the temporal optic vesicle on the operated side by the bead, but not on the unoperated side where expression was restricted to the dorsal presumptive neural retina. Scale bar = 0.1 mm.

B Operated side of the head of the embryo shown in **A**. *Tbx2* mRNA was detected in the dorsal and temporal aspects of the optic vesicle adjacent to the BMP4-soaked bead (marked by arrow). Dorsal (**d**) orientation of the developing eye is indicated for this figure and **C**. Dotted line marks the plane of section of **D** and **F**.

C Unoperated side of the head of the embryo shown in **A**. *Tbx2* mRNA was detected in the dorsal aspect of the unoperated optic vesicle. Dotted line marks the plane of section of **E** and **G**. Scale bar = 0.1 mm for **B** and **C**.

D Transverse section through the dorsal operated optic vesicle and the bead (marked by an asterisk) shown in **B**. *Tbx2* was expressed in the presumptive neural retina (**p-nr**: the distal neuroepithelium, borders marked by dotted lines, directly opposed to the surface ectoderm, **se**) and in the temporal region of the presumptive retinal pigmented epithelium (**r-rpe**). The **p-nr** was not thickened compared with **p-rpe** and if anything was thinner (nr: rpe thickness ratio 5:6). *Tbx2* expression in the optic vesicle appeared stronger on the ventricular aspect of the neuroepithelium.

E Transverse section through the dorsal unoperated optic vesicle shown in **C**. *Tbx2* expression was restricted to the presumptive neural retina (**p-nr**: distal neuroepithelium in contact with surface ectoderm, **se**, marked by dotted lines). *Tbx2* expression in the optic vesicle appeared stronger on the ventricular aspect of the **p-nr**. In this unoperated optic vesicle the **p-nr** was thickened with respect to the presumptive retinal pigmented epithelium, **p-rpe** (nr: rpe thickness ratio 10:7).

F Transverse section through the operated optic vesicle shown in **B** ventral to the section in **D**. *Tbx2* mRNA was detected at this level in the **p-nr** (opposed to the surface ectoderm, bordered by dotted lines) and in the temporal **p-rpe** (arrow) ventral to the bead (seen in **D**). *Tbx2* expression was also expressed in the ventral peri-ocular mesenchyme (**m**) at this level. *Tbx2* expression in the optic vesicle appeared stronger on the ventricular aspect of the neuroepithelium. The naso-temporal axis for this figure and for **A** and **E** is indicated.

G Transverse section through the unoperated optic vesicle shown in **C** ventral to the section in **E**. *Tbx2* expression was detected at this level in the **p-nr** (bordered by dotted lines). *Tbx2* mRNA was also detected in the peri-ocular mesenchyme (**m**) at this level. *Tbx2* expression in the optic vesicle appeared stronger on the ventricular aspect of the neuroepithelium. Scale bar = 50 μm for **D-G**.

BMP4-soaked beads induce *Tbx2* in cultured E9.5 embryos

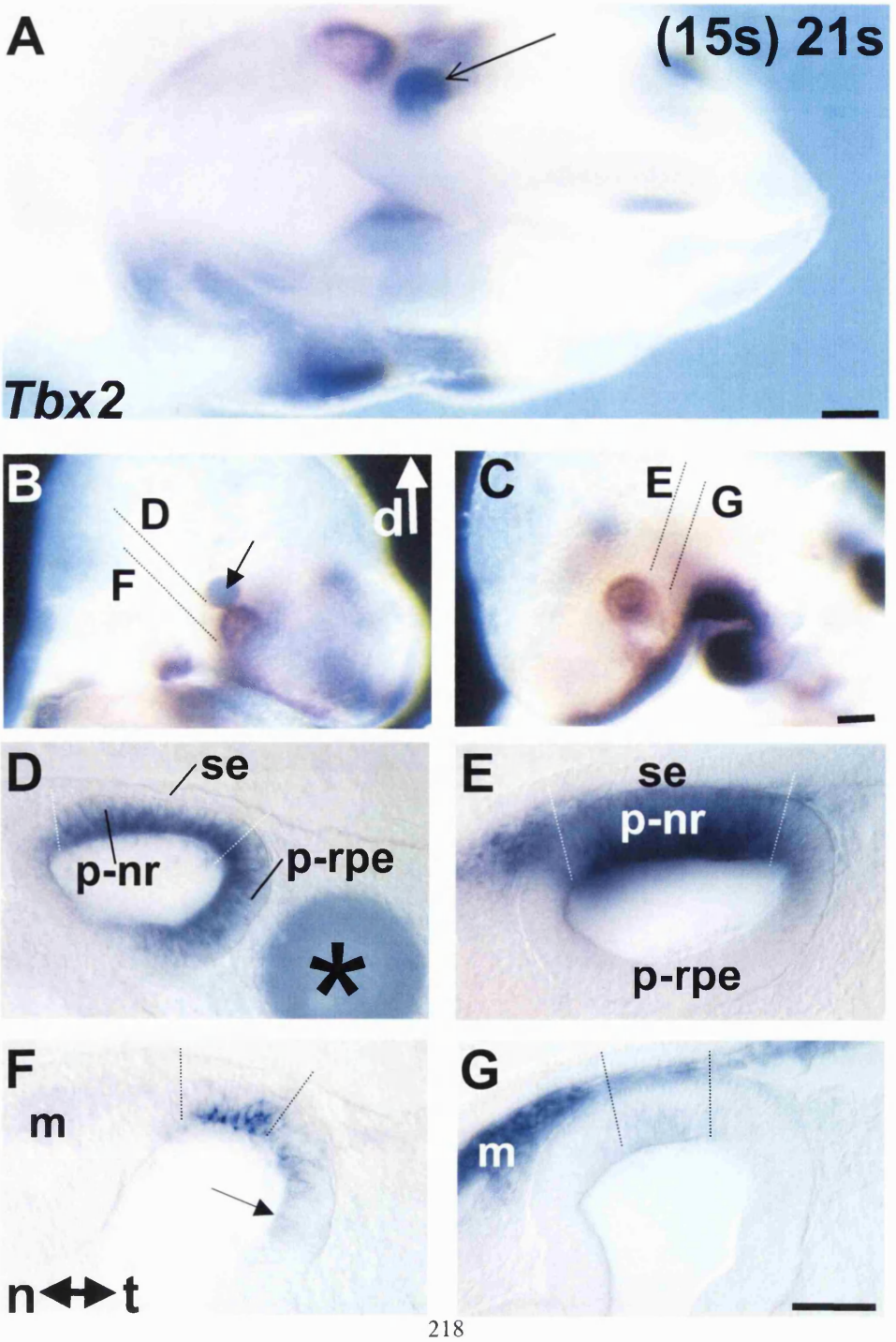

Figure 5.5

Tbx5 is upregulated in the temporal optic vesicle by a BMP4-soaked bead placed in the temporal peri-ocular mesenchyme of E9.5 mouse embryos after 18 hours in culture (**A-E**):

A Dorsal view of an E9.5 mouse embryo at the 25 somite stage following culture for 18 hours with a BMP4-soaked bead (arrow) and whole mount *in situ* hybridisation for *Tbx5*. The mean somite stage of uncultured littermates was 16 paired somites (bracketed). *Tbx5* was upregulated in the temporal optic vesicle on the operated side by the bead, but not on the unoperated side where expression was restricted to the dorsal presumptive neural retina. Scale bar = 0.1 mm.

B Operated side of the head of the embryo shown in **A**. *Tbx5* mRNA was detected in the dorsal and temporal aspects of the optic vesicle adjacent to the BMP4-soaked bead (marked by arrow). Dorsal (**d**) orientation of the developing eye is indicated for this figure and for **C**. Dotted line marks the plane of section of **D** and **F**.

C Unoperated side of the head of the embryo shown in **A**. *Tbx5* mRNA was detected in the dorsal aspect of the unoperated optic vesicle only. Dotted line marks the plane of section of **E** and **G**. Scale bar = 0.1 mm for **B** and **D**.

D Transverse section through the dorsal operated optic vesicle and the bead (marked by an asterisk) shown in **B**. *Tbx5* was expressed in the presumptive neural retina (**p-nr**: the distal neuroepithelium bordered by dotted lines and opposed to the surface ectoderm, **se**) and in the temporal region of the presumptive retinal pigmented epithelium (**p-rpe**). The **p-nr** was not thickened compared with **p-rpe** (nr: rpe thickness ratio 1:1).

E Transverse section through the dorsal unoperated optic vesicle shown in **C**. *Tbx5* transcripts were restricted to the presumptive neural retina (**p-nr**; marked by dotted lines and opposed to the surface ectoderm, **se**). The **p-nr** was thickened compared with the presumptive retinal pigmented epithelium, **p-rpe** (nr: rpe thickness ratio 3:2).

F Transverse section through the operated optic vesicle shown in **B** ventral to the section in **D**. *Tbx5* mRNA was detected at this level in the ventricular aspect of the **p-nr** (opposed to the surface ectoderm, **se**, bordered by dotted lines). *Tbx5* expression in the optic vesicle appeared stronger on the ventricular aspect of the neuroepithelium. The naso-temporal axis for this figure and for **A** and **E** is indicated.

G Transverse section through the unoperated optic vesicle shown in **C** ventral to the section in **E**. *Tbx5* expression was detected at this level in ventricular aspect of the **p-nr** (opposed to the surface ectoderm, **se**, bordered by dotted lines). Scale bar = 50 μm for **D-G**.

BMP4-soaked beads induce *Tbx5* in cultured E9.5 embryos

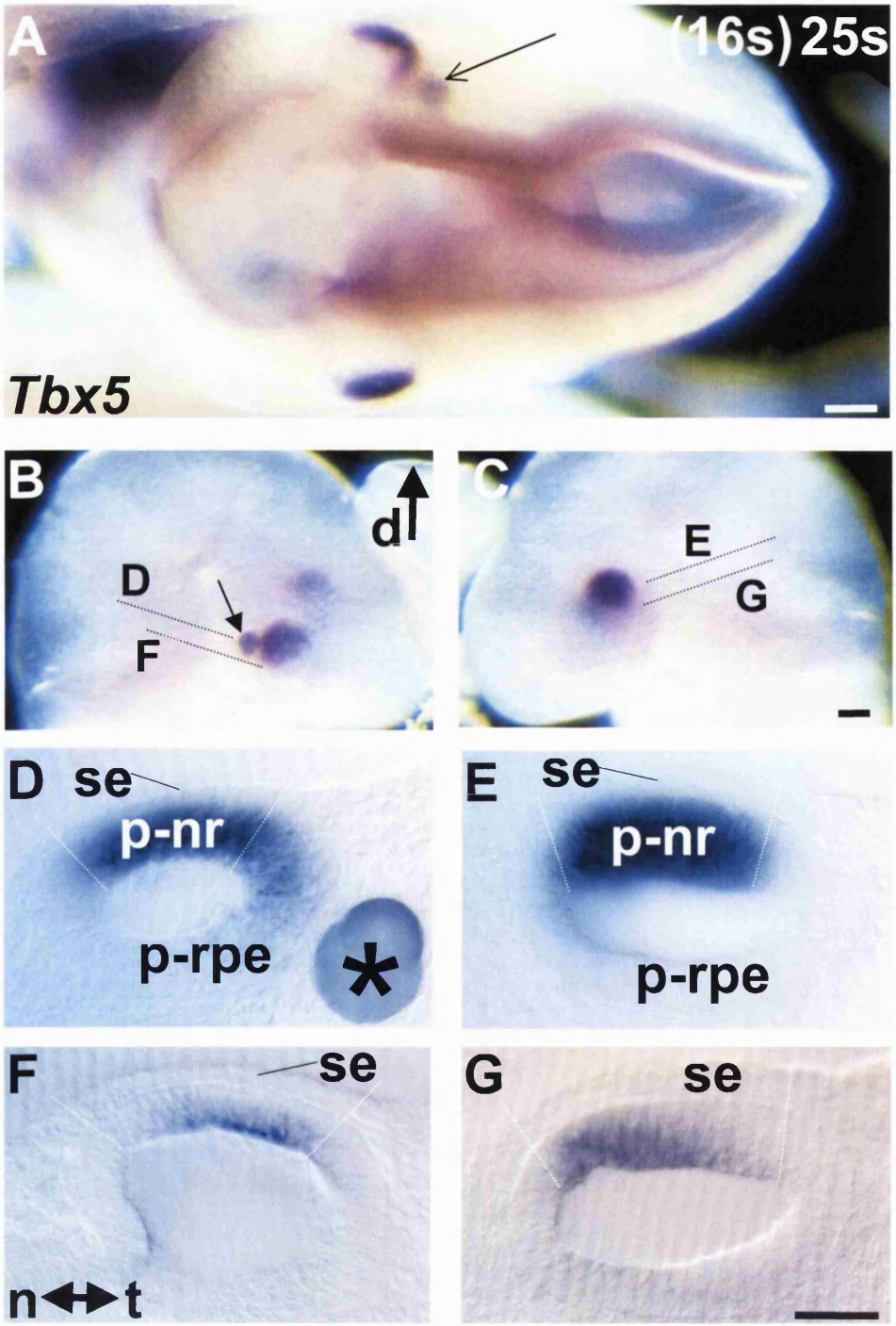

5.5B) but not on the unoperated side (**Fig. 5.5C**). Transverse sectioning revealed that *Tbx5* expression extended temporally into the presumptive RPE (bead marked by as asterisk, **Fig. 5.5D**) whereas on the unoperated side *Tbx5* expression was firmly restricted to the presumptive neural retina (**Fig. 5.5E**). Ectopic *Tbx5* expression did not extend as far temporally in response to the bead as did *Tbx2* expression. In addition, *Tbx5* upregulation was not observed in the temporal optic vesicle ventral to the bead (**Fig. 5.5F, G**).

The assessment of any morphological changes occurring after BMP bead implantation can only be carried out in healthy cultures that showed an expected degree of growth and development. Although numbers are currently too small to determine definitively whether ectopic BMP4 at a concentration of 113 μgml^{-1} caused morphological alterations in the developing optic vesicle, these data are consistent with this notion. Optic vesicles with implanted BMP4-soaked beads were more rounded and did not display a thickening of the presumptive neural retina (**Fig. 5.4, 5.5**). *Tbx2* and *Tbx5* were upregulated even in cultures in which satisfactory growth and development were not achieved (**Fig. 5.6**).

5.4. BMP4-soaked beads induce *Tbx2*, but not *Tbx5*, in the developing eyes of mouse embryos cultured at E11.5

Operations were performed on E11.5 mouse embryos prior to culture. After ensuring the amnion was torn away, agarose beads were implanted into the ventral mesenchyme immediately adjacent to the optic cup or into the lens vesicle. Beads were implanted into the ventral mesenchyme to provide an ectopic source of BMP4 at the opposite side of the optic cup to the endogenous dorsal *Bmp4* expression. To address the concern that diffusing BMP4 may not readily cross the mesenchymal-epithelial boundary and the pigmented epithelium to enter the neural retina, beads were also placed within the optic cup. The lens vesicle proved to be the only technically feasible location within the optic cup to implant beads without damaging to the retina. The space between the neural retina and the lens was too narrow at the E11.5 stage to allow bead implantation.

Figure 5.6

Tbx2 and *Tbx5* are upregulated by exogenous BMP4 even in embryos that did not display good growth and development in culture (**A-G**):

A Dorsal view of the head of an E9.5 mouse embryo at the 17 somite stage following culture for 18 hours with a BMP4-soaked bead (arrow) and whole mount *in situ* hybridisation for *Tbx2*. The mean somite stage of uncultured littermates was 16 paired somites (bracketed). Despite poor growth and development in this embryo during culture, *Tbx2* was upregulated in the optic vesicle on the operated side by the bead. On the unoperated side *Tbx2* expression was restricted to the dorsal presumptive neural retina. Temporal is indicated as up. Scale bar = 0.1 mm.

B Transverse section through the dorsal optic vesicle and the BMP4-soaked bead (marked by asterisk) on the operated side of the embryonic head shown in **A**. *Tbx2* mRNA was detected throughout the dorsal optic vesicle including presumptive RPE (the proximal neuroepithelium adjacent to the extra-ocular mesenchyme and the bead). The naso-temporal axis for this figure and for **C**, **E** and **F** is indicated.

C Transverse section through the dorsal optic vesicle on the unoperated side of the embryonic head shown in **A**. *Tbx2* mRNA was detected in the ventricular aspect of a small portion of the presumptive neural retina (the distal neuroepithelium directly opposed to the surface ectoderm). Scale bar = 50 μm.

D Operated side of the head of an E9.5 mouse embryo at the 17 somite stage following culture for 18 hours with a BMP4-soaked bead (arrow) and whole mount *in situ* hybridisation for *Tbx5*. The mean somite stage of uncultured littermates was 15 paired somites (bracketed). *Tbx5* was upregulated on the temporal aspect of the optic vesicle (delayed in development compared with the unoperated side, see **G**) by the bead. Dotted lines mark the planes of section through the dorsal (**E**) and ventral (**F**) optic vesicles. Scale bar = 0.2 mm for **D** and **G**.

E Transverse section through the head of the embryo shown in **D** at the level of the dorsal operated (**o**, top) and dorsal unoperated (**u**, bottom) optic vesicles. On the operated side of the head *Tbx5* was expressed in the distal optic vesicle (which was delayed in development compared with the unoperated side) in a domain that extended temporally beside the bead (marked by asterisk). On the unoperated side the dorsal optic vesicle was clearly distinguished from the prosencephalic neuroectoderm (**n**) and *Tbx5* was expressed throughout the distal optic vesicle (arrow) and not more proximally.

F Transverse section through the head of the embryo shown in **D** at a more ventral level to that shown in **E**. *Tbx5* transcripts were detected distally and temporally (arrow) in the operated optic vesicle (**o**) by the bead (marked by asterisk). *Tbx5* could not be detected in the ventral unoperated optic vesicle (**u**). Scale bar = 50 μm for **E** and **F**.

G Unoperated side of the head of the embryo shown in **D**. *Tbx5* was expressed in the dorsal aspect of the optic vesicle (arrow). Dorsal (**d**) orientation is indicated for this figure and **D**. Dotted lines mark the planes of section through the dorsal (**E**) and ventral (**F**) optic vesicles.

BMP4-soaked beads induce *Tbx2* and *Tbx5* in cultured E9.5 embryos

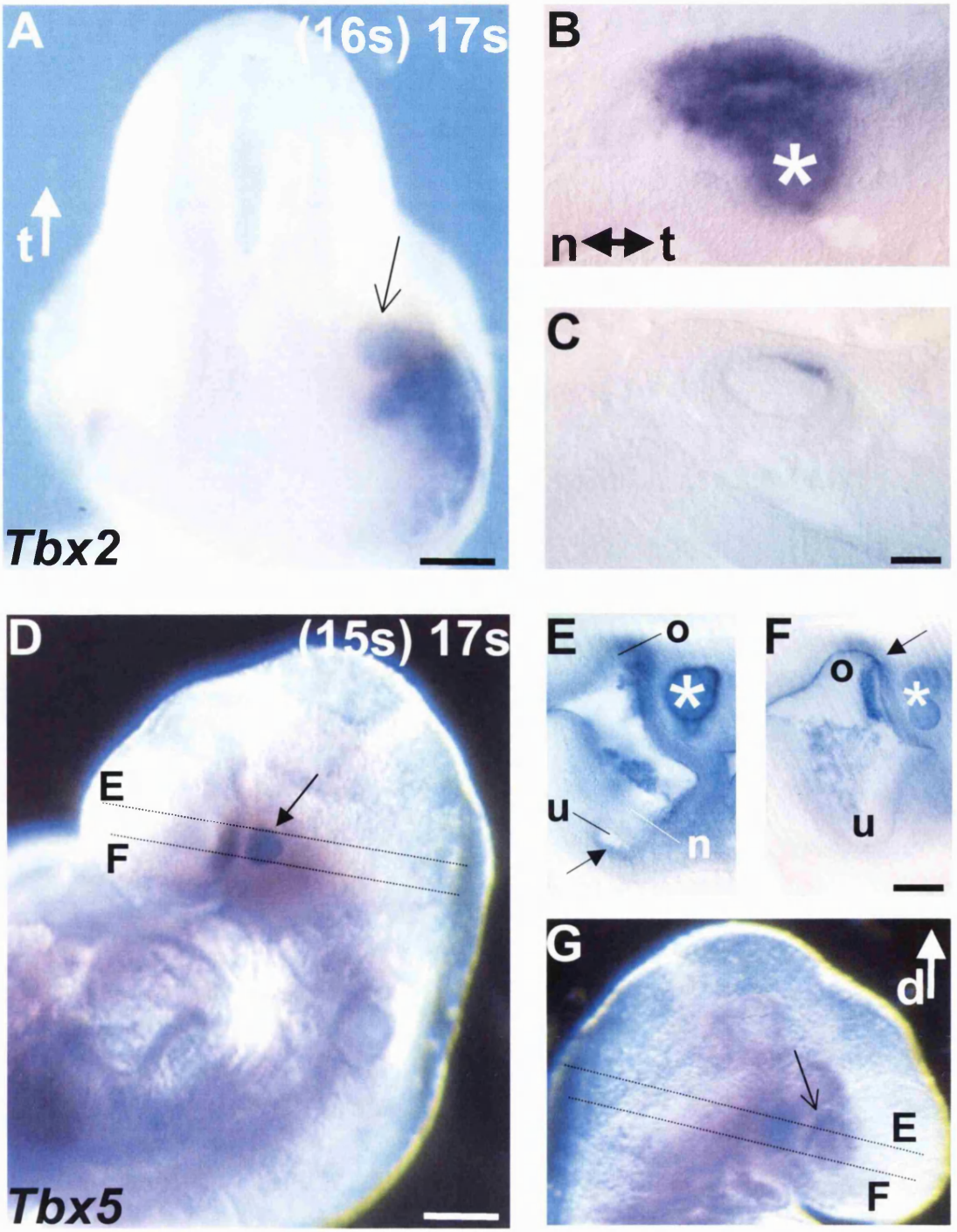

BMP4-soaked beads induce Tbx2 expression in the developing optic cup

Beads soaked in 113 μgml^{-1} BMP4 were implanted into the lens vesicle prior to culture of E11.5 mouse embryos. After the culture period, embryos were examined for *Tbx2* and *Tbx5* expression. In the unoperated eye of a cultured E11.5 embryo, *Tbx2* was normally expressed throughout the dorsal hemiretina (**Fig. 5.7A**). In the eye with a BMP4-soaked bead occupying the lens vesicle, *Tbx2* expression expanded into the ventral retina, and, more strikingly, was induced in the lens (**Fig. 5.7B**; asterisk marks the bead). Transverse vibratome sections showed that expression was indeed induced in the lens tissue of the operated eye and was not simply 'trapping' of the hybridisation signal in the lens vesicle (**Fig. 5.7C-H**; asterisk marks the bead). Expression was also seen to extend further ventrally in peripheral regions of the neural retina on the operated side in these sections. This result was repeated in other E11.5 mouse embryo analysed for *Tbx2* expression after overnight culture with BMP4 (**Fig. 5.8A, B** shows a second example; asterisk marks the bead). When *Tbx5* was examined in a similarly cultured embryo, no alterations in the normal expression pattern were seen (**Fig. 5.8C, D**; asterisk marks the bead, see also **Table 5.1**). *Tbx5* expression was sharply restricted to the dorsal quadrant of the retina with no gene induction in the lens in both the operated and the unoperated eye (**Fig. 5.8C, D**). The effect of BMP4 on *Tbx2* was apparent even in some embryos that had not faired well in culture. One such embryo was analysed by dorso-ventral sectioning through the optic cup (compared with transverse sections shown in **Fig. 5.7**). The BMP4-soaked bead induced *Tbx2* expression in the lens and ventral retina of the left eye (**Fig. 5.8E-G**; asterisk marks the bead), while in the right eye a BSA-soaked bead had no effect (**Fig. 5.8H-K**; asterisk marks the bead).

Fig. 5.9A-F shows an E11.5 mouse embryo analysed for *Tbx2* expression and vibratome sectioned along the dorso-ventral axis of the optic cup after overnight culture with BMP4-soaked beads in the lens vesicle. The vibratome sections show expression in the peripheral tip of the ventral retina (the part of ventral retina nearest the bead which is marked by an asterisk), as well as in the lens vesicle, on the operated side only (**B, C** compared with **E, F**). When BMP4-soaked beads were implanted into the ventral mesenchyme, less conclusive observations were made. In one embryo out of three tested, the ventrally located bead appeared to upregulate *Tbx2* expression in the ventral optic cup (**Fig. 5.9G-M**; asterisk marks the bead). This was

Figure 5.7

Tbx2 is upregulated in the ventral retina and lens by a BMP4-soaked bead placed in the lens vesicle of E11.5 mouse embryos after 18 hours in culture (**A-H**):

A Unoperated eye of an E11.5 mouse embryo at the 51 somite stage following culture for 18 hours and whole mount *in situ* hybridisation for *Tbx2*. The pre-culture somite number was 42. In the developing eye, *Tbx2* mRNA was detected throughout the dorsal half of the optic cup only (arrows mark limits of expression domain). Dotted lines mark the planes of section through dorsal to more ventral optic cup for **C**, **E** and **G**. Dorsal (**d**) orientation of the developing eye is indicated for this figure and for **B**. Nasal (**n**) orientation is indicated.

B Operated eye of the cultured E11.5 mouse shown in **A**. *Tbx2* expression was extended into the ventral optic cup (marked by arrows) and in the developing lens when a BMP4-soaked bead (marked by an asterisk) was implanted into the lens vesicle prior to culture. On the unoperated side *Tbx2* expression was restricted to the dorsal presumptive neural retina. Dotted lines mark the planes of section through dorsal to more ventral optic cup for **D**, **F** and **H**. Nasal (**n**) orientation is indicated. Somite number is indicated (pre-culture somite number is bracketed).

C Transverse section through the dorsal aspect of the unoperated optic cup shown in **A**. *Tbx2* mRNA was detected in the neural retina (**nr**) and not in the lens (**le**). More signal was detected on the temporal side in all sections of both eyes because the sections were skewed and this side is more dorsal than the nasal side (see **A** and **B**). The naso-temporal axis for **C** through to **H** is indicated.

D Transverse section through the dorsal aspect of the operated optic cup shown in **B** at the level of the section shown in **C**. *Tbx2* was expressed in both nasal and temporal aspects of the dorsal retina. *Tbx2* transcripts were also detected in the developing lens around the bead (which is marked by an asterisk), but not in the presumptive corneal epithelium (**c**).

E Transverse section through the unoperated optic cup shown in **A**, parallel to the section shown in **C**. *Tbx2* was expressed in the dorsal neural retina seen on the temporal side and not in the lens.

F Transverse section through the operated optic cup shown in **B** at the level of the section shown in **E** and parallel to the section shown in **D**. *Tbx2* was expressed in both dorso-temporal and ventro-nasal aspects of the neural retina. *Tbx2* transcripts were also detected in the developing lens tissue around the bead (which is marked by an asterisk), but not in the presumptive corneal epithelium.

G Transverse section through the ventral aspect of the unoperated optic cup shown in **A** and parallel to the sections shown in **C** and **E**. *Tbx2* mRNA was not detected in the ventral neural retina or the lens. Transcripts were detected in the ventral peri-ocular mesenchyme (**m**) seen on the nasal side.

H Transverse section through the ventral aspect of the operated optic cup shown in **B** at the level of the section shown in **G** and parallel to the sections shown in **D** and **F**. *Tbx2* was expressed in the temporally and in nasal retina (which is also more ventral due to skewed sectioning, see **B**, and is marked by an arrowhead). *Tbx2* was also expressed in the developing lens and the ventral peri-ocular mesenchyme (**m**), but not in the presumptive corneal epithelium (surface ectoderm). Scale bar = 0.1 mm for all figures.

BMP4-soaked beads induce *Tbx2* in cultured E11.5 embryos (I)

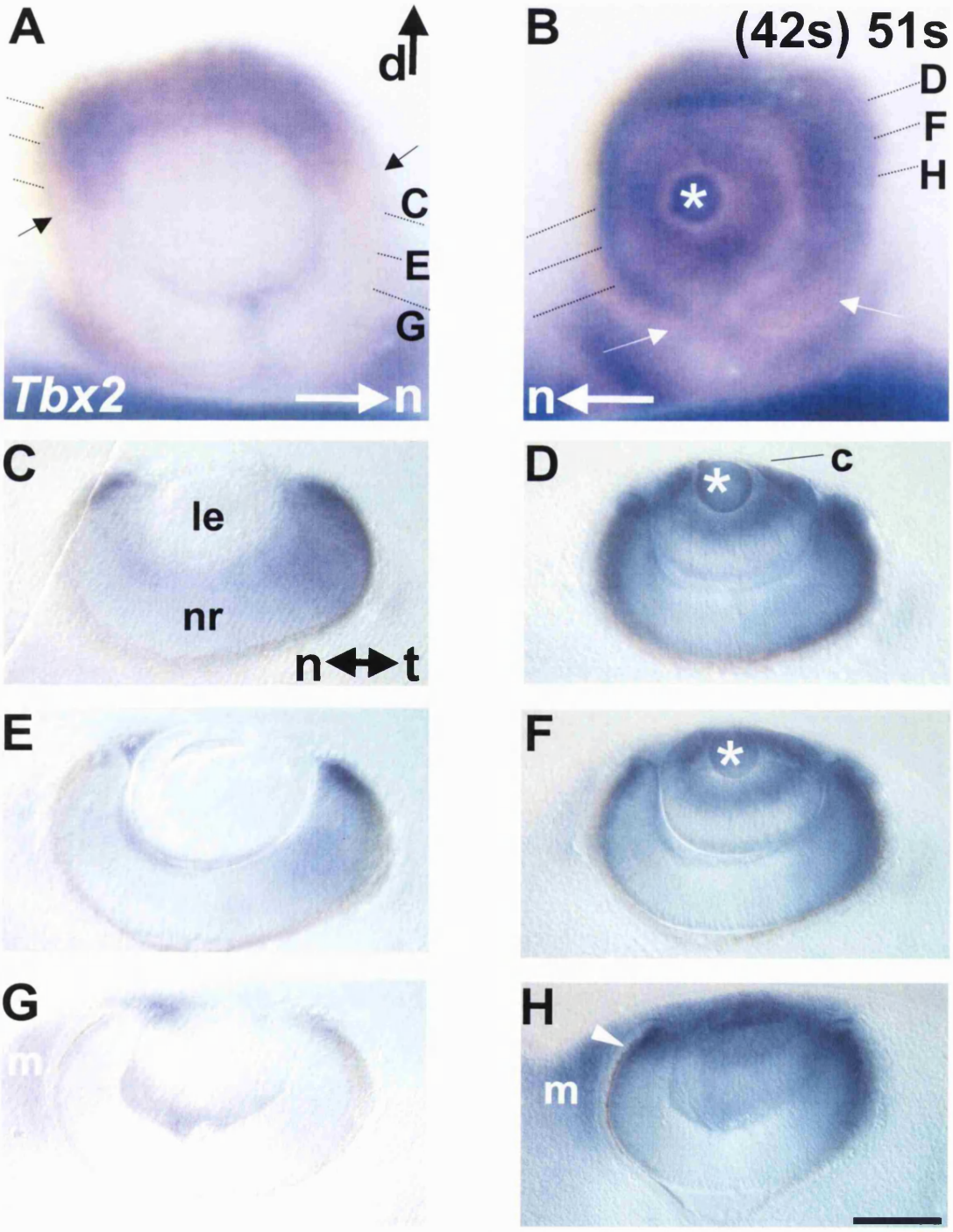

Figure 5.8

E11.5 mouse embryos cultured for 18 hours with a BMP4-soaked bead in the lens vesicle upregulate *Tbx2* but not *Tbx5* (**A-K**):

A Operated eye of an E11.5 mouse embryo at the 49 somite stage following culture for 18 hours and whole mount *in situ* hybridisation for *Tbx2*. The pre-culture somite number was 42. *Tbx2* was upregulated in the ventral optic cup (arrows) and in the developing lens to be expressed throughout the eye when a BMP4-soaked bead (marked by an asterisk) was implanted into the lens vesicle prior to culture. Dorsal (**d**) orientation of the eye is indicated for all figures.

B Unoperated eye of the cultured E11.5 mouse shown in **A**. *Tbx2* was expressed in the dorsal hemiretina (arrows mark domain). Low level expression was detected ventrally in this embryo. Somite number is indicated on the bottom right (pre-culture somite number is bracketed).

C Operated eye of an E11.5 mouse embryo at the 48 somite stage (pre-culture somite number was 38) following culture for 18 hours and whole mount *in situ* hybridisation for *Tbx5*. *Tbx5* was not upregulated when a BMP4-soaked bead (marked by an asterisk) was implanted into the lens vesicle prior to culture. *Tbx5* was expressed in the dorsal optic cup quadrant (arrows).

D Unoperated eye of the cultured E11.5 mouse shown in **C**. In the developing eye, *Tbx5* mRNA was detected throughout the dorsal quadrant of the optic cup (arrows mark domain). Somite number is indicated on the bottom right (pre-culture somite number is bracketed).

E Operated eye of an E11.5 mouse embryo at the 43 somite stage following culture for 18 hours and whole mount *in situ* hybridisation for *Tbx2*. The pre-culture somite number was 38 (bracketed). *Tbx2* was upregulated ventrally (arrow) and in the lens when a BMP4-soaked bead (marked by an asterisk) was implanted into the lens vesicle prior to culture. Dotted lines mark the planes of section through the optic cup along the dorso-ventral axis shown in **F** and **G**.

F Section through the optic cup in **E** along its dorso-ventral axis. *Tbx2* transcripts were detected in the dorsal and (to a lesser degree) ventral neural retina (arrow) and in the anterior wall of the lens vesicle by the bead (marked by asterisk). Bleeding (**b**) during culture has distorted the shape of the optic cup. Bleeding occurred in both optic cups during culture.

G Parallel section to that shown in **F**. *Tbx2* was upregulated in ventral retina (arrow) and lens by the bead (marked by asterisk). Bleeding (**b**) during culture has distorted the shape of the optic cup.

H Control operated eye of the E11.5 mouse embryo shown in **E**. *Tbx2* expression was normally restricted to the dorsal retina (domain marked by arrows) when a BSA-soaked bead (marked by an asterisk) was implanted into the lens vesicle prior to culture. Dotted lines mark the planes of section through the optic cup along the dorso-ventral axis shown in **J** and **K**.

J Section through the optic cup in **H** along its dorso-ventral axis. *Tbx2* was normally expressed in the dorsal retina (domain boundary marked by arrow) in a gradient that diminished ventrally (bead marked by asterisk). Bleeding (**b**) has occurred during culture and collected behind the optic cup.

K Parallel section to that shown in **J**. *Tbx2* was expressed in the dorsal retina in a gradient that diminished ventrally (arrow). An asterisk marks the bead. Scale bar = 0.1 mm for all figures.

BMP4-soaked beads induce *Tbx2*, but not *Tbx5*, in cultured E11.5 embryos

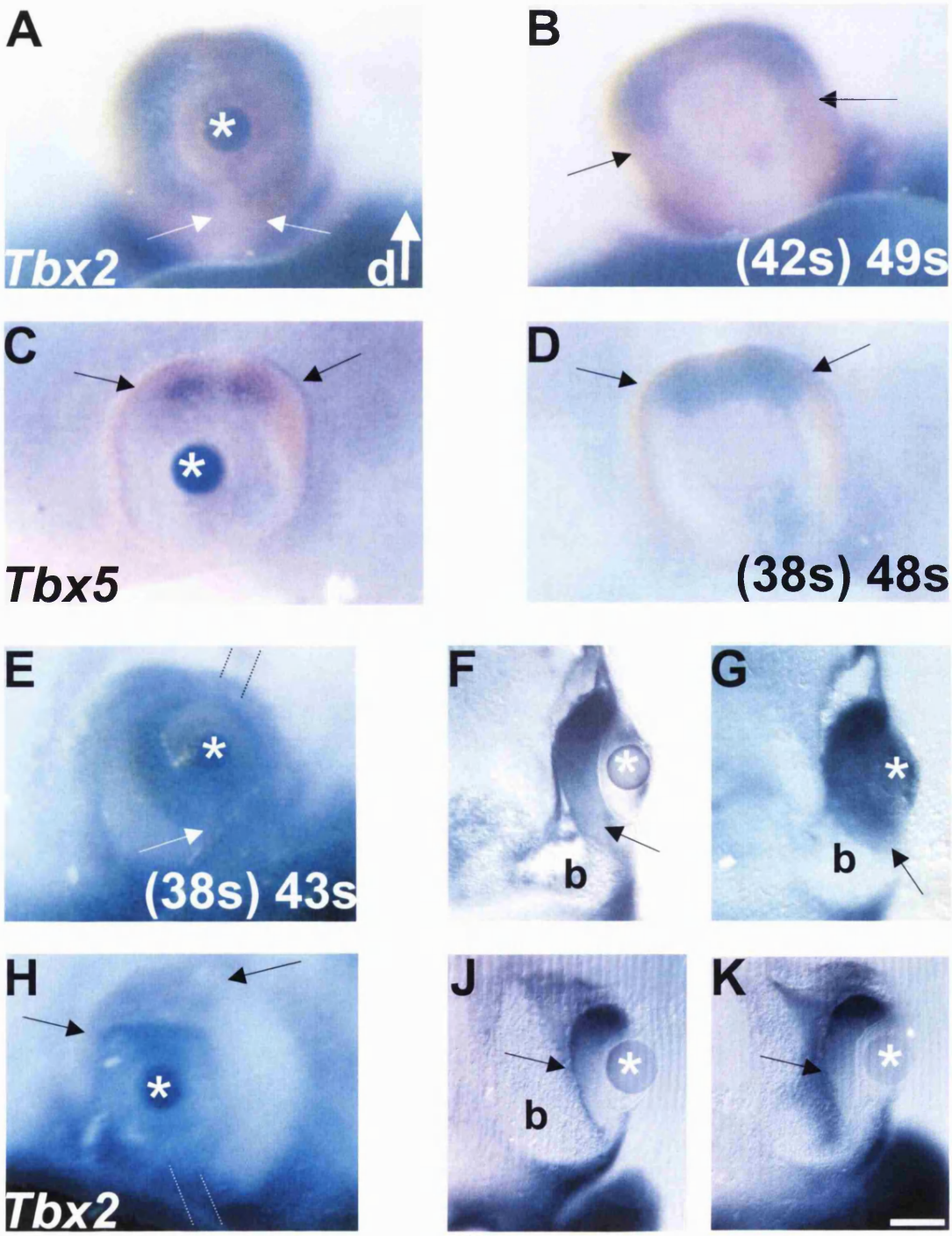

Figure 5.9

Tbx2 is upregulated in the E11.5 mouse optic cup after 18 hours in culture by a BMP4-soaked bead in the lens vesicle or the ventral extra-ocular mesenchyme (**A-M**):

A Operated eye of an E11.5 mouse embryo at the 51 somite stage following culture for 18 hours and whole mount *in situ* hybridisation for *Tbx2*. When a BMP4-soaked bead (marked by an asterisk) was implanted into the lens vesicle prior to culture, *Tbx2* was upregulated in the ventral retina (arrows show extended expression domain) and lens. Dotted lines mark the planes of section through the optic cup along the dorso-ventral axis shown in **B** and **C**. Dorsal (**d**) orientation of the developing eye is indicated for all figures.

B Section through the optic cup in **A** along its dorso-ventral axis. *Tbx2* mRNA was localised to the dorsal retina, the peripheral ventral retina (arrowhead) and the lens (bead marked by asterisk).

C Parallel section to that shown in **B**. *Tbx2* mRNA was localised to the dorsal retina (arrow marks ventral limit), the peripheral ventral retina (arrowhead) and the lens (bead marked by asterisk).

D Unoperated eye of the E11.5 mouse embryo shown in **A**. *Tbx2* expression was restricted to the dorsal half of the optic cup (arrows indicate ventral limits of expression domain). Dotted lines mark the planes of section through the optic cup along the dorso-ventral axis shown in **E** and **F**. Somite number is indicated (pre-culture somite number is bracketed).

E Section through the optic cup in **D** along its dorso-ventral axis. *Tbx2* was expressed in the dorsal retina in a gradient that diminished ventrally (ventral limit of expression marked by arrow).

F Parallel section to that shown in **E**. *Tbx2* was normally expressed in the dorsal retina in a gradient that diminished ventrally (ventral limit of expression marked by arrow).

G Operated eye of an E11.5 mouse embryo at the 43 somite stage following culture for 18 hours and whole mount *in situ* hybridisation for *Tbx2*. When a BMP4-soaked bead (marked by an asterisk) was implanted into the ventral peri-ocular mesenchyme prior to culture, *Tbx2* was upregulated in the ventral retina. Arrow shows ventral extension of *Tbx2* expression. Dotted lines mark the planes of section through the optic cup along the dorso-ventral axis shown in **H** and **J**.

H Section through the optic cup in **A** along its dorso-ventral axis. *Tbx2* was upregulated in ventral retina (arrow) but not in the peri-ocular mesenchyme around the bead (marked by asterisk).

J Parallel section to that shown in **B**. *Tbx2* was upregulated in ventral retina (arrow) but not in the peri-ocular mesenchyme around the bead (marked by asterisk).

K Unoperated eye of the E11.5 mouse embryo shown in **G**. *Tbx2* expression was restricted to the dorsal half of the optic cup (arrows indicate ventral limits of expression domain). Dotted lines mark the planes of section through the optic cup along the dorso-ventral axis shown in **L** and **M**. Somite number is indicated (pre-culture somite number is bracketed).

L Section through the optic cup in **K** along its dorso-ventral axis. *Tbx2* was normally expressed in the dorsal retina in a gradient that diminished ventrally (arrow shows ventral limit of expression).

M Parallel section to that shown in **L**. *Tbx2* was normally expressed in the dorsal retina in a gradient that diminished ventrally (arrow shows ventral limit).Scale bar = 0.1 mm for all figures.

BMP4-soaked beads induce *Tbx2* in cultured E11.5 embryos (II)

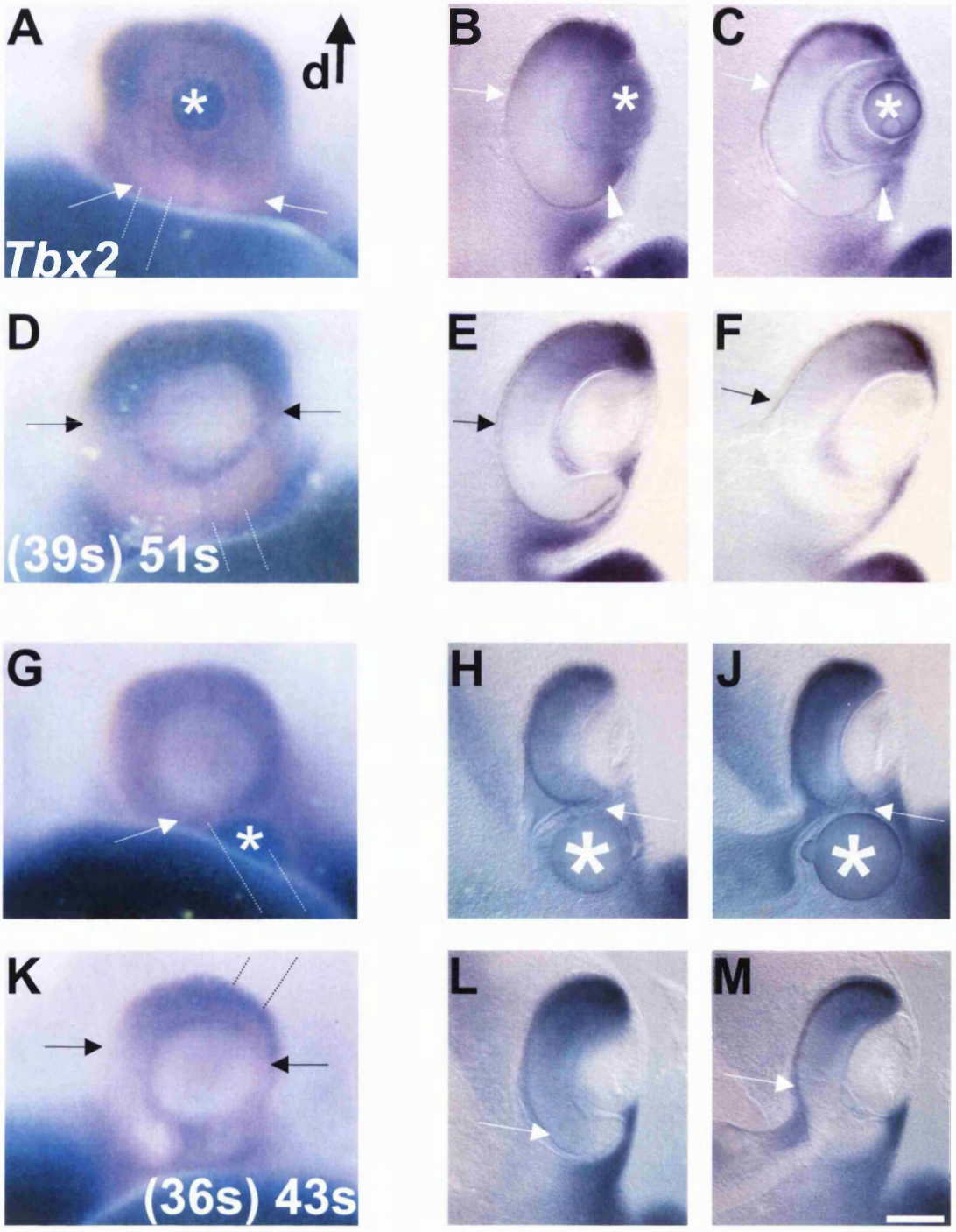

not convincingly reproduced (not shown) in other embryos. This variation may reflect the difficulty of BMP4 diffusion into the optic cup across the biological barriers (RPE, mesenchyme boundary) and may result from subtle variations in the positioning of the bead and tissue damage during surgery.

An effect on *Tbx5* expression was not seen after culture when BMP4-soaked beads were implanted into the ventral mesenchyme of E11.5 mouse embryos (not shown). No dramatic alterations in morphology that were attributable to the beads were seen in E11.5 cultures, though in several cases the operated eye was slightly smaller than the unoperated eye (compare **Fig. 5.7A** with **B** and **Fig. 5.9A** with **D**).

No effect was seen when beads at a 20 μgml^{-1} rather than a 113 μgml^{-1} BMP4 concentration were used (n = 4, not shown). Beads were soaked in BMP4 diluted in 0.1% BSA in PBS to a concentration of 20 μgml^{-1} BMP4 prior to implantation. These beads had no effect on Tbx5 expression (n = 4, not shown).

DISCUSSION

This chapter provides evidence that in the developing mouse eye, BMP4 regulates *omb*-related T-box genes. This is the first demonstration that the *omb*-related T-box genes are downstream targets of BMP signalling in the developing mouse eye. In *Drosophila*, BMP2/4 orthologue decapentaplegic (DPP) regulates *omb* in the *Drosophila* wing, leg and genital imaginal discs (Brook and Cohen, 1996; Grimm and Pflugfelder, 1996; Gorfinkiel *et al.*, 1999). Other work has shown that in the chick, BMP2 regulates *omb*-related T-box genes in the developing heart and limb (Rodriguez-Esteban *et al.*, 1999; Yamada *et al.*, 2000). In a recent study of the chick retina, *Bmp4* misexpression can induce *Tbx5* expression ventrally (Koshiba-Takeuchi *et al.*, 2000). Considered together, these data indicate that BMP2/4 regulation of *omb*-related T-box genes is an evolutionarily conserved pathway between vertebrates and invertebrates acting in the development and patterning of different tissues.

Table 5.2 shows the numbers of embryos for which results have been obtained in the present study. Implications of the findings of this work and further applications of the embryo culture system for analysis of eye development are discussed in this section.

5.5. *Tbx2* and *Tbx5* are regulated by BMP4 in the developing mouse optic vesicle

The ectopic induction of *Tbx2* and *Tbx5* expression in the mouse optic vesicle by BMP4 demonstrates that in the undifferentiated neuroepithelium of the optic vesicle, ectopic BMP4 activity is sufficient for *Tbx2* and *Tbx5* upregulation. Considered together with the normal co-expression of *Bmp4* with *Tbx2* and *Tbx5* in the dorsal retina (see **Chapter 4**), this study provides strong evidence that BMP4 regulates *Tbx2* and *Tbx5* during retinal development.

It is possible that the human recombinant BMP4 at the concentration used may have inductive properties absent in the endogenous mouse BMP4 source. However given the structural (96.8% amino acid homology, Entrez Protein accession nos. P12644 and P21275) and functional (Furuta and Hogan, 1998) similarities of mouse and human BMP4, this seems unlikely. The concentration used in the present study (113 μgml^{-1}) is far greater than the 1-5 μgml^{-1} used to rescue defective lens induction in *Bmp4* mutants (Furuta and Hogan, 1998), although these latter experiments were conducted using eye explants rather than whole embryo cultures. The concentration of BMP4 used in this chapter is similar to the 100 μgml^{-1} used in other examples of genetic regulation by BMP4 in mice (Kim *et al.*, 1998; Zhang *et al.*, 1999; Bei *et al.*, 2000; Zhang *et al.*, 2000). Although the human recombinant BMP4 used in these studies (and numerous ones in the chick) is all derived from the Genetics Institute (MA, USA), different batches can show substantial variation in their degree of biological activity (Y. P. Chen, personal communication). In this study a single batch of BMP4 was used and low concentrations (20 μgml^{-1} or lower) were found to have no effect.

Since (ectopic) BMP4 is sufficient for *Tbx2* and *Tbx5* expression in the temporal optic vesicle (where *Bmp4* is normally not expressed), it seems likely that endogenous *Bmp4* expression is necessary and sufficient for *Tbx2* and *Tbx5* expression in the optic vesicle. Thus the dorsal restriction of *Tbx2* and *Tbx5* expression in the developing

Table 5.2. T-box gene induction by BMP4 in the developing mouse retina

Ectopic *Tbx* expression after culture with beads	BSA-soaked beads		BMP4-soaked beads	
	Tbx5	*Tbx2*	*Tbx5*	*Tbx2*
E9.5 Culture with beads in temporal mesenchyme	0/2	-	3/3	2/2
E11.5 Culture with beads in ventral mesenchyme	-	0/1	0/3	1/3
E11.5 Culture with beads in the lens vesicle	-	0/3	0/1	5/7

This table shows the number of times ectopic *Tbx* gene expression was detected in the developing mouse eye after implantation of beads soaked in 0.1% BSA in PBS, or in 113 μg/ml BMP4.

retina could be explained by the dorsal restriction of *Bmp4* expression. It is a less straightforward suggestion than it first appears; other factors in the dorsal retina could potentially substitute for BMP4 activity. *Growth and differentiation factor 6* (*Gdf6*), a TGFβ family member, is co-expressed with *Bmp4* in the dorsal retina of *Xenopus* embryos (Hemmati-Brivanlou and Thomsen, 1995; Chang and Hemmati-Brivanlou, 1999). The zebrafish *Gdf6* orthologue *Radar* has also been detected in the dorsal retina (Rissi *et al.*, 1995; Davidson *et al.*, 1999). GDF6 can form heterodimers with BMP molecules and can bind Noggin with an affinity approaching that of BMP4 (Zimmerman *et al.*, 1996; Chang and Hemmati-Brivanlou, 1999). GDF6 may regulate T-box genes in partnership with BMP4, and could potentially do so alone. Currently no data exists on GDF6 in the mouse or chick retina.

The bead implantation and embryo culture system of the present study could be employed to examine whether *Tbx* gene expression was abolished by exogenously applied Noggin in the dorsal retina. Noggin is a diffusible molecule capable of blocking BMP4 activity (Zimmerman *et al.*, 1996; Chang *et al.*, 1999). *Noggin* expression has been detected in the dorsal E3 chick retina by some (Belecky-Adams and Adler, 2001; Trousse *et al.*, 2001), but not by others (Sakuta *et al.*, 2001). *Noggin* expression was not detected in the mouse optic vesicles (J. Holt and P. Ybot-Gonzalez, unpublished observations). Endogenous Noggin in the dorsal retina could act to modulate BMP4 activity. An excess of ectopic Noggin to this region might be expected to block completely the endogenous BMP4 signal. The abolition of *Tbx* expression would demonstrate that BMP4 (and other molecules such as GDF6 also responsive to Noggin) is necessary as well as sufficient for T-box gene induction in the dorsal retina.

Recently a new BMP4 antagonist has been identified in the chick called *Ventroptin*. Its expression in the developing retina was detected from the optic vesicle stage and in the optic cup *Ventroptin* mRNA was strongly detected in the ventral retina (Sakuta *et al.*, 2001). Like Noggin, Ventroptin binds BMP4 with high affinity. It does not bind other TGFβ superfamily members BMP7, TGFβ and Activin. Furthermore, *Ventroptin* over-expression in the chick eye can downregulate the expression of *Bmp4* (Sakuta *et al.*, 2001). Ventroptin could thus be used as an alternative to Noggin to inhibit BMP4, though as yet, unlike Noggin, no recombinant protein has been purified

for experimental use. The present study demonstrates that BMP4 can overcome the effect of any blocking factors or negative regulators that might normally suppress *Tbx* expression in ectopic areas of the retina.

It is not clear whether BMP4 regulation of *Tbx2* and *Tbx5* is achieved as a direct consequence of BMP4 signal transducers (such as SMAD complexes) binding to *Tbx* regulatory regions. Indirect regulation through the actions of an intermediate gene cannot be ruled out. If T-box genes are directly regulated by BMP4, a regulatory relationship might be predicted wherever co-expression of *Bmp4* with *Tbx2* and *Tbx5* occurred. It would be of interest to carry out a time course study of T-box response to BMP4. The current study cultured embryos for at least 16 hours. Shorter culture times could also be used and might provide evidence supporting direct regulation. In *Drosophila*, molecular dissection of cis-regulatory sequences of the *omb* T-box gene revealed a DPP response element (Sivasankaran *et al.*, 2000). This suggests *omb* is a direct target of DPP signalling. Furthermore, given the many similarities between *Drosophila* and vertebrates in genetic regulation, this finding supports the idea that *omb*-related T-box genes *Tbx2*, *Tbx3* and *Tbx5* might be direct targets of signalling by DPP homologue BMP4. The finding of SMAD binding sites in the regulatory elements of mouse T-box genes would help confirm this notion. If BMP4 signalling can directly induce *Tbx* genes, this does not rule out other factors being important for their expression. In the *Drosophila* wing, synergistic signalling by multiple ligands is required for *omb* expression to overcome the limitations imposed by DPP receptor concentration levels (Haerry *et al.*, 1998).

A recent study found that BMP4 promoted moderate levels of cell death in the chick retina (Trousse *et al.*, 2001). Many other studies have shown that BMP4 mediates apoptosis during the development of other systems (Graham *et al.*, 1994; Ganan *et al.*, 1996; Zou and Niswander, 1996; Zhao and Rivkees, 2000). Although levels of cell death were not analysed in the current study, this could be an interesting area of future work, particularly in view of the possible reduction in eye size seen following bead implantation and culture.

5.6. *Tbx2* and *Tbx5* respond differently to BMP4 in the developing mouse optic cup

In the developing E11.5 mouse optic cup, BMP4 beads induced *Tbx2*, but not *Tbx5*, expression when placed in the lens vesicle. This is in contrast to the earlier stage examined when the two T-box genes responded similarly to BMP4. Furthermore *Tbx2* was induced in the developing lens, a structure that does not normally express T-box genes and might not be expected to be capable of doing so.

Tbx2 induction in the neural retina

Tbx2, but not *Tbx5*, was upregulated in the ventral neural retina in response to BMP4. This suggests that BMP4 contributes to the continued expression of *Tbx2*, but not *Tbx5*, at later stages. It demonstrates that *Tbx2* and *Tbx5* may be regulated in different ways in the optic cup. These results bear similarities to those obtained in the chick heart: BMP2 was found to induce *Tbx2* and *Tbx3* but not *Tbx5* in the heart where both T-box genes are similarly expressed at early stages (Yamada *et al.*, 2000). In the chick limb bud, BMP2 can induce *Tbx2*, *Tbx3* (J.-P. Revelli, unpublished observations, cited in Yamada *et al.*, 2000) and *Tbx5* (Rodriguez-Esteban *et al.*, 1999). This shows that *Tbx5* can respond differently from *Tbx2* and *Tbx3* to BMPs in a tissue dependent manner. *Tbx3*, expressed in the dorsal mouse optic vesicle and optic cup (Chapman *et al.*, 1996; Sowden *et al.*, 2001), is also likely to be regulated by BMP4 in the developing retina.

The induction of *Tbx2* but not *Tbx5* in the retina may be caused by reduced sensitivity, rather **than** a lack of responsiveness, of *Tbx5* to BMP4. *Tbx5* and *Bmp4* expression is co-incident whereas *Tbx2* is expressed in a broader domain in the developing retina (**Chapter 4**). The extent of up-regulation in response to BMP4 was greater for *Tbx2* than for *Tbx5* in the optic vesicle (see **5.3.** above). These facts could be explained by a greater responsiveness of *Tbx2* to BMP4 in general. In this model *Tbx5* expression depends on the high levels of BMP4 close to its source (be it the dorsal expression domain or the bead), while *Tbx2* is induced in a wider area by lower levels of diffusing BMP4. Thus *Tbx5* is insensitive to the levels of BMP4 that reach the ventral neural retina from the bead in the lens vesicle, while *Tbx2* is not. *Ventroptin* encodes a novel BMP4 antagonist and is expressed in the ventral (and nasal) retina of the chick

following formation of the optic cup (Sakuta *et al.*, 2001). Mouse Ventroptin homologues in the ventral optic cup but not the temporal optic vesicle would also account for the more profound induction of *Tbx* genes by BMP4 observed in the latter.

Alternatively (or even additionally) BMP4 may maintain *Tbx5* expression in the dorsal optic cup but be unable to induce ectopic expression because of inhibitory factors that suppress *Tbx5* but not *Tbx2* expression. In **Chapter 4** the expression domains of *Tbx2* and *Tbx5* were compared with the transcription factors that pattern the early optic cup and demarcate retinal territories. It seems likely that the factors that regulate ventral expression of *Vax2* may also repress expression of *Tbx5*. Indeed misexpression of *Vax2* itself in dorsal chick retina will repress *Tbx5* expression (Schulte *et al.*, 1999).

It is not clear why only a low level of successful *Tbx2* induction in the retina by BMP4-soaked beads placed in the ventral peri-ocular mesenchyme was achieved. Lack of *Tbx2* (or *Tbx5*) upregulation following bead placement in the ventral peri-ocular mesenchyme may be due to a barrier to BMP4 diffusion into the optic cup that is not present in the optic vesicle. In the developing optic vesicle, the undifferentiated extra-ocular mesenchyme is essential for retinal pigmented epithelium (RPE) development (Fuhrmann *et al.*, 2000). This regulation is likely achieved through secreted Activin. Activin can substitute for extra-ocular mesenchyme to promote RPE development in the proximal optic vesicle (Fuhrmann *et al.*, 2000). Following formation of the optic cup, such interactions between the developing mesenchymal tissues and the eye are not known to occur. A barrier to diffusion of morphogens at the optic cup stage may exist to prevent disruption of eye development. Such a barrier could serve to allow retinal patterning and development to occur without interference from the inductive events of mesenchymal differentiation, and *vice versa*. More simply, BMP4 from beads in the ventral peri-ocular mesenchyme may be more affected by Ventroptin than BMP4 from beads in the lens vesicle. Ventroptin homologues in the ventral mouse RPE would provide an added level of blockage to BMP4 molecules diffusing from outside the optic cup compared with diffusion from the lens vesicle.

It is interesting that *Tbx2* and *Tbx5* were apparently not upregulated in the ventral peri-ocular mesenchyme by BMP4-soaked beads placed there at E9.5 or E11. *Tbx2* is normally expressed in this ventral location in the maxillary mesenchyme whereas *Tbx5* is not normally expressed at these sites (**Chapter 3**). This suggests that the regulation of *Tbx2* is different in this tissue to that in the developing eye.

Tbx2 induction in the developing lens

The induction of *Tbx2* expression in the lens vesicle shows that BMP4 is the only missing ingredient for *Tbx2* induction in the normal developing lens. *Tbx2* was not induced by BMP4 in the presumptive lens placode (the surface ectoderm overlying the optic vesicles at E9.5), though this may be because the bead was never positioned close enough this to this tissue. Even so, BMP4 would not be expected to induce *Tbx2* in the surface ectoderm. Whereas both *Bmp4* and *Tbx2* are expressed in the dorsal optic vesicle, *Bmp4* is expressed alone in the surface ectoderm without any sign of *Tbx2* expression (**Chapter 4**). *Bmp4* transcripts can be detected in the surface ectoderm right up to formation of the lens placode, when *Bmp4* is sharply downregulated (**Chapter 4**; Furuta and Hogan, 1998).

Which molecule(s) allow *Tbx2* induction in response to BMP4 in the developing lens but not in the prospective lens placode? Such a molecule or molecules might provide the competence for the *Tbx2* upregulation seen in the neural retina and could be expected to be present in the optic vesicle and the optic cup, as well as in the lens. Alternatively the removal of inhibiting factors in the developing lens to allow transcription of lens specific genes could inadvertently permit *Tbx2* induction in response to BMP4.

5.7. Ectopic BMP4 seems to alter mouse eye morphogenesis

One important question that has not been conclusively answered in this study is that of whether ectopic BMP4 can alter eye morphogenesis. Recent evidence in the chick shows BMP4 can promote proliferation and cell death in the retina (Trousse *et al.*, 2001). This is supported by new findings with BMP4-soaked beads and *Noggin* misexpression in the developing chick prosencephalon (Ohkubo *et al.*, 2002). Both ectopic BMP4 and misexpression of *Noggin* caused hypoplasia of the developing telecephalic and optic vesicles. However, BMP4-induced hypoplasia seemed to be

predominantly mediated by apoptosis, while hypoplasia due to *Noggin* misexpression was associated only with a decrease in proliferating cells (Ohkubo *et al.*, 2002). In the optic vesicles of 22- to 25-somite mouse embryos, the dorsal retina appears substantially smaller in the *Bmp4* null mutant (see Fig. 3 in Furuta and Hogan, 1998), suggesting mouse *Bmp4* may also promote proliferation in the eye. Mouse *Bmp4* electroporated into ventral chick optic cups produce eyes with deformities of ventral eye structures that seem larger and more rounded (Koshiba-Takeuchi *et al.*, 2000). In the present study, cultures at E9.5 show subtle effects of BMP4 on eye morphology and at E11.5 BMP4 bead-implanted eyes appeared to be smaller than the unoperated eyes. This work has recently been followed up and a reduction in eye size along the dorso-ventral, but not the naso-temporal, axis has been confirmed in the E11.5 cultures (H. Behesti and J. Sowden, unpublished).

It will be interesting in future work to culture embryos with beads at E10.5, when optic cup formation is just about to occur. Physical alterations caused by BMP4 would be expected to be far more apparent during this critical phase of eye morphogenesis, when an optic cup is being forged from the optic vesicle. Proliferation could be examined in the cultures with BrdU labelling or with the analysis of markers of proliferation such as H3 or PCNA. TUNEL could be used to look for BMP4-induced apoptosis. T-box genes could mediate the proliferative effects of BMP4. In the current study, *Tbx2* and *Tbx5* were consistently observed in the ventricular region of the optic vesicle, the site of proliferating neuroblasts (Dyer and Cepko, 2001). When *Tbx5* was electroporated into the eye vesicles of stage 8 chick embryos, optic cups formed that were elongated along the dorsal and ventral axis (Koshiba-Takeuchi *et al.*, 2000). *Tbx5* deficiency is known to cause severe hypoplasia in the mouse heart (Bruneau *et al.*, 2001), though overexpression studies in transgenic chick hearts suggest that *Tbx5* may act as a cellular arrest signal (Hatcher *et al.*, 2001).

5.8. Conclusion

This chapter has demonstrated that *Tbx2* and *Tbx5* are regulated by BMP4 in the developing mouse retina. *Tbx2* was shown to be more responsive to BMP4 than *Tbx5*, which could not be induced in the optic cup. Indeed BMP4 was found to induce *Tbx2* even in the developing lens vesicle, a structure normally devoid of both *Tbx2* and

Bmp4 expression. *Tbx2* was not upregulated in the ventral peri-ocular mesenchyme however, a site of normal *Tbx2* expression.

Another conclusion that must emerge from this work is the validity of the embryo culture method as a manipulable model of *in vivo* mouse eye development. This has more applications both in and outside of this study as it leaves the mouse embryo accessible to manipulation throughout early eye morphogenesis, and during the development of other tissues. Future work with this system has the potential to further clarify the precise nature of the regulatory network governing eye development in the mouse.

CHAPTER 6

Transgenic misexpression of *Tbx5* in the developing mouse retina

INTRODUCTION

Chapter 3 demonstrated that *TBX5*/*Tbx5* is asymmetrically expressed within the human and mouse eye in the dorsal retina throughout its formation and that of its projections. This conserved expression in mammals suggested a role for *TBX5*/*Tbx5* in the regulation of genes that provide dorso-ventral identity to the retina. This is important for morphogenesis, axon guidance and regional variation in cellular distribution. One good way to test this hypothesis would be to misexpress *TBX5*/*Tbx5* in ventral parts of the embryonic eye and then look for any abnormalities in shape, gene expression and topographic mapping that might arise. Indeed such a strategy has recently been used with *Tbx5* during chick eye development (Koshiba-Takeuchi *et al.*, 2000). A retroviral construct designed to express chick *Tbx5* was injected into the early chick eye during development. Widespread misexpression in the ventral eye dorsalised the ventral retina and its projections (Koshiba-Takeuchi *et al.*, 2000). The chick is a convenient system for developmental misexpression studies because it is very accessible. Operations can be performed on the developing chick with relative ease and minimal disruption by cutting a small window in the eggshell. The use of viruses in the chick offers a quick method to test the effects of ectopic gene expression. However, using this method it is difficult to consistently misexpress a viral construct in the same group of cells. I elected to use a different approach in order to investigate the role of asymmetric T-box gene expression during the development of the mouse visual system.

Mouse transgenesis and the establishment of lines of transgenic mice, compared with the chick system, offers a significant advantage in that it consistently gives clearly defined ectopic expression in animals that are almost identical genetically. It also provides the possibility of further analysis through the crossing of mice with other transgenic/mutant mouse strains. Furthermore, this method allows effective genetic misexpression in mammals and thus may be of greater relevance to human biology. This is of particular importance in view of the difference between the chick and mammalian visual systems, most notably the monocular vision of the chick compared with the binocular mammalian visual system.

This chapter is concerned with the preparation of a construct for the transgenic misexpression of *Tbx5* in ventral retina during mouse eye development. The transgene construct described in this chapter uses the α-element and p0 promoter of the *Pax6* gene (α-p0) to drive ectopic *Tbx5* expression in specific regions of the eye. These regulatory elements direct reporter gene expression first in the nasal and temporal developing neural retina at embryonic days 9 to 10.5 (E9-E10.5). α-p0 activity has spread into the ventral retina by E12.5-E13.5 and remains in all but the dorsal-most retina in the mature eye at postnatal day 1 (P1), when it is also active in the iris. Up to P10 at least, α-p0 activity is excluded from the central (proximal) retina and includes all cellular layers of the peripheral/distal retina (Kammandel *et al.*, 1999; Marquardt *et al.*, 2001).

This transgene is therefore expected to extend the normally dorsal expression of *Tbx5* into ventral retina during mouse retinal development. If mouse *Tbx5* plays a prominent role in dorso-ventral patterning then the expression of other dorso-ventral markers may be altered. In the chick optic cup, misexpression of *Tbx5* led to a downregulation of ventral transcription factor genes *Vax* and *Pax2*. Ventral patterning molecules *Ephb2* and *Ephb3* were downregulated whilst their dorsal partners *Efnb1* and *Efnb2* were upregulated and ventral RGC projections to the tectum became dorsalised (Koshiba-Takeuchi *et al.*, 2000). In mice, loss of ventral *Ephb2* and *Ephb3* expression leads to errors in RGC axon guidance to the optic disc, particularly affecting dorsal axons (Birgbauer *et al.*, 2000). The aim of my experiment is to see whether the expression of these genes is similarly disrupted following *Tbx5* misexpression in the ventral mouse retina, and if so whether defective axon guidance of ventral and of dorsal RGC axons occurs to the optic disc or to central targets. Establishment of a transgenic mouse line misexpressing *Tbx5* will allow analysis of projection patterns at different points during development.

A disruption of the retinotopic map in the superior colliculus (SC) could potentially affect other sensory modalities. Visual map development in superficial layers of the ferret SC guides the development of the auditory representation in deeper layers (King *et al.*, 1988). Dorsal and ventral retina-derived axons are segregated in the optic nerve and tract (Chan and Chung, 1999). It would thus be of interest to examine topography within the optic nerve and tract of *Tbx5* misexpressing transgenic mice. Patterning

along the dorso-ventral axis of the retina is not entirely divorced from that along the naso-temporal axis (Feldheim *et al.*, 2000; Sakuta *et al.*, 2001). It might be of interest to examine the expression of naso-temporal markers in *Tbx5* misexpressing mice such as forkhead genes *Foxg1* and *Foxd2* to see if the two longitudinal axes of the retina interact at the level of transcription factor gene expression.

Birds and fish have monocular vision (*i.e.* the left visual field is viewed with the left eye and the right visual field with the right eye), whilst mammals (and frogs) have binocular vision (both visual fields are represented by information from both eyes). Axons from both eyes enter the ipsilateral or contralateral optic tract so that RGCs providing information about the right visual field project to the left brain and those receiving from the left visual field project to the right brain. Species with monocular vision project all their RGC axons to the contralateral brain. Ipsilaterally projecting retinal axons in mice are derived from a small population of RGCs in the ventro-temporal retina (Drager and Olsen, 1980). A similar population project ipsilaterally in *Xenopus*, where ipsilateral routing of axons at the optic chiasm is regulated by EFNB proteins (Nakagawa *et al.*, 2000). If *Tbx5* misexpression were to disrupt the dorso-ventral asymmetry of *Ephb* and *Efnb* expression in the mouse retina as in the chick (Koshiba-Takeuchi *et al.*, 2000) then defects in the ipsilateral projection might be expected.

The ultimate aims of the transgenic study are to examine the consequences of misexpressing *Tbx5* for:

(1) the expression of dorso-ventral markers *Tbx2*, *Tbx3*, *Vax2*, *Pax2*, *Ephb2*, *Ephb3*, *Efnb1* and *Efnb2* as well as naso-temporal markers such as *Foxg1* and *Foxd2*.
(2) RGC axon guidance to the optic disc and intra-retinal connectivity.
(3) topographic visual (and auditory) mapping to the SC and visual mapping to other retino-recipient areas such as the lateral geniculate nucleus (LGN).
(4) the development of the ipsilateral retinal projection.
(5) topographic order within the optic nerve and tract.

My primary aim was to build a construct that could misexpress *Tbx5* in the developing retina, inject it into mouse embryos and establish a line of trangene-expressing mice for future analyses. The work undertaken to achieve this aim is detailed in this

chapter. Isolation of fertilised eggs for microinjection and injection of DNA was performed by Katie Gardener in the transgenic facility at the Institute of Child Health. All other aspects of the work outlined I carried out myself.

RESULTS

6.1. *Tbx5* is incorporated into *α-p0-ires-gfp-intron-pA*

A DNA construct was built for microinjection into mouse zygotes to generate transgenic mice with the construct incorporated into their genome. The construct was based on one received from Peter Gruss, Germany. This consisted of the α-p0; an internal ribosomal entry site (ires); the *green fluorescent protein* (*gfp*) gene; the small t-intron from simian virus 40 (to increase efficiency of RNA processing, see Huang and Gorman, 1990); and a poly-A tail (essential for RNA processing); all contained within the pSL1170 plasmid vector. A modified form of the construct received from Germany has been used in mice leading to successful transcription and translation of the *gfp* gene (Marquardt *et al.*, 2001).

A full-length *Tbx5* cDNA isolated in our laboratory from a mouse E15 retinal cDNA library in the pBK-CMV vector was used to prepare the transgene construct. The coding region of the mouse *Tbx5* cDNA was inserted into the *α-p0-ires-gfp-intron-pA* plasmid between the p0 region and the ires. This would enable simultaneous expression of *gfp* and *Tbx5* driven by the α-element and p0 promoter of *Pax6*. My initial cloning strategy was to utilise a *Nru*I site and a *Sac*II site present in the polylinker between the p0 and the ires. The aim was to insert the *Tbx5* cDNA using a blunted 5' site and a 3' downstream *Sac*II site. An initial construct ('faulty' construct 1) was generated that from restriction digests and sequencing of the cDNA insert appeared to contain the correctly inserted *Tbx5* cDNA. Several attempts to generate founder transgenic mice with this original construct were made (see **Table 6.1**) before discovery of a small deletion through sequencing. The construct contained a 105 base pair deletion in a critical region of the p0 promoter. The failure of this cloning strategy was explained by the discovery of a second *Sac*II site in a linker region immediately 3' to the p0.

Table 6.1. Summary of results following micro-injection of a 'faulty' construct 1 (*α-p0-Tbx5-ires-gfp-intron-pA*)

DNA batch	Injected DNA concentration	No. foster mothers	Results	PCR detection of transgene
1	~10 $ng\mu l^{-1}$	16	embryos die *in utero*	No transgenics (13 embryos)
2	~2 $ng\mu l^{-1}$	6	20 pups	2 x transgenics (1 male, 1 dead)
3	~2 $ng\mu l^{-1}$	3	15 pups	No transgenics

Each foster mother received 10-20 injected eggs. A single surviving transgenic founder mouse (male) was obtained from 35 pups. This was mated with a non-transgenic female mouse. 9 pups were born and found to be non-transgenic before cessation of work to focus on a revised *α-p0-Tbx5-ires-gfp-intron-pA* generated with an alternate and ultimately successful cloning strategy.

In the new strategy, to enable precise excision and insertion of the *Tbx5* cDNA, it was first necessary to manipulate a *Tbx5* cDNA clone so that the *Tbx5* coding region was closely flanked by *Sac*II restriction enzyme sites. Site-directed mutagenesis was performed to create a *Sac*II site immediately downstream of the stop codon. The *Tbx5* cDNA was then sub-cloned into the pBII-KS vector to provide an upstream *Sac*II site. The two *Sac*II sites were then utilised to excise the *Tbx5* coding region. This was inserted into the *Sac*II sites contained between the p0 and the ires of the *α-p0-ires-gfp-intron-pA* construct from Peter Gruss. The whole sub-cloning procedure is outlined in **Fig. 6.1**.

Following completion of the construct, the *Tbx5* insert was sequenced entirely, to ensure correct orientation and an absence of mistakes. The leader sequence between the transcriptional start site of the p0 promoter and the start codon (ATG) for *Tbx5* was sequenced and examined to build confidence in the biological viability of the construct. This leader sequence is 260 base pairs long and is composed of various linkers from different cloning steps (**Fig. 6.2**). The *Tbx5* messenger RNA transcribed from the construct will thus contain an artificially long 5' untranslated region (utr), composed of unusual genetic elements that could potentially disrupt translation. The sequence of this region was examined for rogue start codons upstream of the true *Tbx5* start codon. Three were identified; two of these were found to belong to the endogenous *Tbx5* 5' utr. One of the endogenous ATGs was followed by an in-frame stop codon before the genuine start codon. In eukaryotes, the genetic context of the ATG is very important for initiation and only one coding region will be read (Lewin, 1994). All the start codons were compared with the Kozak consensus, the favoured sequence flanking an 'ATG' sequence essential for the recognition of it as a start codon. The Kozak consensus was determined by examination of a multitude of vertebrate messenger RNAs (Kozak, 1987). The presence of an 'ATG' start codon upstream of the true start codon for *Tbx5* with a genetic context approximating that of the Kozak consensus would arouse fears of inappropriate translation. As it was, the genetic context of the rogue ATG's approximated only very loosely to the Kozak consensus while the true start codon approximated very well (**Fig. 6.2**). The entire sequence of the *Tbx5* cDNA and flanking regions in the construct is shown in **Fig. 6.3**.

Figure 6.1

The α-p0-ires-gfp-intron-pA construct (in the pSL1170 plasmid vector) was received from Peter Gruss, Germany. This figure shows how I set about inserting the coding region of the *Tbx5* cDNA between the *Pax6* p0 promoter and the internal ribosomal entry site (ires).

A The *Tbx5* cDNA was isolated from an E15 mouse retina cDNA library in the pBK-CMV phagemid vector, inserted into *Eco*RI. The pBK-CMV vector with *Tbx5* was isolated from a large-scale preparation of *Escherichia.coli*. The *Eco*RI sites are marked. Restriction enzyme sites used for subcloning are also marked: *Bam*HI (**brown** band), *Sac*II (**red** band) and *Xho*I (**black** band).

B A primer pair complementary to the area across the end of the *Tbx5* coding region but including a mutation immediately 3' to the TAA stop codon (the beginning of the 3' untranslated region or utr) were designed and synthesised (see below). 3 bases of 34 (highlighted in yellow, below) were altered in each mutant primer to create a *Sac*II site (ccgcgg) immediately 3' to the stop codon (highlighted in green, below). New vectors containing the mutation were synthesised by a modified PCR using the mutant primers (site-directed mutagenesis). The original vectors were selectively destroyed by digestion with *Dpn*I, a restriction enzyme specific for methylated DNA (DNA synthesised by *Escherichia coli* is methylated; by PCR it is not). *Sac*II, **red** bands in figure.

Forward primer: GGAGTGAGAATAGCTAAccGCgGACCTGTGCCAG

Reverse primer: CTGGCACAGGTCcGCggTTAGCTATTCTCACTCC

C After sequencing the *Tbx5* coding region to check for errors following PCR, the 3' utr was excised by digestion with *Sac*II. The vector backbone and *Tbx5* coding region was isolated by gel extraction and then ligated to give the *Tbx5* gene with a single *Sac*II site in place of the 3' utr, in the pBK-CMV vector. *Bam*HI, **brown** bands; *Sac*II, **red** bands; *Xho*I, **black** bands.

D In order to place a *Sac*II site upstream of the *Tbx5* gene, the gene was transferred into the pBII-KS vector. pBK-CMV/*Tbx5* was cut with *Bam*HI and *Xho*I, as was pBII-KS. The *Tbx5* insert and the pBII-KS vector backbone were gel extracted and ligated together. This produced a vector with a *Sac*II site upstream of *Tbx5*, in the pBII-KS multiple cloning site, as well as one immediately downstream of the *Tbx5* stop codon. *Bam*HI, **brown** bands; *Sac*II, **red** bands; *Xho*I, **black** bands.

E *Sac*II was used to excise the *Tbx5* coding region (and 5' utr) from the pBII-KS plasmid vector and to linearise the pSL1170 vector and *α-p0-ires-gfp-intron-pA* construct. Purified fragments were obtained by gel extraction and ligated together to insert the gene. The completed construct could then be sequenced to check for errors and correct *Tbx5* orientation. *Sac*II, **red** bands.

Building of
α-p0-Tbx5-ires-gfp-intron-pA

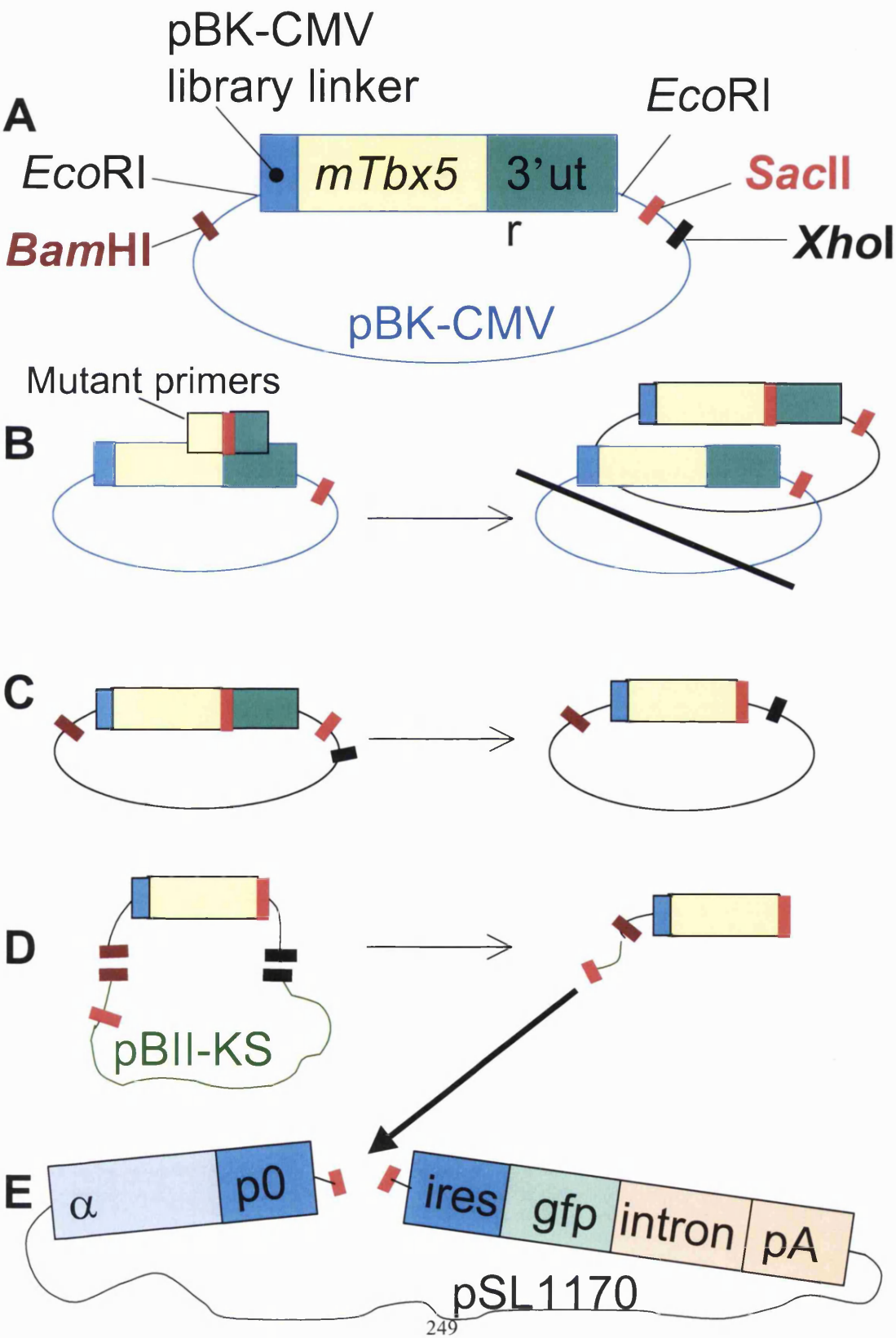

Figure 6.2

Sequencing the completed *α-p0-Tbx5-ires-gfp-intron-pA* construct.

A The complete *α-p0-Tbx5-ires-gfp-intron-pA* construct is displayed here within the pSL1170 plasmid vector.

B The region around the *Tbx5* gene is shown in close-up and the location of sites for sense and antisense primers are illustrated with black arrows (labelled **F1-6** and **R1-3**). These have been utilised to sequence the entire region shown in **B**. This DNA sequence is shown in **Fig. 6.3**. *Sac*II sites, **red** lines.

C The 5' leader sequence between the *Pax6* p0 promoter and the *Tbx5* start codon is shown in close-up and has been examined in more detail. There are 260 bases between the transcriptional start site of the *Pax6* p0 promoter and the *Tbx5* start codon (ATG). This leader region (depicted) contains a fragment of the *LacZ* gene and a piece of plasmid linker derived from the original *α-p0-ires-gfp-intron-pA* construct. Then comes the *Sac*II site (indicated by **red** line), a small piece of pBII-KS linker, followed by a piece of pBK-CMV linker and the pBK-CMV library linker. After this comes the 5' untranslated region (utr) of the *Tbx5* gene. Three ATG start codons (**1-3**) were identified upstream of the true start ATG (**4**) of the *Tbx5* gene (see also **Fig. 3A, B**). The genetic context of these ATGs was compared with the Kozak consensus (see **1-4** below). This is the favoured sequence surrounding an ATG so that it may be recognised as a start codon.

The Kozak consensus: (GCC)GCC(A/G)CCATGG. Regions flanking the ATG (highlighted in yellow) facilitate transcription, other regions (highlighted in green) are less influential and more varied.

2 GATCCTAGAATGC, poor homology to the Kozak consensus.

3 AGAGACACCATGC, reasonable but imperfect approximation to Kozak consensus. An in-frame TAA stop codon follows 34 bases later.

4 CGGTGGCGAATGC, no homology to the Kozak consensus.

5 CTGCGCACCATGG, true *Tbx5* start codon, good approximation to Kozak consensus.

Analysis of the *Tbx5* leader in *α-p0-Tbx5-ires-gfp-intron-pA*

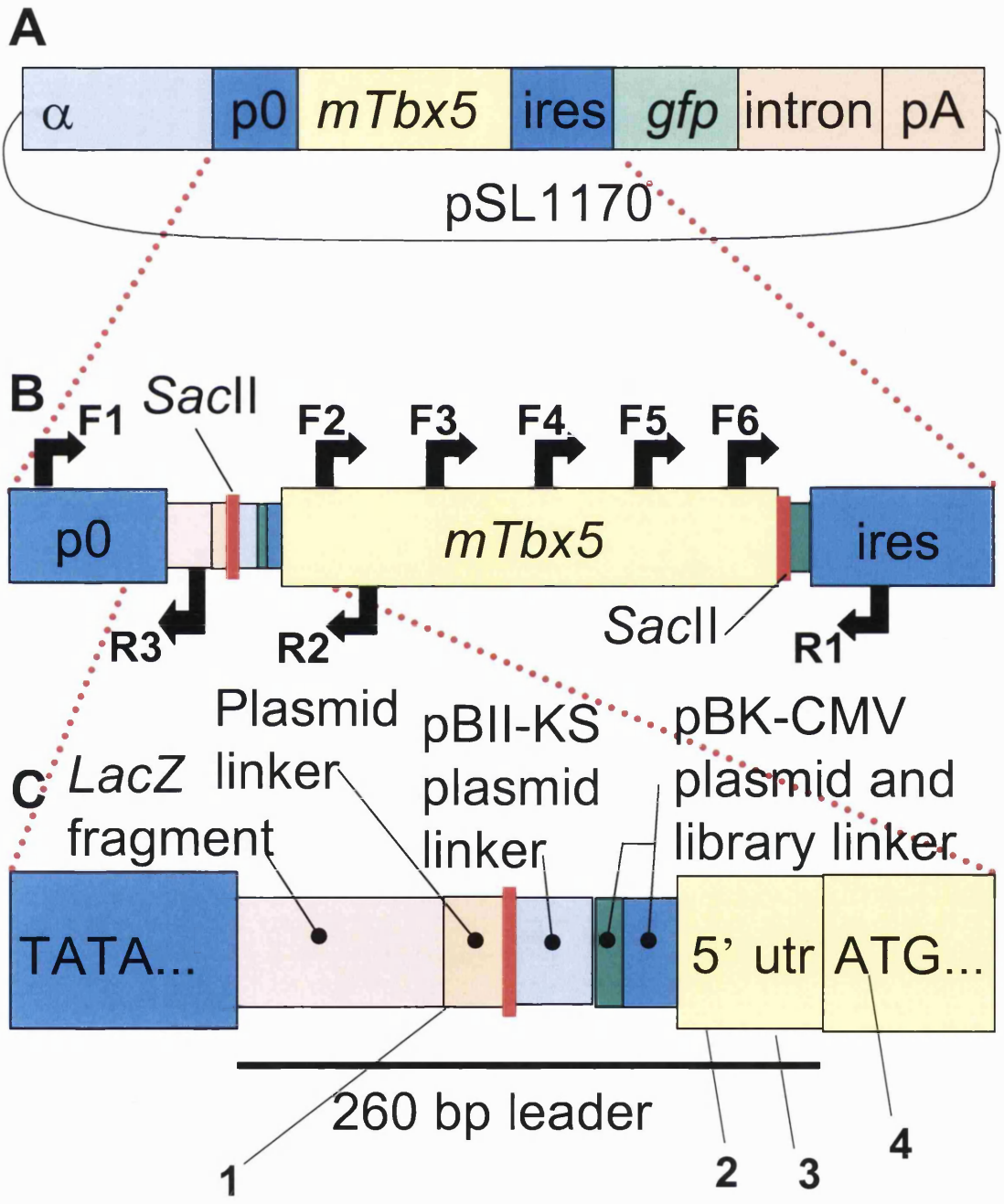

Figure 6.3

The rough locations of the primer sites for sequencing are shown in **Fig 6.2B**. The primers used are listed here:

Forward primers:		*Reverse primers:*	
GCCTAAGAGCAAGTACAGTGGG --	**F1**	CAAACGCACACCGGCCTTATTC --	**R1**
GAGCCCGACATCCTAGCTCC ----	**F2**	GGAACTTCAGCCACAGTTCACG --	**R2**
ACTCAGCGAGGCAATATGGT ----	**F3**	CTCCTCCATCCTAAGAGTCTTC --	**R3**
GGGCAGTGATGACCTGGAGTTA --	**F4**		
GGCCTGAGTACCTCTTACAGGA --	**F5**		
CCCCCAGAGTTTCTCTACACTC --	**F6**		

The sequence of the *Pax6* p0 promoter, the linker sequences and 5' untranslated region (utr) of the *Tbx5* cDNA, the *Tbx5* coding region itself, and the beginning of the internal ribosomal entry site (ires) are shown (**A-C**):

A The p0 promoter sequence is shown from the *Xba*I site (**blue**) that joins it to the α-element. In **red** are CCAAT and ATATTAA boxes and the bold '**A**' shows the transcriptional start site. The region from the transcriptional start site is the beginning of the *LacZ* gene. After 68 bases is a short piece of plasmid linker joined by blunted *Bgl*I (**magenta**) and *Xba*I (**blue**) sites. This contains the first **ATG** and the *Sac*II site to which the manipulated *Tbx5* cDNA was inserted.

B The manipulated *Tbx5* insert, flanked by *Sac*II sites (**cyan**), is shown. The *Sac*II site begins a piece of pBII-KS plasmid linker that joins the pBK-CMV plasmid linker at the *Bam*HI site (**green**). The *Eco*RI site (**orange**) begins the pBK-CMV library linker and the start of the *Tbx5* cDNA is an '**A**' (in bold). Start (**ATG**) and the stop (**TAA**) codons are marked.

C A piece of plasmid linker joins the *Sac*II site to the *Eco*RI site (**orange**). From this begins the ires, of which the first 79 bases are shown.

The sequence of *Tbx5* within *α-p0-Tbx5-ires-gfp-intron-pA*

A

TCTAGAGAAC CTAAAGGCCC AGGCTACGGG GTCACTTAGA GAGATAACTG GCTGGCCTAA
GAGCAAGTAC AGTGGGATCC GCGTACTGGA TGGCCCCTGA ACTCCGCAGG ACCTGTTTAC
TTGAAAGTAG GGGGAGGGGG GCTTAAGCCG AACCTCAGGG AGGACAATAC CAGCCAGAGG
CAGGCTGGGC GTGTGCAGTT ACCGGCCAGA CCCCTGAAGA CTCTTAGGAT GGAGGAGTCA
GACTCTGCCT GAAGAGAGGG AGTCTCCCGC CGGGCCAGAG AGCTAATCTG CCGAGCTGAA
CCCAACTCTG GCCGCCGTGA CGTCATCCGC GCCCGGCAAC CAATGAGGGC ATTGCTGGCG
TGGATATTAA GGAAAGTTAG CGCCTGCCGG AGCACCCTCT TTTCTTATCG TTGACATTTA
AACTCTGGGC AGGTCCTCGC GTAGAACCCG GTTGTCAGAT CCTAGAATGC ATTCCGC

B

GGTGGCGGCC GCTCTAGAAC TAGTGGATCC AAAGAATTCG GCACGAGAGA GACACCATGC
CTGCACCCCC ACCTGGCCTC CGGCTTTCCT GCTAAGAAGA AGAAGGGCGG TGGCGAATGC
ATCCCCCTGT TCAGAGCGAG AATAGAACCT CGCGCGGGCA CAGGAACCCC TGCGCACCAT
GGCCGATACA GATGAAGGCT TTGGCCTGGC GCGCACGCCT CTGGAGCCTG ATTCCCAAGA
CAGGTCTTGC GATTCGAAAC CTGAGAGTGC TCTGGGGGCT CCCAGCAAGT CTCCATCATC
CCCGCAGGCT GCCTTCACCC AGCAGGGCAT GGAAGGAATC AAGGTGTTTC TTCATGAACG
TGAACTGTGG CTGAAGTTCC ACGAAGTGGG CACAGAGATG ATCATCACCA AGGCAGGGAG
GAGAATGTTT CCTAGTTACA AAGTGAAGGT GACTGGCCTT AATCCCAAAA CGAAGTATAT
TCTTCTCATG GATATTGTTC CCGCAGACGA CCACAGATAT AAATTTGCTG ATAACAAATG
GTCCGTAACT GGCAAAGCAG AGCCTGCCAT GCCGGGGCGC CTTTATGTGC ACCCGGACTC

CCCAGCAACC GGAGCCCACT GGATGCGACA ACTTGTCTCC TTCCAGAAGC TCAAACTCAC
CAACAACCAC CTGGACCCGT TTGGACACAT TATCCTGAAC TCCATGCACA AATACCAGCC
CCGATTACAC ATCGTGAAAG CAGACGAAAA TAATGGGTTC GGTTCAAAGA ACACTGCGTT
TTGCACCCAC GTCTTCCCGG AGACAGCTTT TATCGCTGTG ACTTCGTACC AGAATCACAA
GATCACACAG CTGAAAATTG AGAACAACCC CTTCGCCAAA GGCTTTCGGG GCAGTGATGA
CCTGGAGTTA CACAGGATGT CTCGGATGCA AAGTAAAGAG TATCCTGTGG TTCCCAGGAG
CACAGTGAGG CACAAAGTCA CCTCCAACCA CAGCCCCTTC AGCAGCGAGA CCCGAGCTCT
CTCCACCTCA TCCAATTTAG GGTCCCAGTA CCAGTGTGAG AATGGTGTCT CTGGCCCCTC
CCAGGACCTT CTGCCCCCAC CTAACCCATA CCCACTGGCC CAGGAGCACA GCCAAATTTA
CCACTGTACC AAGAGGAAAG ATGAGGAATG TTCCAGCACG GAGCACCCCT ATAAGAAGCC

GTACATGGAG ACATCCCCCA GCGAGGAAGA CACCTTCTAT CGCTCGGGCT ACCCCCAGCA
GCAGGGCCTG AGTACCTCTT ACAGGACAGA GTCGGCCCAG CGGCAGGCCT GCATGTATGC
CAGCTCCGCT CCCCCCAGCG AGCCCGTGCC TAGCCTGGAG GACATCAGCT GTAACACATG
GCCCAGCATG CCCTCCTATA GCAGCTGTAC CGTCACCACC GTGCAGCCCA TGGACCGTCT
TCCCTACCAG CACTTCTCCG CTCATTTCAC CTCGGGGCCC CTGGTCCCTC GGTTGGCTGG
CATGGCCAAC CATGGTTCTC CCCAGCTCGG CGAAGGGATG TTTCAGCACC AGACCTCAGT
GGCCCATCAG CCTGTGGTCA GGCAGTGCGG GCCTCAGACT GGCCTTCAGT CTCCGGGCGG
CCTCCAGCCC CCAGAGTTTC TCTACACTCA CGGCGTGCCC AGGACCCTGT CCCCCCATCA
GTATCACTCG GTACACGGCG TCGGCATGGT GCCAGAGTGG AGTGAGAATA GCTAACCGC

C

GGTGGCGGCC GAGGTCGACG GTATCGATAA GCTTGATATC GAATTCCGCC CCCCCCCCTC
TCCCTCCCCC CCCCCTAACG TTACTGGCCG AAGCCGCTTG GAATAAGGCC GGTGTGCGTT

6.2. *α-p0-Tbx5-ires-gfp-intron-pA* is incorporated into transgenic mice

The *α-p0-Tbx5-ires-gfp-intron-pA* construct was excised from the pSL1170 vector using *Nhe*I and *Xho*I restriction enzymes. The linearised and isolated construct was gel purified after electrophoresis and diluted to 2-10 ng/μl in injection buffer made with embryo-tested water. If the DNA concentration is too high, the embryos lyse and cannot be implanted in pseudopregnant female mice. If the concentration is too low then the DNA will not be incorporated into the mouse genome (Hogan *et al.*, 1994). Gel electrophoresis with at least 3 different construct dilutions and 2 dilutions of a quantifiable DNA ladder was performed. Construct concentrations were determined by comparison of band intensities on the gel photograph.

In an effort to quickly determine the activity of the construct and to generate transient transgenic embryos, injected embryos were removed from pregnant foster mothers at approximately the 25-somite stage of development. *α-p0-Tbx5-ires-gfp-intron-pA* was injected into mouse embryos at an initial concentration of ~2 ng/μl (**Table 6.2**). Embryos were viewed under a microscope with ultra-violet light for gfp fluorescence and their yolk sacs were analysed using PCR with construct-specific primers to determine transgenic status. Neither gfp fluorescence nor presence of the transgene was detected in 16 embryos from 2 litters. The concentration of injected DNA was increased to improve transmission and foster mothers were allowed to litter down to focus on the establishment of transgenic lines.

DNA was injected at ~10 ng/μl. 1 transgenic female mouse was obtained from 8 pups as determined using PCR of tail tip DNA (**Fig. 6.4A**). A concentration between 5 and 10 ng/μl was aimed for in further DNA preparations for embryo injection, those in the order of 10 ng/μl frequently had a deleterious effect on the single cell embryos that then had to be discarded. No further transgenic founders have been obtained to date. The single founder was mated with a stud male of the inbred CBA/Ca strain. Out of 7 pups, one transgenic F1 male was obtained (**Fig. 6.4B**), showing that the transgenic line was indeed transmitting the transgene to subsequent generations. This mouse has not produced any offspring despite many attempts and so appears to be sterile. The founder female has also not produced any further surviving litters.

Table 6.2. Results following injection of *α-p0-Tbx5-ires-gfp-intron-pA* (construct 2)

DNA batch	Injected DNA concentration	No. foster mothers	Results	PCR detection of transgene
1	~2 ngμl^{-1}	2	16 embryos (transient Tg)	No transgenics
2	~10 ngμl^{-1}	2	8 pups	1 x transgenics (female)
3	~5 ngμl^{-1}	2	3 pups	No transgenics
4	~5 ngμl^{-1}	3	7 pups	No transgenics

Figure 6.4

Mouse tail tips were analysed using PCR for the presence of the *α-p0-Tbx5-ires-gfp-intron-pA* construct. To show presence of the transgene, 2 sets of primers specific for the *α-p0-Tbx5-ires-gfp-intron-pA* construct were used. One pair was specific for a region 5' to *Tbx5* (the forward primer covered the α-element/p0 join; the reverse primer, a piece of the pBII-KS plasmid linker).

5' pair:
Forward primer – GCTGCCCAGTATCTAGAGAACC
Reverse primer – GGATCCACTAGTTCTAGAGCGG
Product = 522 base pairs (**b**)

The second primer pair were specific for a region at the 3' end of *Tbx5* (the reverse primer matched a region of the internal ribosomal entry site, ires).

3' pair:
Forward primer – CCCCCAGAGTTTCTCTACACTC (**F6** – see **Fig.6.3**)
Reverse primer – CAAACGCACACCGGCCTTATTC (**R1** – see **Fig.6.3**)
Product = 600 base pairs (**b**)

2 transgenic mice were identified through PCR analysis (**A, B**):

A 1 transgenic female mouse was obtained following injections of DNA construct (~10 ng/μl) into mouse embryos. PCR using both the 5' and the 3' primers on tail-tip DNA from this mouse (+ **ve**) gave products of the correct size (**522** and **600 b**). PCR on DNA from littermates (**- ve**) and control (**c**) samples (without DNA) gave no product at all. Band sizes were determined with reference to a DNA ladder (**L**).

B 1 transgenic male mouse was obtained following breeding from the transgenic female in **A** with a non-transgenic male. PCR using both the 5' and the 3' primers on tail-tip DNA from this mouse (+ **ve**) gave products of the correct size (**522** and **600 b**). PCR on DNA from littermates (**- ve**) and control (**c**) samples (without DNA) gave no product at all. **L**, DNA ladder.

α-p0-Tbx5-ires-gfp-intron-pA is incorporated into transgenic mice

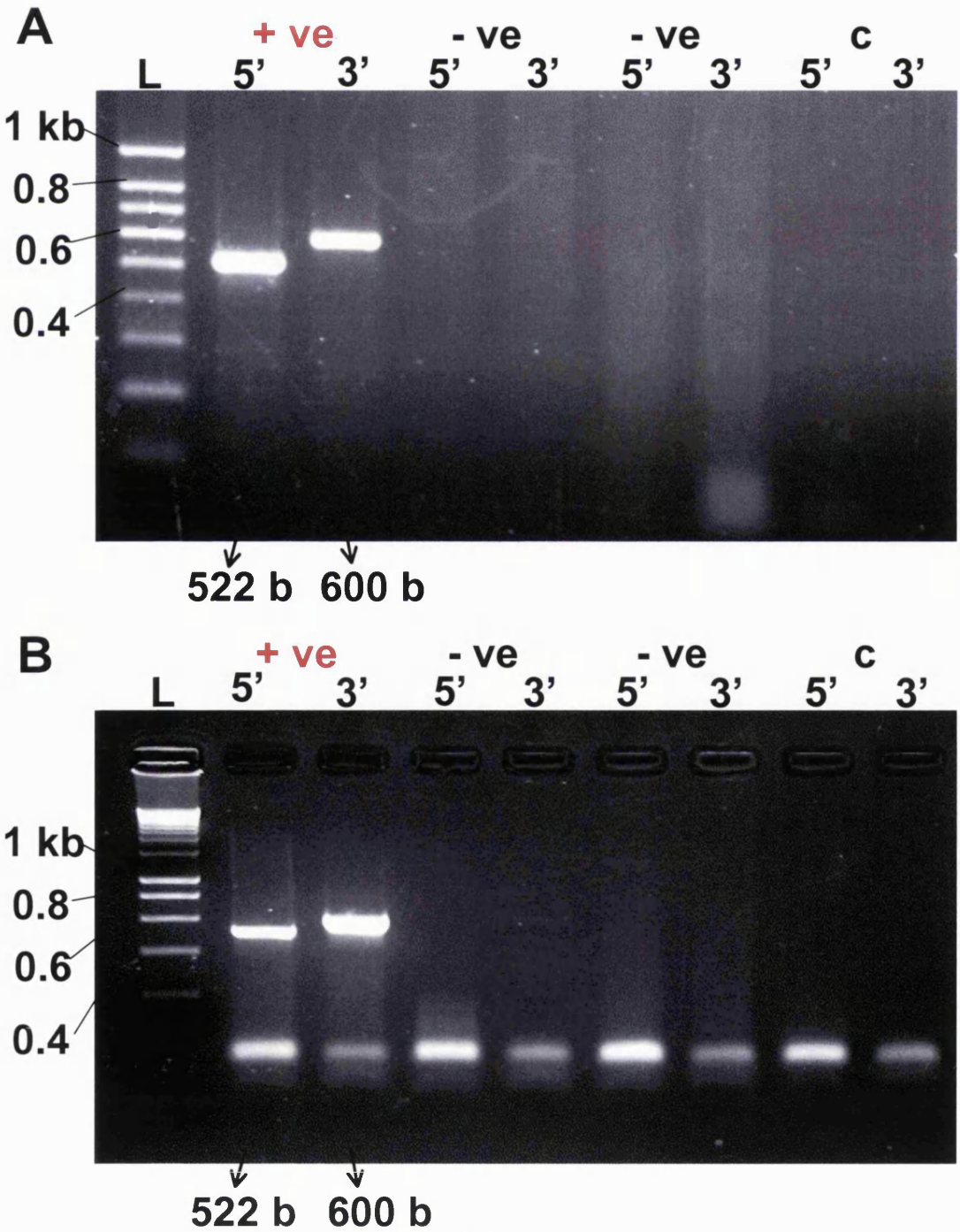

DISCUSSION

The building of a construct for the misexpression of *Tbx5* in the developing ventral retina of transgenic mice has been described. The construct was successfully incorporated into the mouse genome but a viable transgene line has not been established due to the low numbers of mice born to the founder mouse and the apparent sterility of the transgenic F1 male obtained. This means the biological viability of the construct remains to be confirmed. Reasons for the low frequency of transgenic mice generated and the future directions for this project are discussed below.

6.3. Low frequencies of transgenic mice were generated

The main problems that hindered the generation of transgenic mice were the small litter sizes and the eating of neonatal mice by their mothers. Because of this embryo injection and implantation into pseudopregnant mice was carried out many times for a very low number of potential founder mice (**Table 6.2**, experiments where all offspring were eaten or none were born are not included on this table). Furthermore, the frequency of transgenesis in the embryos that did survive was low. Out of 34 surviving injected mouse embryos brought to term, the transgene was detected in only one, a female mouse. This gives a frequency of successful transgenesis of only 8.8%.

If incorporation of the transgene into the mouse genome was affecting embryo health one may observe all of the problems described above. Small litter sizes may be due to death and reabsorption of embryos *in utero*. Eating of offspring can occur if the mother senses the neonatal mice are in poor health. A low frequency of transgenic mice might be due to the preferential death of transgenic embryos. Expression of *α-p0-Tbx5-ires-gfp-intron-pA* should be completely restricted to the developing eye (Kammandel *et al.*, 1999; Marquardt *et al.*, 2001). Because of this *α-p0-Tbx5-ires-gfp-intron-pA* itself is not predicted to cause any negative effects on development or on the general health of transgenic mouse embryos. This may not be the case (1) if α-p0 drives expression of *Tbx5*/*gfp* in tissues and at time-points not examined by

Kammandel *et al.* and Marquardt *et al.* so causing toxicity of the developing embryo; or (2) if transgenes disrupted the function of endogenous gene(s) on entering the genome. Point (1) seems unlikely firstly because there is no evidence that α-p0 can drive expression in any tissue but the eye and secondly because an F1 transgenic mouse was generated. Point (2) is a potential hazard in every injected embryo, but given the large numbers injected it seems unlikely that this could account for the consistently poor yield of transgenic offspring. Approximately 5-15% of transgenic lines carry phenotypically visible insertional mutations (Hogan *et al.*, 1994).

Toxicity of the DNA preparation could potentially impair embryo health *in utero* and so contribute to the small litter sizes and eating of offspring. Moreover, an impure DNA preparation might prevent an optimal DNA concentration being injected (due to increased toxicity of high concentrations) and so reduce the efficiency of transgene uptake. For this reason it would be worth using alternative DNA purification methods (such as those detailed in p228-231 of Hogan *et al.*, 1994) in future attempts to generate transgenic mice with this construct.

Though small litter sizes and rejection (and eating) of mouse offspring by their mothers can occur if the neonates are not in good health, it may also be a sign that the conditions of the mother are not optimal. Although the impurity of the DNA preparation may have contributed to this, it is unlikely to be the only factor. In this study, problems were not just encountered with breeding of foster mothers (which are generally more likely to reject offspring), but were also encountered with the natural breeding of the founder female obtained, for whom 4 pregnancies yielded 7 pups, one of which was transgenic. Furthermore, low litter size and the eating of mouse pups was a difficulty encountered by other users of the transgenic unit at the Institute of Child Health. Sub-optimal conditions of the mice could be due to many factors. The light/dark cycle may be disrupted, the diet may be inappropriate or the holding room temperature may too high or too low. In addition, frequent disturbance of the mice (particularly during late pregnancy) by animal house users and staff could stress the mice and cause abortion or rejection of offspring. These issues were discussed with animal house staff and faults were discovered in the regulation of the light/dark cycle in some of the holding rooms. These problems have now been rectified. Switching

pregnant mothers to a high fat diet (10%) can reduce the incidence of the eating of offspring. In future breeding attempts it may be worth switching to such a diet.

6.4. Future work

Future work must begin with the analysis of the existing transgenic mice. The founder female is probably now too old to produce further offspring. The F1 transgenic male will soon be beyond the optimal age for mating and must be assumed sterile. The eyes of both these mice can be taken and cryosectioned. Sections can be viewed under fluorescent microscopy for the presence of gfp and *in situ* hybridisation could be performed to see if *Tbx5* is ectopically expressed. Whilst α-p0 driven gene expression has only been examined up to postnatal stages and so is not known to persist into adulthood, it might reasonably be expected to do so. In the postnatal eye, α-p0 drives gene expression in the iris and the peripheral retina. As the expression of *Pax6* in these tissues remains the same into adulthood (Davis and Reed, 1996; Macdonald and Wilson, 1996), the regulation of *Pax6* might also be expected to remain the same in the adult (and hence misexpression of *Tbx5* by α-p0). Alternatively, it may be worth examining the RGC projections of the F1 transgenic male (the ways of doing this are discussed below), perhaps after first examining the eyes of the founder mother and finding gfp fluorescence and/or ectopic *Tbx5* expression. If any abnormalities attributable to the construct are found, it will be worth further attempts to generate transgenic lines with *α-p0-Tbx5-ires-gfp-intron-pA*.

The analysis of transgenic mice generated with the *α-p0-Tbx5-ires-gfp-intron-pA* construct would be divided into two broad areas of study: (1) the analysis of markers of different retinal territories using *in situ* hybridisation and (2) the analysis of RGC projections using standard anterograde and retrograde tracing methods. For (1), expression of patterning genes *Tbx2*, *Tbx3*, *Tbx5*, *Vax2*, *Pax2*, *Ephb2*, *Ephb3*, *Efnb1*, *Efnb2*, *Foxg1* and *Foxd2* would be examined in transgenic embryos (as described above in the introduction) and compared with wild type littermates. Analysis of the projections would occur at different points in the retinofugal pathways and would consider any effect on the ipsilateral retinal projections (described above in the introduction). DiI (Molecular probes, USA) would be injected into localised regions of the retina of transgenic and non-transgenic littermates and anterogradely-labelled

projections compared. Retrograde labelling using DiI, DiO and DiASP crystals (Molecular probes, USA), which fluoresce at different wavelengths, simultaneously implanted into different target structures (such as the optic tract, SC or LGN) would allow multiple labelling of different RGC populations in a single animal. Retrograde labelling could also be used for topographical analysis of auditory and somatosensory maps in the SC. Horseradish peroxidase (HRP) and rhodamine-soaked beads could also be used for retrograde labelling.

Crystal implants would be made either in neonatal mice *in vivo* (possible only for intra-retinal injections) or in fixed preparations of prenatal or neonatal mice (fixed preparations allow more localised implants but axon transport is passive and slow). Analysis of late prenatal/early neonatal mice would enable analysis of topography in retino-recipient areas prior to the refinement of retinofugal connections. Analysis of late neonatal/adult mice would allow analysis of mature topographic maps after the refinement of retinofugal connections. In the rat, initial connections are made in the SC by postnatal day 1 (P1) and mature, refined connections established by P12 (Simon and O'Leary, 1992). Anterogradely labelled SC and LGN could be examined using whole mount preparations of these structures or by exposing the SC in whole brains. Axon topography within the optic nerve and tract would best be examined using transverse sections through these pathways. Retrogradely labelled retinas could be examined using retinal whole mounts. Retinas anterogradely labelled during the peak period of RGC axon guidance to the optic disc (E13.5 to E17.5) could be examined with retinal whole mounts for aberrant projections to the optic disc. Retinas could also be sectioned and examined histologically for differences in intra-retinal connectivity and neuronal morphology in *Tbx5* misexpressing cells (identified with gfp fluorescence). gfp fluorescence would also allow the isolation of populations of cells that are misexpressing *Tbx5*. This could have further applications beyond the immediate scope of this project such as the screening for downstream targets of *Tbx5* using Genechip microarray technology. For all experiments described above, transgenic animals would be compared with non-transgenic littermates to ensure that aberrant projections never occurred in wild type mice.

If the phenotype of α-p0 driven *Tbx5*-misexpressing mice proved to be interesting, they could be crossed with other transgenic animals for further analysis of *Tbx5* gene

function. One possibility would be the crossing of α-p0 driven *Tbx5*-misexpressing mice with mice transgenic for the bacterial β-galactosidase gene driven by multiple copies of a RA-sensitive response element or RARE (Wagner *et al.*, 2000). Labelling of LacZ in RARE-driven β-galactosidase expressing mice labels dorsal and ventral populations of RGCs and their axons (Wagner *et al.*, 2000), as defined by the dorsal and ventral retinal RA synthesis domains (McCaffery *et al.*, 1999; Drager *et al.*, 2001). Because these domains are separated in the retina by a *CYP26* expressing equatorial band (CYP26 actively degrades RA; McCaffery *et al.*, 1999) and RGC axons show dorso-ventral topography in the optic nerve and tract (Chan *et al.*, 1999), these two populations of RGC axons can be tracked independently. By crossing these mice with α-p0 driven *Tbx5*-misexpressing mice, effects of *Tbx5* misexpression on axon topography in the optic nerve and tract could be visualised with LacZ labelling of whole mount embryos and compared to non-crossed RARE-driven β-galactosidase expressing mice. This is assuming that RA synthesis would not be affected by *Tbx5* misexpression. If it were, this would itself be highly informative and contribute to the understanding of the genetic hierarchy that controls dorso-ventral retinal patterning.

α-p0 driven *Tbx5*-misexpressing mice could also be crossed onto other transgenic/mutant strains such as *Ephb2/Ephb3* knockout mice (Birgbauer *et al.*, 2000; Birgbauer *et al.*, 2001). Based on chick studies (Koshiba-Takeuchi *et al.*, 2000), *Tbx5* misexpression in the eye might be expected to suppress *Ephb2* and *Ephb3* expression and promote *Efnb1* and *Efnb2* expression in the retina. Crossing with *Ephb2/Ephb3* knockout mice would determine whether disruptions in topography caused by *Tbx5* misexpression in the retina depended on axonal EFNB interacting with EPHB2/EPHB3 in target regions.

6.5. Conclusion

This chapter has chronicled the construction of a transgene for the misexpression of *Tbx5* and *gfp* in the developing mouse retina and its introduction into transgenic mice. Because of the problems encountered establishing a transmitting line of mice for this construct, analysis of transgenic mice has not been undertaken. Future work will concentrate on establishing lines from new founder transgenic mice. Another possible route to test the constructs activity is to electroporate in into mouse embryos using the

embryos culture system. It is hoped that this project will determine the importance of *Tbx5* for dorso-ventral patterning and retinotopic mapping in the mouse. The discovery of abnormalities in the retino-collicular projection of transgenic mice would further the understanding of how topographic connections are made and might have implications for the development of other neural maps. Furthermore, the transgenic mice generated in this project would provide a valuable resource for further research in this field.

CHAPTER 7

Discussion

I conclude this thesis by summarising the work contained herein and detailing how it adds to our current understanding of development and patterning of the retina. I discuss this work in the context of other research in the field and present a model for dorso-ventral patterning of the mammalian retina based on these data. Lastly I suggest future directions for the continuing study of dorso-ventral patterning and T-box genes in retinal development.

In recent years, work in developmental biology and genetics has provided new insight into the mechanisms involved in eye development, disease and evolution, using a variety of approaches. Greater understanding of the cell cycle, of apoptosis, of key signalling molecules and of transcription factors have all played their part. Gene mutations underlying congenital/developmental eye defects, retinal dystrophies and glaucoma are fast being uncovered. Understanding genetics has already contributed to diagnosis of eye disorders, the assessment of prognosis and genetic counselling. It may not be long before gene therapy, fast becoming a reality in clinical medicine, may be applied to the treatment of eye disease. The future offers the promise of stem cell therapies with the potential for regeneration of diseased tissues including the retina. Outside of the eye, understanding how neuronal connections are established (such as those of RGCs to the brain) could well have implications in axonal regeneration within the central nervous system. Other new therapies are likely to emerge from a better knowledge of eye development and its regulation. These may depend on greater understanding of protein/gene interactions – to which this thesis contributes. The startling conservation of regulatory mechanisms in eye development between vertebrates and invertebrates has sparked debate over the evolutionary origin (or origins?) of photoreception. On the more practical level, analogous regulatory networks have validated the study of invertebrate systems as models of vertebrate eye development. The conservation is evident in this thesis, with homologous DPP/*omb* (in *Drosophila*) and BMP/*Tbx* (in mouse) regulation.

7.1. Summary

I have shown that *Drosophila omb*-related T-box genes are expressed in the dorsal mouse and human retina during early eye development (**Chapter 3**). I found that their expression becomes restricted to different layers during retinal stratification. Thus

they are likely to have distinct roles in dorsal patterning and lamination of the retina. Human *TBX5* and mouse *Tbx2* and *Tbx5* all showed gradients of expression across the dorso-ventral axis of the retina in RGCs at a time when their projections are reaching central brain targets. These three genes are therefore good candidates for regulating axon guidance molecules in the dorsal retina. Homeobox-containing paired box gene *Pax6* has been shown to be important for the polarised expression of *Tbx5* and ventral homeobox gene *Vax2* (**Chapter 4**). This was determined by the analysis of expression in *Pax6* null *Small eye* (*Sey*) mouse embryos. Expression of TGFβ-family member *Bmp4* has been shown to coincide with those of T-box genes in the developing mouse retina (**Chapter 4**). A whole embryo culture system was used to demonstrate that BMP4 regulates the expression of *Tbx2* and *Tbx5* in the developing mouse retina (**Chapter 5**). Both *Tbx2* and *Tbx5* were ectopically upregulated in the optic vesicle in response to implanted human recombinant BMP4-soaked beads. *Tbx2* was found to be more responsive to ectopic BMP4 than *Tbx5*. The genesis of transgenic mice to directly test the function of *Tbx5* in the developing mouse retina has been described, but phenotypic analysis has been hampered by difficulties in breeding (**Chapter 6**).

This thesis has also examined in detail the distribution of POU-domain transcription factor POU4F2 in the developing human retina (**Chapter 3**). This work suggests a wider role for POU4F2 in the development of retinal precursors than its known role in developing RGCs (Erkman *et al.*, 1996; Gan *et al.*, 1996; Gan *et al.*, 1999). Expression of *Drosophila H15*-related T-box gene *Tbx20* has been examined in the developing mouse embryo (**Chapter 3**). *Tbx20* was expressed in developing ventral hindbrain nuclei and with *Tbx5* in the developing heart in complementary and overlapping patterns. Expression of newly cloned forkhead transcription factor gene *Foxn4* was examined in the developing mouse embryo and its asymmetric retinal expression (across both dorso-ventral and naso-temporal axes) was compared with that of *Bmp4*, *Tbx2*, *Tbx5* and *Vax2* (**Chapter 4**). Dorso-ventral patterning was found to occur in *Chx10* null *ocular retardation* (*or*) mouse eyes (**Chapter 4**) and the whole mouse embryo culture system was validated for use as a manipulable model of mammalian eye development (**Chapter 5**).

The underlying theme throughout this thesis is that of dorso-ventral patterning of the mammalian retina and the putative involvement of T-box genes in this process, with

the mouse used as the primary model of mammalian eye development. Dorso-ventral patterning polarises the retina across this axis. This allows cells of the retina to respond to inductive events in a manner appropriate to their dorso-ventral position. The essential nature of this process needs reiterating:

(1) Invagination of the optic vesicle occurs on its ventral aspect. Dorsal neuroepithelium then sweeps ventrally with both nasal and temporal aspects extending around the lens to meet and fuse at the ventral fissure. Dorso-ventral polarity is thus essential for eye morphogenesis to occur.
(2) After formation of the optic cup, the retina becomes stratified into distinct cellular layers. Differentiating RGCs migrate to the inner retina and project their axons through the optic stalk (the early optic nerve) to central targets in the brain. RGC axons form topographical maps through their synapse pattern in target areas. This pattern formation largely depends on positional identity of the RGCs. Dorso-ventral patterning is therefore required for the axon guidance of RGCs.
(3) Position-dependent features of the retina require some kind of positional identity among retinal neurons. Across the dorso-ventral axis of the retina these include asymmetric cellular or chemical distributions. Examples are RGC distributions or synthesis of opsin types in photoreceptors.
(4) Dorso-ventral patterning of the retina is an evolutionarily conserved feature of the vertebrate eye. This suggests it is an essential feature during development of the cameral eye of vertebrates.

The work of this thesis must be placed in the broader context of its field. In the following sections, models for dorso-ventral patterning of the mammalian retina and for the probable roles of *omb*-related T-box genes are presented. These models incorporate the results from this thesis into the wider body of research on dorso-ventral patterning in the developing retina. This thesis is concluded with suggestions for future investigation in this field.

7.2. Dorso-ventral patterning of the developing retina

Patterning of tissues in the developing retina occurs through a variety of different mechanisms, but some general principles are known. For the most part, polarised expression of genes encoding secreted signalling molecules seems to be important.

These signalling centres (or polarising zones) may be specified through numerous inductive events originating from spatial asymmetries at the earliest stages of embryo development (Zernicka-Goetz, 2002). Polarising zones are believed to define 'patterning axes' within developing tissues. This may be achieved through the diffusion of signalling molecules and/or propagation of a patterning signal through secondary relay mechanisms across developing tissue axes (Reilly and Melton, 1996; Kerszberg, 1999; Sanson, 2001). Evidence supports such mechanisms of action for BMP4, Sonic hedgehog (SHH) and retinoid signalling (Eichele and Thaller, 1987; Jones and Smith, 1998; Zeng *et al.*, 2001), all implicated in dorso-ventral patterning of the retina (see below). Different levels of signalling molecules are hypothesised to induce expression of position-specific networks of transcription factors which control the expression of genes that effect the positional characteristics of individual cells. The molecular players that control retinal patterning can thus be tentatively categorised into three types and placed in a putative regulatory hierarchy:

(1) Extrinsic regulators: extra-cellular signalling molecules and their receptors that bind cells to activate intracellular pathways and transcription factors.
(2) Intrinsic regulators: transcription factors that regulate the expression of multiple genes necessary to provide a cell with a particular phenotype.
(3) Effector molecules: molecules that effect the cell phenotype in response to extracellular signalling (*e.g.* cell cycle regulators, cytoskeletal elements or cell surface molecules to effect proliferation, cell migration and axon guidance).

There are a number of problems with presenting this linear patterning hierarchy. Patterning does not occur in a simple linear sequence, but rather is an ongoing inductive process involving the interaction and feedback of many factors at many levels. Extrinsic signals are transduced through the activation of intracellular signalling pathways that result in the formation of transcriptional complexes in the nucleus. These function by binding and regulating target genes (often, but not necessarily, encoding transcription factors). Extrinsic and intrinsic mechanisms regulate the levels of different transcription factors. These function co-operatively or independently to regulate effector genes (and those encoding other transcription factors or signalling molecules). Effector molecules (for example cell surface molecules that respond to the environment in a position-dependent way) may themselves act as extrinsic regulators by taking part in inductive interactions with

other cells. Despite the inevitable complexity, the above categorisation provides a good framework on which to build a theoretical model of retinal patterning. Rather than embrace complexity from the outset, it is more prudent to build a simplistic model based on known interactions between patterning molecules and adapt it as new evidence is accumulated.

Dorso-ventral patterning of the neural retina

Candidate molecules for the provision of dorso-ventral identity to the developing retina (see **Chapter 1: 1.3.**) can be grouped into a regulatory hierarchy with extrinsic regulators at the top, followed by intrinsic regulators, and effector molecules at the bottom. They are described and grouped below. They and their interactions are illustrated in **Fig. 7.1**. This model of dorso-ventral patterning combines understanding of patterning of the mouse and chick eye, although findings from other systems are mentioned when relevant. The model includes the findings of this thesis and other work published during the course of this thesis, particularly work examining patterning of the chick eye. From current data, overt patterning mechanisms appear similar between mouse and chick eyes. Subtle differences are known (such as in Eph/ephrin distributions and *Mitf* expression) and are expected because of the differences in the mouse and chick visual systems. For example, the presence of an ipsilateral RGC axon projection in the mouse will necessitate patterning differences at the optic chiasm.

(1) Extrinsic regulators: diffusible molecules BMP4 and (low-level) retinoic acid (RA) in dorsal retina; SHH and (high-level) RA in ventral retina

- RA is known to be important in formation of the ventral retina from studies in mouse (Warkany and Schraffenberger, 1946; Kastner *et al.*, 1997) and zebrafish (Marsh-Armstrong *et al.*, 1994; Hyatt *et al.*, 1996). RA can also promote expression of ventral markers. In mice, TLX, an enhancer of RA signalling, positively regulates *Pax2* (Yu *et al.*, 2000). RA treatment in zebrafish and *Xenopus* extended the ventral *pax2* and *Vax2* expression domains respectively (Hyatt *et al.*, 1996; Sasagawa *et al.*, 2002). In zebrafish, RA reduced expression of the dorsal marker *mshC* (Hyatt *et al.*, 1996), a zebrafish *Msx* orthologue (Ekker *et al.*, 1997). Analysis of retinoid synthesis and signalling levels suggest that high RA levels are involved in the specification of ventral retina, while low RA levels

Figure 7.1

This diagram is based primarily on work in the developing chick and mouse unless stated below. It illustrates the molecules currently implicated in dorso-ventral patterning of the neural retina with their known interactions. The optic cup and lens are represented schematically and the dorso-ventral axis is illustrated. SHH, derived from a ventral forebrain source, is shown as a positive regulator of *Pax2* and *Vax2* in ventral retina. *Six6/9* is expressed in the ventral optic vesicle and may be involved in patterning of the ventral retina. SHH is a negative regulator of *Bmp4* expression, it also negatively regulates *Pax6* to restrict its expression to the developing neural retina. BMP4, active in dorsal retina, is a positive regulator of dorsally expressed *Msx2*, *Tbx2* and *Tbx5*. *Tbx2* and *Tbx3* are expressed in dorsal retina and in *Xenopus* can repress *Pax2* expression and downstream elements of the SHH pathway (indicated). Expression of *Hmx3* and *Tbx20* has also been reported in the dorsal retina. The involvement of *Pax6* in establishing the polarised levels of active retinoids (such as retinoic acid, RA) in dorsal (low levels, ↓) and ventral (high levels, ↑) retina is indicated. RA is can positively regulate of *Pax2* in zebrafish (indicated). *Efnb* and *Ephb* genes are illustrated as downstream targets of *Tbx5* and *Vax2* in dorsal and ventral retina respectively.

Molecules implicated in dorso-ventral patterning of the neural retina

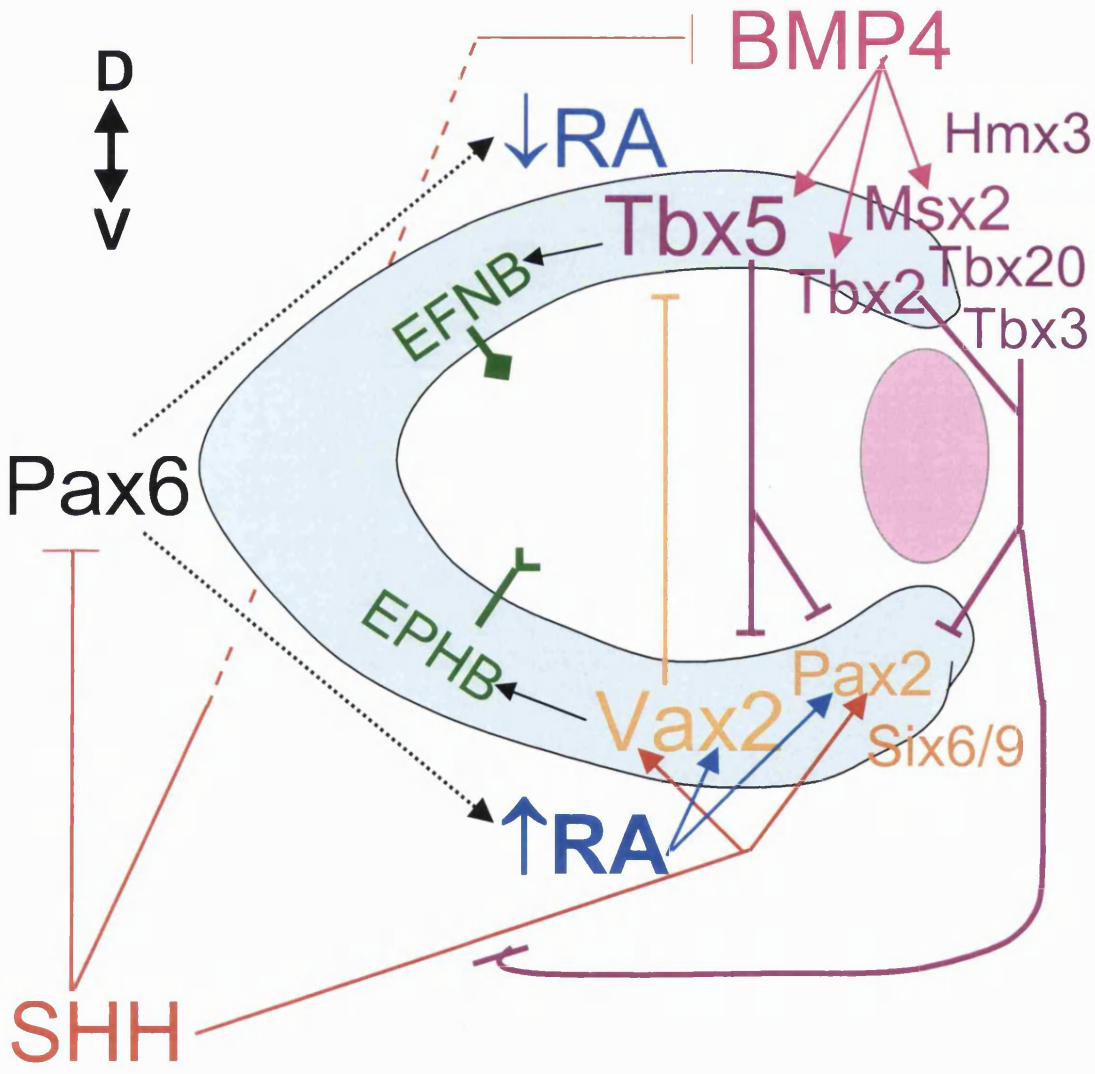

are involved in the specification of dorsal retina (McCaffery *et al.*, 1999; Wagner *et al.*, 2000; Drager *et al.*, 2001). In the optic vesicles of *Pax6*-null mouse embryos, RA signalling, production and sequestration were significantly decreased (Enwright and Grainger, 2000). In work from this thesis, polarised *Tbx5* and *Vax2* expression were disrupted in the *Pax6*-null optic vesicle, an effect that may be due to reduced RA signalling (**Chapter 4**).

- In the ventral chick optic cup, SHH positively regulates *Vax* (orthologous to *Vax2*) and *Pax2*, and negatively regulates *Bmp4* and *Pax6* expression (Zhang and Yang, 2001). These relations are conserved in *Xenopus*, except that SHH does not appear to regulate *Bmp4* expression (Sasagawa *et al.*, 2002). In the dorsal optic cup, BMP4 has been implicated in the positive regulation of mouse *Msx2* and chick *Tbx5* and the negative regulation of chick *Vax*, *Pax2* and *Ventroptin* (Furuta and Hogan, 1998; Koshiba-Takeuchi *et al.*, 2000; Sakuta *et al.*, 2001). Work from this thesis has implicated BMP4 in the positive regulation of mouse *Tbx2* and *Tbx5* (**Chapter 5**). In *Xenopus*, BMP4 signalling positively regulates *Tbx2/3/5* and *Pax6*, and negatively regulates *Vax2* and *Pax2* (Sasagawa *et al.*, 2002). Chick Ventroptin shares some homology with BMP antagonist Chordin. It can block BMP4 function *in vivo*, downregulate retinal *Bmp4* and *Tbx5* expression and upregulate expression of *Vax* (Sakuta *et al.*, 2001). Polarised *Ventroptin* expression is first evident in the early ventral optic cup and later is strongly expressed in ventral and in nasal retina in a double gradient pattern. Retinal *Ventroptin* misexpression causes defects in the chick retino-tectal projection across both dorso-ventral and antero-posterior axes (Sakuta *et al.*, 2001).

(2) Intrinsic regulators: transcription factors Tbx2, Tbx3, Tbx5, Tbx20, Msx2 and Hmx3 in dorsal retina; Vax2, Pax2 and Six6/9 (Optx2) in ventral retina; Pax6.

- *Tbx5* misexpression in the developing chick eye dorsalises the ventral retino-tectal projection and induces *Efnb1* and *Efnb2* expression whilst repressing that of *Vax*, *Ephb2* and *Ephb3* (Koshiba-Takeuchi *et al.*, 2000). In *Xenopus* embryos, misexpression of *Tbx2* and *Tbx3* downregulated Gli1, Gli2 and Ptc2, all members of the SHH signalling pathway. *Pax2* expression was similarly repressed by *Tbx2* and *Tbx3* misexpression (Takabatake *et al.*, 2002; Wong *et al.*, 2002). *Xenopus Tbx3* misexpression also downregulates *Netrin-1* (also named *XNet1*, involved in

the guidance of axons to the optic disc; de la Torre *et al.*, 1997; Hopker *et al.*, 1999) in the ventral retina (Wong *et al.*, 2002). Expression of *Tbx2* and *Tbx5* (**Chapter 3**), *Tbx20* (Carson *et al.*, 2000; Kraus *et al.*, 2001), *Msx2* (Monaghan *et al.*, 1991; Furuta and Hogan, 1998) and *Hmx3* (fused to the *LacZ* reporter gene; Weidong *et al.*, 2000) has been described in restricted dorsal domains of the developing mouse retina. This implicates them in the provision of dorsal retinal identity. In this thesis, *TBX2*, *TBX3* and *TBX5* were expressed in overlapping domains of the dorsal human optic cup (**Chapter 3**), consistent with work in other vertebrate species.

- Both *Vax2* and *Pax2* are expressed in ventral retina where they are implicated in the development of ventral eye structures (Torres *et al.*, 1996; Barbieri *et al.*, 1999; Bertuzzi *et al.*, 1999). *Six6/9* is expressed in the ventral optic vesicles and may also be involved in ventral retina specification and development (Jean *et al.*, 1999; López-Ríos *et al.*, 1999). Misexpression of chick *Vax* or mouse *Vax2* in the developing chick eye disrupts the dorsal retino-tectal projection and induces *Pax2*, *Ephb2* and *Ephb3* expression whilst repressing that of *Tbx5*, *Efnb1* and *Efnb2* (Schulte *et al.*, 1999). Loss of *Vax2* in mouse knockouts leads to upregulation of *Efnb1* and *Efnb2* and downregulation of *Ephb2* and *Ephb3*, but no alteration in *Pax2*, *Tbx5*, *Six6/9* and *Foxg1* expression (Barbieri *et al.*, 2002; Mui *et al.*, 2002). In these knockouts the ventral RGC projection was dorsalised. Ventro-temporal retina was more severely affected than ventro-nasal retina, suggesting an interaction/overlap between dorso-ventral and naso-temporal patterning mechanisms (Mui *et al.*, 2002).

- *Pax6* has been proposed to regulate patterning indirectly in dorsal and ventral retina by permitting retinal cells to respond to RA signalling (**Chapter 4**).

(3) Effector molecules: EFNB in dorsal retina; EPHB in ventral retina.

- *Ephb2* and *Ephb3*, both of which encode Eph receptor tyrosine kinases (RTKs) of the B class) show restricted expression in the ventral chick retina, as does *Epha7* (Sefton *et al.*, 1997; Connor *et al.*, 1998). *Efnb1* and *Efnb2*, which both encode ephrin binding partners of EPHB RTKs, are expressed in the dorsal chick retina (Braisted *et al.*, 1997). In the mouse, asymmetric expression of *Ephb2* and *Efnb2*

has been detected in ventral and dorsal retina respectively (Birgbauer *et al.*, 2000). EPHB/EFNB interactions can guide axons, through repulsive mechanisms, during the formation of neuronal networks (Henkemeyer *et al.*, 1996; Orioli and Klein, 1997; Wang and Anderson, 1997). Repulsive EPHB/EFNB interactions are implicated in RGC axon pathfinding to the optic disk in mice (Birgbauer *et al.*, 2000; Birgbauer *et al.*, 2001) and formation of the ipsilateral projection in *Xenopus* (Nakagawa *et al.*, 2000). *XNet1* is expressed in ventral retina and can be downregulated by *Tbx3* misexpression (Wong *et al.*, 2002). The ventral retina is the site of the developing optic disc, where Netrin-1 guides axons towards it and into the optic nerve (de la Torre *et al.*, 1997; Hopker *et al.*, 1999). Netrin-1 has not been implicated in dorso-ventral patterning.

In summary, co-ordinated retinoid, BMP4 and SHH signalling are proposed to be the master controllers of dorso-ventral patterning in the developing eye. These are able to do so by virtue of the asymmetric expression/synthesis of the morphogens themselves, their receptors or binding partners and other downstream components of the signalling pathways. BMP4 and SHH signalling are known to regulate the expression of dorsal and ventral transcription factors respectively (**Chapter 5**; Furuta and Hogan, 1998; Koshiba-Takeuchi *et al.*, 2000; Zhang and Yang, 2001). In *Pax6* null mouse embryos, *Pax2* expression is upregulated suggesting SHH signalling (which regulates *Pax2* expression; Zhang and Yang, 2001) can still occur. Likewise *Bmp4* and *Bmpr-I* receptor genes are expressed in essentially the correct areas of the *Pax6* null optic vesicle (Furuta and Hogan, 1998), suggesting BMP4 might be available for retinal signalling in the absence of *Pax6*. Despite this, expression of *Tbx5* and *Vax2* are disrupted in the *Pax6* optic vesicle (**Chapter 4**), suggesting that the normal regulation of these genes by BMP4 (**Chapter 5**; Koshiba-Takeuchi *et al.*, 2000) and SHH (Zhang and Yang, 2001) respectively, is insufficient or unable to occur. Retinoid signalling defines dorsal and ventral compartments of the retina that correspond to receptive areas of the upper and lower visual fields (Wagner *et al.*, 2000). The disruption of retinoid signalling in *Pax6* null optic vesicles (Enwright and Grainger, 2000) provides a putative explanation for the requirement of *Pax6* in dorso-ventral retinal patterning. Thus retinoid signalling is proposed to control dorso-ventral identity by allowing dorsal and ventral retina to respond appropriately to diffusible morphogens such as BMP4 and SHH. These morphogens, via the differential

regulation of transcription factor networks across the dorso-ventral axis of the retina, may then control the expression of effector genes of positional identity.

As presented, RA signalling can be viewed as an independent patterning system that modulates the action of different morphogens by setting boundaries of where they may act and altering the responsiveness of different areas to them. This model, though tentative, is consistent with the known interactions of patterning molecules along the dorso-ventral axis of the retina (see **Fig. 7.1**) and can thus be considered a good base from which to design further experiments. One problem is the apparent absence of a RA signalling system across the dorso-ventral axis of the retina at early stages of chick eye development (Mey *et al.*, 2001). It may be that this analysis, which identified similar RA synthesis and degradation patterns to the mouse only after formation of the optic cup, was not sensitive enough to detect reduced levels at earlier stages. Alternatively this could reflect a genuine difference between the chick and mouse. In this instance, RA signalling could still be involved in the definition of boundaries (for example, of the upper and lower visual receptive fields), but could not be required for the early retina to respond to the action of BMP4 and SHH in the chick.

Dorso-ventral patterning of the RPE

One interesting feature that has not been included in **Fig. 7.1** is that of dorso-ventral patterning of the retinal pigmented epithelium (RPE). Recent analysis of mouse mutants combined with chick embryo manipulations has provided new understanding of RPE development. These studies identified molecules implicated in determining a neural retina versus RPE state, but they also highlighted dorso-ventral distinctions in these fate decisions. It appears that the RPE, like the neural retina, is divided at the molecular level into dorsal and ventral compartments.

Growth arrest specific gene 1 (*Gas1*), which encodes a membrane-anchored protein capable of cell-autonomous suppression of proliferation, shows generalised expression in the developing eye. In *Gas1* mutant mouse embryos, a secondary ventral neural retina forms where the ventral RPE should be (Lee *et al.*, 2001). In this secondary ventral neural retina, RPE-specific genes *Mitf* (encoding a bHLH transcription factor) and *Tyrosine related protein gene 2* (*Tyrp2*) were downregulated

while proneural bHLH gene *Math5* was upregulated. Despite generalised *Gas1* expression in wild-type eyes, formation of neural retina instead of RPE occurred in a sharply defined ventral compartment of the mutant outer retina (Lee *et al.*, 2001). This suggests either *Gas1* is not involved in dorsal RPE development, or there are other factors, specific to the dorsal RPE, that can compensate for loss of *Gas1* function. The injection of hybridoma cells producing anti-SHH IgG antibodies into the vitreous of stage 17 chick embryos resulted in a similar phenotype to that observed in *Gas1* mutant mice (Zhang and Yang, 2001). A well-defined ventral compartment of the RPE assumed a morphology that resembled neural retina in hybridoma injected optic cups. This suggested that ventral and not dorsal RPE depends on SHH for its differentiation. In this ventral region, expression of homeobox gene *Otx2*, a marker of RPE, was specifically downregulated (Zhang and Yang, 2001) and this may account for the loss of RPE specification (see below).

Similar phenotypes to those described above for ventral RPE in *Gas1* mutant and SHH-blocked eyes have also been described for the dorsal RPE. *Mitf* is expressed throughout developing RPE and associated with the onset and maintenance of pigmentation (Fuhrmann *et al.*, 2000; Nguyen and Arnheiter, 2000). Loss of *Mitf* function in the *microphthalmia* mutant mouse results in defective RPE specification. The ventral RPE initially develops normally but then fails to acquire pigmentation or a differentiated cuboidal morphology. The dorsal outer optic cup forms a secondary neural retina, which develops all major retinal cell types along a similar time course to the wild type (Bumsted and Barnstable, 2000). This demonstrates that the ventral retina is uniquely responsive to RPE-specifying factor(s) that can function in the absence of *Mitf* to promote specification (but not differentiation) of RPE over neural retina. *Otx2* expression was specifically downregulated in the dorsal mutant RPE area and this could account for the loss of RPE specification (see below).

The expression of homeobox genes *Otx1* and *Otx2* (orthologous to *Drosophila* head gap gene *orthodenticle*) is essential for the specification of anterior neuroectoderm and the development of the rostral head and the eyes (Acampora *et al.*, 1995; Matsuo *et al.*, 1995; Suda *et al.*, 1999). *Otx1* and *Otx2* are expressed throughout the early optic vesicle (Simeone *et al.*, 1993). Expression of these genes then becomes restricted to the dorsal optic vesicle in a complementary pattern to *Pax2*, later to the

outer layer of the optic cup, the presumptive RPE (Bovolenta *et al.*, 1997; Martinez-Morales *et al.*, 2001). Reductions in *Otx1* and *Otx2* activity in mutant mice leads to an expansion of the *Pax2* expression domain in the optic vesicle and a loss of RPE specification (with a downregulation of pigmentation genes *Mitf* and *Tyrosinase*) in the optic cup. Neural retina and optic stalk tissue was expanded in the optic cups of these mutants as determined by analysis of *Six3*, *Pax2* and *Pax6* expression (Martinez-Morales *et al.*, 2001).

These data are consistent with the suggestions above that localised reductions in *Otx2* expression may account for the failure of dorsal and ventral RPE specification in *microphthalmia* mutants and SHH blocking experiments respectively. Though *Otx2* and other RPE-specifying genes are expressed throughout the developing RPE, it is clear that they are differently regulated in dorsal and ventral retina. Different groups of transcription factors are likely to be operating in dorsal and ventral RPE. Through mutual positive interactions, such as those between Otx and Mitf in the dorsal RPE (Nguyen and Arnheiter, 2000; Martinez-Morales *et al.*, 2001), different sets of transcription factors could function co-operatively to regulate the same network of RPE genes in dorsal and ventral retina (Bentley *et al.*, 1994). T-box genes could potentially be involved in the regulation of the dorsal RPE compartment. The dorsal expression domains of mouse *Tbx2* and *Tbx5* extend into the dorsal RPE (**Chapter 3**). Mitf could potentially regulate the dorsal RPE expression domains of these genes. The *Tbx2* promoter contains a full consensus Mitf recognition element and *Tbx2* expression can be induced by Mitf in melanocytes (Carreira *et al.*, 2000).

The functional significance of the dorso-ventral compartmentalisation of the RPE is not immediately clear. It has been hypothesised that RPE patterning might help direct that of the neural retina (Lee *et al.*, 2001). Although this remains an intriguing possibility, compartmentalisation of the RPE may be a simple reflection of the way that dorso-ventral patterning occurs in the developing eye. In mice, RA is differentially synthesised across the dorso-ventral axis of the developing eye before the specification of neural retina and RPE (McCaffery *et al.*, 1992; McCaffery *et al.*, 1993). Disruptions in RA signalling affect ventral RPE as well as ventral neural retina (Hyatt *et al.*, 1992; Marsh-Armstrong *et al.*, 1994; Kastner *et al.*, 1997). It is likely that the differential RA signalling that defines dorsal and ventral compartments in the

neural retina (McCaffery *et al.*, 1999) also defines dorsal and ventral compartments in the neighbouring RPE. Signalling molecule SHH, derived from expressing cells in the ventral prosencephalic midline (Huh *et al.*, 1999; Zhang and Yang, 2001), is prominent in the ventral RPE (Zhang and Yang, 2001). The same may also be true of BMP4, derived from the dorsal neural retina (**Chapter 4**; Furuta and Hogan, 1998), in the dorsal RPE. Interestingly, BMP genes *Bmp5* and *Bmp7* show restricted expression to the ventral RPE in the chick optic cup (Belecky-Adams and Adler, 2001; Trousse *et al.*, 2001). Given the different molecular environments of dorsal and ventral RPE, it is perhaps not surprising that they are differentially regulated.

7.3. The role of *omb*-related T-box genes in the developing retina

T-box proteins in the developing retina, as transcription factors, function by regulating other genes. To consider their effect on development one must ask which genes are regulated by them and in what way. Transcription factors seem to function as either gene activators or gene repressors, though recent work has shown that the same protein can have both roles. Some transcription factors will activate or repress transcription according to the nature of the binding site in a target gene, or the availability of co-factors that bind the transcription factor (Latchman, 2001). Transcription factors can act in association with other transcription factors. This may be through the formation of homodimers (pairs of the same factor) or of heterodimers (pairs of related transcription factors). Alternatively, different transcription factors may bind the same gene and form part of a single transcriptional complex to regulate expression (for example, Hiroi *et al.*, 2001). This co-operation of different transcription factors taken with their considerable inter-regulation suggests a tendency to function in networks rather than in isolation. This means that the analysis of transcription factor function within a given tissue must consider its wider position within a regulatory hierarchy governing development of that tissue.

TBX2 and TBX3 seem able to act as repressors of transcription (Carreira *et al.*, 1998; He *et al.*, 1999). A conserved C-terminal repressor domain was identified in human TBX2 and in human and *Xenopus* Tbx3/TBX3 and shown to repress transcription when fused to the binding domain of Gal4 (He *et al.*, 1999). Tbx5 seems to act as an activator of transcription, it can associate with homeodomain protein Nkx2-5 to activate *cardiac-specific natriuretic peptide precursor type A* in cultured cardiac cells

(Hiroi *et al.*, 2001). *Tbx5* misexpression in chick eyes causes upregulation of dorsal markers and downregulation of ventral markers (Koshiba-Takeuchi *et al.*, 2000), while *Tbx2* and *Tbx3* misexpression in *Xenopus* causes only a downregulation of ventral markers (Takabatake *et al.*, 2002; Wong *et al.*, 2002). If Tbx5 is primarily an activator of transcription and Tbx2/Tbx3 are repressors, *Tbx5* misexpression may be repressing ventral genes by upregulating *Tbx2* or *Tbx3* expression. Predicted dimerisation residues are identical for TBX2, TBX3 and TBX5 and the potential for function as heterodimers *in vivo* exists for these proteins (Muller and Herrmann, 1997; Meins *et al.*, 2000; but see Sinha *et al.*, 2000). This would add another level of complexity to the possible interactions of these genes.

It seems likely that during early retinogenesis Tbx2, Tbx3 and Tbx5 work together – and perhaps in tandem with other dorsal transcription factors, such as Hmx3, Msx2 or Tbx20 – to induce genes that supply dorsal characteristics and repress those that provide ventral characteristics. The concept of *Tbx2*, *Tbx3* and *Tbx5* working together in this way is particularly attractive given their differential patterns of expression and primary activator/repressor roles. To set graded cellular identity across the dorso-ventral axis of the retina, a more localised dorsal activator (*Tbx5*) would work well with a broadly expressed set of ventral repressors (*Tbx2* and *Tbx3*). Moving from the ventral to the dorsal retina, cellular identity could be shaped by first the withdrawal of ventral factors (such as EPHB2/3) and then by the gradual introduction of dorsal elements (such as EFNB1/2).

As downstream targets of BMP4 signalling, *omb*-related T-box genes are likely to mediate some of the effects of BMP4. The involvement of *Tbx5* in retinal proliferation has been discussed previously (**Chapter 5: 5.7.**). TBX2 and TBX3 are known to promote proliferation through inhibition of p14ARF, which causes a p53-dependent proliferation arrest (Lingbeek *et al.*, 2002). Morphogenesis occurs with dorso-ventral asymmetry and coincides with asymmetric *Tbx* expression. T-box proteins could regulate aspects of eye morphogenesis. This might include regulating proliferation. It might include the ability to respond to signalling molecules from the surface ectoderm/developing lens. T-box proteins could conceivably be regulating secreted molecules that signal lens induction. BMP4 is essential for lens induction (Furuta and Hogan, 1998), it is possible that this effect is indirect via the regulation of other

factors by T-box genes. The restriction of *omb*-related T-box gene expression to differentiating cells in the optic cup and later to emerging lamina during retinal stratification (**Chapter 3**) suggest later roles in the differentiation of different cell types and the provision of laminar characteristics. Potential roles of T-box genes in the developing retina are illustrated in **Fig. 7.2**. Misexpression of *Tbx5* in the mouse retina will hopefully provide further insights into the roles of this gene in retinal development (**Chapter 6**).

7.4. Future directions

Many questions remain concerning retinal T-box gene function and dorso-ventral patterning of the retina. What are the precise interactions of retinoid, SHH and BMP4 signalling systems? How do they combine to regulate the asymmetric expression of transcription factors and do they act directly on other types of genes? Do *omb*-related T-box genes occupy a distinct functional class of transcription factors, regulating specific aspects of dorso-ventral patterning and morphogenesis, or do they act in concert with other dorsal transcription factors? Finally, what genes are regulated by the T-box genes and precisely how do they pattern the developing eye? Answers to this final question are already emerging with the study of Eph/ephrin signalling and its regulation. Eph/ephrin signalling can guide developing axons through contact repulsion and through other mechanisms that remain to be elucidated. Targeted deletions of Eph and ephrin genes in the superior colliculus could help us further understand how topographical connections are made. This in turn should shed light on exactly how dorso-ventral and naso-temporal patterning pathways interact. The discovery of other downstream targets of retinal transcription factors (T-box and otherwise) and signalling molecules are likely to be forthcoming with the use of Genechip microarray technology. This approach will be particularly powerful if expression profiles of cells with aberrant axonal projections can be analysed. With the further unravelling and better characterisation of the human genome, opportunities for the analysis of transcription factor consensus sites in target genes will increase. This will be important for identifying target genes of transcription factors in the eye, but also for understanding the complex interactions between different retinal transcription factors. More studies on the roles of retinal transcription factors to determine the nature of their regulatory power be it activating, repressing, or both, will also help to define their precise roles in the retina.

Figure 7.2

These diagrams present some of the potential roles of the *omb*-related T-box genes (*Tbx*) during eye morphogenesis.

A Cartoon of the developing mouse optic vesicle. *Bmp4* and *Tbx* expression is shown in the dorsal retina and a pink arrow indicates the regulation of *Tbx* by BMP4. Thick blue arrows point to potential roles of *Tbx* in optic vesicle invagination, retinal proliferation and the regulation of lens signalling molecules. Potential retina-derived signalling factors are shown (thin blue arrows) to induce lens formation. The dorso-ventral axis is indicated: **d**, dorsal and **v**, ventral.

B Cartoon of the developing mouse optic cup. *Bmp4* and *Tbx* expression is shown in the dorsal retina and a pink arrow indicates the regulation of *Tbx* by BMP4. Blue arrows point to roles of *Tbx* in retinal proliferation and the regulation of *Eph/EfnB*, *Pax2* and downstream SHH signalling components. *Tbx* expression is also shown in the site of developing ganglion cells, where it may be involved in cellular differentiation (red arrow). The dorso-ventral and proximo-distal axes are indicated: **d**, dorsal; **v**, ventral; **P**, proximal; **D**, distal.

Potential roles of T-box genes during eye morphogenesis

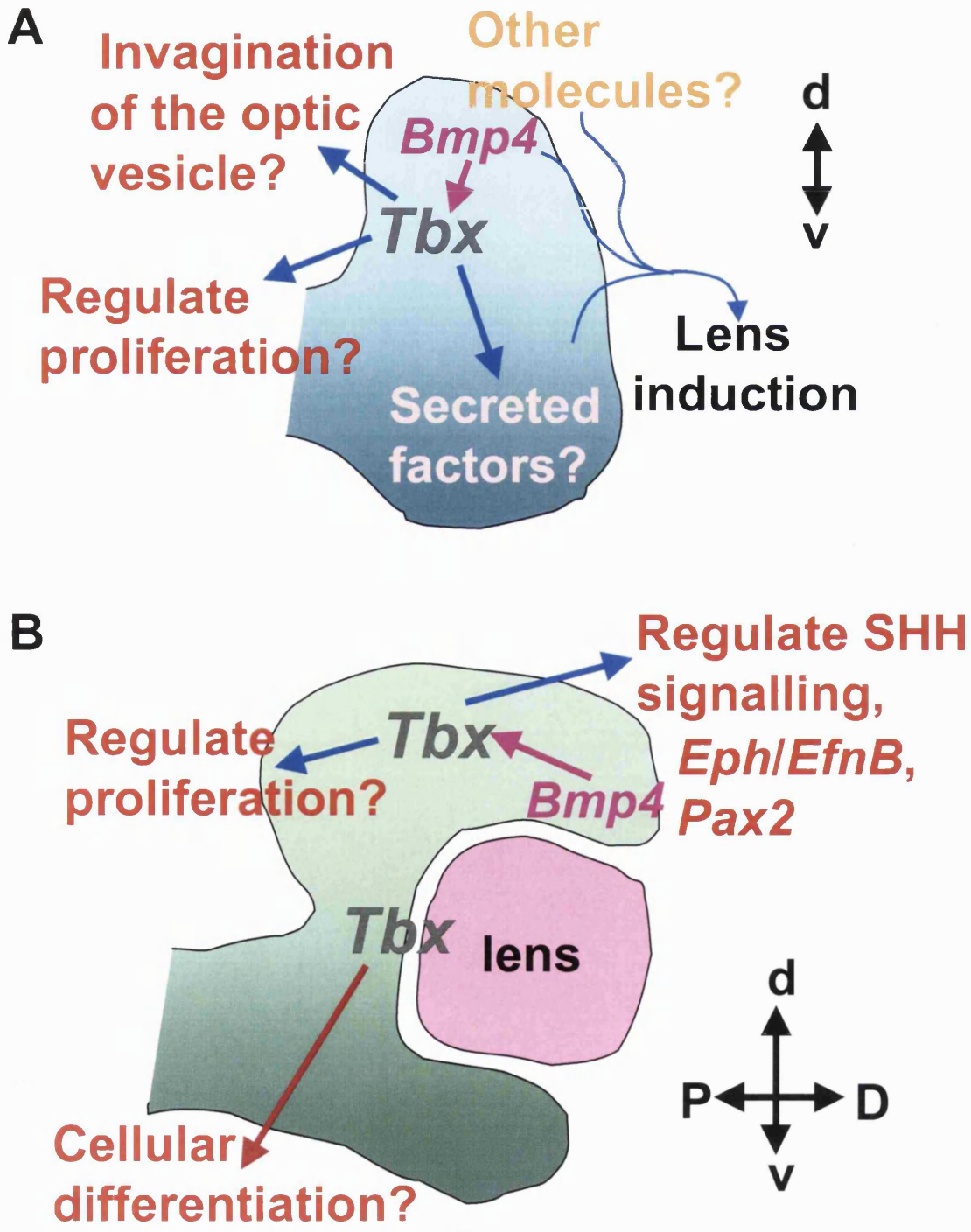

Appendix I

Expression of mouse *Tbx5* in *Drosophila Melanogaster*

Phylogenetic analysis shows that the mouse *Tbx2/3/4/5* T-box gene subfamily is closely related to the fruit fly (*Drosophila Melanogaster*) T-box gene, *optomotor blind* or *omb* (Agulnik *et al.*, 1996). Indeed the T-box regions (defined by the domain of homology between T-box genes) of *omb* and mouse *Tbx2* encode amino acid sequences that share 87% homology (Agulnik *et al.*, 1996). This homology prompted the question of whether *omb*-related T-box genes could substitute for *omb* in the fly. The analysis of *Tbx5* function has been a prominent aim of this thesis. While *Tbx5* shows less structural homology than *Tbx2* and *Tbx3* with *omb*, the prospect of a mutual role in axon guidance for *Tbx5* and *omb* suggested that *Tbx5* might possess more functional homology. *omb* mutations cause severe disruption in axonal connectivity within the fly optic lobes, indicating an important role in the guidance of optic neurons (Pflugfelder and Heisenberg, 1995). *Tbx5* shows strong expression in developing retinal ganglion cells (RGCs) of the dorsal retina, suggesting involvement in the topographic mapping of dorsal RGC axons (**Chapter 3**).

For expression in *Drosophila*, it would be prudent to strip a mouse gene of its untranslated regions (which might contain regulatory/processing elements). During the subcloning steps in **Chapter 6**, a mouse *Tbx5* (*mTbx5*) clone was obtained with the 3' untranslated region (utr) of the gene deleted. The suspicion of functional homology with *omb*, combined with the ready availability of the isolated *Tbx5* coding region, prompted the choice of *Tbx5* for expression in the fly. The *Tbx5* clone with the 3' utr removed was further modified to isolate the coding region, provide a suitable transcription-initiation site and prepare it for expression in *Drosophila* (see below). The result was two constructs that could be used to express *mTbx5* in *Drosophila*. The primary aims are to examine:

(1) The consequences of *mTbx5* misexpression in differentiating photoreceptor cells of the *Drosophila* eye imaginal disc.

(2) The similarities/differences between the effects of eye disc misexpression of *mTbx5* and *omb*.
(3) Whether *mTbx5* will rescue the phenotype of the *optomotor blind* (*omb*) mutant fly.

Analysis of function of constructs is being performed in collaboration with Gert Pflugfelder, Germany. Two constructs have been built. In the first a sequence coding for a MYC epitope tag was used to allow identification of Tbx5-containing cells and comparison and quantification of cellular construct levels, using available monoclonal antibodies (Evan *et al.*, 1985). This construct was designated M-*mTbx5*/pUAST, I will also refer to it as the **M** construct for convenience. In the other (the control or **C** construct, designated C-*mTbx5*/pUAST), no *MYC* sequence is used. This will test whether any results (or lack of) obtained with M-*mTbx5*/pUAST have been influenced by the presence of the MYC tag at the N-terminal end of the Tbx5 protein.

The building of the M/C-mTbx5/pUAST constructs

The first step in building these constructs used a plasmid from **Chapter 6**: pBK-CMV with mutagenised mouse *Tbx5* cDNA minus the 3' untranslated region or utr (see **Chapter 6, Fig. 6.1C**). *Drosophila* nuclear genes exhibit a significantly different translation start consensus sequence (the Cavener consensus; Cavener, 1987) to that described by Kozak (based primarily on vertebrate mRNA sequences; Kozak, 1987). The 5' utr of the *Tbx5* cDNA was thus replaced with a sequence based on the Cavener consensus (that in the **M** construct included the *MYC* sequence immediately downstream of the ATG), using *Bss*HII (**Fig. A.1-A.2**). This was to enable efficient transgene expression in *Drosophila* cells. The modified *Tbx5* cDNA was then transferred into the germline transformation vector pUAST, via *Eco*RI and *Kpn*I (**Fig. A.3**). This vector allows GAL4-induced expression of an inserted open reading frame using the *GAL4/UAS*$_G$ binary system. Sequences of the M/C-*mTbx5* insert and flanking regions of the pUAST vector are given in **Fig. A.4**.

Predicted outcomes of M/C-mTbx5/pUAST expression in Drosophila

The first step will be to incorporate the two constructs into fly lines. The presence of a MYC tag at the N-terminal end of OMB does not impair its functional specificity in *Drosophila* (Porsch, 2002). Problems with MYC tag interference with *Tbx5* function

Figure A.1

The first step in the building of the M/C-*mTbx5*/pUAST constructs was to replace the 5' untranslated region (utr) of the mouse *Tbx5* cDNA (**A-C**):

A Two double-stranded DNA linkers used to replace the 5' utr of the *Tbx5* cDNA are shown. The *MYC*-containing or **M** linker above, and below it the control or **C** linker. Both linkers end with 5' overhangs compatible with ligation of DNA ends cut using *Bss*HII (**red**). Both linkers contain an *Eco*RI site (**cyan**) and a sequence (*CAAAATG*) to provide a favourable genetic context for expression in *Drosophila*. The **dark yellow** '**G**' forms a part of both the *Eco*RI site and the *Bss*HII-compatible end. The first 26 base pairs of the mouse *Tbx5* cDNA coding region (which ends with a *Bss*HII site) follow the **ATG** in the control linker. The **M** linker is identical to the control or **C** linker, but for an insertion of the *MYC* sequence (**blue**) immediately downstream of the **ATG**. Two pairs of complementary synthetic oligonucleotides were annealed to make the linkers:

1. MYC-tag sense: CGCGAATTCAAA***ATG***GAGCAGAAGCTGATCTCCGAGGAGGACC
   TGAACGCCGATACAGATGAGGGCTTTGGCCTGG
2. MYC-tag antisense: CGCGCCAGGCCAAAGCCCTCATCTGTATCGGCGTTCAGGTCCT
   CCTCGGAGATCAGCTTCTGCTC***CATTTT***GAATT
3. control sense: CGCGAATTCAAA***ATG***GCCGATACAGATGAGGGCTTTGGCCTGG
4. control antisense: CGCGCCAGGCCAAAGCCCTCATCTGTATCGGC***CATTTT***GAATT

B This cartoon depicts the removal of the 5' region of *mTbx5* using *Bss*HII. This 5' region ran from the *Bss*HII site located in the multiple cloning site of pBK-CMV (upstream to *mTbx5*) to the *Bss*HII site located 26 bases into the coding region of the *Tbx5* gene. The *mTbx5* 5' utr and sites for *Bss*HII (**red**), *Nhe*I (**pink**), *Sac*II (**brown**) and *Kpn*I (**green**) are labelled.

C This cartoon shows the insertion of the two linkers into the cut *mTbx5* to complete the exchange of the mouse *Tbx5* 5' utr with a context suitable for expression in *Drosophila*. Various components of the linkers including the *Eco*RI site (**cyan**), the *MYC* sequence (**blue**) and the *mTbx5* start are labelled.

Building of the *Tbx5*/pUAST constructs for expression in *Drosophila Melanogaster* (I)

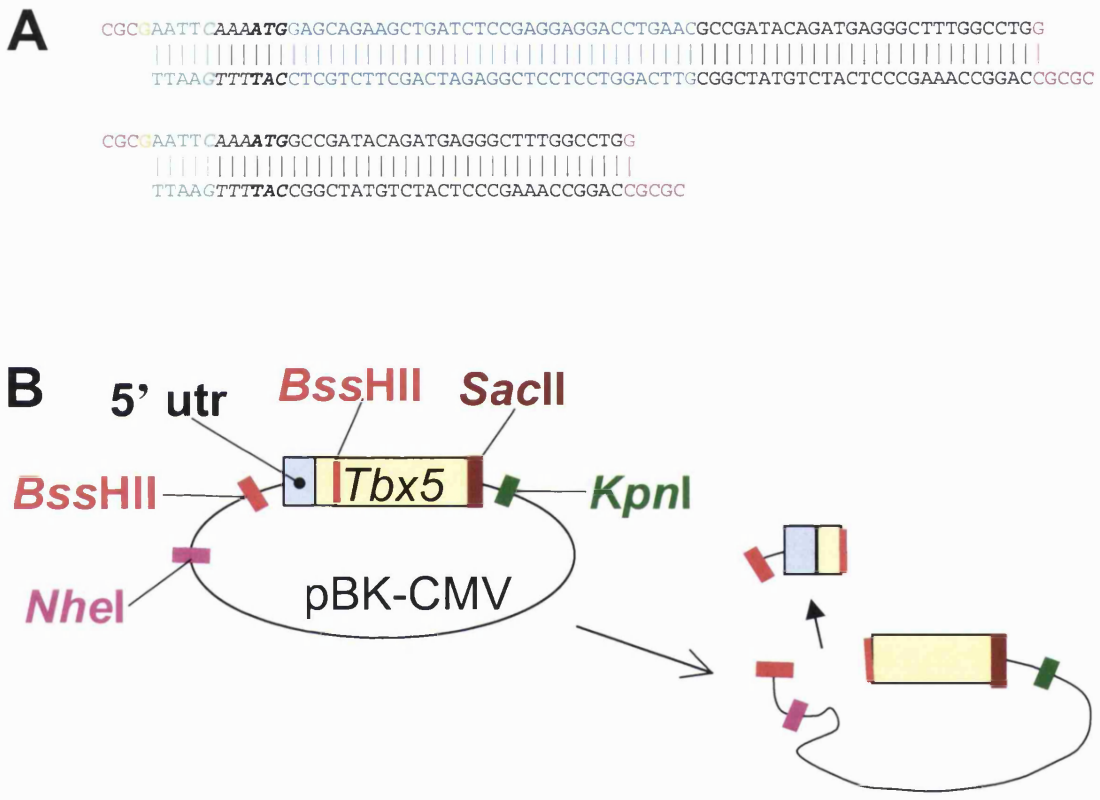

Figure A.2

Following the introduction of the **M** and **C** linkers into the *Bss*HII sites of the *Tbx5* plasmid, correct linker insertion and orientation needed to be checked (**A, B**):

A Ligated linker and plasmid were electroporated into *Escherichia coli* and several clones were obtained for both **M** and **C** ligations (7 and 17 respectively). A colony PCR was performed on the clones using primers flanking the region of the insert to determine which had taken up the insert. 4 control reactions were carried out with no DNA sample to ensure that the samples were not contaminated (**-**). The primers were expected to amplify a fragment of 199 base pairs (bp) if the linker had not been taken up and the cut vector had re-circularised. If the **C** linker or the **M** linker had been taken up then fragments of 242 and 265 bp respectively were expected.

Forward primer: GACCTTGATTACGCCAAGCTCG (**CMV-5'F**)
Reverse primer: CACCTTGATTCCTTCCATGCCC (***mTbx5*-R**)

Fragments of ~200 bp were amplified in the majority of the clones, suggesting that they contained only re-circularised vector. However, bands ~240 bp were amplified from 2 '**C**' clones (**C1** and **C5**) and ~260 bp from 3 '**M**' clones (**M3**, **M5** and **M17**). This suggested that these clones contained vector with linkers successfully incorporated. Clone **M4** was larger than expected at ~400 bp, suggesting that multiple copies of the **M** linker had been taken up.

B Clones that appeared to contain a single copy of the linker (**C1**, **C5**, **M3**, **M5** and **M17**) were amplified and the DNA was extracted. DNA was digested (**d**) with *Nhe*I (site present in the vector, see previous figure) and *Eco*RI (site present in the 5' end of the linker) and run with an uncut DNA sample (**U**). This was done (1) to confirm the presence of a single copy of the linker and (2) to determine the linker orientation. The digestion was expected to release a 185 bp fragment if a single linker was correctly inserted. If a single linker was inserted in the reverse orientation, then a 220 or a 253 bp fragment was expected for the **C** and the **M** linkers respectively. Fragments under 200 bp were released from all samples, indicating that the linker had inserted correctly in **C1**, **C5**, **M3**, **M5** and **M17**.

Colony PCR and diagnostic digests for the detection of inserted DNA linkers

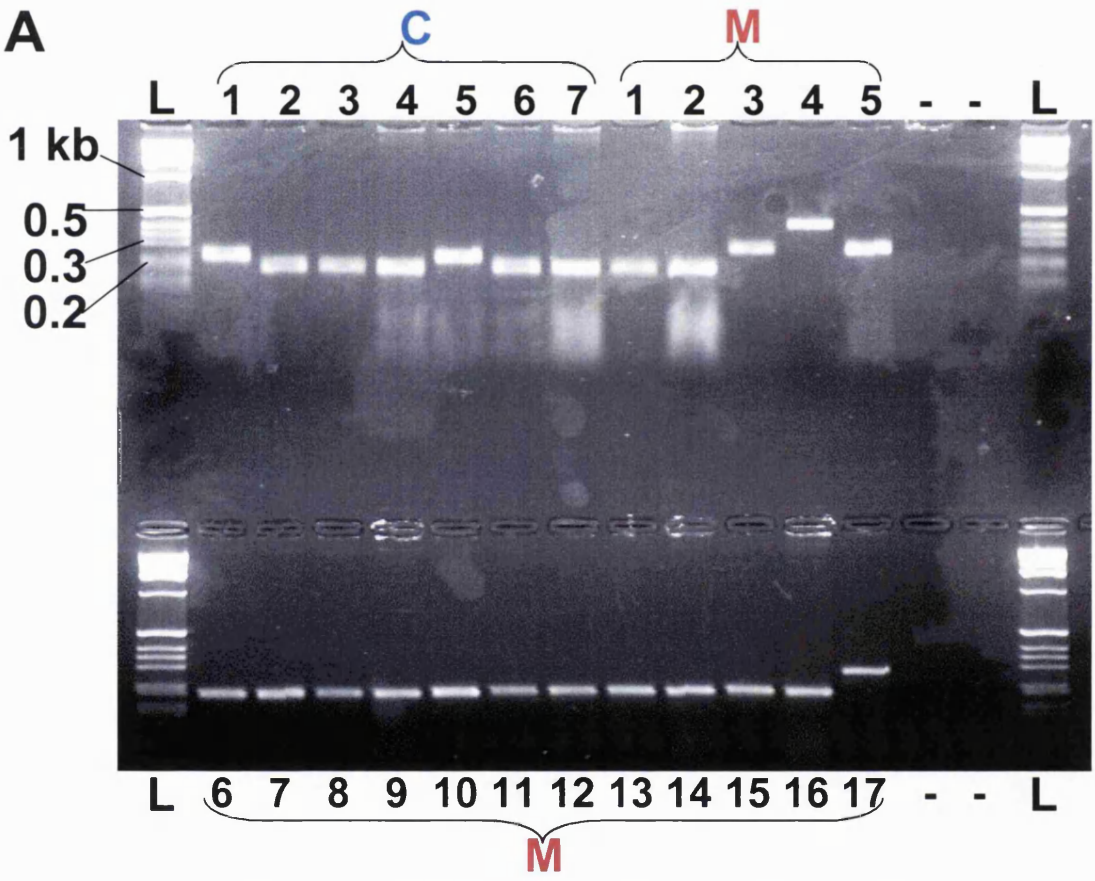

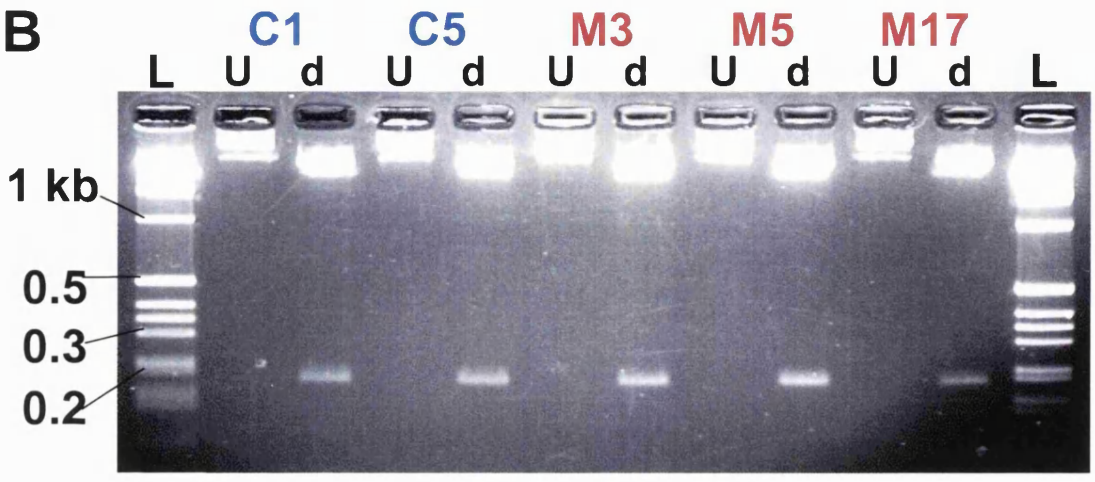

Figure A.3

M-*mTbx5* and C-*mTbx5* were excised and isolated from pBK-CMV (plasmids from clones **M3** and **C1** were used) using *Eco*RI and *Kpn*I followed by gel extraction. The multiple cloning site (MCS) of the pUAST vector was cut using *Eco*RI and *Kpn*I, gel extracted and then ligated with the isolated M-*mTbx5* or C-*mTbx5* to complete the two constructs (**A**, **B**):

A M-*mTbx5* and C-*mTbx5* were removed from pBK-CMV using *Eco*RI and *Kpn*I and transferred into *Eco*RI and *Kpn*I in the pUAST vector MCS. *Eco*RI (**cyan**) and *Kpn*I (**green**) sites are labelled and marked. *Bss*HII (**red**) and *Nhe*I (**pink**) sites are also marked.

B The completed constructs, M-*mTbx5*/pUAST and C-*mTbx5*/pUAST, are shown.

Building of the *Tbx5*/pUAST constructs for expression in *Drosophila Melanogaster* (II)

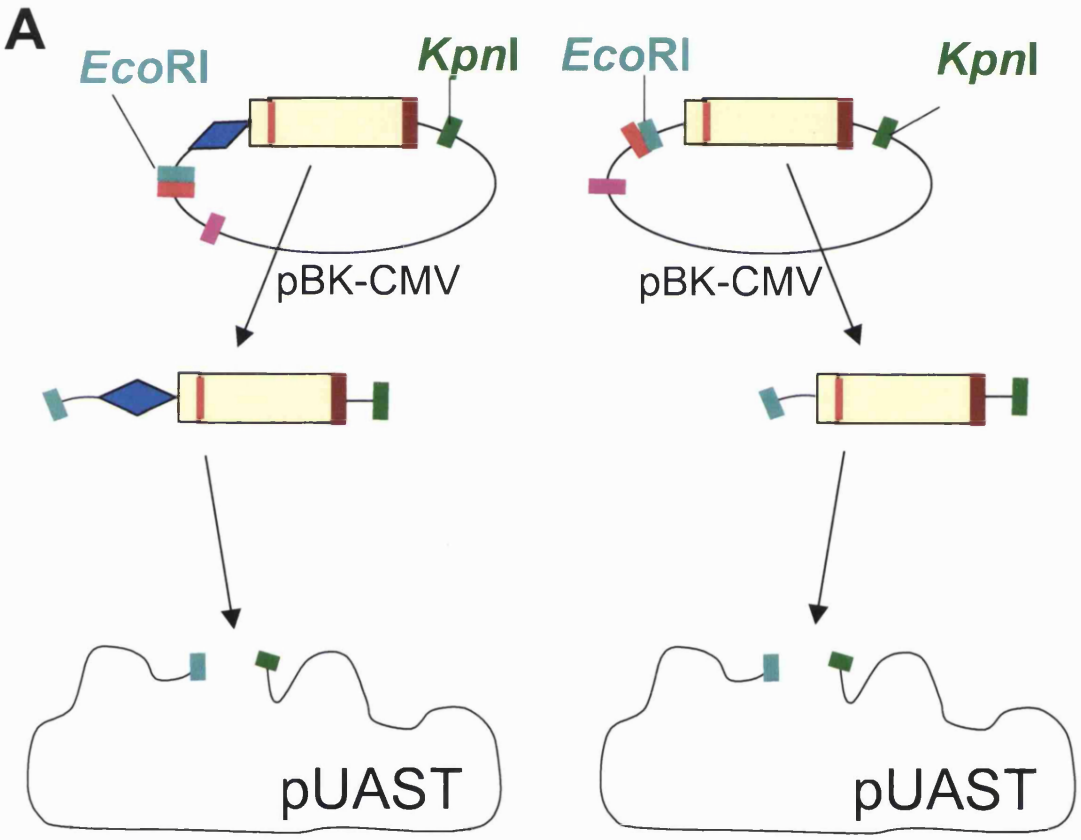

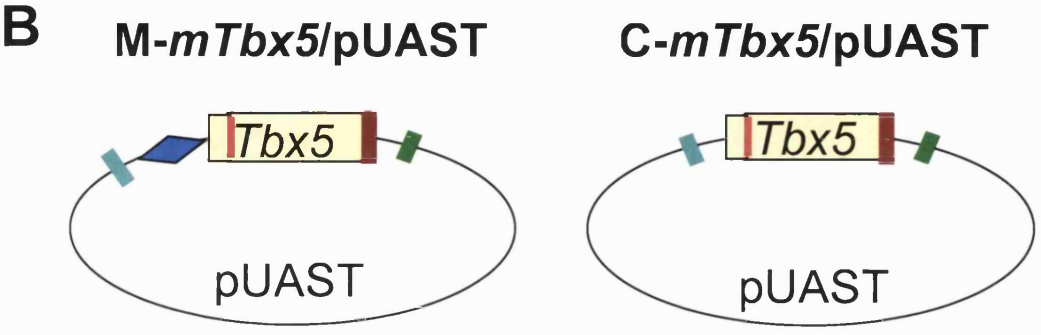

Figure A.4

The *Tbx5* cDNA and its flanking regions in the M/C-*mTbx5*/pUAST constructs were examined through sequencing to confirm that there were no mistakes in this area (particularly in the **C** and **M** linker region). Clones C1 and M3 were Primers **F2-F6** and **R2** from **Chapter 6**, **Fig. 6.2B** were used for sequencing (locations of the primer sites on the *Tbx5* cDNA, as part of *α-p0-Tbx5-ires-gfp-intron-pA*, are shown in **Fig 6.2B**). The primers used are listed here:

Forward primers:		*Reverse primers:*	
GAGCCCGACATCCTAGCTCC ----	**F2**	GGAACTTCAGCCACAGTTCACG --	**R2**
ACTCAGCGAGGCAATATGGT ----	**F3**		
GGGCAGTGATGACCTGGAGTTA --	**F4**		
GGCCTGAGTACCTCTTACAGGA --	**F5**		
CCCCCAGAGTTTCTCTACACTC --	**F6**		

The sequence of the modified *Tbx5* cDNA insert and surrounding regions of the pUAST multiple cloning site (MCS) are shown (**A**-**C**):

A 180 bases of the pUAST MCS are shown up to the *Eco*RI site (**cyan**) where the modified *Tbx5* cDNA was inserted.

B The manipulated *Tbx5* cDNA insert, flanked by an *Eco*RI site (**cyan**) at the 5' end and a *Kpn*I site (**green**) at the 3' end, is shown. The end of the *Eco*RI site begins a sequence that approximates to the Cavener consensus, italicised (*CAAA**ATG***). The **ATG** is in bold. This is followed by the *MYC* sequence (**blue**) in M-*mTbx5*/pUAST. This region is absent in C-*mTbx5*/pUAST. The *mTbx5* coding region then follows. The *Bss*HII site 28 bases into the *Tbx5* coding region, utilised to replace the endogenous *mTbx5* 5' utr with the **M** and **C** linkers, is shown in **red**) begins the pBK-CMV library linker and the start of the *Tbx5* cDNA is an '**A**' (in bold). The stop (**TAA**) codon is marked as is the downstream *Sac*II site (**pink**) where the *Tbx5* coding region was inserted into pBK-CMV.

C 180 bases of the pUAST MCS are shown from the *Kpn*I site (**green**) where the modified *Tbx5* cDNA was inserted.

The sequence of *Tbx5* within the *Tbx5*/pUAST constructs

A

AAGCGAAAGC TAAGCAAATA AACAAGCGCA GCTGAACAAG CTAAACAATC TGCAGTAAAG
TGCAAGTTAA AGTGAATCAA TTAAAAGTAA CCAGCAACCA AGTAAATCAA CTGCAACTAC
TGAAATCTGC CAAGAAGTAA TTATTGAATA CAAGAAGAGA ACTCTGAATA GGGAATTGGG

B

AATTCAAAAT GGAGCAGAAG CTGATCTCCG AGGAGGACCT GAACGCCGAT ACAGATGAGG
GCTTTGGCCT GGCGCGCACG CCTCTGGAGC CTGATTCCCA AGACAGGTCT TGCGATTCGA
AACCTGAGAG TGCTCTGGGG GCTCCCAGCA AGTCTCCATC ATCCCCGCAG GCTGCCTTCA
CCCAGCAGGG CATGGAAGGA ATCAAGGTGT TTCTTCATGA ACGTGAACTG TGGCTGAAGT
TCCACGAAGT GGGCACAGAG ATGATCATCA CCAAGGCAGG GAGGAGAATG TTTCCTAGTT
ACAAAGTGAA GGTGACTGGC CTTAATCCCA AAACGAAGTA TATTCTTCTC ATGGATATTG
TTCCCGCAGA CGACCACAGA TATAAATTTG CTGATAACAA ATGGTCCGTA ACTGGCAAAG
CAGAGCCTGC CATGCCGGGG CGCCTTTATG TGCACCCGGA CTCCCCAGCA ACCGGAGCCC
ACTGGATGCG ACAACTTGTC TCCTTCCAGA AGCTCAAACT CACCAACAAC CACCTGGACC
CGTTTGGACA CATTATCCTG AACTCCATGC ACAAATACCA GCCCCGATTA CACATCGTGA

AAGCAGACGA AAATAATGGG TTCGGTTCAA AGAACACTGC GTTTTGCACC CACGTCTTCC
CGGAGACAGC TTTTATCGCT GTGACTTCGT ACCAGAATCA CAAGATCACA CAGCTGAAAA
TTGAGAACAA CCCCTTCGCC AAAGGCTTTC GGGGCAGTGA TGACCTGGAG TTACACAGGA
TGTCTCGGAT GCAAAGTAAA GAGTATCCTG TGGTTCCCAG GAGCACAGTG AGGCACAAAG
TCACCTCCAA CCACAGCCCC TTCAGCAGCG AGACCCGAGC TCTCTCCACC TCATCCAATT
TAGGGTCCCA GTACCAGTGT GAGAATGGTG TCTCTGGCCC CTCCCAGGAC CTTCTGCCCC
CACCTAACCC ATACCCACTG GCCCAGGAGC ACAGCCAAAT TTACCACTGT ACCAAGAGGA
AAGATGAGGA ATGTTCCAGC ACGGAGCACC CCTATAAGAA GCCGTACATG GAGACATCCC
CCAGCGAGGA AGACACCTTC TATCGCTCGG GCTACCCCCA GCAGCAGGGC CTGAGTACCT
CTTACAGGAC AGAGTCGGCC CAGCGGCAGG CCTGCATGTA TGCCAGCTCC GCTCCCCCCA

GCGAGCCCGT GCCTAGCCTG GAGGACATCA GCTGTAACAC ATGGCCCAGC ATGCCCTCCT
ATAGCAGCTG TACCGTCACC ACCGTGCAGC CCATGGACCG TCTTCCCTAC CAGCACTTCT
CCGCTCATTT CACCTCGGGG CCCCTGGTCC CTCGGTTGGC TGGCATGGCC AACCATGGTT
CTCCCCAGCT CGGCGAAGGG ATGTTTCAGC ACCAGACCTC AGTGGCCCAT CAGCCTGTGG
TCAGGCAGTG CGGGCCTCAG ACTGGCCTTC AGTCTCCGGG CGGCCTCCAG CCCCCAGAGT
TTCTCTACAC TCACGGCGTG CCCAGGACCC TGTCCCCCCA TCAGTATCAC TCGGTACACG
GCGTCGGCAT GGTGCCAGAG TGGAGTGAGA ATAGCTAACC GCGGGCCCAT CGATTTTCCA
CCCGGGTGGG G

C

TACCTCTAGA GGATCTTTGT GAAGGAACCT TACTTCTGTG GTGTGACATA ATTGGACAAA
CTACCTACAG AGATTTAAAG CTCTAAGGTA AATATAAAAT TTTTAAGTGT ATAATGTGTT
AAACTACTGA TTCTAATTGT TTGTGTATTT TAGATTCCAA CCTATGGAAC TGATGAATGG

(in the **M** construct) are therefore not predicted, but cannot be excluded, hence the need for an additional construct (the **C** construct) to control for this possibility. Transgenic fly lines with these constructs will be crossed with flies expressing *Gal4* under control of a *glass* enhancer in primary experiments. This will provide strong *Gal4* expression (and so activate M/C-*mTbx5* expression) in all cells behind the morphogenetic furrow, *i.e.* differentiating photoreceptors (Ellis *et al.*, 1993). Experiments by Matthias Porsch and Gert Pflugfelder have used the same *Gal4* driver to misexpress *Drosophila* T-box genes *omb* and *omb-related gene-1* (*org-1*) in the same population of cells (Porsch, 2002). Misexpression of *org-1*, of the *Tbx1* subfamily (Porsch *et al.*, 1998), produced quite normal-looking eyes, albeit with a roughened appearance. *omb* misexpression led to degenerate ommatidia and diffuse pigmentation. OMB/ORG-1 domain swap experiments revealed that T-domain, N-terminal and C-terminal regions of OMB could promote the *omb* misexpression phenotype (Porsch, 2002).

It is uncertain what the effect of *Tbx5* misexpression in differentiating *Drosophila* photoreceptors will be. There are two main reasons why a different result to that with *omb* misexpression might occur. The obvious reason is the species difference. *mTbx5* may have no effect at all, or produce a different phenotype to *omb* altogether. In work out of my laboratory in collaboration with Alison Woollard (Oxford, UK), mouse *Tbx20* was misexpressed in the *C. elegans male abnormal* (*mab-9*) mutant (deficient in *Tbx20* orthologue *tbx12*; Woollard and Hodgkin, 2000). Preliminary data suggests a worsening of the *mab-9* phenotype, despite the orthologous status of mouse *Tbx20* with *tbx12*.

The second reason that *Tbx5* might not produce a similar phenotype to *omb* in *Drosophila* photoreceptors, is if *mTbx5* is not functionally orthologous to *omb*. Despite being the only known member of the *Tbx2/3/4/5* subfamily in *Drosophila*, *omb* has been strongly linked to the *Tbx2/3* branch by phylogenetic analysis (Agulnik *et al.*, 1996). This analysis suggested (with 99% confidence) that the duplication event proposed to generate *Tbx2/3* and *Tbx4/5* precursors occurred well before the divergence of *omb* from the *Tbx2/3* branch (see **Chapter 1, Fig. 1.6** for T-box phylogenetic tree). The existence of an ancient metazoan *Tbx4/5* gene was thus postulated (Agulnik *et al.*, 1996). This would imply that an invertebrate *Tbx4/5*

orthologue was either lost during evolution or awaits discovery (perhaps the 'true' *mTbx5* orthologue in the fly). *Tbx2* and *Tbx3* seem to function primarily as transcriptional repressors (Carreira *et al.*, 1998; He *et al.*, 1999) while *mTbx5* is known to function as an activator of transcription (Bruneau *et al.*, 2001). Thus if *omb* is functionally closer to *Tbx2/3* then *mTbx5* may, even if it were capable of action in *Drosophila*, act not only on different types of genes to *omb* but in different ways.

If interesting results are obtained, domain swap experiments will be considered to determine whether it is only the homologous T-box region of *mTbx5* that is active in *Drosophila*. In the light of these experiments, the possibility of further experiments, such as attempts to rescue the *omb* phenotype with *Tbx5*, can be investigated.

Appendix II

Expression of *CRX/Crx* during mammalian eye development

Cone-rod homeobox gene (*CRX*) is a member of the *OTX*-like homeobox gene family, a family of genes that encode paired-like homeodomain transcription factors. Mutations in *CRX* cause severe eye disease and blindness in humans (Furukawa *et al.*, 1997; Sohocki *et al.*, 1998). *Crx*-null mice fail to develop the light-detecting outer segments of rod and cone photoreceptors and are blind (Furukawa *et al.*, 1999). Members of my laboratory and that of Cheryl Gregory-Evans (Imperial College London) have been interested in the role of *CRX* in retinal development for some time. We collaborated to examine the developmental expression of *CRX/Crx* in the human and mouse eye (Bibb *et al.*, 2001). This is the first time *CRX* expression has been examined in the human eye. The aims of these experiments were (1) to provide insight into the pathophysiology of retinal dystrophies caused by *CRX* mutations in humans and (2) to validate the use of rodent models for the understanding of *CRX*-linked human disease. My role in this study was to carry out *in situ* hybridisation of *CRX* during human eye development, to prepare human sections for immunohistochemistry and to prepare RNA samples for RT-PCR analysis from human tissues.

Using RT-PCR, *CRX* expression was found to begin between 9.5 and 10.5 weeks post-conception (wpc) in the human eye. This is the stage just prior to the onset of photoreceptor development, when the inner and outer layers of the early retina are well established. In the mouse, the onset of *Crx* expression was found to be at embryonic day 10.5 (E10.5), a comparatively early stage of development. At this stage the optic cup has only just formed and retinal stratification has yet to begin. In both cases expression was detected at later stages, including adult retina. Using *in situ* hybidisation, human *CRX* expression was first detected at 13 wpc in the outermost neural retina, the site of differentiating photoreceptors. The later onset of *CRX* expression detected with this method was thought to be due to the reduced sensitivity of this technique. By 15 wpc, when all three cellular layers of the mature neural retina are established, strong *CRX* expression was detected in the outer nuclear layer (ONL)

in the human eye. CRX protein was first detected (using immunohistochemistry) in the ONL at this stage. *CRX* expression was also detected in the inner nuclear layer (INL) at 15 wpc where labelling was punctate, suggesting only a subset of retinal cells expressed *CRX* in this layer. ONL and the weaker INL expression of *CRX* were similarly detected in the adult human retina. *In situ* hybridisation and immunohistochemistry revealed *Crx* expression and protein distribution in both the ONL and the INL of the adult mouse retina. Interestingly, strong INL expression of *Crx* was detected in mice lacking rod and cone photoreceptors, which do not possess an ONL of the retina.

This study has shown that the expression of human *CRX* and mouse *Crx* are broadly similar, with strong expression in cells of the developing ONL and weaker expression in a subset of cells of the INL. This is consistent with previous observations in mice (Chen *et al.*, 2000) and in zebrafish (Liu *et al.*, 2001), suggesting evolutionarily conserved functions of this gene in retinal development. *Crx* was expressed in mice with a complete absence of rod and cone photoreceptors (*rd/rd,cl* mice). It is possible that this INL expression is in other photoreceptor types. The regulation of circadian rhythms depends on the presence of eyes and hence retinal photoreceptors. Circadian entrainment is attenuated in *Crx* null mice (Furukawa *et al.*, 1999). In *rd/rd,cl* mice however, circadian behaviour and physiology are unaffected (Freedman *et al.*, 1999; Lucas *et al.*, 1999). Taken together, these data suggest that *Crx* is active in non-rod non-cone photoreceptors to control regulation of circadian rhythms. Furthermore, these photoreceptors may correspond to the *Crx*-expressing subset of cells in the INL. This possibility is under current investigation by Cheryl Gregory-Evans and colleagues.

One difference that was highlighted between human *CRX* and mouse *Crx* expression was the earlier onset of expression in the mouse. It is not clear what the role of Crx might be in the newly formed mouse optic cup. At this stage the neural retina contains undifferentiated retinal precursors and *Crx* may have roles in differentiation outside photoreception at this time, perhaps contributing to the complex transcription factor network that controls retinal differentiation. Another feature that arises from this temporal discrepancy in *CRX/Crx* expression is that human CRX becomes an unsuitable candidate for the induction of early expressed photoreceptor genes, some of

which are transactivated by CRX *in vitro* (Chen *et al.*, 1997). The late detection of CRX protein, relative to *CRX* expression, in the human, might reflect limitations to the sensitivity of the immunohistochemistry, but could indicate post-translational control of *CRX* expression. The importance of CRX/Crx in photoreception suggests it can regulate the expression of effector molecules essential for phototransduction. This suggestion is supported by microarray analysis of *Crx* +/+ and -/- retinas (Livesey *et al.*, 2000). Transcription factors tend to function in networks. The same is likely to be true of *CRX/Crx* in the regulation of photoreceptor-specific genes. The relationship of CRX/Crx with other photoreceptor transcription factors, as well to downstream targets, will need to be elucidated to fully understand its role in phototransduction.

Appendix III

Published research papers

1. Sowden JC, Holt JKL, Meins M, Smith HK, Bhattacharya SS (2001) Expression of *Drosophila omb*-related T-box genes in the developing human and mouse neural retina. Investigative Ophthalmology & Visual Science 42(13): 3095-3102.

2. Gouge A, Holt JKL, Hardy AP, Sowden JC, Smith HK (2001) Foxn4 - a new member of the forkhead gene family is expressed in the retina. Mechanisms of Development 107(1-2): 203-206.

3. Bibb LC, Holt JKL, Tarttelin EE, Hodges MD, Gregory-Evans K, Rutherford A, Lucas RJ, Sowden JC and Gregory-Evans (2001) Temporal and spatial expression patterns of the CRX transcription factor and its downstream targets. Critical differences during human and mouse eye development. Human Molecular Genetics 10(15): 1571-1579.

References

Acampora, D., S. Mazan, et al. (1995). Forebrain and midbrain regions are deleted in Otx2-/- mutants due to a defective anterior neuroectoderm specification during gastrulation. *Development* **121**(10): 3279-90.

Agulnik, S. I., N. Garvey, et al. (1996). Evolution of mouse T-box genes by tandem duplication and cluster dispersion. *Genetics* **144**(1): 249-54.

Ahn, D., I. Ruvinsky, et al. (2000). tbx20, a new vertebrate T-box gene expressed in the cranial motor neurons and developing cardiovascular structures in zebrafish. *Mech Dev* **95**(1-2): 253-8.

Altshuler, D. M., D. L. Turner, et al. (1991). Specification of cell type in the vertebrate retina. *Development of the visual system*. D. M.-K. Lam and C. J. Shatz. Cambridge, Massachusetts, MIT Press**:** 37-58.

Andreazzoli, M., G. Gestri, et al. (1999). Role of Xrx1 in Xenopus eye and anterior brain development. *Development* **126**(11): 2451-60.

Ang, H. L. and G. Duester (1999). Retinoic acid biosynthetic enzyme ALDH1 localizes in a subset of retinoid-dependent tissues during xenopus development. *Dev Dyn* **215**(3): 264-72.

Araujo, H., M. Menezes, et al. (1997). Blockage of 9-O-acetyl gangliosides induces microtubule depolymerisation in growth cones and neurites. *Eur. J. Cell Biol.* **72**: 202-13.

Ashery-Padan, R., T. Marquardt, et al. (2000). Pax6 activity in the lens primordium is required for lens formation and for correct placement of a single retina in the eye. *Genes Dev* **14**(21): 2701-11.

Austin, C. P., D. E. Feldman, et al. (1995). Vertebrate retinal ganglion cells are selected from competent progenitors by the action of Notch. *Development* **121**(11): 3637-50.

Azuma, N., A. Hirakiyama, et al. (2000). Mutations of a human homologue of the Drosophila eyes absent gene (EYA1) detected in patients with congenital cataracts and ocular anterior segment anomalies. *Hum Mol Genet* **9**(3): 363-6.

Baker, N. E. (2001). Master regulatory genes; telling them what to do. *Bioessays* **23**(9): 763-6.

Bamshad, M., R. C. Lin, et al. (1997). Mutations in human TBX3 alter limb, apocrine and genital development in ulnar-mammary syndrome. *Nat Genet* **16**(3): 311-5.

Barbieri, A. M., V. Broccoli, et al. (2002). Vax2 inactivation in mouse determines alteration of the eye dorsal-ventral axis, misrouting of the optic fibres and eye coloboma. *Development* **129**(3): 805-13.

Barbieri, A. M., G. Lupo, et al. (1999). A homeobox gene, vax2, controls the patterning of the eye dorsoventral axis. *Proc. Natl. Acad. Sci. USA* **96**(19): 10729-34.

Basson, C. T., D. R. Bachinsky, et al. (1997). Mutations in human TBX5 cause limb and cardiac malformations in Holt-Oram syndrome. *Nat. Genet.* **15**: 30-5.

Basson, C. T., T. Huang, et al. (1999). Different TBX5 interactions in heart and limb defined by Holt-Oram syndrome mutations. *Proc Natl Acad Sci U S A* **96**(6): 2919-24.

Begemann, G. and P. W. Ingham (2000). Developmental regulation of Tbx5 in zebrafish embryogenesis. *Mech Dev* **90**(2): 299-304.

Bei, M., K. Kratochwil, et al. (2000). BMP4 rescues a non-cell-autonomous function of Msx1 in tooth development. *Development* **127**(21): 4711-8.

Belecky-Adams, T. and R. Adler (2001). Developmental expression patterns of bone morphogenetic proteins, receptors, and binding proteins in the chick retina. *J Comp Neurol* **430**(4): 562-72.

Belecky-Adams, T., S. Tomarev, et al. (1997). Pax-6, Prox 1, and Chx10 homeobox gene expression correlates with phenotypic fate of retinal precursor cells. *Invest Ophthalmol Vis Sci* **38**(7): 1293-303.

Belecky-Adams, T. L., D. Scheurer, et al. (1999). Activin family members in the developing chick retina: expression patterns, protein distribution, and in vitro effects. *Dev Biol* **210**(1): 107-23.

Bellairs, R. and M. Osmond (1998). *The Atlas of Chick Development.* London, Academic Press.

Belloni, E., M. Muenke, et al. (1996). Identification of Sonic hedgehog as a candidate gene responsible for holoprosencephaly. *Nat Genet* **14**(3): 353-6.

Benson, D. W., G. M. Silberbach, et al. (1999). Mutations in the cardiac transcription factor NKX2.5 affect diverse cardiac developmental pathways. *J Clin Invest* **104**(11): 1567-73.

Bentley, N. J., T. Eisen, et al. (1994). Melanocyte-specific expression of the human tyrosinase promoter: activation by the microphthalmia gene product and role of the initiator. *Mol Cell Biol* **14**(12): 7996-8006.

Berggren, K., P. McCaffery, et al. (1999). Differential distribution of retinoic acid synthesis in the chicken embryo as determined by immunolocalization of the retinoic acid synthetic enzyme, RALDH-2. *Dev Biol* **210**(2): 288-304.

Bernards, A. and I. K. Hariharan (2001). Of flies and men--studying human disease in Drosophila. *Curr Opin Genet Dev* **11**(3): 274-8.

Bernier, G., F. Panitz, et al. (2000). Expanded retina territory by midbrain transformation upon overexpression of Six6 (Optx2) in Xenopus embryos. *Mech Dev* **93**(1-2): 59-69.

Bertuzzi, S., R. Hindges, et al. (1999). The homeodomain protein vax1 is required for axon guidance and major tract formation in the developing forebrain. *Genes Dev* **13**(23): 3092-105.

Bessant, D. A., R. R. Ali, et al. (2001). Molecular genetics and prospects for therapy of the inherited retinal dystrophies. *Curr Opin Genet Dev* **11**(3): 307-16.

Bibb, L. C., J. K. Holt, et al. (2001). Temporal and spatial expression patterns of the CRX transcription factor and its downstream targets. Critical differences during human and mouse eye development. *Hum Mol Genet* **10**(15): 1571-9.

Birgbauer, E., C. A. Cowan, et al. (2000). Kinase independent function of EphB receptors in retinal axon pathfinding to the optic disc from dorsal but not ventral retina. *Development* **127**(6): 1231-41.

Birgbauer, E., S. F. Oster, et al. (2001). Retinal axon growth cones respond to EphB extracellular domains as inhibitory axon guidance cues. *Development* **128**(15): 3041-8.

Bollag, R. J., Z. Siegfried, et al. (1994). An ancient family of embryonically expressed mouse genes sharing a conserved protein motif with the T locus. *Nat Genet* **7**(3): 383-9.

Bora, N., S. J. Conway, et al. (1998). Transient overexpression of the Microphthalmia gene in the eyes of Microphthalmia vitiligo mutant mice. *Dev Dyn* **213**(3): 283-92.

Bovolenta, P., A. Mallamaci, et al. (1997). Implication of OTX2 in pigment epithelium determination and neural retina differentiation. *J Neurosci* **17**(11): 4243-52.

Braisted, J. E., T. McLaughlin, et al. (1997). Graded and lamina-specific distributions of ligands of EphB receptor tyrosine kinases in the developing retinotectal system. *Dev. Biol.* **191**: 14-28.

Braybrook, C., K. Doudney, et al. (2001). The T-box transcription factor gene TBX22 is mutated in X-linked cleft palate and ankyloglossia. *Nat Genet* **29**(2): 179-83.

Brook, W. J. and S. M. Cohen (1996). Antagonistic interactions between wingless and decapentaplegic responsible for dorsal-ventral pattern in the Drosophila Leg. *Science* **273**(5280): 1373-7.

Brown, N. L., S. Patel, et al. (2001). Math5 is required for retinal ganglion cell and optic nerve formation. *Development* **128**(13): 2497-508.

Brummelkamp, T. R., R. M. Kortlever, et al. (2002). TBX-3, the gene mutated in Ulnar-Mammary Syndrome, is a negative regulator of p19ARF and inhibits senescence. *J Biol Chem* **277**(8): 6567-72.

Bruneau, B. G., M. Logan, et al. (1999). Chamber-specific cardiac expression of Tbx5 and heart defects in Holt-Oram syndrome. *Dev Biol* **211**(1): 100-8.

Bruneau, B. G., G. Nemer, et al. (2001). A murine model of holt-oram syndrome defines roles of the t-box transcription factor tbx5 in cardiogenesis and disease. *Cell* **106**(6): 709-21.

Bumsted, K. M. and C. J. Barnstable (2000). Dorsal retinal pigment epithelium differentiates as neural retina in the microphthalmia (mi/mi) mouse. *Invest Ophthalmol Vis Sci* **41**(3): 903-8.

Burmeister, M., J. Novak, et al. (1996). Ocular retardation mouse caused by Chx10 homeobox null allele: impaired retinal progenitor proliferation and bipolar cell differentiation. *Nat Genet* **12**(4): 376-84.

Campbell, C., K. Goodrich, et al. (1995). Cloning and mapping of a human gene (TBX2) sharing a highly conserved protein motif with the Drosophila omb gene. *Genomics* **28**(2): 255-60.

Carreira, S., T. J. Dexter, et al. (1998). Brachyury-related transcription factor Tbx2 and repression of the melanocyte-specific TRP-1 promoter. *Mol Cell Biol* **18**(9): 5099-108.

Carreira, S., B. Liu, et al. (2000). The gene encoding the T-box factor Tbx2 is a target for the microphthalmia-associated transcription factor in melanocytes. *J Biol Chem* **275**(29): 21920-7.

Carson, C. T., E. R. Kinzler, et al. (2000). Tbx12, a novel T-box gene, is expressed during early stages of heart and retinal development. *Mech Dev* **96**(1): 137-40.

Cavener, D. R. (1987). Comparison of the consensus sequence flanking translational start sites in Drosophila and vertebrates. *Nucleic Acids Res* **15**(4): 1353-61.

Cepko, C. L., C. P. Austin, et al. (1996). Cell fate determination in the vertebrate retina. *Proc Natl Acad Sci U S A* **93**(2): 589-95.

Chader, G. J. (2002). Animal models in research on retinal degenerations: past progress and future hope. *Vision Res* **42**(4): 393-9.

Chambon, P. (1996). A decade of molecular biology of retinoic acid receptors. *Faseb J* **10**(9): 940-54.

Chan, S. O. and K. Y. Chung (1999). Changes in axon arrangement in the retinofugal pathway of mouse embryos: confocal microscopy study using single- and double-dye label. *J Comp Neurol* **406**(2): 251-62.

Chan, S. O., K. Y. Chung, et al. (1999). The effects of early prenatal monocular enucleation on the routing of uncrossed retinofugal axons and the cellular environment at the chiasm of mouse embryos. *Eur J Neurosci* **11**(9): 3225-35.

Chan, S. O. and R. W. Guillery (1994). Changes in fiber order in the optic nerve and tract of rat embryos. *J Comp Neurol* **344**(1): 20-32.

Chang, C. and A. Hemmati-Brivanlou (1999). Xenopus GDF6, a new antagonist of noggin and a partner of BMPs. *Development* **126**(15): 3347-57.

Chang, W., F. D. Nunes, et al. (1999). Ectopic noggin blocks sensory and nonsensory organ morphogenesis in the chicken inner ear. *Dev Biol* **216**(1): 369-81.

Chapman, D. L., N. Garvey, et al. (1996). Expression of the T-box family genes, Tbx1-Tbx5, during early mouse development. *Dev. Dyn.* **206**(4): 379-90.

Chen, S., B. McMahon, et al. (2000). Localisation of the CRX protein in the mature and developing mouse retina. *Invest Ophthalmol Vis Sci* **41**: S392.

Chen, S., Q. L. Wang, et al. (1997). Crx, a novel Otx-like paired-homeodomain protein, binds to and transactivates photoreceptor cell-specific genes. *Neuron* **19**(5): 1017-30.

Cheng, H. J., M. Nakamoto, et al. (1995). Complementary gradients in expression and binding of elf-1 and mek4 in development of the topographical retinotectal projection map. *Cell* **82**: 371-81.

Chiang, C., Y. Litingtung, et al. (1996). Cyclopia and defective axial patterning in mice lacking Sonic hedgehog gene function. *Nature* **383**(6599): 407-13.

Chow, L., E. M. Levine, et al. (1998). The nuclear receptor transcription factor, retinoid-related orphan receptor beta, regulates retinal progenitor proliferation. *Mech Dev* **77**(2): 149-64.

Chow, R. L., C. R. Altmann, et al. (1999). Pax6 induces ectopic eyes in a vertebrate. *Development* **126**(19): 4213-22.

Chow, R. L. and R. A. Lang (2001). Early eye development in vertebrates. *Annu Rev Cell Dev Biol* **17**: 255-96.

Chung, K. Y., D. K. Shum, et al. (2000). Expression of chondroitin sulfate proteoglycans in the chiasm of mouse embryos. *J Comp Neurol* **417**(2): 153-63.

Collinson, J. M., R. E. Hill, et al. (2000). Different roles for Pax6 in the optic vesicle and facial epithelium mediate early morphogenesis of the murine eye. *Development* **127**(5): 945-56.

Connor, R. J., P. Menzel, et al. (1998). Expression and tyrosine phosphorylation of Eph receptors suggest multiple mechanisms in patterning of the visual system. *Dev Biol* **193**(1): 21-35.

Constantine-Paton, M., A. S. Blum, et al. (1986). A cell surface molecule distributed in a dorsoventral gradient in the perinatal rat retina. *Nature* **324**: 459-62.

Copp, A., P. Cogram, et al. (1997). Neurulation and neural tube closure defects. *Methods in Molecular Biology, Vol. 136: Developmental Biology Protocols*. R. S. Tuan and C. W. Lo. Totowa, NJ, Humana Press Inc. **II:** 135-59.

Davidson, A. J., J. H. Postlethwait, et al. (1999). Isolation of zebrafish gdf7 and comparative genetic mapping of genes belonging to the growth/differentiation factor 5, 6, 7 subgroup of the TGF-beta superfamily. *Genome Res* **9**(2): 121-9.

Davis, J. A. and R. R. Reed (1996). Role of Olf-1 and Pax-6 transcription factors in neurodevelopment. *J Neurosci* **16**(16): 5082-94.

Davy, A. and S. M. Robbins (2000). Ephrin-A5 modulates cell adhesion and morphology in an integrin-dependent manner. *Embo J* **19**(20): 5396-405.

de Iongh, R. and J. W. McAvoy (1993). Spatio-temporal distribution of acidic and basic FGF indicates a role for FGF in rat lens morphogenesis. *Dev Dyn* **198**(3): 190-202.

de la Torre, J. R., V. H. Hopker, et al. (1997). Turning of retinal growth cones in a netrin-1 gradient mediated by the netrin receptor DCC. *Neuron* **19**(6): 1211-24.

Dewulf, N., K. Verschueren, et al. (1995). Distinct spatial and temporal expression patterns of two type I receptors for bone morphogenetic proteins during mouse embryogenesis. *Endocrinology* **136**(6): 2652-63.

Dheen, T., I. Sleptsova-Friedrich, et al. (1999). Zebrafish tbx-c functions during formation of midline structures. *Development* **126**(12): 2703-13.

Dono, R., G. Texido, et al. (1998). Impaired cerebral cortex development and blood pressure regulation in FGF-2-deficient mice. *Embo J* **17**(15): 4213-25.

Dowling, J. E. and G. Wald (1960). The biological function of vitamin A acid. *Proc Natl Acad Sci U S A* **46**: 587-608.

Drager, U. C., H. Li, et al. (2001). Retinoic acid synthesis and breakdown in the developing mouse retina. *Prog Brain Res* **131**: 579-87.

Drager, U. C. and J. F. Olsen (1980). Origins of crossed and uncrossed retinal projections in pigmented and albino mice. *J Comp Neurol* **191**(3): 383-412.

Drager, U. C. and J. F. Olsen (1981). Ganglion cell distribution in the retina of the mouse. *Invest Ophthalmol Vis Sci* **20**(3): 285-93.

Drescher, U., C. Kremoser, et al. (1995). In vitro guidance of retinal ganglion cell axons by RAGS, a 25 kDa tectal protein related to ligands for Eph receptor tyrosine kinases. *Cell* **82**(3): 359-70.

Dudley, A. T., R. E. Godin, et al. (1999). Interaction between FGF and BMP signaling pathways regulates development of metanephric mesenchyme. *Genes Dev* **13**(12): 1601-13.

Dudley, A. T. and E. J. Robertson (1997). Overlapping expression domains of bone morphogenetic protein family members potentially account for limited tissue defects in BMP7 deficient embryos. *Dev Dyn* **208**(3): 349-62.

Dyer, M. A. and C. L. Cepko (2001). Regulating proliferation during retinal development. *Nat Rev Neurosci* **2**(5): 333-42.

Eblaghie, M. C., S.-J. Song, et al. (2002). *Specifying position and identity: expression of Tbx2 and Tbx3 in limb and mammary gland.* T box genes in development and disease, University of Nottingham.

Ehrlich, D. and R. Mark (1984). The course of axons of retinal ganglion cells within the optic nerve and tract of the chick (Gallus gallus). *J Comp Neurol* **223**(4): 583-91.

Eichele, G. and C. Thaller (1987). Characterization of concentration gradients of a morphogenetically active retinoid in the chick limb bud. *J Cell Biol* **105**(4): 1917-23.

Ekker, M., M. A. Akimenko, et al. (1997). Relationships among msx gene structure and function in zebrafish and other vertebrates. *Mol Biol Evol* **14**(10): 1008-22.

Ekker, S. C., A. R. Ungar, et al. (1995). Patterning activities of vertebrate hedgehog proteins in the developing eye and brain. *Curr Biol* **5**(8): 944-55.

Ellis, M. C., E. M. O'Neill, et al. (1993). Expression of Drosophila glass protein and evidence for negative regulation of its activity in non-neuronal cells by another DNA-binding protein. *Development* **119**(3): 855-65.

England, M. A. (1996). *Life before birth*. London, Mosby-Wolfe.

Enwright, J. F., 3rd and R. M. Grainger (2000). Altered Retinoid Signaling in the Heads of Small eye Mouse Embryos. *Dev Biol* **221**(1): 10-22.

Eph Nomenclature Committee (1997). Unified nomenclature for Eph family receptors and their ligands, the ephrins. *Cell* **90**(3): 403-4.

Ericson, J., S. Norlin, et al. (1998). Integrated FGF and BMP signaling controls the progression of progenitor cell differentiation and the emergence of pattern in the embryonic anterior pituitary. *Development* **125**(6): 1005-15.

Erkman, L., R. J. McEvilly, et al. (1996). Role of transcription factors Brn-3.1 and Brn-3.2 in auditory and visual system development. *Nature* **381**(6583): 603-6.

Erkman, L., P. A. Yates, et al. (2000). A POU domain transcription factor-dependent program regulates axon pathfinding in the vertebrate visual system. *Neuron* **28**(3): 779-92.

Evan, G. I., G. K. Lewis, et al. (1985). Isolation of monoclonal antibodies specific for human c-myc proto-oncogene product. *Mol Cell Biol* **5**(12): 3610-6.

Faber, S. C., P. Dimanlig, et al. (2001). Fgf receptor signaling plays a role in lens induction. *Development* **128**(22): 4425-38.

Feldheim, D. A., Y. I. Kim, et al. (2000). Genetic analysis of ephrin-A2 and ephrin-A5 shows their requirement in multiple aspects of retinocollicular mapping. *Neuron* **25**(3): 563-74.

Ferda Percin, E., L. A. Ploder, et al. (2000). Human microphthalmia associated with mutations in the retinal homeobox gene CHX10. *Nat Genet* **25**(4): 397-401.

Fougerousse, F., P. Bullen, et al. (2000). Human-mouse differences in the embryonic expression patterns of developmental control genes and disease genes. *Hum Mol Genet* **9**(2): 165-73.

Francis-West, P. H., T. Tatla, et al. (1994). Expression patterns of the bone morphogenetic protein genes Bmp-4 and Bmp-2 in the developing chick face suggest a role in outgrowth of the primordia. *Devl. Dynamics* **201**: 168-78.

Freedman, M. S., R. J. Lucas, et al. (1999). Regulation of mammalian circadian behavior by non-rod, non-cone, ocular photoreceptors. *Science* **284**(5413): 502-4.

Fuhrmann, S., E. M. Levine, et al. (2000). Extraocular mesenchyme patterns the optic vesicle during early eye development in the embryonic chick. *Development* **127**(21): 4599-609.

Furukawa, T., E. M. Morrow, et al. (1997). Crx, a novel otx-like homeobox gene, shows photoreceptor-specific expression and regulates photoreceptor differentiation. *Cell* **91**(4): 531-41.

Furukawa, T., E. M. Morrow, et al. (1999). Retinopathy and attenuated circadian entrainment in Crx-deficient mice. *Nat Genet* **23**(4): 466-70.

Furuta, Y. and B. L. M. Hogan (1998). BMP4 is essential for lens induction in the mouse embryo. *Genes Dev* **12**(23): 3764-75.

Gale, N. W., S. J. Holland, et al. (1996). Eph receptors and ligands comprise two major specificity subclasses and are reciprocally compartmentalized during embryogenesis. *Neuron* **17**(1): 9-19.

Gan, L., S. W. Wang, et al. (1999). POU domain factor Brn-3b is essential for retinal ganglion cell differentiation and survival but not for initial cell fate specification. *Dev. Biol.* **210**(2): 469-80.

Gan, L., M. Xiang, et al. (1996). POU domain factor Brn-3b is required for the development of a large set of retinal ganglion cells. *Proc. Natl. Acad. Sci. USA* **93**(9): 3920-5.

Ganan, Y., D. Macias, et al. (1996). Role of TGF beta s and BMPs as signals controlling the position of the digits and the areas of interdigital cell death in the developing chick limb autopod. *Development* **122**(8): 2349-57.

Gibson-Brown, J. J., S. I. Agulnik, et al. (1996). Evidence of a role for T-box genes in the evolution of limb morphogenesis and the specification of forelimb/hindlimb identity. *Mech. Dev.* **56**(1-2): 93-101.

Gibson-Brown, J. J., I. A. S, et al. (1998). Expression of T-box genes Tbx2-Tbx5 during chick organogenesis. *Mech. Dev.* **74**(1-2): 165-9.

Gibson-Brown, J. J., I. A. Sergei, et al. (1998). Involvement of T-box genes Tbx2-Tbx5 in vertebrate limb specification and development. *Development* **125**: 2499-509.

Godement, P., J. Salaun, et al. (1984). Prenatal and postnatal development of retinogeniculate and retinocollicular projections in the mouse. *J Comp Neurol* **230**(4): 552-75.

Gorfinkiel, N., L. Sánchez, et al. (1999). Drosophila trerminalia as an appendage-like structure. *Mech. Dev.* **86**: 113-23.

Gouge, A., J. Holt, et al. (2001). Foxn4 - a new member of the forkhead gene family is expressed in the retina. *Mech Dev* **107**(1-2): 203-6.

Graham, A., P. Francis-West, et al. (1994). The signalling molecule BMP4 mediates apoptosis in the rhombencephalic neural crest. *Nature* **372**(6507): 684-6.

Griffin, K. J., J. Stoller, et al. (2000). A conserved role for H15-related T-box transcription factors in zebrafish and Drosophila heart formation. *Dev Biol* **218**(2): 235-47.

Grimm, S. and G. O. Pflugfelder (1996). Control of the gene optomotor-blind in Drosophila wing development by decapentaplegic and wingless. *Science* **271**(5255): 1601-4.

Grindley, J. C., D. R. Davidson, et al. (1995). The role of Pax-6 in eye and nasal development. *Development* **121**(5): 1433-42.

Grindley, J. C., L. K. Hargett, et al. (1997). Disruption of PAX6 function in mice homozygous for the Pax6Sey-1Neu mutation produces abnormalities in the early development and regionalization of the diencephalon. *Mech Dev* **64**(1-2): 111-26.

Grun, F., Y. Hirose, et al. (2000). ALDH6, a cytosolic retinaldehyde dehydrogenase prominently expressed in sensory neuroepithelia during development. *J Biol Chem.*

Guillemot, F. and C. L. Cepko (1992). Retinal fate and ganglion cell differentiation are potentiated by acidic FGF in an in vitro assay of early retinal development. *Development* **114**(3): 743-54.

Haerry, T. E., O. Khalsa, et al. (1998). Synergistic signaling by two BMP ligands through the SAX and TKV receptors controls wing growth and patterning in Drosophila. *Development* **125**(20): 3977-87.

Halder, G., P. Callaerts, et al. (1995). Induction of ectopic eyes by targeted expression of the eyeless gene in Drosophila. *Science* **267**(5205): 1788-92.

Hanson, I. and V. Van Heyningen (1995). Pax6: more than meets the eye. *Trends Genet* **11**(7): 268-72.

Harland, R. (2000). Neural induction. *Curr Opin Genet Dev* **10**(4): 357-62.

Harris, W. A. and C. E. Holt (1995). From tags to RAGS: chemoaffinity finally has receptors and ligands. *Neuron* **15**(2): 241-4.

Hatcher, C. J., M. S. Kim, et al. (2001). TBX5 Transcription Factor Regulates Cell Proliferation during Cardiogenesis. *Dev Biol* **230**(2): 177-88.

Hatini, V., W. Tao, et al. (1994). Expression of winged helix genes, BF-1 and BF-2, define adjacent domains within the developing forebrain and retina. *J Neurobiol* **25**(10): 1293-309.

Hazama, M., A. Aono, et al. (1995). Efficient expression of a heterodimer of bone morphogenetic protein subunits using a baculovirus expression system. *Biochem Biophys Res Commun* **209**(3): 859-66.

He, M., L. Wen, et al. (1999). Transcription repression by Xenopus ET and its human ortholog TBX3, a gene involved in ulnar-mammary syndrome. *Proc Natl Acad Sci U S A* **96**(18): 10212-7.

Heanue, T. A., R. J. Davis, et al. (2002). Dach1, a vertebrate homologue of Drosophila dachshund, is expressed in the developing eye and ear of both chick and mouse and is regulated independently of Pax and Eya genes. *Mech Dev* **111**(1-2): 75-87.

Hemmati-Brivanlou, A. and G. H. Thomsen (1995). Ventral mesodermal patterning in Xenopus embryos: expression patterns and activities of BMP-2 and BMP-4. *Dev Genet* **17**(1): 78-89.

Henkemeyer, M., D. Orioli, et al. (1996). Nuk controls pathfinding of commisural axons in the mammalian central nervous system. *Cell* **86**: 35-46.

Herrmann, B. G., S. Labeit, et al. (1990). Cloning of the T gene required in mesoderm formation in the mouse. *Nature* **343**(6259): 617-22.

Hill, R. E., J. Favor, et al. (1991). Mouse small eye results from mutations in a paired-like homeobox-containing gene. *Nature* **354**(6354): 522-5.

Hinds, J. W. and P. L. Hinds (1978). Early development of amacrine cells in the mouse retina: an electron microscopic, serial section analysis. *J Comp Neurol* **179**(2): 277-300.

Hinds, J. W. and P. L. Hinds (1983). Development of retinal amacrine cells in the mouse embryo: evidence for two modes of formation. *J Comp Neurol* **213**(1): 1-23.

Hiroi, Y., S. Kudoh, et al. (2001). Tbx5 associates with Nkx2-5 and synergistically promotes cardiomyocyte differentiation. *Nat Genet* **28**(3): 276-80.

Hogan, B., R. Beddington, et al. (1994). *Manipulation of the mouse embryo, a laboratory manual.* New York, Cold Spring Harbour Laboratory Press.

Holder, N. and R. Klein (1999). Eph receptors and ephrins: effectors of morphogenesis. *Development* **126**: 2033-44.

Holland, S. J., N. W. Gale, et al. (1996). Bidirectional signalling through the EPH-family receptor Nuk and its transmembrane ligands. *Nature* **383**(6602): 722-5.

Holt, C. E., T. W. Bertsch, et al. (1988). Cellular determination in the Xenopus retina is independent of lineage and birth date. *Neuron* **1**(1): 15-26.

Hopker, V. H., D. Shewan, et al. (1999). Growth-cone attraction to netrin-1 is converted to repulsion by laminin-1. *Nature* **401**(6748): 69-73.

Horb, M. E. and G. H. Thomsen (1999). Tbx5 is essential for heart development. *Development* **126**(8): 1739-51.

Hornberger, M. R., D. Dutting, et al. (1999). Modulation of EphA receptor function by coexpressed ephrinA ligands on retinal ganglion cell axons. *Neuron* **22**(4): 731-42.

Huang, M. T. and C. M. Gorman (1990). Intervening sequences increase efficiency of RNA 3' processing and accumulation of cytoplasmic RNA. *Nucleic Acids Res* **18**(4): 937-47.

Huh, S., V. Hatini, et al. (1999). Dorsal-Ventral patterning defects in the eye of BF-1 deficient mice associated with a restricted loss of shh expression. *Development* **211**: 53-63.

Hutcheson, D. A. and M. L. Vetter (2001). The bHLH factors Xath5 and XNeuroD can upregulate the expression of XBrn3d, a POU-homeodomain transcription factor. *Dev Biol* **232**(2): 327-38.

Hyatt, G. A., E. A. Schmitt, et al. (1996). Retinoic acid establishes ventral retinal characteristics. *Development* **122**(1): 195-204.

Hyatt, G. A., E. A. Schmitt, et al. (1992). Retinoic acid-induced duplication of the zebrafish retina. *Proc Natl Acad Sci U S A* **89**(17): 8293-7.

Hyer, J., T. Mima, et al. (1998). FGF1 patterns the optic vesicle by directing the placement of the neural retina domain. *Development* **125**(5): 869-77.

Imagawa, T., Y. Fujita, et al. (1999). Quantitative studies of the optic nerve fiber layer in the chicken retina. *J. Vet. Med. Sci.* **61**(8): 883-9.

Jacobs, J. J., P. Keblusek, et al. (2000). Senescence bypass screen identifies TBX2, which represses Cdkn2a (p19ARF) and is amplified in a subset of human breast cancers. *Nat Genet* **26**(3): 291-9.

Jean, D., G. Bernier, et al. (1999). Six6 (Optx2) is a novel murine Six3-related homeobox gene that demarcates the presumptive pituitary/hypothalamic axis and the ventral optic stalk. *Mech Dev* **84**(1-2): 31-40.

Jensen, A. M. and V. A. Wallace (1997). Expression of Sonic hedgehog and its putative role as a precursor cell mitogen in the developing mouse retina. *Development* **124**(2): 363-71.

Jerome, L. A. and V. E. Papaioannou (2001). DiGeorge syndrome phenotype in mice mutant for the T-box gene, Tbx1. *Nat Genet* **27**(3): 286-91.

Jones, C. M. and J. C. Smith (1998). Establishment of a BMP-4 morphogen gradient by long-range inhibition. *Dev Biol* **194**(1): 12-7.

Kammandel, B., K. Chowdhury, et al. (1999). Distinct cis-essential modules direct the time-space pattern of the Pax6 gene activity. *Dev Biol* **205**(1): 79-97.

Kastner, P., J. M. Grondona, et al. (1994). Genetic analysis of RXR alpha developmental function: convergence of RXR and RAR signaling pathways in heart and eye morphogenesis. *Cell* **78**(6): 987-1003.

Kastner, P., M. Mark, et al. (1997). Genetic evidence that the retinoid signal is transduced by heterodimeric RXR/RAR functional units during mouse development. *Development* **124**(2): 313-26.

Kastner, P., N. Messaddeq, et al. (1997). Vitamin A deficiency and mutations of RXRalpha, RXRbeta and RARalpha lead to early differentiation of embryonic ventricular cardiomyocytes. *Development* **124**(23): 4749-58.

Kaufman, M. H. (1992). *The Atlas of Mouse Development*. London, Academic Press Ltd.

Kenyon, K. L., N. Zaghloul, et al. (2001). Transcription factors of the anterior neural plate alter cell movements of epidermal progenitors to specify a retinal fate. *Dev Biol* **240**(1): 77-91.

Kerszberg, M. (1999). Morphogen propagation and action: towards molecular models. *Semin Cell Dev Biol* **10**(3): 297-302.

Kim, H. J., D. P. Rice, et al. (1998). FGF-, BMP- and Shh-mediated signalling pathways in the regulation of cranial suture morphogenesis and calvarial bone development. *Development* **125**(7): 1241-51.

King, A. J., M. E. Hutchings, et al. (1988). Developmental plasticity in the visual and auditory representations in the mammalian superior colliculus. *Nature* **332**(6159): 73-6.

Kioussi, C., S. O'Connell, et al. (1999). Pax6 is essential for establishing ventral-dorsal cell boundaries in pituitary gland development. *Proc Natl Acad Sci U S A* **96**(25): 14378-82.

Kispert, A., B. Koschorz, et al. (1995). The T protein encoded by Brachyury is a tissue-specific transcription factor. *Embo J* **14**(19): 4763-72.

Kobayashi, M., R. T. Yu, et al. (2000). Cell-type-specific regulation of the retinoic acid receptor mediated by the orphan nuclear receptor TLX. *Mol Cell Biol* **20**(23): 8731-9.

Koenig, B. B., J. S. Cook, et al. (1994). Characterization and cloning of a receptor for BMP-2 and BMP-4 from NIH 3T3 cells. *Mol Cell Biol* **14**(9): 5961-74.

Koshiba-Takeuchi, K., J. K. Takeuchi, et al. (2000). Tbx5 and the retinotectum projection. *Science* **287**(5450): 134-7.

Kozak, M. (1987). An analysis of 5'-noncoding sequences from 699 vertebrate messenger RNAs. *Nucleic Acids Res* **15**(20): 8125-48.

Kraus, F., B. Haenig, et al. (2001). Cloning and expression analysis of the mouse T-box gene tbx20. *Mech Dev* **100**(1): 87-91.

Krauss, S., J. P. Concordet, et al. (1993). A functionally conserved homolog of the Drosophila segment polarity gene hh is expressed in tissues with polarizing activity in zebrafish embryos. *Cell* **75**(7): 1431-44.

Latchman, D. S. (1998). *Eukaryotic transcription factors*, Academic Press.

Latchman, D. S. (2001). Transcription factors: bound to activate or repress. *Trends Biochem Sci* **26**(4): 211-3.

Law, D. J., T. Gebuhr, et al. (1995). Identification, characterization, and localization to chromosome 17q21-22 of the human TBX2 homolog, member of a conserved developmental gene family. *Mamm Genome* **6**(11): 793-7.

Lee, C. S., N. R. May, et al. (2001). Transdifferentiation of the ventral retinal pigmented epithelium to neural retina in the growth arrest specific gene 1 mutant. *Dev Biol* **236**(1): 17-29.

Letsou, A., K. Arora, et al. (1995). Drosophila Dpp signaling is mediated by the punt gene product: a dual ligand-binding type II receptor of the TGF beta receptor family. *Cell* **80**(6): 899-908.

Lewin, B. (1994). *Genes V*. Oxford, Oxford University Press.

Li, H.-S., C. Tierney, et al. (1997). A single morphogenetic field gives rise to two retina primordia under the influence of the prechordal plate. *Development* **124**: 603-15.

Li, H. S., J. M. Yang, et al. (1994). Pax-6 is first expressed in a region of ectoderm anterior to the early neural plate: implications for stepwise determination of the lens. *Dev Biol* **162**(1): 181-94.

Li, Q. Y., R. A. Newbury-Ecob, et al. (1997). Holt-Oram syndrome is caused by mutations in TBX5, a member of the Brachyury (T) gene family. *Nat. Genet.* **15**(1): 21-9.

Lingbeek, M. E., J. J. Jacobs, et al. (2002). The T-box Repressors TBX2 and TBX3 Specifically Regulate the Tumor Suppressor Gene p14ARF via a Variant T-site in the Initiator. *J Biol Chem* **277**(29): 26120-7.

Liu, F., F. Ventura, et al. (1995). Human type II receptor for bone morphogenic proteins (BMPs): extension of the two-kinase receptor model to the BMPs. *Mol Cell Biol* **15**(7): 3479-86.

Liu, I. S., J. D. Chen, et al. (1994). Developmental expression of a novel murine homeobox gene (Chx10): evidence for roles in determination of the neuroretina and inner nuclear layer. *Neuron* **13**(2): 377-93.

Liu, Y., Y. Shen, et al. (2001). Isolation and characterization of a zebrafish homologue of the cone rod homeobox gene. *Invest Ophthalmol Vis Sci* **42**(2): 481-7.

Livesey, F. J. and C. L. Cepko (2001). Vertebrate neural cell-fate determination: lessons from the retina. *Nat Rev Neurosci* **2**(2): 109-18.

Livesey, F. J., T. Furukawa, et al. (2000). Microarray analysis of the transcriptional network controlled by the photoreceptor homeobox gene Crx. *Curr Biol* **10**(6): 301-10.

Logan, M., H. G. Simon, et al. (1998). Differential regulation of T-box and homeobox transcription factors suggests roles in controlling chick limb-type identity. *Development* **125**(15): 2825-35.

Logan, M. and C. J. Tabin (1999). Role of Pitx1 upstream of Tbx4 in specification of hindlimb identity. *Science* **283**(5408): 1736-9.

Lohnes, D., M. Mark, et al. (1994). Function of the retinoic acid receptors (RARs) during development (I). Craniofacial and skeletal abnormalities in RAR double mutants. *Development* **120**(10): 2723-48.

Loosli, F., S. Winkler, et al. (1999). Six3 overexpression initiates the formation of ectopic retina. *Genes Dev* **13**(6): 649-54.

López-Ríos, J., M. E. Gallardo, et al. (1999). Six9 (Optx2), a new member of the Six gene family of transcription factors, is expressed at early stages of vertebrate ocular and pituitary development. *Mech. Dev.* **83**: 155-9.

Lough, J., M. Barron, et al. (1996). Combined BMP-2 and FGF-4, but neither factor alone, induces cardiogenesis in non-precardiac embryonic mesoderm. *Dev Biol* **178**(1): 198-202.

Lucas, R. J., M. S. Freedman, et al. (1999). Regulation of the mammalian pineal by non-rod, non-cone, ocular photoreceptors. *Science* **284**(5413): 505-7.

Macdonald, R., K. A. Barth, et al. (1995). Midline signalling is required for Pax gene regulation and patterning of the eyes. *Development* **121**(10): 3267-78.

Macdonald, R. and S. W. Wilson (1996). Pax proteins and eye development. *Curr. Op. Neurobiol.* **6**: 49-56.

Mangelsdorf, D. J. and R. M. Evans (1995). The RXR heterodimers and orphan receptors. *Cell* **83**(6): 841-50.

Mann, I. (1964). *The development of the human eye.* London, British Medical Association.

Marin-Teva, J. L., M. A. Cuadros, et al. (1999). Naturally occurring cell death and migration of microglial precursors in the quail retina during normal development. *J. Comp. Neurol.* **412**(2): 255-75.

Marquardt, T., R. Ashery-Padan, et al. (2001). Pax6 is required for the multipotent state of retinal progenitor cells. *Cell* **105**(1): 43-55.

Marsh-Armstrong, N., P. McCaffery, et al. (1994). Retinoic acid is necessary for development of the ventral retina in zebrafish. *Proc. Natl. Acad. Sci. U.S.A.* **91**: 7286-90.

Martinez-Morales, J. R., M. Signore, et al. (2001). Otx genes are required for tissue specification in the developing eye. *Development* **128**(11): 2019-30.

Maslim, J., M. Webster, et al. (1986). Stages in the structural differentiation of retinal ganglion cells. *J Comp Neurol* **254**(3): 382-402.

Massague, J. (1998). TGF-beta signal transduction. *Annu Rev Biochem* **67**: 753-91.

Mathers, P. H., A. Grinberg, et al. (1997). The Rx homeobox gene is essential for vertebrate eye development. *Nature* **387**(6633): 603-7.

Matise, M. P. and A. L. Joyner (1997). Expression patterns of developmental control genes in normal and Engrailed-1 mutant mouse spinal cord reveal early diversity in developing interneurons. *J Neurosci* **17**(20): 7805-16.

Matsuo, I., S. Kuratani, et al. (1995). Mouse Otx2 functions in the formation and patterning of rostral head. *Genes Dev* **9**(21): 2646-58.

McAvoy, J. W., C. G. Chamberlain, et al. (1991). The role of fibroblast growth factor in eye lens development. *Ann N Y Acad Sci* **638**: 256-74.

McCabe, K. L., E. C. Gunther, et al. (1999). The development of the pattern of retinal ganglion cells in the chick retina: mechanisms that control differentiation. *Development* **126**(24): 5713-24.

McCaffery, P., M. O. Lee, et al. (1992). Asymmetrical retinoic acid synthesis in the dorsoventral axis of the retina. *Development* **115**: 371-82.

McCaffery, P., K. C. Posch, et al. (1993). Changing patterns of the retinoic acid system in the developing retina. *Dev. Biol.* **158**: 390-9.

McCaffery, P., E. Wagner, et al. (1999). Dorsal and ventral retinal territories defined by retinoic acid synthesis, break-down and nuclear receptor expression. *Mech. Dev.* **85**: 203-14.

McLoon, S. C. (1991). A monoclonal antibody that distinguishes between temporal and nasal retinal axons. *J Neurosci* **11**: 1470-7.

McWhirter, J. R., M. Goulding, et al. (1997). A novel fibroblast growth factor gene expressed in the developing nervous system is a downstream target of the chimeric homeodomain oncoprotein E2A-Pbx1. *Development* **124**(17): 3221-32.

Meins, M., D. J. Henderson, et al. (2000). Characterization of the human TBX20 gene, a new member of the T-Box gene family closely related to the drosophila H15 gene. *Genomics* **67**(3): 317-32.

Mendez-Otero, R. and J. E. Friedman (1996). Role of acetylated gangliosides on neurite extension. *Eur. J. Cell Biol.* **71**: 192-8.

Merscher, S., B. Funke, et al. (2001). TBX1 is responsible for cardiovascular defects in velo-cardio-facial/DiGeorge syndrome. *Cell* **104**(4): 619-29.

Mey, J., P. McCaffery, et al. (2001). Sources and sink of retinoic acid in the embryonic chick retina: distribution of aldehyde dehydrogenase activities, CRABP-I, and sites of retinoic acid inactivation. *Brain Res Dev Brain Res* **127**(2): 135-48.

Mic, F. A., A. Molotkov, et al. (2000). RALDH3, a retinaldehyde dehydrogenase that generates retinoic acid, is expressed in the ventral retina, otic vesicle and olfactory pit during mouse development. *Mech Dev* **97**(1-2): 227-30.

Miller, D. L., S. Ortega, et al. (2000). Compensation by fibroblast growth factor 1 (FGF1) does not account for the mild phenotypic defects observed in FGF2 null mice. *Mol Cell Biol* **20**(6): 2260-8.

Monaghan, A. P., D. R. Davidson, et al. (1991). The Msh-like homeobox genes define domains in the developing vertebrate eye. *Development* **112**(4): 1053-61.

Moskal, J. R., D. Trisler, et al. (1986). Purification of a membrane protein distributed in a topographic gradient in chicken retina. *Proc. Natl. Acad. Sci. USA* **83**(13): 4730-3.

Mui, S. H., R. Hindges, et al. (2002). The homeodomain protein Vax2 patterns the dorsoventral and nasotemporal axes of the eye. *Development* **129**(3): 797-804.

Muller, C. W. and B. G. Herrmann (1997). Crystallographic structure of the T domain-DNA complex of the Brachyury transcription factor. *Nature* **389**(6653): 884-8.

Muller, F., S. Albert, et al. (2000). Direct action of the nodal-related signal cyclops in induction of sonic hedgehog in the ventral midline of the CNS. *Development* **127**(18): 3889-97.

Nakagawa, S., C. Brennan, et al. (2000). Ephrin-B regulates the Ipsilateral routing of retinal axons at the optic chiasm. *Neuron* **25**(3): 599-610.

Nakamura, H. and D. D. O'Leary (1989). Inaccuracies in initial growth and arborization of chick retinotectal axons followed by course corrections and axon remodeling to develop topographic order. *J Neurosci* **9**(11): 3776-95.

Newbury-Ecob, R. A., R. Leanage, et al. (1996). Holt-Oram syndrome: a clinical genetic study. *J Med Genet* **33**(4): 300-7.

Nguyen, M. and H. Arnheiter (2000). Signaling and transcriptional regulation in early mammalian eye development: a link between FGF and MITF. *Development* **127**(16): 3581-91.

Nicholls, J. G., A. R. Martin, et al. (2001). *From neuron to brain*. Sunderland, Sinauer Associates Incorporated.

Nishimatsu, S. and G. H. Thomsen (1998). Ventral mesoderm induction and patterning by bone morphogenetic protein heterodimers in Xenopus embryos. *Mech Dev* **74**(1-2): 75-88.

Nohno, T., T. Ishikawa, et al. (1995). Identification of a human type II receptor for bone morphogenetic protein-4 that forms differential heteromeric complexes with bone morphogenetic protein type I receptors. *J Biol Chem* **270**(38): 22522-6.

Nornes, H. O., G. R. Dressler, et al. (1990). Spatially and temporally restricted expression of Pax2 during murine neurogenesis. *Development* **109**(4): 797-809.

Ohkubo, Y., C. Chiang, et al. (2002). Coordinate regulation and synergistic actions of BMP4, SHH and FGF8 in the rostral prosencephalon regulate morphogenesis of the telencephalic and optic vesicles. *Neuroscience* **111**(1): 1-17.

Ohsaki, K., T. Morimitsu, et al. (1999). Expression of the Vax family homeobox genes suggests multiple roles in eye development. *Genes Cells* **4**(5): 267-76.

Ohuchi, H., J. Takeuchi, et al. (1998). Correlation of wing-leg identity in ectopic FGF-induced chimeric limbs with the differential expression of chick Tbx5 and Tbx4. *Development* **125**(1): 51-60.

Orioli, D. and R. Klein (1997). The Eph receptor family: axonal guidance by contact repulsion. *Trends Genet* **13**(9): 354-9.

Ortega, S., M. Ittmann, et al. (1998). Neuronal defects and delayed wound healing in mice lacking fibroblast growth factor 2. *Proc Natl Acad Sci U S A* **95**(10): 5672-7.

Papaioannou, V. E. (2001). T-box genes in development: from hydra to humans. *Int Rev Cytol* **207**: 1-70.

Papalopulu, N. and C. Kintner (1996). A Xenopus gene, Xbr-1, defines a novel class of homeobox genes and is expressed in the dorsal ciliary margin of the eye. *Dev Biol* **174**(1): 104-14.

Pera, E. and M. Kessel (1997). Patterning of the chick forebrain analage by the prechordal plate. *Development* **124**: 201-5.

Pflugfelder, G. O. and M. Heisenberg (1995). Optomotor-blind of Drosophila Melanogaster: a neurogenetic approach to optic lobe development and optomotor behaviour. *Comp. Biochem. Physiol.* **110A**: 185-202.

Pflugfelder, G. O., H. Roth, et al. (1992). A homology domain shared between Drosophila optomotor-blind and mouse Brachyury is involved in DNA binding. *Biochem Biophys Res Commun* **186**(2): 918-25.

Plaza, S., H. Hennemann, et al. (1999). Evidence that POU factor Brn-3B regulates expression of Pax-6 in neuroretina cells. *J Neurobiol* **41**(3): 349-58.

Poeck, B., A. Hofbauer, et al. (1993). Expression of the Drosophila optomotor-blind gene transcript in neuronal and glial cells of the developing nervous system. *Development* **117**(3): 1017-29.

Polyak (1941). *The Retina*. Chicago, The University of Chicago Press.

Porsch, M. (2002). Mapping of specificity determinants in OMB and ORG-1. *Lehrstuhl fur Genetik und Neurobiologie, Biozentrum*. Wurzburg, Universitat Wurzburg**:** 61-84.

Porsch, M., K. Hofmeyer, et al. (1998). Isolation of a Drosophila T-box gene closely related to human TBX1. *Gene* **212**(2): 237-48.

Porter, F. D., J. Drago, et al. (1997). Lhx2, a LIM homeobox gene, is required for eye, forebrain, and definitive erythrocyte development. *Development* **124**(15): 2935-44.

Prada, C., L. Puelles, et al. (1981). A golgi study on the early sequence of differentiation of ganglion cells in the chick embryo retina. *Anat Embryol (Berl)* **161**(3): 305-17.

Pratt, T., T. Vitalis, et al. (2000). A role for Pax6 in the normal development of dorsal thalamus and its cortical connections. *Development* **127**(23): 5167-78.

Puschel, A. W., P. Gruss, et al. (1992). Sequence and expression pattern of pax-6 are highly conserved between zebrafish and mice. *Development* **114**(3): 643-51.

Rager, G. and B. von Oeynhausen (1979). Ingrowth and ramification of retinal fibers in the developing optic tectum of the chick embryo. *Exp. Brain Res.* **35**: 213-27.

Reese, B. E. and G. E. Baker (1993). The re-establishment of the representation of the dorso-ventral retinal axis in the chiasmatic region of the ferret. *Vis Neurosci* **10**(5): 957-68.

Reilly, K. M. and D. A. Melton (1996). Short-range signaling by candidate morphogens of the TGF beta family and evidence for a relay mechanism of induction. *Cell* **86**(5): 743-54.

Reuter, T. E., R. H. White, et al. (1971). Rhodopsin and porphyropsin fields in the adult bullfrog retina. *J Gen Physiol* **58**(4): 351-71.

Rhodes, R. H. (1979). A light microscopic study of the developing human neural retina. *Am J Anat* 154(2): 195-209.

Rissi, M., J. Wittbrodt, et al. (1995). Zebrafish Radar: a new member of the TGF-beta superfamily defines dorsal regions of the neural plate and the embryonic retina. *Mech. Dev.* **49**(3): 223-34.

Rodieck, R. W. (1998). Informing the brain. *The first steps in seeing*: 266-91.

Rodriguez-Esteban, C., T. Tsukui, et al. (1999). The T-box genes Tbx4 and Tbx5 regulate limb outgrowth and identity. *Nature* **398**: 814-8.

Roessler, E., E. Belloni, et al. (1996). Mutations in the human Sonic Hedgehog gene cause holoprosencephaly. *Nat Genet* **14**(3): 357-60.

Rohlich, P., T. van Veen, et al. (1994). Two different visual pigments in one retinal cone cell. *Neuron* **13**(5): 1159-66.

Rosenzweig, B. L., T. Imamura, et al. (1995). Cloning and characterization of a human type II receptor for bone morphogenetic proteins. *Proc Natl Acad Sci U S A* **92**(17): 7632-6.

Roskies, A., G. C. Friedman, et al. (1995). Mechanisms and molecules controlling the development of retinal maps. *Perspect Dev Neurobiol* **3**(1): 63-75.

Roskies, A. L. and D. D. O'Leary (1994). Control of topographic retinal axon branching by inhibitory membrane-bound molecules. *Science* **265**(5173): 799-803.

Ruvinsky, I., A. C. Oates, et al. (2000). The evolution of paired appendages in vertebrates: T-box genes in the zebrafish. *Dev Genes Evol* **210**(2): 82-91.

Sakuta, H., R. Suzuki, et al. (2001). Ventroptin: a BMP-4 antagonist expressed in a double-gradient pattern in the retina. *Science* **293**(5527): 111-5.

Sampath, K., A. L. Rubinstein, et al. (1998). Induction of the zebrafish ventral brain and floorplate requires cyclops/nodal signalling. *Nature* **395**(6698): 185-9.

Sanson, B. (2001). Generating patterns from fields of cells. Examples from Drosophila segmentation. *EMBO Rep* **2**(12): 1083-8.

Sasagawa, S., T. Takabatake, et al. (2002). Axes establishment during eye morphogenesis in Xenopus by coordinate and antagonistic actions of BMP4, Shh, and RA. *Genesis* **33**(2): 86-96.

Schauerte, H. E., F. J. van Eeden, et al. (1998). Sonic hedgehog is not required for the induction of medial floor plate cells in the zebrafish. *Development* **125**(15): 2983-93.

Schmitt, E. A. and J. E. Dowling (1996). Comparison of topographical patterns of ganglion and photoreceptor cell differentiation in the retina of the zebrafish, Danio rerio. *J Comp Neurol* **371**(2): 222-34.

Schmitt, E. A. and J. E. Dowling (1999). Early retinal development in the zebrafish, Danio rerio: light and electron microscopic analyses. *J Comp Neurol* **404**(4): 515-36.

Schott, J. J., D. W. Benson, et al. (1998). Congenital heart disease caused by mutations in the transcription factor NKX2-5. *Science* **281**(5373): 108-11.

Schulte, D. and C. L. Cepko (2000). Two homeobox genes define the domain of EphA3 expression in the developing chick retina. *Development* **127**(23): 5033-45.

Schulte, D., T. Furukawa, et al. (1999). Misexpression of the Emx-related homeobox genes cVax and mVax2 ventralizes the retina and perturbs the retinotectal map. *Neuron* **24**(3): 541-53.

Schwarz, M., F. Cecconi, et al. (2000). Spatial specification of mammalian eye territories by reciprocal transcriptional repression of Pax2 and Pax6. *Development* **127**(20): 4325-34.

Sefton, M., M. Araujo, et al. (1997). Novel expression gradients of Eph-like receptor tyrosine kinases in the developing chick retina. *Dev. Biol.* **188**(2): 363-8.

Sefton, M. and M. A. Nieto (1997). Multiple roles of Eph-like kinases and their ligands during development. *Cell Tissue Res.* **290**(2): 243-50.

Sidman, R. L. (1961). Histogenesis of the mouse retina studied with thymidine-H_3. *The Structure of the Eye*. G. K. Smelser. New York, Academic Press: 487-505.

Silver, J. and J. Sapiro (1981). Axon guidance during development of the optic nerve: the role of pigmented epithelia and other extrinsic factors. *J. Brain Res.* **202**: 521-38.

Simeone, A., D. Acampora, et al. (1993). A vertebrate gene related to orthodenticle contains a homeodomain of the bicoid class and demarcates anterior neuroectoderm in the gastrulating mouse embryo. *Embo J* **12**(7): 2735-47.

Simon, D. K. and D. D. O'Leary (1991). Relationship of retinotopic ordering of axons in the optic pathway to the formation of visual maps in central targets. *J Comp Neurol* **307**(3): 393-404.

Simon, D. K. and D. D. O'Leary (1992). Development of topographic order in the mammalian retinocollicular projection. *J Neurosci* **12**(4): 1212-32.

Simon, D. K. and D. D. O'Leary (1992). Influence of position along the medial-lateral axis of the superior colliculus on the topographic targeting and survival of retinal axons. *Brain Res Dev Brain Res* **69**(2): 167-72.

Simon, D. K. and D. D. O'Leary (1992). Responses of retinal axons in vivo and in vitro to position-encoding molecules in the embryonic superior colliculus. *Neuron* **9**(5): 977-89.

Sinclair, C. S., C. Adem, et al. (2002). TBX2 is preferentially amplified in BRCA1- and BRCA2-related breast tumors. *Cancer Res* **62**(13): 3587-91.

Sinha, S., S. Abraham, et al. (2000). Differential DNA binding and transcription modulation by three T-box proteins, T, TBX1 and TBX2. *Gene* **258**(1-2): 15-29.

Sivasankaran, R., M. A. Vigano, et al. (2000). Direct transcriptional control of the Dpp target omb by the DNA binding protein Brinker. *Embo J* **19**(22): 6162-72.

Snow, R. L. and J. A. Robson (1994). Ganglion cell neurogenesis, migration and early differentiation in the chick retina. *Neuroscience* **58**(2): 399-409.

Sohocki, M. M., L. S. Sullivan, et al. (1998). A range of clinical phenotypes associated with mutations in CRX, a photoreceptor transcription-factor gene. *Am J Hum Genet* **63**(5): 1307-15.

Sowden, J. C., J. K. Holt, et al. (2001). Expression of Drosophila omb-Related T-Box Genes in the Developing Human and Mouse Neural Retina. *Invest Ophthalmol Vis Sci* **42**(13): 3095-102.

Sperry, R. W. (1943). Visuomotor co-ordination in the newt (Triturus viridescens) after regeneration of the optic nerve. *J. Comp. Neurol.* **79**: 33-55.

Sperry, R. W. (1963). Chemoaffinity in the orderly growth of nerve fiber patterns and connections. *Proc. Natl. Acad. Sci. USA* **50**: 703-10.

Spira, A. W. and M. J. Hollenberg (1973). Human retinal development: ultrastructure of the inner retinal layers. *Dev Biol* **31**(1): 1-21.

Stone, E. M., V. C. Sheffield, et al. (2001). Molecular genetics of age-related macular degeneration. *Hum Mol Genet* **10**(20): 2285-92.

Stoykova, A., D. Treichel, et al. (2000). Pax6 modulates the dorsoventral patterning of the mammalian telencephalon. *J Neurosci* **20**(21): 8042-50.

Straznicky, K. and D. Tay (1977). Retinal growth in double dorsal and double ventral eyes in Xenopus. *J. Embryol. Exp. Morphol.* **40**: 175-85.

Stull, D. L. and K. C. Wikler (2000). Retinoid-dependent gene expression regulates early morphological events in the development of the murine retina. *J Comp Neurol* **417**(3): 289-98.

Suda, Y., J. Nakabayashi, et al. (1999). Functional equivalency between Otx2 and Otx1 in development of the rostral head. *Development* **126**(4): 743-57.

Suzuki, A., E. Kaneko, et al. (1997). Mesoderm induction by BMP-4 and -7 heterodimers. *Biochem Biophys Res Commun* **232**(1): 153-6.

Suzuki, R., T. Shintani, et al. (2000). Identification of RALDH-3, a novel retinaldehyde dehydrogenase, expressed in the ventral region of the retina. *Mech Dev* **98**(1-2): 37-50.

Szeto, D. P., C. Rodriguez-Esteban, et al. (1999). Role of the Bicoid-related homeodomain factor Pitx1 in specifying hindlimb morphogenesis and pituitary development. *Genes Dev* **13**(4): 484-94.

Takabatake, Y., T. Takabatake, et al. (2002). Conserved expression control and shared activity between cognate T-box genes Tbx2 and Tbx3 in connection with Sonic hedgehog signaling during Xenopus eye development. *Dev Growth Differ* **44**(4): 257-71.

Takabatake, Y., T. Takabatake, et al. (2000). Conserved and divergent expression of T-box genes Tbx2-Tbx5 in Xenopus. *Mech Dev* **91**(1-2): 433-7.

Takeuchi, J. K., K. Koshiba-Takeuchi, et al. (1999). Tbx5 and Tbx4 genes determine the wing/leg identity of limb buds. *Nature* **398**: 810-4.

Tamura, K., S. Yonei-Tamura, et al. (1999). Differential expression of Tbx4 and Tbx5 in Zebrafish Fin buds. *Mech. Dev.* **87**(1-2): 181-4.

ten Dijke, P., H. Yamashita, et al. (1994). Identification of type I receptors for osteogenic protein-1 and bone morphogenetic protein-4. *J Biol Chem* **269**(25): 16985-8.

Thor, S., J. Ericson, et al. (1991). The homeodomain LIM protein Isl-1 is expressed in subsets of neurons and endocrine cells in the adult rat. *Neuron* **7**(6): 881-9.

Toresson, H., S. S. Potter, et al. (2000). Genetic control of dorsal-ventral identity in the telencephalon: opposing roles for Pax6 and Gsh2. *Development* **127**(20): 4361-71.

Torres, M., E. Gomez-Pardo, et al. (1996). Pax2 contributes to inner ear patterning and optic nerve trajectory. *Development* **122**(11): 3381-91.

Toy, J., J. M. Yang, et al. (1998). The optx2 homeobox gene is expressed in early precursors of the eye and activates retina-specific genes. *Proc Natl Acad Sci U S A* **95**(18): 10643-8.

Trisler, D. (1990). Cell recognition and pattern formation in the developing nervous system. *J. Exp. Biol.* **153**: 11-27.

Trisler, D. and F. Collins (1987). Corresponding spatial gradients of TOP molecules in the developing retina and optic tectum. *Science* **237**(4819): 1208-9.

Trousse, F., P. Esteve, et al. (2001). Bmp4 mediates apoptotic cell death in the developing chick eye. *J Neurosci* **21**(4): 1292-301.

Trowe, T., S. Klostermann, et al. (1996). Mutations disrupting the ordering and topographic mapping of axons in the retinotectal projection of the zebrafish, Danio rerio. *Development* **123**: 439-50.

Turner, D. L., E. Y. Snyder, et al. (1990). Lineage-independent determination of cell type in the embryonic mouse retina. *Neuron* **4**(6): 833-45.

Vetter, M. L. and N. L. Brown (2001). The role of basic helix-loop-helix genes in vertebrate retinogenesis. *Semin Cell Dev Biol* **12**(6): 491-8.

Vogel-Hopker, A., T. Momose, et al. (2000). Multiple functions of fibroblast growth factor-8 (FGF-8) in chick eye development. *Mech Dev* **94**(1-2): 25-36.

Wagner, E., P. McCaffery, et al. (2000). Retinoic acid in the formation of the dorsoventral retina and its central projections. *Dev Biol* **222**(2): 460-70.

Wallace, V. A. and M. C. Raff (1999). A role for Sonic hedgehog in axon-to-astrocyte signalling in the rodent optic nerve. *Development* **126**(13): 2901-9.

Walter, J., S. Henke-Fahle, et al. (1987). Avoidance of posterior tectal membranes by temporal retinal axons. *Development* **101**(4): 909-13.

Walter, J., B. Kern-Veits, et al. (1987). Recognition of position-specific properties of tectal cell membranes by retinal axons in vitro. *Development* **101**(4): 685-96.

Wang, H. U. and D. J. Anderson (1997). Eph family transmembrane ligands can mediate repulsive guidance of trunk neural crest migration and motor axon outgrowth. *Neuron* **18**(3): 383-96.

Wang, S. S., R. Y. Tsai, et al. (1997). The characterization of the Olf-1/EBF-like HLH transcription factor family: implications in olfactory gene regulation and neuronal development. *J Neurosci* **17**(11): 4149-58.

Wang, S. W., B. S. Kim, et al. (2001). Requirement for math5 in the development of retinal ganglion cells. *Genes Dev* **15**(1): 24-9.

Warkany, J. and E. Schraffenberger (1946). Congenital malformations induced in rats by maternal vitamin A deficiency I. Defects of the eye. *Arch. Opthal.* **35**: 150-69.

Watanabe, M., U. Rutishauser, et al. (1991). Formation of the retinal ganglion cell and optic fiber layers. *J Neurobiol* **22**(1): 85-96.

Wawersik, S. and R. L. Maas (2000). Vertebrate eye development as modeled in Drosophila. *Hum Mol Genet* **9**(6): 917-25.

Wawersik, S., P. Purcell, et al. (1999). BMP7 acts in murine lens placode development. *Dev Biol* **207**(1): 176-88.

Weidong, W., P. Lo, et al. (2000). Hmx: an evolutionary conserved homeobox gene family expressed in the developing nervous system in mice and Drosophila. *Mech Dev* **99**: 123-37.

West, S. K. (2000). Looking forward to 20/20: a focus on the epidemiology of eye diseases. *Epidemiol Rev* **22**(1): 64-70.

Wetts, R. and S. E. Fraser (1988). Multipotent precursors can give rise to all major cell types of the frog retina. *Science* **239**(4844): 1142-5.

Winslow, J. W., P. Moran, et al. (1995). Cloning of AL-1, a ligand for an Eph-related tyrosine kinase receptor involved in axon bundle formation. *Neuron* **14**: 973-81.

Wong, K., Y. Peng, et al. (2002). Retina dorsal/ventral patterning by Xenopus TBX3. *Biochem Biophys Res Commun* **290**(2): 737-42.

Woo, K. and S. Fraser (1995). Order and coherence in the fate map of the zebrafish nervous system. *Development* **121**: 2595-609.

Woollard, A. and J. Hodgkin (2000). The caenorhabditis elegans fate-determining gene mab-9 encodes a T-box protein required to pattern the posterior hindgut. *Genes Dev* **14**(5): 596-603.

Wu, H. H., R. J. Cork, et al. (2000). Refinement of the ipsilateral retinocollicular projection is disrupted in double endothelial and neuronal nitric oxide synthase gene knockout mice. *Brain Res Dev Brain Res* **120**(1): 105-11.

Xiang, M. (1998). Requirement for Brn-3b in early differentiation of postmitotic retinal ganglion cell precursors. *Dev Biol* **197**(2): 155-69.

Xiang, M., L. Zhou, et al. (1995). The Brn-3 family of POU-domain factors: primary structure, binding specificity, and expression in subsets of retinal ganglion cells and somatosensory neurons. *J Neurosci* **15**(7 Pt 1): 4762-85.

Xiang, M., L. Zhou, et al. (1993). Brn-3b: a POU domain gene expressed in a subset of retinal ganglion cells. *Neuron* **11**(4): 689-701.

Xu, P. X., X. Zhang, et al. (1999). Regulation of Pax6 expression is conserved between mice and flies. *Development* **126**(2): 383-95.

Xu, Q., G. Mellitzer, et al. (1999). In vivo cell sorting in complementary segmental domains mediated by Eph receptors and ephrins. *Nature* **399**(6733): 267-71.

Yamada, M., J. P. Revelli, et al. (2000). Expression of Chick Tbx-2, Tbx-3, and Tbx-5 Genes during Early Heart Development: Evidence for BMP2 Induction of Tbx2. *Dev Biol* **228**(1): 95-105.

Yamashita, H., P. ten Dijke, et al. (1995). Osteogenic protein-1 binds to activin type II receptors and induces certain activin-like effects. *J Cell Biol* **130**(1): 217-26.

Young, R. W. (1985). Cell differentiation in the retina of the mouse. *Anat Rec* **212**(2): 199-205.

Yu, R. T., M. Y. Chiang, et al. (2000). The orphan nuclear receptor Tlx regulates Pax2 and is essential for vision. *Proc Natl Acad Sci U S A* **97**(6): 2621-5.

Zeng, X., J. A. Goetz, et al. (2001). A freely diffusible form of Sonic hedgehog mediates long-range signalling. *Nature* **411**(6838): 716-20.

Zernicka-Goetz, M. (2002). Patterning of the embryo: the first spatial decisions in the life of a mouse. *Development* **129**(4): 815-29.

Zhang, X. M. and X. J. Yang (2001). Regulation of retinal ganglion cell production by Sonic hedgehog. *Development* **128**(6): 943-57.

Zhang, X. M. and X. J. Yang (2001). Temporal and spatial effects of Sonic hedgehog signaling in chick eye morphogenesis. *Dev Biol* **233**(2): 271-90.

Zhang, Y., Z. Zhang, et al. (2000). A new function of BMP4: dual role for BMP4 in regulation of Sonic hedgehog expression in the mouse tooth germ. *Development* **127**(7): 1431-43.

Zhang, Y., X. Zhao, et al. (1999). Msx1 is required for the induction of Patched by Sonic hedgehog in the mammalian tooth germ. *Dev Dyn* **215**(1): 45-53.

Zhao, S., F. C. Hung, et al. (2001). Patterning the optic neuroepithelium by FGF signaling and Ras activation. *Development* **128**(24): 5051-60.

Zhao, Z. and S. A. Rivkees (2000). Programmed cell death in the developing heart: regulation by BMP4 and FGF2. *Dev Dyn* **217**(4): 388-400.

Zhou, H., T. Yoshioka, et al. (1996). Retina-derived POU-domain factor-1: a complex POU-domain gene implicated in the development of retinal ganglion and amacrine cells. *J Neurosci* **16**(7): 2261-74.

Zimmerman, L. B., J. M. De Jesus-Escobar, et al. (1996). The Spemann organizer signal noggin binds and inactivates bone morphogenetic protein 4. *Cell* **86**(4): 599-606.

Zou, H. and L. Niswander (1996). Requirement for BMP signaling in interdigital apoptosis and scale formation. *Science* **272**(5262): 738-41.

Zuber, M. E., M. Perron, et al. (1999). Giant eyes in Xenopus laevis by overexpression of XOptx2. *Cell* **98**(3): 341-52.